THE ACID LEACHING OF URANIUM DIOXIDE WITH PEROXYGENS

by

SIMON FRANCIS WATTS, B.Sc.

A Thesis submitted for the degree of Doctor of Philosophy of the University of London and for the Diploma of Membership of Imperial College.

Metallurgy Department
Royal School of Mines
Imperial College
London S.W.7.

September 1985

ABSTRACT

The anodic oxidation of uranium dioxide has been studied in low pH sulphate systems. It is proposed that the anodic half cell reaction proceeds by a mechanism involving intermediate uranium oxides. The rate determining steps in the anodic oxidation of uranium dioxide appear to be the oxidation of U_3O_7 and U_8O_{19} at less oxidising potentials ($E \leq$ 611 mV (SHE)), and the oxidation of U_3O_8 at more oxidising potentials ($E >$ 750 mV (SHE)).

The leaching of UO_2 with both hydrogen peroxide and peroxymonosulphuric acid at low pH in sulphate systems has been studied and the results treated using multi-linear regression analysis. Activation energies, anodic transfer coefficients, and various kinetic parameters have been evaluated. Mass transfer coefficients for both systems have also been estimated. These data indicate that the leaching of UO_2 in the presence of both hydrogen peroxide and peroxymonosulphuric acid are chemically rate limited, and further that the rate limiting step is within the anodic half cell reaction mechanism.

A dissolution mechanism consistent with the kinetic and electrochemical data is proposed, and certain other phenomena are explained.

To my Parents, who never quite
knowing what it was all about,
encouraged me through it all.

Thank you, Michael Cooke and
Colin O'Prey, who in the Lord
inspired me and set my feet
on this road.

"... Auxillium ab alto..."

CONTENTS

		Page
Abstract		2
Contents		6
List of Figures		9
List of Plates		13
List of Graphs		14
List of Tables		16
Glossary of Symbols		20
SECTION 1. LITERATURE SURVEY		25
1.1	HETEROGENEOUS REACTIONS	27
1.2	LEACHING MODELS	30
1.3	URANIUM OXIDES	32
1.4	THE SULPHATE-BISULPHATE EQUILIBRIUM	39
1.5	PREVIOUS WORK	42
1.5.1	The Anodic Reaction	42
1.5.2	The Cathodic Reaction	59
SECTION 2. EXPERIMENTAL PROCEDURE		67
2.1	APPARATUS AND EXPERIMENTAL PROCEDURE	67
2.1.1	Reagents	67
2.1.2	Chemical Leaching studies	74
2.1.3	Electrochemically Driven Leaching Studies	80
2.1.4	Methods of Analysis	99
2.1.5	Treatment of Kinetic Results	107

		Page
SECTION 3. RESULTS AND DISCUSSION		119
3.1	INTRODUCTION	119
3.2	THE ANODIC OXIDATION OF UO_2	119
3.2.1	Cyclic Voltammetry	119
3.2.2	Cathodic Stripping Voltammetry	140
3.2.3	Summary of the Voltammetry Results	163
3.2.4	Chronoamperometry	169
3.2.5	Summary of Results	186
3.3	THE MECHANISM OF THE FULL LEACHING SYSTEM	196
3.3.1	Introduction	196
3.3.2	Peroxymonosulphuric Acid System	197
3.3.3	Hydrogen Peroxide System	219
3.3.4	Microscopy and Steady State Electrochemistry	229
3.4	THE PRACTICAL APPLICATION OF ELECTROCHEMISTRY TO REAL SYSTEMS	243
3.4.1	Introduction	243
3.4.2	The Problems	243
3.4.3	The Electrochemical Cell	250
SECTION 4. SUMMARY OF RESULTS AND CONCLUSIONS		252
4.1	THE ANODIC OXIDATION OF UO_2	252
4.2	THE LEACHING OF UO_2 WITH OXIDISING AGENT	255
4.2.1	Peroxymonosulphuric Acid	255
4.2.2	Hydrogen Peroxide	258
4.3	THE MAJOR WEAKNESSES OF THIS WORK	260
4.4	THE COURSE OF FUTURE WORK	261

		Page
APPENDIX 1.	The Fundamental Electrochemistry	262
APPENDIX 2.	The Computer Programs and Potential Models	292
APPENDIX 3.	The Composition Data and Kinetic Results	316
APPENDIX 4.	The Minitab Regression Outputs for the Hydrogen Peroxide and Peroxymonosulphuric Acid Systems	329
ACKNOWLEDGEMENTS		352
REFERENCES		354

LIST OF FIGURES

No.	Title	Page
1.	The structure of uranium dioxide.	
	(a) The fluorite structure	33
	(b) The uranium and oxygen sublattices.	34
2.	A schematic diagram of the leaching apparatus.	77
3.	A schematic distram of the electrochemical cell.	81
4.	A block and schematic diagram of the electrochemical system.	82
5.	A schematic diagram of a UO_2 electrode.	88
6.	A schematic diagram of the carbon paste electrode holder.	89
7.	A summary of the electrolytic experiments carried out in this project.	97
8.	Cyclic voltammograms with varying anodic limits at pH 1.5 (this work).	121
9.	Cyclic voltammograms with varying anodic and cathodic limits at pH 9.2 (this work).	122
10.	A comparison of cyclic voltammograms from this work (a) and Sunder et al.[45] (b).	123 & 124
11.	A comparison of cyclic voltammograms at different pHs (this work).	130

LIST OF FIGURES (continued)

No.	Title	Page
12.	A comparison of anodic oxidation areas found by cyclic voltammograms at different pHs (this work and Sunder et al.[44,45,47,49]).	131
13.	A comparison of cyclic voltammograms obtained using different uranium oxides in carbon paste electrodes (this work).	132
14.	Single cyclic voltammograms obtained using U_2O_5 in carbon paste electrodes (this work).	135
15.	Single voltammogram obtained using U_3O_7 in carbon paste electrodes (this work).	136
16.	A comparison of the oxidation areas shown in Figures 13, 14 and 15.	137
17.	A single cyclic voltammogram obtained using $UO_4.4H_2O$ in a carbon paste electrode (this work).	138
18.	Cathodic stripping voltammograms at various potentials as shown (this work).	142-146
19.	Extracts of the Minitab multilinear regression output	
	(a) The peroxymonosulphuric acid system	202
	(b) The hydrogen peroxide system.	203

LIST OF FIGURES (continued)

No.	Title	Page
A1.	The differences of polarity in the electrochemical and electrolytic systems.	265
A2.	A comparison of reversible and irreversible reactions.	268
A3.	Current density overpotential curve for simple system, $\alpha = 0.5$, $n = 1$.	269
A4.	The effect of potential on the activation energy.	283
A5.	A cyclic voltammogram displaying double layer polarity inversion.	288
A6.	The computer programs used to calculate the compositions of the kinetic runs.	302
	(a) Peroxymonosulphuric acid (NUNA).	302
	(b) Hydrogen peroxide (NINA).	305
A7.	The computer program used to process the uranium concentration data from the kinetic runs (SARAH).	308
A8.	The Minitab regression output from which the hydrogen peroxide potential model was taken (MTX 2).	310
A9.	The Minitab regression output from which the peroxymonosulphuric acid potential model was taken (MTX 1).	313

LIST OF FIGURES (continued)

No.	Title	Page
A10.	The Minitab regression output for the kinetic analysis of the peroxymonosulphuric acid system.	330-340
A11.	The Minitab regression output for the kinetic analysis of the hydrogen peroxide system.	341-351

LIST OF PLATES

No.	Title	Page
1.	Unleached uranium dioxide spheres at various magnifications.	242-243
2.	Leached uranium dioxide spheres from run 212.	
3.	Leached uranium dioxide spheres from run 203.	
4.	Uranium dioxide electrodes under various conditions.	

LIST OF GRAPHS

No.	Title	Page
1.	The measured impedance of some uranium dioxide electrodes.	87
2.	The variation of cathodic charge with time measured at different potentials (this work).	161
3.	A comparison of the variation of the anodic and cathodic charges with time at E = 111 mV SHE.	162
4.	The Tafel plot for the anodic oxidation of UO_2	177
5.	The effect of pH on the oxidation of UO_2.	189
6.	The effect of sulphate on the oxidation of UO_2.	190
7.	The effect of hydrogen peroxide on the oxidation of UO_2.	191
8.	The effect of peroxymonosulphate on the oxidation of UO_2.	192
9.	A comparison of predicted and experimental rate constants for the peroxymonosulphuric acid system.	199
10.	A comparison of predicted and experimental rate constants for the hydrogen peroxide system.	200

LIST OF GRAPHS (continued)

No.		Title	Page
11.	(a)	The variation of the electrochemical contribution to the activation energy ($\Delta G^{\neq}_{e,cont}$) with potential.	212
	(b)	The variation of the activation energy at the potential of measurement ($\Delta G^{\neq}_{E=E}$) with potential.	213
12.		The potential imposed on a UO_2 surface by different oxidising agents.	238
13.		Comparison of steady state current and corrosion current data.	239
14.		The absolute leaching rate of UO_2 with different oxidising agents.	240

LIST OF TABLES

No.	Title	Page
1.	Lattice constants of some uranium oxides.	35
2.	Comparison of X.R.D. pattern data A.S.T.M. No. 31-1424 (U_3O_8) with the patterns of the product of the stoichiometry determination of the UO_2 used in the chemical kinetic runs and the UO_2 used in the electrode fabrication.	113
3.	Comparison of X.R.D. powder patterns of uranium oxides used in this work with various A.S.T.M. standards.	
	(a) Comparison of A.S.T.M. pattern 5-0550 (UO_2) with the pattern of the UO_2 (Koch-Light) that was used for synthesis and carbon paste electrodes. The pattern of the UO_2 used in the chemical runs is also given.	114
	(b) Comparison of A.S.T.M. pattern 24-1172 (U_3O_8) with the pattern of the U_3O_8 (Koch-Light) that was used for synthesis and carbon paste electrodes.	115
	(c) Comparison of A.S.T.M. pattern 15-4 (U_3O_7) with the pattern of the U_3O_7 synthesised and used in carbon paste electrodes.	116

LIST OF TABLES (continued)

No.	Title	Page
3.	(d) Comparison of A.S.T.M. pattern 32-1403 (U_2O_5) with the pattern of the U_2O_5 synthesised and used in carbon paste electrodes.	117
	(e) Comparison of A.S.T.M. pattern 16-207 ($UO_4.2H_2O$) and A.S.T.M. pattern 16-206 ($UO_4.4H_2O$) with the pattern of the $UO_4.2H_2O$ that was used for carbon paste electrodes.	118
4.	Resistivity data for six electrodes used in this project.	85
5.	Oxidation and reduction area analysis of the voltammograms that appear in Figure 8.	125
6.	Oxidation and reduction area analysis of the voltammograms that appear in Figure 9.	126
7.	A summary of the cathodically stripped intermediates from the voltammograms that appear in Figure 18.	147
8.	A summary of the characterised structures of some known uranium oxides in the stoichiometric range UO_2 to UO_3.	152
9.	An analysis of system structures after Jones[91]	153
10.	The cathodic and anodic charge data from the cathodic stripping voltammetry (this work).	158

LIST OF TABLES (continued)

No.	Title	Page
11.	Film thicknesses of proposed intermediates (calculated with molecular formulae) at different potentials.	159
12.	Film thicknesses and partial charges for proposed intermediates (calculated using empirical formulae) at different potentials.	160
13.	The steady-state current and potential data for the anodic oxidation of UO_2.	174
14.	The calculated anodic transfer coefficients for reaction steps in the proposed mechanism.	175
15.	The results from the experimental Tafel slope analysis.	176
16.	The steady-state current and potential data for the reaction order determinations.	
	(a) The effect of pH on the UO_2 to UO_2^{2+} half cell reaction, [TS] = 1 M.	187
	(b) The effect of sulphate on the UO_2 to UO_2^{2+} half cell reaction, pH = 1.5.	187
	(c) The effect of hydrogen peroxide on the UO_2 to UO_2^{2+} half cell reaction pH = 1.5, [TS] = 1 M.	188
	(d) The effect of peroxymonosulphuric acid on the UO_2 to UO_2^{2+} half cell reaction, pH = 1.5, [TS] = 1 M.	188

LIST OF TABLES (continued)

No.	Title	Page
17.	Experimental rate constants and theoretical mass transfer coefficients for the hydrogen peroxide and peroxymonosulphuric acid systems.	198
18.	An analysis of the results of the multilinear regression analysis of the kinetic runs containing peroxymonosulphuric acid and hydrogen peroxide respectively.	214 & 215
19.	The corrosion potential and rate data for both systems at T = 30°C	234
	(a) Hydrogen peroxide system	234
	(b) Peroxymonosulphuric acid system	235
20.	Comparisons of the absolute leaching rates of UO_2 with different oxidising agents.	236
A1.	The kinetic and initial composition data for all peroxymonosulphuric acid runs.	319-321
A2.	The composition data for all the peroxymonosulphuric acid runs from Table A1 used in the multilinear regression analysis.	322-323
A3.	The kinetic and initial composition data for all hydrogen peroxide runs.	325-326
A4.	The composition data for all the hydrogen peroxide runs from Table A3 used in the multilinear regression analysis.	327-328

GLOSSARY

(i) Roman Symbols

A	Area (cm^2)
A	constant [Arrhenius equation]
a	The number of electrons transferred in the rate determining step [Butler-Volmer equation]
C_{Ab}	The concentration of A in the bulk of the solution (mols cm^{-3})
C_{As}	The concentration of A at the electrode surface (mols cm^{-3})
C_d	The capacitance of a capacitor (Farads)
D_1	Impeller diameter (in) [Harriot correlations]
D	Diffusion coefficient ($cm^2 sec^{-1}$)
d	Particle diameter (cms)
d	Thickness of a solid layer (cms)
E	Potential (mV or V as specified)
E_c	Corrosion potential (mV)
E^o	The standard potential of a half cell reaction (mV or V as specified)
F	The Faraday constant (9.6786×10^4 (mol^{-1}))
$\Delta G_{e,cont.}$	The electrochemical contribution to the activation energy (kJ mol^{-1})
$\Delta G_{E=E}$	The measured activation energy at E=E (kJ mol^{-1})
$\Delta G_{o,c}$	The electrochemical activation energy at E=0 on the scale of use, also termed the absolute chemical activation energy (kJ mol^{-1})

ΔG^{o}	The standard Gibb's free energy for a specified process
g	Gravitational acceleration (cm sec^{2}) [Harriot correlations]
I	Agitation intensity ($in^{\frac{2}{3}}$, min^{-1}) [Harriot correlations]
I	Current (μA or as specified)
$\varphi = i$	Current density (μA cm^{-2})
φ_{o}	Exchange current density
I_{TOT}	Total ionic strength (also μ)
K_{12}	First dissociation constant of sulphuric acid ($H_2SO_4 \longrightarrow HSO_4^- + H^+$)
K_1	Second dissociation constant of sulphuric acid ($HSO_4^- \longrightarrow SO_4^{2-} + H^+$)
$K_1 \ldots K_n$	Equilibrium constants for reactions 1 to n
k	Minimum mass transfer coefficient (cm sec^{-1}) [Harriot correlations]
k_{200}	The standard mass transfer coefficient (cm sec^{-1}) [Harriot correlations]
k'	Rate constant (cm sec^{-1})
k_o	Concentration of potentially reactive sites (cm^{-2})
k_f	The forward (cathodic) rate constant (cm sec^{-1})
k_b	The backward (anodic) rate constant (cm sec^{-1})
k_f^{o}	The forward (cathodic) rate constant at E=0 on the scale of use (cm sec^{-1})
k_b^{o}	The backward (anodic) rate constant at E=0 on the scale of use (cm sec^{-1})

k^o	The standard or intrinsic rate constant (cm sec^{-1}). The value of k_f^o and k_b^o at E^o.
k_L	The linear rate constant ($cm^4 mol^{-1} sec^{-1}$)
k_M	The mass transfer coefficient (cm sec^{-1})
L	The length of material through which a current is forced [resistivity measurements]
M	Molar (mols $litre^{-1}$)
M	Molecular mass (AMU)
M	number of moles of substance (mols)
N	Stirrer speed (rpm) [Harriot correlations]
n	Total number of electrons transferred in the overall process
n_A	Flux of A [mass transfer]
Q	Dray coefficient [Harriot correlations]
Q_A	The anodic charge (C or μC as specified)
Q_C	The cathodic charge (C or μC as specified)
q	The charge on one plate of a capacitor (C)
R	The universal gas constant (8.314 J k^{-1} mol^{-1})
$R_{T=T}$	Resistance at specified temperature T=T (Ω or kΩ as specified)
R_e	The Reynolds number = vd/ν Harriot correlations
r	An arbitrary factor, the value of which is dependent on the mechanism of a process [Butler-Volmer equation]
r_o	The initial radius of a particle (cms)
S	The cross-sectional area (cm^{-2}) [Resistance measurements]

Sc	The Schmidt number = $\frac{D}{\nu}$ [Harriot correlations]
Sh	The Sherwood number $\frac{k^{+}d}{D}$ [Harriot correlations]
T	Tank diameter (ins) [Harriot correlations]
T	Absolute temperature (K)
t	Time (seconds or minutes as specified)
U_o	Free stream velocity [mass transfer]
V	The absolute reaction rate = $\frac{dn}{dt}$ (moles cm^{-2} sec^{-1})
V	Particle molar volume (cm^3 mol^{-1}) = $\frac{M}{\rho}$
v	Velocity (cm sec^{-1}) [Harriot correlations]
x	The order of reaction with respect to species x
y	The order of reaction with respect to species y
Z	Suspension depth (in) [Harriot correlation]

(ii) Greek Symbols

α	The proportion of the mineral initially added that has dissolved
$\overleftarrow{\alpha}$	The anodic transfer coefficient
$\vec{\alpha}$	The cathodic transfer coefficient
	In simple systems it is often assumed that $\overleftarrow{\alpha} = \vec{\alpha} = \beta$. In this case the transfer coefficient is often represented by α.
β	The symmetry factor
γ_{H^+}	The activity coefficient of hydrogen ion in the sulphate system at specified total ionic strength and pH.
δ	The thickness of the diffusion layer (cm)
η	The overpotential (mV)

θ	Surface coverage at E=E
θ_e	Surface coverage at $E=E^o$
μ	Total ionic strength (molar) also I_{TOT}.
ν	The number of times the rate determining step must occur in a reaction cycle
ν	Kinematic viscosity ($cm^2\ sec^{-1}$)
ρ	Density ($g\ cm^{-3}$)
$\rho_{T=T}$	Resistivity at ambient temperature
σ	Roughness factor
σ	Stoichiometry factor
$\vec{\phi}$	The number of electrons transferred before the rate determining step
$\overleftarrow{\phi}$	The number of electrons transferred after the rate determining step
Φ_e	The potential drop across the solid solution interface (V or mV as specified)
χ	Distance from the leading edge of solid (diffusion layer studies)

SECTION 1

INTRODUCTION

The uses of uranium, unlike many other commodities, are strictly limited. The two principle uses are for power generation, and for military application. In the past (1942-1974) the world's military requirements amounted to approximately 50% of the cumulative world output for that period[18]. Such requirements, however, now do not play such a major part, and power generation currently accounts for approximately 95% of uranium production.

Unlike many other commodities, uranium cannot be easily replaced by other substances. This means that until fusion power becomes a commercially viable process (estimated at 2040 A.D.) there will be a steady demand for uranium. At the present time production of uranium exceeds demand by approximately 15%. This results in low uranium prices in the world markets. This low price, along with normal commercial pressure has prompted many producers to search for ways to exploit the vast reserves of low grade ore, and also to make their present operations more economic. Some of the practical results of this drive for economy are the virtual demise of the higher cost carbonate leach process, and the growth of the in situ and microbiological mining operations.

The major ore minerals for uranium are the simple oxides. As these oxides contain both uranium IV and

uranium VI, only the latter of which is soluble in aqueous systems, any uranium IV present must be oxidized to uranium VI. This is usually accomplished by the addition of oxidizing agents, e.g. pyrolusite (MnO_2) or sodium chlorate. These oxidizing agents maintain the iron in solution in the III oxidation state, which then itself oxidizes the uranium IV. Recent work[33,34] however, has indicated that hydrogen peroxide and Caro's acid (peroxymonosulphuric acid) may be more economic oxidizing agents for some ores. It has also been found that both these oxidizing agents are able to efficiently oxidize UO_2 without the presence of iron, and do not share the environmental problems of other oxidizing agents. It is known that the oxidation of UO_2 at low pH is an electrochemical process. Although much is known about it, the process is still not fully understood.

The purposes of this project are:

(a) to investigate the anodic oxidation of uranium dioxide

(b) to investigate the behaviour of hydrogen peroxide and peroxymonosulphuric acid as a part of that reaction system

(c) to draw mechanistic conclusions from these investigations.

1.1. HETEROGENEOUS SYSTEMS

In a heterogeneous reaction system, any reaction taking place between the two phases must take place at their interface. There are a number of stages in any heterogeneous reaction[1].

a) Mass transfer of reactants and products between the solid and liquid phases.

b) Chemical reaction between adsorbed species and/or the solid surface itself.

The slowest step will determine the overall rate of reaction and is termed the rate determining step. It should be noted[2] that the rate determining step can change depending on reaction conditions. Furthermore, frequently there may not be a single rate determining step because several steps may have approximately equal effects in determining the rate. The relative importance of these steps may change in the course of the reaction. It is therefore important to understand how each individual step interacts as part of the whole mechanism.

a) Mass Transfer Controlled Reactions

In a stirred system only 3 regions can be deemed to exist. The solid surface, the bulk liquid phase, and between these the static 'diffusion' layer. This diffusion layer has concentration gradients of all reactants and products which are diffusing. These concentration gradients are normally assumed to be linear (the Nernst-Merriam

approximation). Levitch[3] devised an equation for the calculation of the thickness of the diffusion layer (δ)

$$\delta = D^{\frac{1}{3}} v^{1/6} \sqrt{X/U_o} \qquad (1)$$

where δ = thickness of the diffusion layer

v = viscosity

U_o = free stream velocity

X = distance from leading edge of solid

D = diffusion coefficient

It can be seen from the equation that stirring speed (related to U_o) affects δ, and therefore will affect the rate of mass transfer. It should however be noted, that even if stirring speed is increased to the point that the rate of reaction remains constant, this simply means that the diffusion layer (δ) is at a minimum thickness, and mass transfer may still be rate limiting. In the absence of other forces, diffusion to the interface is controlled by Fick's law of diffusion, when A is the species diffusing.

$$n_A = K_m (C_{Ab} - C_{As}) \qquad (2)$$

where: n_A = flux of A

C_{Ab} = concentration of A in the bulk of the solution

C_{As} = concentration of A at the solid surface

K_m = mass transfer coefficient (cm sec^{-2})

Obviously, the rate of mass transfer is at a maximum when $C_{As} = 0$, i.e. the diffusing species reacts as soon as it arrives at the interface. If this were the case the reaction

is said to be mass transfer controlled with respect to A. The mass transfer coefficient (K_m) can be viewed as the 'rate constant' for the diffusion of a specific species. Although it can be calculated for certain very well defined cases, it is usually estimated from empirical correlations involving the Sherwood number as a function of the Reynolds and Schmidt numbers. In this work the suspended particle correlations by Harriot[4] were used. The mass transfer coefficient can then be compared to the experimentally determined rate constants, to determine whether mass transport of species A is rate controlling. Typical activation energies for mass transfer controlled reactions are 10-30 KJ mol^{-1}.[5]

b) Chemically controlled reactions

A reaction which is not mass transfer controlled is chemically controlled. Chemically controlled reactions consist broadly of 3 stages:

(a) adsorption of reactants

(b) reaction on the surface

(c) desorbtion of soluble products

Adsorption of reactants is usually rapid, very often with a slow surface reaction. Many surface reactions have been found to be electrochemical in nature, thus by manipulation of the potential, different steps may become rate limiting. In some reactions where the products are not soluble, a product layer can build up. Frequently in these cases although initially the reaction is surface controlled, eventually diffusion through this product layer becomes

rate controlling. Typical activation energies for chemically controlled reactions are 45-100 KJ mol^{-1}.[6]

1.2. LEACHING MODELS

Although leaching models were not extensively used in this work, correlation to a leaching model can be indicative of mechanistic processes. There are many leaching models in the literature. Wadsworth[2] presents a concise summary and derivations of the more applicable models. No attempt to derive any of these models will be carried out here. Interested readers are referred to reference 2. By necessity, a leaching model contains many assumptions, and often as a consequence is of little value when applied to real systems. Usually the most uncertain assumptions concern particle size distribution, uniformity of particle shape and the agitation conditions.

In this work, however, almost monosize spheroidal particles were employed, thus giving greater validity to some of the underlying assumptions. Because of this, a few models were investigated.

The models were:

(a) a shrinking particle model where the kinetics are controlled by the surface area available for reaction and dissolution occurs by a uniform removal of material from a symmetric particle.

The model is expressed mathematically as:

$$1 - (1 - \alpha)^{-\frac{1}{3}} = kt \qquad (3)$$

where:

$$k = \frac{k_L[C]^x}{r_o} \qquad (4)$$

k_L = the linear rate constant ($cm^4 mol^{-1} sec^{-1}$)

$k_L = Vk_o k'$ for chemical control

$k_L = \frac{VD}{\delta\sigma}$ for diffusion control

V = the particle molar volume ($cm^3 mole^{-1}$)

r_o = initial particle radius (cm)

k' = rate constant ($cm^3 sec^{-1}$)

k_o = the concentration of potentially reactive sites (cm^{-2})

t = time (secs)

α = the fraction of the mineral dissolved

σ = a stoichiometry factor which represents the number of mols of the diffusing species required for each mol of metal value released by the reaction.

(b) A shrinking particle model (as above) but as the dissolution proceeds a product layer forms. Diffusion through this product layer of both reactants and products is rate determining. The model is expressed mathematically as:

$$1 - \tfrac{2}{3}\alpha - (1 - \alpha)^{\frac{2}{3}} = \frac{2VD}{\sigma r_o^2} \cdot [C]^x.t \qquad (5)$$

A combination of these two models gives a new model applicable to cases where the product film is itself dissolving. Model (a) was found to give a satisfactory

fit to experimental results, therefore no other models were investigated.

1.3. URANIUM OXIDES

Like many uranium compounds, the uranium oxides are all to some extent stoichiometrically variable. A practical consequence of this is the existence of 48 cards in the A.S.T.M. card index of X-ray diffraction patterns for UO_2 to UO_3 compounds. Although exact empirical formulae can be misleading, the range of uranium oxides is not a continuous series. There are discrete crystal structures, and individual oxides can be identified. Sometimes, however, quite where the boundaries between them lie would seem to be a moot point.

Range $UO_{1.75}$ - $UO_{2.30}$

All the compounds in this range have a fluorite structure. See Figure 1. The suggestion[9] that the uranium sublattice develops vacancies to accommodate the extra oxygen (above UO_2) was dismissed when theoretical and X-ray density data showed no substantial amount of uranium was missing from the lattice. It now seems that the extra oxygen occupies interstitial positions in the lattice[24], hence these initial oxidation reactions are fairly reversible.

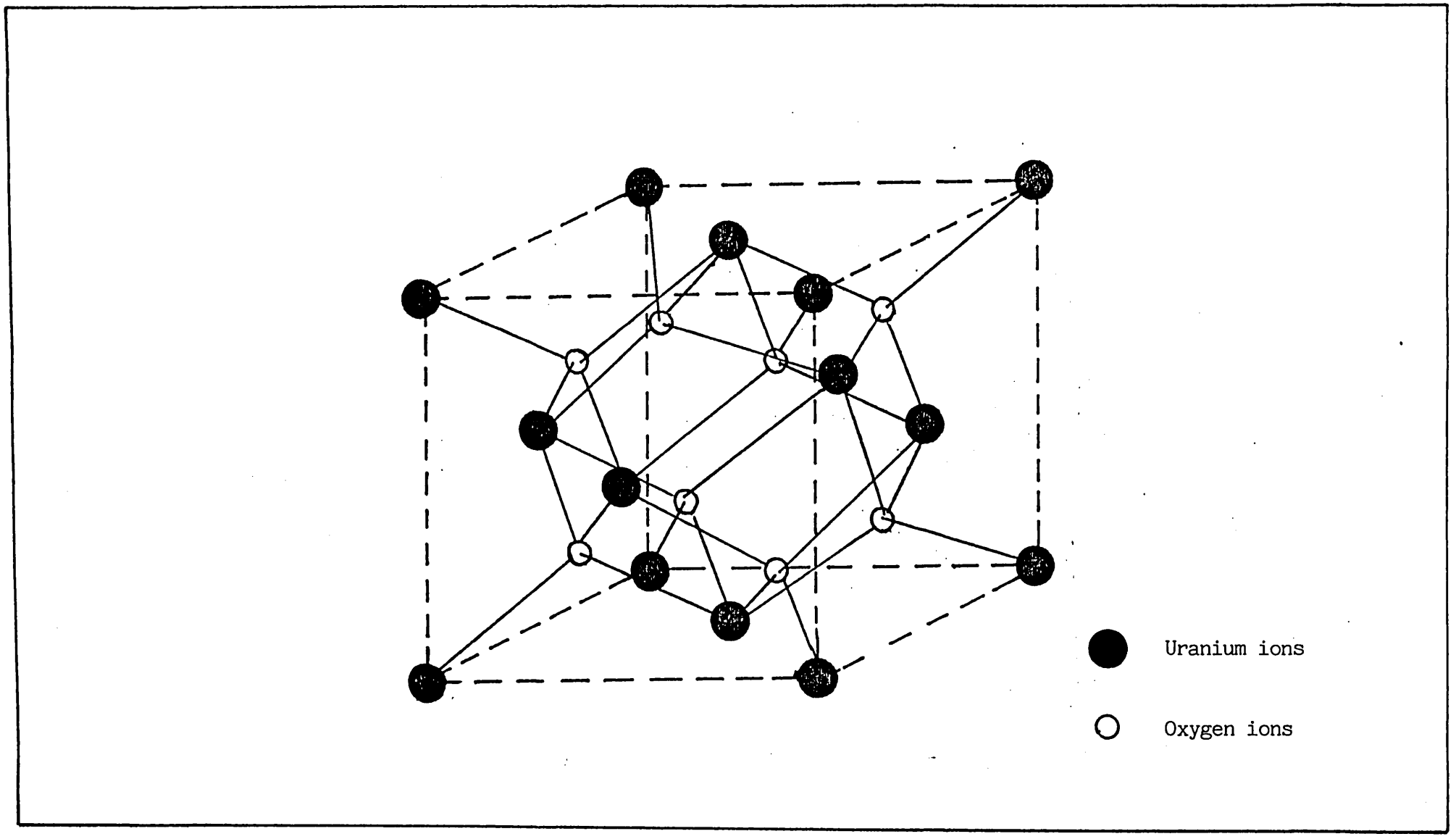
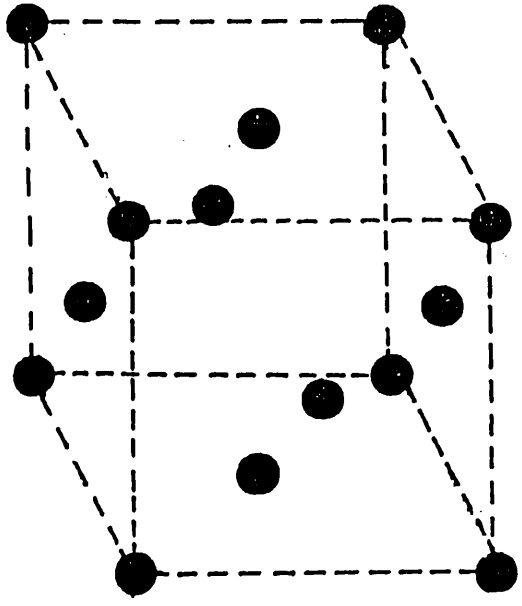


FIG. 1(a). The fluorite structure.

(i) The Uranium Sublattice



(ii) The Oxygen Sublattice

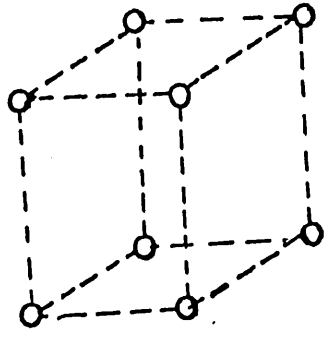


FIG. 1(b). The uranium and oxygen sublattices.

$UO_{1.75}$ or U_4O_7

This homogeneous face centred cubic phase has a lattice constant of 5.477 Å and was first detected by Zachariasen[8]. However, the fact that similar phases have been observed before in monophasic regions and the uniform change in lattice constants between different oxides, (see Table 1), allows the possibility that U_4O_7 could be the lower limit of the range of solid solutions known as "UO_2".

TABLE 1: Lattice constants of some uranium oxides

Oxide	Lattice constant a_o (Å)
$UO_{1.75}$ (U_4O_7)	5.477
$UO_{2.00}$	5.460
$UO_{2.25}$ (U_4O_9)	5.441
$UO_{2.30}$ (U_3O_7)	5.430

It should be noted that lattice constants of uranium oxides depend very much on the history, preparation and composition of the sample. Variations between apparently identical samples can be as high as $\pm$0.005 Å.

$UO_{2.00}$

Like U_4O_7, UO_2 has a fluorite structure with a face centred cubic lattice. Many estimates of lattice parameters

have been made[9,10,11,12,13], probably the most reliable of which is a_0 = 5.4581 Å after Rundle et al.[7] Swanson et al.[19] report a_0 = 5.4682 Å, and this value appears in the A.S.T.M. collection. The discrepancy between these data reflect the difficulty in comparing oxide samples with widely different histories.

$UO_{2.25}$ or U_4O_9

Like the other oxides in this group U_4O_9 has a cubic structure with a lattice constant determined as a_0 = 5.441 Å,[22] and a_0 = 5.440 Å.[23] The agreement between these two figures is remarkable. Rundle et al.[9] report the lattice constant of UO_2 to be a_0 = 5.4719 Å, decreasing to a_0 = 5.4406 Å with increasing oxygen content. This suggests that U_4O_9 is simply another oxygen rich UO_2. However, recent work by Paquette et al.[24] has shown U_4O_9 to be the thermodynamically stable phase ($0.3 < E < 0.5$ V SCE) at 100°C and pH ~1.5.

$UO_{2.30}$ or U_3O_7

Two sets of workers[14,15] independently studying the low temperature oxidation of UO_2 discovered this blueish/black phase which had a crystal structure similar to UO_2, but was less symmetric. The lattice constant (a_o) was determined as 5.40 Å. It has been suggested[7] that U_3O_7 is the oxygen saturated limit of the range of solid solutions known as "UO_2". Blitz et al.[16] showed that oxygen

adsorbed above $UO_{2.15}$ could be driven off under conditions of high temperature and vacuum. The same authors also showed the long term stability of U_3O_7 under normal atmospheric conditions.

Range $UO_{2.30}$ - $UO_{3.0}$

Transition between different oxides in this range comes about, unlike before, with major changes in the uranium sublattice. In the UO_2 range of compounds the uranium sublattice is cubic. In UO_3 it is hexagonal. The transition between the two is via various orthorhombic compounds, e.g. U_2O_5 and U_3O_8. The transition between U_3O_8 and higher oxides is a continuous one.

$UO_{2.50}$ or U_2O_5

This phase was first prepared by Rundle et al.,[9] and his data appears in the A.S.T.M. index. This orthorhombic oxide has lattice parameters a_o = 8.29 Å, b_o = 31.71 Å and c_o = 6.73 Å. There are 16 molecules of U_2O_5 per unit cell. U_2O_5 is only stable under atmospheric conditions below 270°C.[15] At 900°C it slowly takes up oxygen and becomes U_3O_8.[9] A monoclinic U_2O_5 has been synthesised,[20] as well as two hexagonal forms,[20,21] but it seems that the orthorhombic form is the most stable under ambient temperature. When hydrated this oxide is orthorhombic.[20]

$UO_{2.67}$ or (U_3O_8)

There are 7 cards in the A.S.T.M. index for this oxide. At temperatures less than 400°C it is an orthorhombic compound. The lattice parameters of this oxide are: $a_o = 6.70 \pm 0.02$ Å, $b_o = 11.94 \pm 0.03$ Å, $c_o = 4.14 \pm 0.01$ Å. The unit cell contains two U_3O_8 molecules. U_3O_8 has a wide range of compositions from $UO_{2.92}$ down to possibly $UO_{2.50}$.[9,16,7] This is the reason for the apparent lack of precision in the lattice parameters.

UO_3

The crystal structure of UO_3 is very dependent on the method of preparation and many UO_3 structures are not part of the U_3O_8 to UO_3 progression.[13] Many UO_3 samples are amorphous to X-rays and many are uncharacterized. Colours range from yellow to red and structures include: monoclinic, tetragonal, orthorhombic and hexagonal. Typical hexagonal lattice parameters are: $a_o = 3.963$ Å, $b_o = 4.160$ Å, $c_o = 4.160$ Å. Hydrated forms tend to be orthorhombic. Typical parameters are: $a_o = 14.3$ Å, $b_o = 16.8$ Å, $c_o = 14.7$ Å.

1.4. THE SULPHATE/BISULPHATE EQUILIBRIUM

In any kinetic study the concentrations of the species present must be known, or be amenable to estimation. The present study is in a pH range in which the sulphate/bisulphate equilibrium is incomplete. It is therefore necessary to have reliable information on the values of the appropriate dissociation constants under different conditions of temperature and ionic strength. Sulphuric acid dissociates as follows:

$$H_2SO_4 \underset{K_{12}}{\rightleftharpoons} H^+ + HSO_4^- \qquad (6)$$

$$HSO_4^- \underset{K_1}{\rightleftharpoons} H^+ + SO_4^{2-} \qquad (7)$$

The first dissociation of sulphuric acid is virtually complete at sulphuric acid concentrations below 11 M. Values of the second dissociation constant (K_1) have been the subject of many studies. The result is a plethora of empirical and semi-empirical equations over different ranges of temperature (T) and ionic strength (μ). Most of these works are the subject of an excellent review by Dias[25], and only the most pertinent will be discussed here. For the purposes of this work, concentrations of sulphate and bisulphate must be estimated in an acid system ($0.5 \leq pH \leq 2.5$) in the presence of sodium and/or potassium ions, up to total ionic strengths of $\sim$4.

Baes[26] noted that $\gamma_{\pm}^{3}$ in both pure sulphuric acid solutions and in pure sodium sulphate solutions varied in much the same way with ionic strength (μ). They present an empirical equation for the second dissociation constant (K_1) in terms of total ionic strength (μ) at 25°C:

$$\log K_1 = \log 0.0102 + \frac{2.036\sqrt{\mu}}{1 + 0.4\sqrt{\mu}} \qquad (8)$$

μ is on the molal scale.

This work is based on the assumption that $\gamma_{\pm}^{3}$ varies in the same way with total ionic strength (μ) in sulphuric acid and sodium sulphate solutions. Unfortunately, this assumption becomes untenable at a total ionic strength of ~1.4 (molal scale).

Lindstrom and Wirth[27] studied the dissociation constant (K_1) in sulphuric acid and sodium bisulphate solutions at 25°C and ionic strengths (μ) up to 4.0 on the molar scale. Their results are represented by the empirical equations:

In sulphuric acid solutions:

$$\log K_1 = \log 0.0102 + 2.036\mu^{\frac{1}{2}} - 1.376\mu + 0.8862\mu^{3/2} - 0.217\mu^2 \qquad (9)$$

In sodium bisulphate solutions:

$$\log K_1 = \log 0.0102 + 2.036\mu^{\frac{1}{2}} - 1.543\mu + 0.8297\mu^{3/2} - 0.1703\mu^2 \qquad (10)$$

where μ is on the molar scale.

Lindstrom and Wirth[27] used the observed mean apparent molar volumes of sulphuric acid and sodium bisulphate to obtain estimates of the dissociation constant (K_1). They assumed that the apparent molar volumes of different electrolytes are additive over the range of their study. Young et al.[29] in work on the thermodynamics of mixing show that this assumption is valid.

The most extensive study on the effect of ionic strength (μ) and temperature (T) on the dissociation constant (K_1) in sulphuric acid is that of Marshall and Jones.[28] The range of temperature studied was 25-350°C, at molalities between 0 and 1.0 m (4.8 m below 50°C).

Their results are represented by the semi-empirical equation:

$$\log K_1 = \log K_1^{\circ} = \frac{4S\sqrt{\mu}}{1 + A_k\sqrt{\mu}} \qquad (11)$$

where S is the solubility of $CaSO_4$ at temperature = T (corrected for the use of molal units)

A_k is a parameter that changes with temperature.

K_1° is the thermodynamic equilibrium constant, (i.e. the value of K_1 when $\mu = 0$)

They also propose an empirical equation for the value of the thermodynamic equilibrium constant (K_1) over the temperature range (25 - 350°C).

The equation was:

$$\log K_1^{o} = 56.889 - 19.8858 \log T - \frac{2307.9}{T} - 0.006473T \qquad (12)$$

The temperature (T) is expressed in Kelvin.

Unlike the other works mentioned above, this work is less empirical and attempts are made to correlate terms in the derived equation (11) with terms from the Debye-Huckel equations. In more recent works on activity coefficients in sulphuric acid and sulphate solutions, Majima et al.[30] calculate the concentrations of sulphate and bisulphate by using the correlations of Baes.[26]

1.5. PREVIOUS WORK

1.5.1. The Anodic Reaction

Habashi et al.[35] studied the dissolution of UO_2 in both sulphuric acid and sodium carbonate environments. In the carbonate system their results indicated a reaction order of 0.5 with respect to oxygen pressure, when the carbonate concentration was greater than ~0.1 M, below which the rate was dependent on carbonate concentration. In the sulphuric acid system they concluded that the rate was dependent on H_2SO_4 up to about 0.0025 M H_2SO_4. Above this it was dependent on the pressure of oxygen. They state the reaction is electrochemical in nature. They propose a mechanism and by applying previous work by Habashi on corrosion,[36] present theoretical rate equations. The rate equations and proposed mechanism are presented below:

$$\text{rate} = \frac{k_1 k_2 A P_{O_2}^{\frac{1}{2}} [H^+]}{k_1 P_{O_2} + k_2 [H^+]} \quad (13)$$

$$\text{rate} = \frac{k_1' k_2' A P_{O_2} [CO_3^{2-}]}{k_1' P_{O_2}^{\frac{1}{2}} + k_2' [CO_3^{2-}]} \quad (14)$$

where:

$k_1 k_2 k_1' k_2'$ = rate constants

$[H^+]$ = concentration of hydrogen ions

$[CO_3]$ = concentration of carbonate ions

P_{O_2} = partial pressure of oxygen

A = surface area of oxide in contact with aqueous phase

Cathodic reaction

$$O_2 + 2H_2O + 4e^- \longrightarrow 4OH^- \quad (15)$$

or

$$O_2 + 2H_2O + 2e^- \longrightarrow 2OH^- + H_2O_2 \quad (16)$$

Anodic reaction

oxidation

$$UO_2 \longrightarrow UO_2^{2+} + 2e^- \quad (17)$$

dissolution

$$2UO_2^{2+} + 2H_2O \longrightarrow [UO_2(OH)_2UO_2]^{2+} + 2H^+ \quad (18)$$

$$[UO_2(OH)_2UO_2]^{2+} + H_2O \longrightarrow [UO_2(OH)_2UO_2]OH^+ + H^+ \quad (19)$$

$$[UO_2(OH)_2UO_2]OH^+ + H_2O \longrightarrow HO[UO_2(OH)_2UO_2]OH + H^+ \quad (20)$$

In neutral solutions $UO_2(OH)_2$ is insoluble.

In carbonate solutions $UO_2(OH)_2 + 3CO_3^{2-} \longrightarrow [UO_2(CO_3)_3]^{4-} + 2OH^-$ (21)

In acid solutions $UO_2(OH)_2 + 2H^+ \longrightarrow UO_2^{2+} + 2H_2O$ (22)

They propose that the oxidation reaction is a two electron transfer process in all cases and the differences in rate dependencies are due to the dissolution reaction. Using their own results however, in the sulphuric acid system an order of ~ 1 with respect to P_{O_2} can be calculated. This difference in orders between the acid and alkali systems cannot be explained by the dissolution mechanism proposed but rather by a change in the oxidation reaction mechanism.

Nicol et al.[38] studied the anodic dissolution of UO_2 in carbonate, perchlorate and sulphuric acid media. They propose a simplified mechanism for the acid dissolution of UO_2 as below:

$$UO_2 + H_2O \rightleftharpoons UO_2OH + H^+ + e^- \quad (23)$$

$$UO_2OH \longrightarrow UO_3 + H^+ + e^- \quad (24)$$

$$UO_3 + 2H^+ \longrightarrow UO_2^{2+} + H_2O \quad (25)$$

$$UO_2OH \rightleftharpoons UO_3^- + H^+ \quad (26)$$

Reaction (26) is only noticeable between pH 3-5. They suggest the transformation of an insoluble film of uranium VI oxides to soluble products to be rate limiting. They also suggest this film is multilayered in structure

possibly containing other uranium oxides e.g. U_4O_9, U_3O_7, U_3O_8... with UO_3 as the surface species. They note similarities between UO_3 and UO_2 dissolution. They prove that no soluble uranium V products are formed and establish the stoichiometry of the reaction. They explain various anion and cation effects as the results of specific adsorption and Helmholtz effects. Cyclic voltammograms show at least four reaction intermediates indicating a complex mechanism. They detected two steady-state Tafel regions. The magnitude of the least oxidizing potential Tafel region ($595\ mV \leq E \leq 670\ mV$ SHE) was pH dependent ($dE/d\ln i \simeq 35$ to 40 mV decade^{-1} at pH $\sim$1.5). The more oxidizing potential Tafel region ($850\ mV \leq E \leq 1050\ mV$ SHE) was not pH dependent ($dE/d\ln i \simeq 140$ to 160 mV decade^{-1}). There are two major problems with the low pH section of this work. The first is that the proposed mechanism predicts a Tafel slope of approximately 120 mV decade^{-1} for the second Tafel region, and the second is that the proposed mechanism would produce simple cyclic voltammograms which is not the case.

In further works on the acid system,[41,39] Nicol and Needes confine themselves to restating the data and conclusions already arrived at in the earlier report.[38] They do however, expand their explanation of the effect of sulphate on the rate of reaction. Whereas previously[38] they explained the retarding effect of sulphate under acid conditions ($0 \leq pH \leq 3$) as a function of the specific adsorption of sulphate, they now propose that in addition to this,

sulphate is also involved as a complexing agent in both the anodic dissolution and cathodic charge transfer stages.

In their work on the carbonate system,[38] Nicol and Needes propose two simplified alternative, but kinetically identical mechanisms for UO_2 dissolution:

$$UO_2 + HCO_3^- \longrightarrow UO_2HCO_3 + e^- \quad (27)$$

$$UO_2HCO_3 + OH^- \longrightarrow UO_2CO_3 + H_2O + e^- \quad (28)$$

$$UO_2CO_3 + 2CO_3^{--} \longrightarrow UO_2(CO_3)_3^{4-} \quad (29)$$

or

$$UO_2 + OH^- \longrightarrow UO_2OH + e^- \quad (30)$$

$$UO_2OH + HCO_3^- \longrightarrow UO_2CO_3 + H_2O + e^- \quad (31)$$

$$UO_2CO_3 + 2CO_3^{2-} \longrightarrow UO_2(CO_3)_3^{4-} \quad (32)$$

Cyclic voltammograms presented in this work are complex and again indicate a complex mechanism. They detected one steady-state Tafel region, the magnitude of which was pH dependent (dE/dlni = 70 to 80 mV decade^{-1} at pH = 10). Complex dependencies of the rate on both pH and sulphate concentrations were also found. There are two major problems with the high pH region of this work. The first is that the proposed mechanism predicts a Tafel slope of 120 mV decade^{-1}, the second is that the proposed mechanism would produce simple cyclic voltammograms which is not the case. There is one other internal inconsistency in this work. Nicol and Needes state clearly (and incorrectly) that the number of steady state regions indicates the number

of electron transfers. If this were the case, on the basis of their proposed mechanism one would expect two steady state regions. This will be pursued further, below.

In further work on the alkali system[40,42] Nicol and Needes attempt to clarify the anomalous conclusions reached in the first report about the rate determining step. In this work a two electron transfer process with a subsequent dissolution is proposed.

$$UO_2 + CO_3^{2-} \rightleftharpoons UO_2CO_3 + 2e^- \qquad (33)$$

$$UO_2CO_3 + 2CO_3^{2-} \longrightarrow UO_2(CO_3)_3^{4-} \qquad (34)$$

The dependence of rate on pH as well as carbonate concentration is explained in terms of the effect of pH on the concentration of carbonate present.

$$HCO_3 \rightleftharpoons CO_3 + H^+ \qquad pK_a = 9.5 \qquad (35)$$

Unfortunately, this now leaves the rather complex cyclic voltammograms unexplained. A mechanism involving a $2e^-$ transfer process but also many intermediate oxide species may be appropriate. Nicol and Needes conclude that there is a change in the oxidation mechanism, from low to high pH. The results of Habashi et al.[35] can be made to show similar changes in the oxidation reaction. The conclusion of Nicol and Needes concerning the presence of a film of uranium VI oxide/hydroxide, and the theory that at longer

times the dissolution of the surface film may become rate limiting bears a strong resemblance to work by Habashi et al.[35] Information presented by Sipos et al.[37] on the redox reactions of some uranium species confirms the information presented by Nicol and Needes in their cyclic voltammograms that the oxidation of UO_2 is very irreversible.

There are two further points of interest in the work of Nicol and Needes. In their initial report,[38] the proposed mechanisms for the oxidation of UO_2 are labelled as 'simplified'. They suggest that the oxidation proceeds by intermediate oxides. In later works[39,40,41,42] however, the same mechanism is presented with no provisos, and no mention of intermediate oxides is made. The second point is that throughout this series of papers, Nicol and Needes repeatedly state that the number of steady-state Tafel areas is equal to the number of electron transfer reactions. This is not correct. The presence of a steady-state Tafel area indicates that over the range of that Tafel area, the same rate controlling process(es) are operative. Therefore, two Tafel areas indicate two different rate determining steps over the two potential ranges of the Tafel slopes.

Haque et al.[53] in a review and comparison of different oxidizing agents propose an entirely different type of anodic oxidation mechanism from those proposed previously.[35,38]

$$U^{+4} = UO_2^{+2} + 2H_2O = 2UO_2^{+} + 4H^{+} \quad (36)$$

$$UO_2^{+} + H^{+} = UOOH^{2+} \quad (37)$$

$$UO_2^{+} + UOOH = UO_2^{+2} + UOOH^{+} \quad (38)$$

$$2UO_2^{+} + O_2 = 2UO_2^{2+} + O^{2-} \quad (39)$$

This is an exact copy of the proposed mechanism. Although no retraction or correction has appeared, one assumes that the first part of equation (36) is illustrative, and that the UOOH in equation (38) is meant to be $UOOH^{2+}$. This is only a suggested mechanism and after comparison with work by Nicol and Needes[38-42] it can be dismissed on the grounds of reaction (37) being unlikely and a lack of surface films observed by Nicol et al.[38]

In a preliminary paper on irradiated UO_2 dissolution with oxygen, Johnson et al.[44] conclude that the surface of the UO_2 reacts rapidly with dissolved oxygen to produce oxidized surface films, the thickness and nature of which depend on the redox conditions and solution composition. In the presence of carbonate or some other complexing agent the film is of lesser thickness. X-Ray Photoelectron Spectroscopy (X.P.S.) was used to identify the preliminary film as $UO_{2.50}$. When carbonate was not present, the top layer of the film was found to be UO_3, which was not passivating. No evidence of precipitation U VI was found in either the carbonate or sulphate systems. This preliminary work was carried out in the pH range 9 to 10.5.

After a detailed study of UO_2 dissolution in sulphate solutions ($6 < pH < 11$) Sunder et al.[45] conclude that the oxidation of UO_2 proceeds via a sequence of surface oxide films. In all cases a thin ($\leq$5 molecular layers) film of UO_{2+x} ($x \leq 0.25$) is formed. On top of this film a second film of $UO_{2.30}$ grows. The characteristics of the film structure and their oxides present then depend on redox and solution conditions, as below:

The first step is the dual oxide film formation:

$$UO_2 \longrightarrow UO_{2+x(x\leq 0.25)} \longrightarrow UO_{2.33} \qquad \text{Fast} \qquad (40)$$

$$\text{i.e.} \quad 3UO_2 + H_2O \longrightarrow U_3O_7 + 2H^+ + 2e^- \qquad (40a)$$

Further oxidation involves some intermediate oxidized species, which the authors designate as adsorbed uranyl ion.

$$UO_2 \longrightarrow (UO_2^{2+})_{ads.} + 2e^- \qquad (41)$$

At less oxidizing potentials ($E < 445$ mV SHE), the surface coverage of (UO_2^{2+}) is low, and dissolution predominates.

$$(UO_2^{2+})_{ads.} \longrightarrow (UO_2^{2+})_s \qquad (42)$$

$$(UO_2^{2+})_s + SO_4^{2-} \rightleftharpoons (UO_2SO_4)_s \qquad (43)$$

$$(UO_2SO_4)_s \longrightarrow (UO_2SO_4)_b \qquad (44)$$

where $(\ )_{ads.}$, $(\ )_s$, $(\ )_b$, represent species adsorbed onto, close to the electrode surface, and in the bulk solution respectively. At intermediate potentials (E = 545 mV SHE) dissolution predominates, but is accompanied by film growth:

$$UO_{2.33} + (UO_2^{2+})_{ads.} + \tfrac{2}{3}H_2O \longrightarrow 2UO_{2.5} + 4/3H^+ \quad (45)$$

$$2UO_{2.50} + (UO_2^{2+})_{ads.} + H_2O \longrightarrow 3UO_{2.67} + 2H^+ \quad (46)$$

At more oxidizing potentials ($E \geq$ 645 mV SHE) in the absence of stirring:

$$2UO_{2.5} + 2H^+ \longrightarrow 2(UO_2^{2+})_s + 2e^- + H_2O \quad (47)$$

$$(UO_2^{2+})_s + (z - 1)H_2O \rightleftharpoons UO_3.zH_2O + 2H^+ \quad (48)$$

Cyclic voltammograms presented by Sunder et al.[45] show the presence of at least three surface phases, and bear some resemblance to cyclic voltammograms presented by Nicol et al.[38] The voltammograms from Nicol and Needes do not show as much fine detail as those of Sunder, but this could be due to differences in the pH.[45]

The other major anomaly in the cyclic voltammograms is the potential ranges under which they were obtained. Whilst Nicol and Needes used an A.C. Fluke impedance bridge to estimate the effect of uncompensated cell resistance and double-layer charging on polarization (referred to hereafter as IR drop), a procedure which has been shown

to be inappropriate,[46] it appears that no correction for the IR drop was applied to the voltammograms of Sunder et al.[45] The difference between the voltammograms, potentially, is ~400 mV. Differences in the dry resistances of the electrodes could account for a maximum of 200 mV. The actual potential drop depends on detailed knowledge of the double layer capacitance, which is not presented in either work. There is obviously a potential difference ($100 < \Delta E < 200$ mV) between the two sets of work, but whether this is a real or an apparent effect, it is difficult to say. It is equally obvious however, from the shape of the voltammograms that the same reaction is being studied, and qualitative comparisons are valid. The subject of the IR drop will be more fully discussed in the practical applications section.

The mechanism of UO_2 dissolution proposed by Sunder et al.[45] agrees well with that of Nicol and Needes.[38] The main difference is the origin of the UO_3 found on the surface by both groups. Sunder et al. state it is the result of precipitation, whilst Nicol et al. claim it is an intermediate produced prior to UO_2^{2+} dissolution. The fact that UO_3 does not appear until either the potential is high and/or there is no stirring tends to support Sunder. However, the difficulty with X.P.S. to unambiguously identify a thin layer of one oxide on another, in this case ~5 molecular layers or less of UO_{2+x} ($x \leq 0.25$) on a bulk crystal of UO_2 casts some doubt on whether X.P.S. could

detect the UO_3 in the first place and on the identification of the initial film as UO_{2+x} ($x \leq 0.25$).

In further work on the dissolution of UO_2 in sulphate solution at high pH, Sunder et al.[47] propose a mechanism:

$$UO_2 \longrightarrow UO_{2+x} \longrightarrow UO_{2.33} \quad (40)$$

$$UO_2 \longrightarrow (UO_2^{2+})_{ad.} + 2e^- \quad (41)$$

$$UO_{2.33} + (UO_2^{2+})_{ads.} + \tfrac{2}{3}H_2O \longrightarrow 2UO_{2.5} + 4/3H^+ \quad (45)$$

$$2UO_{2.50} + (UO_2^{2+})_{ads.} + H_2O \longrightarrow 3UO_{2.67} + 2H^+ \quad (46)$$

$$3UO_{2.67} + (UO_2^{2+})_{ads.} + 2H_2O \longrightarrow 4UO_3 + 2H^+ \quad (49)$$

$$(UO_2^{2+})_{ads.} \longrightarrow (UO_2^{2+})_{soln.} \quad (50)$$

As previously the natures of these films depend on solution and redox conditions. In all cases a monolayer of a uranium VI species is formed on the surface (possibly $(UO_2^{2+})_{ads.}$ or UO_3). On top of this a layer whose presence depends on pH of UO_{2+x} (possibly $x = 0.25$) is formed. Layers of $UO_{2.5}$ and $UO_{2.67}$ are then formed according to equations (45) and (46) in amounts which are potential dependent. When $E > -445$ mV SHE a partially passivating slowly soluble UO_3 layer forms on top of the other oxide films. In the intermediate potential range ($-55 \leq E \leq -445$ mV SHE) a surface layer of $UO_{2.5}$ forms according to equation (45), and after about 10 minutes a layer of $UO_{2.67}$ according to equation (46) forms on top of the $UO_{2.5}$ layer. At high

pHs (first detected at pH = 10) and potentials more oxidizing than E = 345 mV SHE it is possible that a film of UO_3 grows on top of the $UO_{2.67}$ layer. This is not a precipitated film as in the lower pH region but a precursor to dissolution via equation (44), similar to that suggested by Nicol et al.[41]

The mechanisms for the neutral and high pH dissolutions are similar. The initially formed uranium VI monolayer in the high pH system may also be present in the lower pH system and be undetected. However, examination of the cyclic voltammograms in both works leads to the conclusion that it is formed and reduced. The reason that $UO_{2.5}$ is formed preferentially to $UO_{2.33}$ in the high pH system is kinetic. In the neutral solutions reactions (45) and (46) do not occur at less oxidizing potentials ($E < 545$mV SHE) because the rate of formation of $(UO_2^{2+})_{ads.}$, (reaction (41)), is slow compared to the desorbtion steps (42 - 44). The observation of Sunder et al.[45] that the cyclic voltammograms obtained at lower pH were less defined is now explained simply by the fact that there are less of those intermediates present to give the peaks on the voltammograms. An increase in the stability of surface oxides with increasing pH is predicted thermodynamically,[48] although in this work the phases formed are not the most stable ones predicted thermodynamically.

In a final piece of work, Sunder et al.[49] apply their knowledge of the uranium dioxide anodic half cell reaction

to the complete uranium dissolution system using a medium of 0.5 M Na_2SO_4 in the presence of carbonate. The pH range under which the study was conducted is $6 < pH < 12.5$. They propose a mechanism:

$$UO_2 \longrightarrow UO_{2+x} \longrightarrow UO_{2.33} \qquad (40)$$

$$3UO_{2.33} + H_2O \longrightarrow 3(UO_2^{2+})_{ads.} + 2OH^- + 4e^- \qquad (51)$$

At low concentrations of carbonate ($[CO_3] < 10^{-4}$ M) the rate is independent of carbonate concentration. Under conditions when $UO_{2.33}$ is the surface film, dissolution takes place via reactions (40), (51), (52), and (53).

$$(UO_2^{2+})_{ads.} + CO_2^{2-} \rightleftharpoons (UO_2CO_3)_{ads.} \qquad (52)$$

$$(UO_2CO_3)_{ads.} + 2CO_3^{3-} \longrightarrow UO_2(CO_3)_3^{4-} \qquad (53)$$

When $10^{-4} < [CO_3] < 10^{-3}$ M at high potentials (E ~545 mV SHE) the rate is controlled by (52). At less oxidizing potentials (E~ 345 mV SHE) the rate is controlled by (51). At more oxidizing potentials ($E \geq$ 545 mV SHE) different oxide films are formed according to reactions (45), (46) and (49). Carbonate orders of 0.5 and 1.0 which are compatible with this mechanism have been previously reported.[42,50,51,52]

Eary and Cathless[63] studied the dissolution of stoichiometric UO_2 in a low pH ($1 < pH < 4$) sulphate system, (0 < sulphate concentration < 0.5 M), with hydrogen peroxide ($10^{-8} < H_2O_2$ concentration $< 10^{-2}$ M) as the

oxidizing agent. The order of reaction with respect to H_2O_2 was 1.01 and the apparent activation energy was 27.4 KJ mol^{-1}. Using the etch patterns on the UO_2, and their kinetic data they propose a mechanism and state that the dissolution process is chemically controlled. They report that the order with respect to pH changes over the range of their study. At low pH ($1.0 \leq pH \leq 3$) the rate of reaction was independent of pH, whereas at higher pH ($3 \leq pH \leq 4.5$) slower rates of reaction were found which exhibited a second order dependence on pH. The point of changeover was dependent on the hydrogen peroxide concentration. At higher hydrogen peroxide concentrations, the changeover point occurred at lower pH values. The rate was found to be independent of the sulphate concentration above $\sim$0.01 M sulphate. It is proposed by the authors that uranium peroxide precipitation on the surface of the UO_2 is responsible for the pH dependence and slower rates encountered at higher pH.

The mechanism gives no oxidation or reduction information, and is principally an adsorption model. It is postulated that hydrogen peroxide adsorbs onto a surface site, and uranyl ion is the reaction product. The model involves competitive adsorption of, for example, sulphate ions. Unfortunately, there seem to be a number of major inconsistencies and errors in this work, and only limited conclusions may be drawn from it. The activation energy data presented are complex, and as activation energy varies with potential, which does not appear to have been considered

in this work, it is hazardous to draw any further conclusions. The authors do not indicate how they determined concentrations of sulphate, bisulphate and hydrogen ions. No sound evidence to prove chemical as opposed to diffusion control is presented, and there seems to be confusion about the definition of the mass transfer coefficients of the system.

Manning[60] surveyed the dissolution of stoichiometric UO_2 in hydrogen peroxide systems at low pH. He reports a lessening of the rate of reaction of approximately an order of magnitude over the pH range 1.5 to 2.5. This is consistent with results reported by Eary et al.[63] However, from the results of Manning[60] an order of reaction with respect to pH of 0.25 can be calculated over the pH range 0.5 to 1.5. This contrasts with the zero order calculated by Eary et al.[63]

SUMMARY

The anodic oxidation of UO_2 is an electrochemical reaction. The oxidation appears to proceed via a complex series of films of different uranium oxides. The sequence and structure of the oxides depends on solution composition, pH and oxidation conditions.

In the alkali system the exact sequence seems fairly well documented.[44,45,47,49] In the acid system, the presence of the multilayered film is suggested, but not proved.[38]

The available kinetic data for the complexing agents (carbonate or sulphate), in the alkali and acid systems respectively, are consistent with this type of mechanism.[42,52]

The interpretation of the sulphate data is made more complex by the adsorption and complexation behaviour of this anion in the acid system.[54,55] Considering the mechanistic simplification employed in the major work in the acid system[38,39,41] the degree of self consistency and agreement with previous work is extraordinary.

1.5.2. The Cathodic Reaction

In a fundamental study the basic process is studied, devoid of complications. Thus in the interest of clarity, work on uranium ore leaching will not be discussed, since, apart from the effect of products of the reaction of gangue in the leaching system on the ionic strength, the presence of iron is implicit in any ore. The presence of iron distorts the cathodic kinetics of any other oxidizing agent, giving mixed or even iron dependent kinetics. For similar reasons studies performed without iron present will be given greater emphasis than those studies involving iron.

Mackay et al.[56] studied the dissolution of synthetic UO_2 in H_2SO_4 systems using oxygen as the oxidizing agent. They found that the reaction order was 0.5 with respect to oxygen (up to 900 psi). The temperature range of the work was 194 to 273°C.

They propose a mechanism:

$$UO_2 + H_2O \longrightarrow UO(OH)_2 \quad \text{rapid hydration} \tag{54}$$

$$OU(OH)_2 \rightleftharpoons OU\begin{matrix}\diagup O^- \\ \diagdown O^-\end{matrix} \tag{55}$$

$$O_2\,(g) \rightleftharpoons O_2\,(aq) \tag{56}$$

$$OU\begin{matrix}\diagup OH \\ \diagdown OH\end{matrix} + O_2\,(g) \rightleftharpoons A^{\neq} \longrightarrow UO_2^{2+} + HO_2^- + OH^- \tag{57}$$

The detection of hydrogen peroxide is reported. This is consistent with the generation of HO_2^- in the reaction. The authors do not carry out any further kinetic analysis, and the mechanism presented is very unclear with regard to any oxidation or reduction processes. At the high temperatures involved, their assumption about the small magnitude of the bisulphate dissociation constant is valid. However from their own data an order with respect to H_2SO_4 of 0.74 (up to $[H_2SO_4] = 0.025$ M), and orders of 0.39 (up to 6×10^{-3} M) and 1.05 (up to 2.5×10^{-2} M) with respect to $[H^+]$ can be calculated.

The order of 0.74 with respect to H_2SO_4 compares very favourably with 0.75 (Eligwe et al.[57,58]) and an order of 0.86 (Eligwe et al.[59]) with respect to Na_2SO_4. All of these latter studies involved the leaching of uranium ore with hydrogen peroxide. The change in hydrogen ion dependence may indicate a change in the rate determining step of the dissolution, or simply that the hydrogen ion is in excess, hence the first order dependence. Enthalpy of activation was determined as 75.6 kJ mol^{-1}. These data indicate a chemically controlled reaction and reflect the unsuitability of oxygen as an oxidizing agent. The order of 0.5 with respect to oxygen may well not be as straightforward as proposed. Nicol et al.[40] in their study of the alkaline system compare a number of oxidizing agents including oxygen, hydrogen peroxide, ferricyanide, and $Cu(NH_3)_4^{2+}$. All display a kinetic order of 0.5. This order could only be explained in terms of a dissociative

mechanism for two of the above. Nicol et al. further studied the reduction of O_2 at a UO_2 surface and found the reaction was first order. The conclusion is that these reaction orders cannot be explained solely in terms of the cathodic half cell reaction. It is stressed that these latter results refer to the alkali system. However, if the same fundamental anodic reaction underlies both systems, it is likely that these findings will be repeated in the acid system. Many of the works in the carbonate system do give orders of about 0.5 with respect to oxidants; e.g. Hiskey[51] reports an order of 0.5 with respect to hydrogen peroxide. Hiskey[52] and Schortmann et al.[31] both report a reaction order of 0.5 with respect to the partial pressure of oxygen. None of the above works attempt to correlate their estimates of activation energy with potential. Hiskey[52] reports an activation energy of 43 to 47 kJ mol^{-1} and Schortmann et al.[31] report an activation energy of 56.3 kJ mol^{-1}. Although these figures suggest chemical control, these activation energy data are complex including both electrochemical and chemical contributions.

In their work on the acid system, Nicol et al.[39] reconcile apparently contradictory works[6,54,60,61,62] on the orders of reaction with respect to the ferric to ferrous ratio. They argue that the same cathodic (and anodic) half cell reactions are involved in all the studies reported above and that the mechanism in no way changes. They ascribe the differences in observed order with respect to the ferric to ferrous ratio to be due to changes in

the leaching potential (engendered by changes in the above ratio), and that as a consequence of the changed ratio, hence potential, the relative magnitudes of the various partial anodic and cathodic currents are changed. The cathodic reaction is described as a series of single electron transfer steps from the $FeSO_4^+$ and $Fe(OH)_2^+$ complexes.

In the major study on cathodic reactions at a UO_2 electrode surface, Nicol et al.[43] examine the electrode kinetics of reduction of a number of oxidizing agents. In common with Sunder et al.[45] they note the presence of a passivating film on the surface of the UO_2 even at less oxidizing potentials (-255 mV $\leq E \leq$ 245 mV SHE). The implication is that the electrode kinetics observed may not be the same as would be seen on a UO_2 surface without this film. With hydrogen peroxide there are three reactions that occur in the potential range of interest. These are the oxidation and reduction of hydrogen peroxide, and the oxidation of UO_2. Nicol et al.[43] used a ring disc electrode to separate the various reaction products. It was found that the oxidation of hydrogen peroxide (59, 61) was much more reversible than its reduction (58, 60) and at pH = 9 both H_2O_2 and OH_2^- are involved in the reduction process (62 to 65).

$$H_2O_2 + 2H^+ + 2e^- \longrightarrow 2H_2O \qquad (58)$$

$$H_2O_2 \longrightarrow O_2 + 2H^+ + 2e^- \qquad (59)$$

$$HO_2^- + H_2O + 2e^- \longrightarrow 3OH^- \qquad (60)$$

$$HO_2^- + OH^- \longrightarrow O_2 + H_2O + 2e^- \quad (61)$$

$$H_2O_2 \rightleftharpoons H^+ + HO_2^- \quad (62)$$

$$H_2O_2 + e^- \longrightarrow OH^- + OH. \quad (63)$$

$$HO_2^- + H_2O + e^- \longrightarrow OH. + 2OH^- \quad (64)$$

$$OH. + e^- \rightleftharpoons OH^- \quad (65)$$

(63) and (64) are parallel rate determining steps.

It should be noted that the pK for reaction (62) is about 11.6 and therefore at low pH HO_2^- should not be present.

The inhibiting effect of FeII on the anodic dissolution of UO_2 was attributed to the formation of FeU_2O_7, which is less soluble than its proposed $UO_2(OH)_2H_2O$ precursor.

As the oxidation of H_2O_2 has been shown to be more reversible than its reduction, the mechanism of its oxidation is also important, inasfar as any reaction intermediates or products may affect the oxidation of UO_2. The proposed mechanism of oxidation of hydrogen peroxide is:

$$H_2O_2 \longrightarrow H^+ + HO_2^- \quad (62)$$

$$H_2O_2 \longrightarrow 2OH. \quad (66)$$

$$HO_2^- \longrightarrow OH. + O^- \quad (67)$$

$$OH. \longrightarrow O + H^+ + e^- \quad (68)$$

$$O^- \longrightarrow O + e^- \quad (69)$$

$$2O \longrightarrow O_2 \quad (70)$$

(68) and (69) are the rate determining steps. In the same work, Nicol and Needes also studied the reduction of oxygen at a UO_2 surface, and conclude that it has two possible reaction pathways. At low current densities, there are no intermediates and the reaction product is water.

$$O_2 + 4H^+ + 4e^- \longrightarrow H_2O \qquad (71)$$

At higher current densities the main pathway is as before, but a second pathway involving two single electron transfers and H_2O_2 as an intermediate also occurs. This auxiliary pathway accounts for about 10% of the overall cathodic current. The authors note that concentrations of sulphate up to about 0.5 M have no effect on the reduction of O_2 at a UO_2 surface. A reaction order of 1 for oxygen reduction is reported (indicating a non-dissociative mechanism) and the authors detected two Tafel regions, the first of which displayed pH dependence. A mechanism is proposed:

$$UO_2| + O_2 + H_2O \rightleftharpoons UO_2\begin{matrix}\diagup H^+ \\ \diagdown O_2\end{matrix} + OH^- \qquad (72)$$

$$UO_2\begin{matrix}\diagup H^+ \\ \diagdown O_2\end{matrix} + e^- \rightleftharpoons UO_2|HO_2 \qquad (73)$$

or

$$UO_2| + O_2 + H_2O + e^- \rightleftharpoons UO_2|HO_2 + OH^- \qquad (74)$$

then:

$$UO_2|HO_2 + e^- \rightleftharpoons UO_2|O + OH^- \qquad (75)$$

$$UO_2|O + H_2O + e^- \rightleftharpoons UO_2|OH + OH^- \quad (76)$$

$$UO_2|OH + e^- \rightleftharpoons UO_2| + OH^- \quad (77)$$

The rate limiting step is (73) at low cathodic potentials, (72) at intermediate potentials, and (74) at high cathodic potentials.

A mechanism of this type explains the detection of H_2O_2 reported by MacKay et al.[56] and the variety of possible pathways are consistent with the order changes with respect to $[H^+]$ that were detected.

SUMMARY

The reduction of oxidizing agents on a UO_2 surface is hindered by the formation of a passivating film. As the cathodic and anodic rates must be equal, a slow irreversible reduction (e.g. oxygen) can lead to that being the rate controlling process in uranium dissolution.

In the potential range of interest, hydrogen peroxide undergoes both oxidation and reduction, the former being the more reversible. This makes evaluation of electrode-kinetic data from leaching studies hazardous. A further complication at high pH is the presence of the peroxyhydroxyl ion.

The reduction of oxygen is an irreversible process with more than one reaction pathway. The major reduction is a two electron transfer process with no detectable intermediates.

SECTION 2

EXPERIMENTAL PROCEDURE

2.1 APPARATUS AND EXPERIMENTAL PROCEDURE

2.1.1 Reagents

All the reagents used in the leaching and electrochemical studies were of A.R. grade, except those listed below:

H_2O_2; Interox Chemicals Ltd., 85% aqueous solution

H_2O_2; BDH Chemicals Ltd., G.P.R., 6% (20 vol) aqueous solution

$UO_2SO_4.3\frac{1}{2}H_2O$; BDH Chemicals Ltd., G.P.R., Assay 97.0%

2.1.1.1 Caro's Acid Preparation

The preparation of Caro's Acid from sulphuric acid (98%) and hydrogen peroxide (85%) was carried out as described in the Interox booklet "Caro's Acid Laboratory Procedure for Hydrometallurgy".[74] The typical reagent ratio used in the preparation was:

SO_3 : H_2O_2

1.5 : 1

After the dilution of product stage, 20 ppm chloride as sodium chloride was added, and the solution was left stirring overnight. The presence of chloride at this concentration destroyed all but a negligible amount of the hydrogen peroxide present.

The solution was then analysed for hydrogen peroxide, peroxymonosulphuric acid and total acid.

The Caro's acid and hydrogen peroxide (6%) were stored in plastic bottles in a refrigerator, to minimise decomposition. No changes in the hydrogen peroxide or peroxymonosulphate concentrations were detected at times up to three weeks.

2.1.1.2 Uranium Oxides

2.1.1.2 (i) Introduction.

All X-ray powder diffraction patterns were determined using Co Kα emission in a Guinier camera. Comparisons with standard (A.S.T.M.) X-ray powder diffraction patterns were carried out on the basis of classifying the lines according to strength and clarity as below.

Strength

s = strong

m = medium

w = weak

v is a suffix indicating 'very'

There are therefore seven classifications of strength i.e. from vs (very strong) to vw (very weak).

Clarity

d = diffuse

b = broad

No symbol in the clarity section indicates that the line is well defined.

e.g. ms, d indicates a diffuse line of medium strong intensity

w indicates a well defined line of weak intensity.

Lines of relative intensity (I/I_{100}) less than 10, (i.e. $I/I_{100} < 10$) in the A.S.T.M. standards are not classified as primary, (for identification purposes), and are not compared.

The same furnace was used for all uranium oxide synthesis. The temperature profile of this furnace was determined, and all synthesis carried out with reference to it.

2.1.1.2 (ii) Uranium Dioxide (UO_2)

(a) UO_2 used in chemical leaching studies

The UO_2 used in the chemical leaching studies was supplied by UKAEA (Harwell) and was in the form of almost monosize, well defined spherical particles. Pictures of some random samples of the uranium dioxide particles appear in Plate 1.

Particle sizes were measured by scanning electron microscopy. The average diameter of the particles was found to be 79 μ. The statistical summary of the data on which the diameter determination was made appears below:

number of samples (n) = 36

mean ($\bar{x}$) = 79 μ

standard deviation (σ_{n-1}) = 2.34

variance (σ^2_{n-1}) = 5.33

The stoichiometry of the uranium dioxide was found to be $UO_{2.03}$. This was determined by weight difference after the UO_2 had been converted to U_3O_8 by heating at 880°C for 24 hours under atmospheric conditions. This method was described by Rabinovitch et al.,[7] and used by Nicol et al.[39] The average equilibrium composition of uranium dioxide in air is $UO_{2.04}$.[7]

The X-ray powder diffraction pattern of the oxidised product is compared with the A.S.T.M. standard pattern for U_3O_8 in Table 2. It can be seen that the two patterns are very similar, with all the primary lines of the standard present in the pattern of the product. The product can therefore be identified as U_3O_8.

Some of the UO_2 spheres were ground to a fine powder using an agate lined grinding mill and an agate mortar and pestle. The X-ray powder diffraction pattern of this oxide is compared with the A.S.T.M. standard pattern for UO_2 in Table 3(a). It can be seen that the two patterns are very similar, with all of the primary lines of the standard present in the pattern of the sample.

The density of the UO_2 was 10.26 cm^3 (93.61% theoretical density). The density was determined by displacement of water in a converted burette after ultra-sonic agitation to remove air bubbles.

(b) UO_2 used in electrode fabrication

The UO_2 used in the electrode fabrication was supplied by UKAEA (Harwell) and was in the form of a uniform slab of thickness 0.559 cm.

The stoichiometry of the uranium dioxide was found to be $UO_{2.04}$, by the same method as previously. The X-ray powder diffraction pattern of the oxidised product is compared with the A.S.T.M. standard pattern for U_3O_8 in Table 2. It can be seen that the two patterns are very similar, with all the primary lines of the standard present in the pattern of the product. The product can therefore be identified as U_3O_8.

The density of the UO_2 was 10.59g cm^3 (96.62% theoretical density). Again this was determined as before.

The resistivity of the UO_2 was measured when it was in electrode form, and will be fully discussed at that point.

(c) UO_2 used in carbon paste electrodes and synthesis

UO_2; Koch-Light Laboratories Ltd., Laboratory reagent Assay 99.97%, depleted uranium.

The X-ray powder diffraction pattern of this oxide is compared to the A.S.T.M. standard in Table 3(a). It can be seen that the two patterns are very similar with all the primary lines of the standard present in the pattern of the sample. The sample can therefore be identified as UO_2.

2.1.1.2 (iii) Other uranium oxides.

(a) U_3O_8 used in carbon paste electrodes and synthesis

U_3O_8; Koch-Light Laboratories Ltd., Laboratory reagent Assay = 99.97%, depleted uranium.

The X-ray powder diffraction pattern of this oxide is compared to the A.S.T.M. standard in Table 3(b). The two patterns are very similar with all the lines of the standard present in the pattern of the sample. There are also two foreign lines present in the pattern, which could be two of the primary lines of U_3O_7. It is possible that a small quantity of U_3O_7 is present in this oxide. Notwithstanding, this oxide can be identified as U_3O_8.

(b) U_3O_7 used in carbon paste electrodes

The U_3O_7 was prepared by evacuating a silica tube closed at one end containing uranium dioxide (10g), and then filling it to a pressure of 700 torr with oxygen before sealing it. The silica tube was then heated in a tube furnace at 220°C for 48 hours. This method was first used and is fully described by Gronvold et al.[15]

The X-ray powder diffraction pattern of this oxide is compared to the A.S.T.M. standard in Table 3(c). The two patterns are very similar, with all the lines of the standard present in the sample. The sample can therefore be identified as U_3O_7.

(c) U_2O_5 used in carbon paste electrodes

The U_2O_5 was prepared by evacuating a silica tube closed at one end, containing 7.8 g U_3O_8 and 2.5 g UO_2 which had been well mixed. Air was then allowed to re-enter the tube to a pressure of 700 torr. The tube was then sealed and heated to 1100°C for 48 hours. This method was first employed and is fully described by Rundle et al.[9]

The X-ray powder diffraction pattern of this oxide is compared to the A.S.T.M. standard in Table 3(d). The two patterns are very similar, with all the lines of the standard present in the sample. A number of the primary lines of UO_2 and U_3O_8 are present in this oxide, indicating that some of these constituent oxides are present in the product. Notwithstanding, this product can be identified as U_2O_5.

(d) UO_3 used in carbon paste electrodes

UO_3; Koch-Light Laboratories Ltd., Laboratory reagent. Assay 99.97%, depleted uranium.

No X-ray powder diffraction pattern for this oxide could be obtained. This indicates that this particular oxide is amorphous to X-rays.

(e) $UO_4.2H_2O$ used in carbon paste electrodes

The $UO_4.2H_2O$ was prepared by G.D. Manning by precipitation. Hydrogen peroxide was added to a solution of uranyl sulphate, and the precipitate filtered off and

washed with ethanol whilst on the filter, and dried. The X-ray powder diffraction pattern of this oxide is compared to the two A.S.T.M. standards for the known uranium peroxides in Table 3(e). The sample oxide contains primary lines of both $UO_4.2H_2O$ and $UO_4.4H_2O$.

The method of preparation and the fact that it is a hydrated compound combine to give the lack of clarity and weakness in the observed sample pattern. It is not possible to state anything further than this oxide is a mixture of the two uranium peroxides.

2.1.2 Chemical Leaching Studies

2.1.2.1 Apparatus

The leaching vessel consisted of a round bottomed wide flanged Quickfit 250 ml glass split flask which had been modified to have a flat bottom. The wide flanged lid had five necks, and the two halves were held together by a metal clip. A glass paddle stirrer was aligned through the central port by way of a P.T.F.E. stirrer guide. The stirrer was driven by an overhead Heidolph variable speed motor, (rotation up to 230 rpm), via a rubber joint.

The remaining four ports were used for:

(a) Holding a combined pH/reference electrode

(b) Holding a combined platinum/reference electrode

(c) Holding a mercury in glass thermometer

(d) Sampling, otherwise stoppered.

In the electrochemical runs, the platinum electrode was replaced by a mercurous sulphate reference electrode. A uranium dioxide electrode was fitted into the remaining port. Sampling was achieved by removing the mercurous sulphate reference electrode.

The use of baffles was deemed unnecessary for the following reasons:

(a) The electrodes and the thermometer acted as their own baffles

(b) The flat bottom of the flask increased turbulence

(c) The uplifting effect of the paddle stirrer

(d) The particles of uranium dioxide were in suspension under the conditions employed.

Most of the kinetic runs were less than 1 hour in duration and the highest temperature employed in this study was 80°C. For this reason, and since tight seals were maintained on all joints, it was deemed unnecessary, and practically difficult, to include a condenser to cut down on evaporation.

Heating was achieved by the use of a heating mantle (electrothermal, 300 watts rating), into which the leaching vessel was placed. The temperature within the vessel was maintained by a 'Fi-monitor' (Fison's Scientific Apparatus) and a Variac placed in the heating circuit. This set-up normally enabled temperature to be controlled to within $\pm$ 1°C. The stirring effectively eliminated temperature gradients within the solution. No external insulation was necessary.

The potential was measured using a combination reference platinum electrode and a Solartron digital voltmeter. Care was taken to correct the potential readings for temperature. Similar precautions were taken when using UO_2 and separate reference electrodes. Figure 2 shows the typical leaching apparatus.

2.1.2.2 Preparation of Leach Solutions

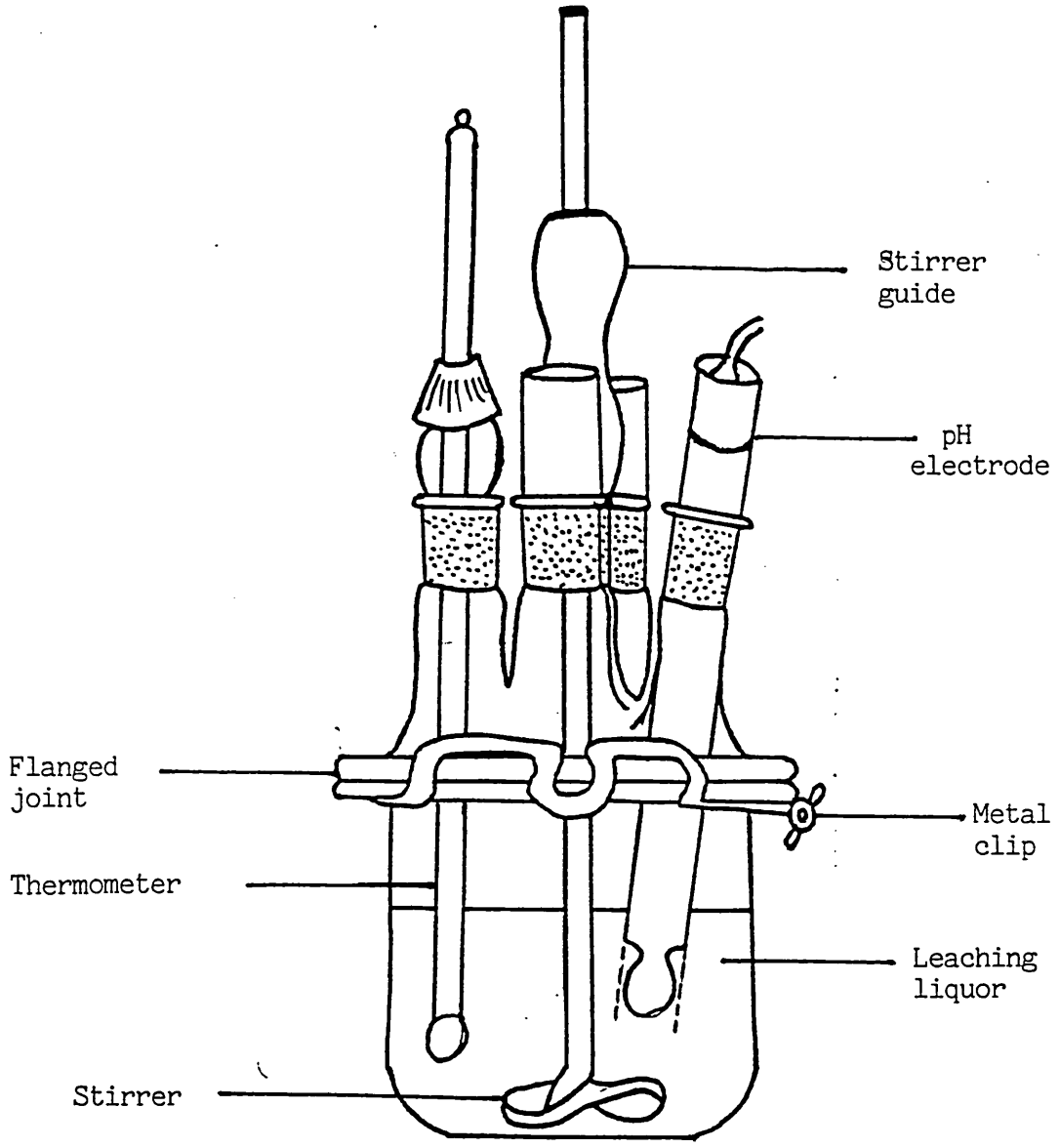
Usually, a stock amount (typically 1 L) of leaching solution was prepared for a series of runs.

If sodium sulphate, nitrate or perchlorate were required, they were weighed into a 1 L beaker and dissolved in about 250 mls of water. Hydrogen peroxide or Caro's acid was then pipetted into the beaker. At this point any sulphuric acid (1 M) required was pipetted into the beaker. Finally, any sodium or potassium hydroxide (10 M) was added to the beaker. The contents of the beaker were quantitatively transferred to a 1 L volumetric flask and diluted to the mark with water.

Due to the viscosity of the 10 M hydroxide solutions, no effective method of measuring the volume of this reagent was discovered, and so analysis of the leach solutions for sodium and/or potassium was carried out using atomic absorption spectroscopy.

Occasionally, leaching solutions were prepared on an 'ad hoc' basis. On these occasions the procedure was

FIG. 2. A schematic diagram of the leaching apparatus.



the same as described above, except that a 250 ml volumetric flask was employed.

Due to an error in density measurements of Caro's Acid, some of the early runs had to be retrospectively analysed for total sulphur using inductively coupled plasma spectroscopy.

2.1.2.3 Dissolution Procedure

At the beginning of a run, the required amount of UO_2 (usually 0.5 g) was weighed to within $\pm$ 0.0002 g of the nominal weight, into a clean, dry weighing boat.

The required amount of leaching solution was either pipetted or added via a funnel to the reaction vessel. The electrodes and thermometer were inserted into the vessel and the stirrer motor started. The vessel was heated to the nominal experimental temperature. The system was left for 15 minutes to allow the electrode assemblies to attain the temperature of their surroundings.

At this point the pH was adjusted to the desired value. Either sulphuric acid (1 M) was pipetted into the vessel, or sodium or potassium hydroxide (10 M) was added from an Oxford macro pipette. Any solutions remaining on the sides of the reaction vessel was washed into the vessel with a little leaching solution.

The system was left for a further two minutes, and then a 2 ml sample was removed. This was used as a blank in the subsequent analysis.

The solid was added to the reaction vessel through the sampling port. If any of the solid adhered to the lid or sides of the vessel, a small quantity of the leaching solution was removed from the vessel and used to wash the solid into the vessel.

2 or 5 ml samples of leach solutions were taken at appropriate times (typically 5 minutes) depending on experimental conditions. This periodic reduction in leaching volume was incorporated in the computer program developed to calculate experimental data, and account was taken of it.

Whenever a sample was taken, the stirrer motor was turned off for a few seconds, to allow the UO_2 to settle out, before the sample was taken.

Leaching times varied between 10 minutes and 24 hours, typically the leaching time was 30-60 minutes. In some runs, the leached particles were kept for microscopic examination.

Stirrer speed was measured by an adjustable stroboscope. Before any other variable was examined, the effect of stirrer speed was established. Stirrer speeds from 100 to 1300 rpm were examined. Below 360 rpm the rate of uranium leaching varied with stirrer speed. Above 1000 rpm the uranium leaching rate became less reproducible. All further experiments were carried out at 625 rpm, this value being well on the 'stirrer speed plateau'.

The pH range studied was from 0.5-2.5, and the temperature range was from 30°C - 80°C.

Care was taken not to allow uranium containing solutions to come into contact with the skin.

2.1.3 Electrochemically Driven Leaching Studies

2.1.3.1 Apparatus

A three electrode two compartment electrochemical cell was specifically constructed for this project. Figure 3 shows the electrochemical cell.

The reference and working compartments were connected by an adjustable luggin probe. The reference cell consisted of a 24 mm internal diameter tube with a 24/29 quickfit female joint at the top. The tube leading from the bottom of the reference compartment to the luggin capillary had a stopcock to prevent seepage of reference electrolyte into the working compartment.

The adjustable luggin probe was made from a glass syringe, the centre plunger having been hollowed out, and a capillary joined to the end as shown.

The working compartment comprised of a flanged beaker (capacity approximately 75 mls), with the barrel of the syringe joined to the side (as shown). The P.T.F.E. lid had holes drilled into it for the counter and working electrodes, thermometer, gas inlet, and condenser. The condenser was connected to a gas bubbler to ensure

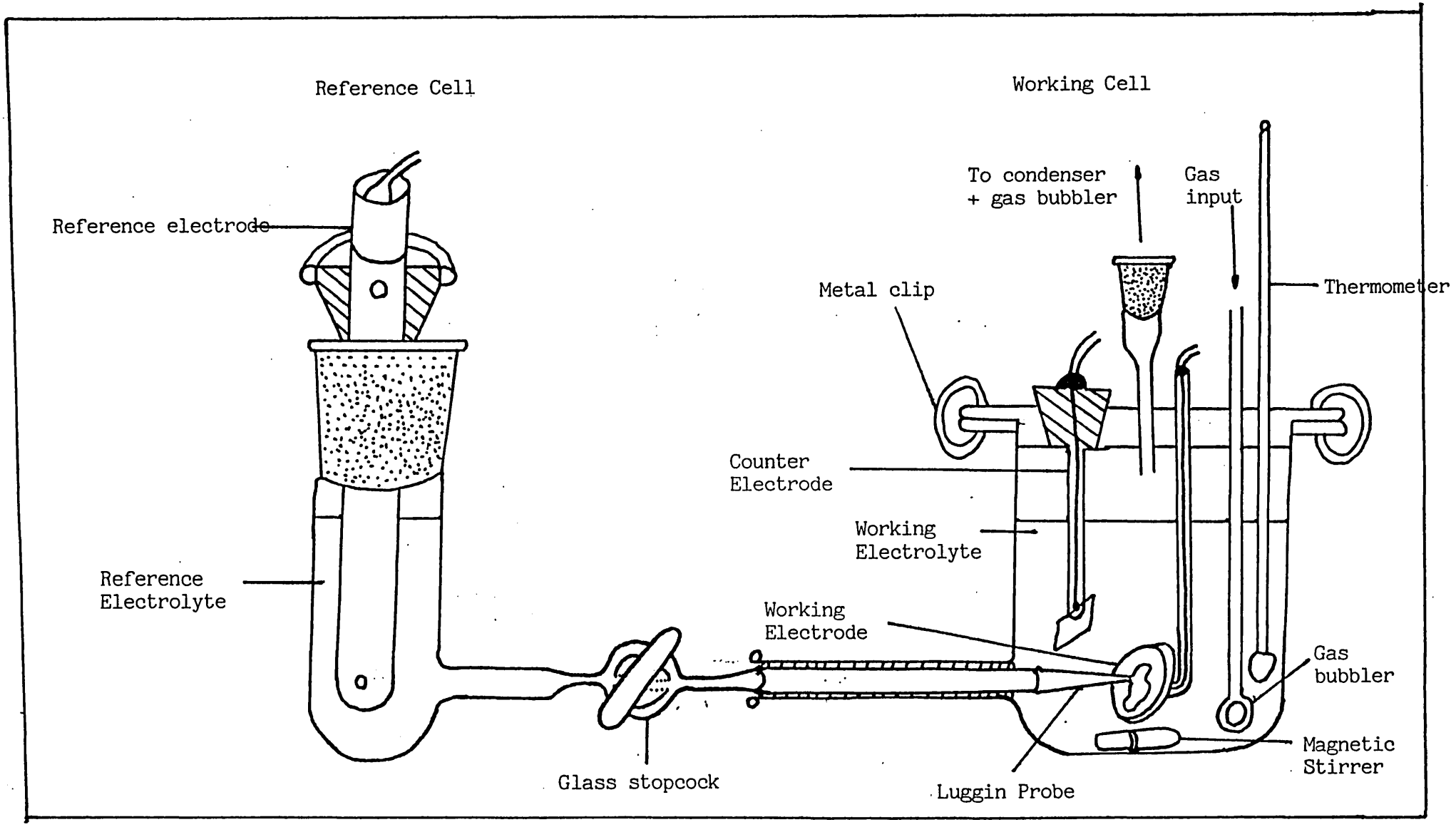


FIG. 3. A schematic diagram of the electrochemical cell.

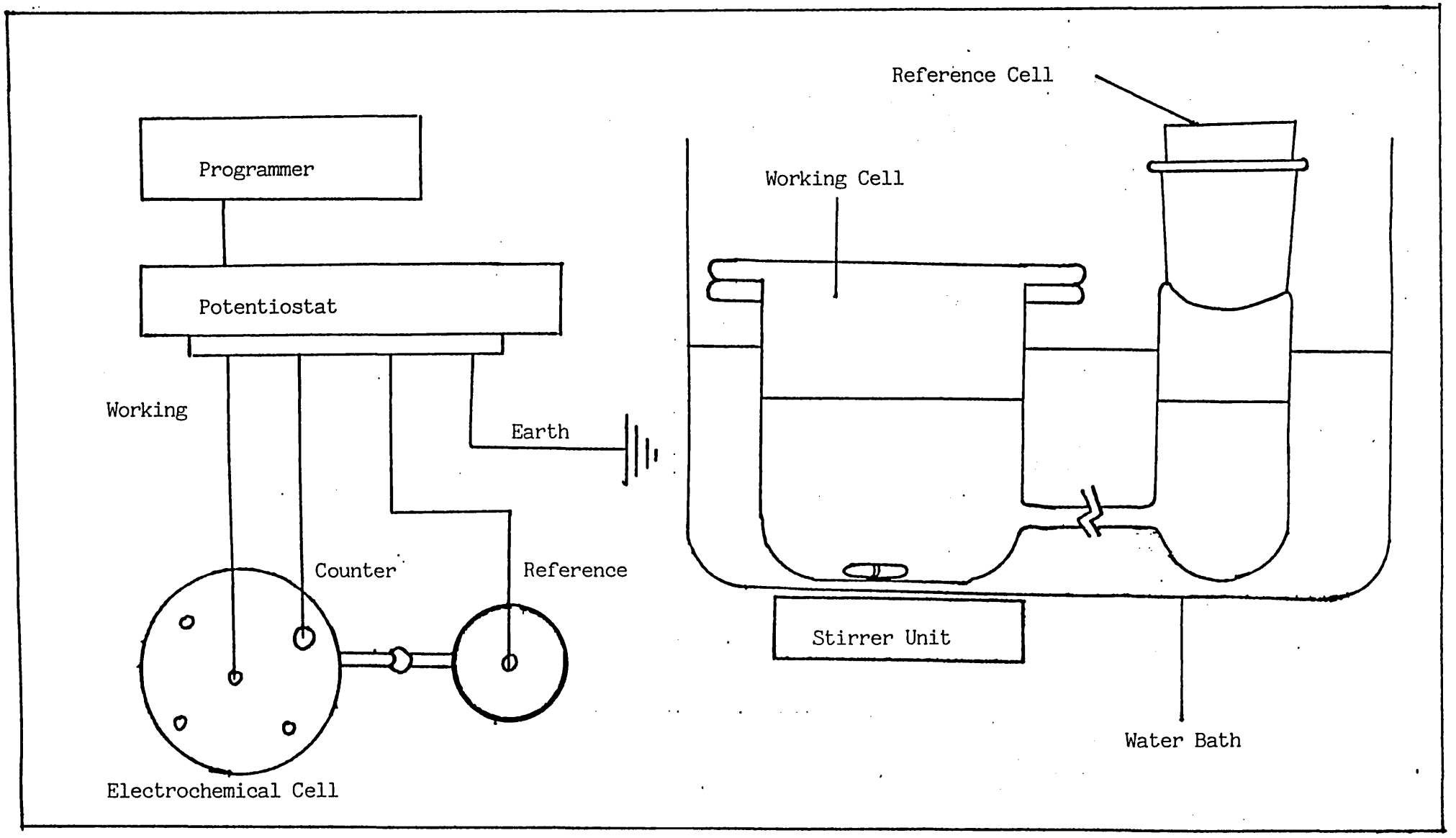


FIG. 4. A block and schematic diagram of the electrochemical system.

that there was a positive pressure of nitrogen within the cell. The lid was connected to the flanged top of the working cell with two metal clips.

If stirring was required, a magnetic stirrer bar was placed in the cell and powered by a magnetic stirrer unit (Gallenkamp). Heating was effected by partially immersing the cell in a water bath at the appropriate temperature. All electrochemical experiments were performed at either 30 or 25°C.

In all studies the counter electrode employed was a platinum flag ($\sim$0.25 cm^2 in area), and the reference electrode was a standard mercurous sulphate reference electrode. The reference half cell reaction and standard reduction potential at 30°C are:

$$Hg_2SO_4 + 2e^- \longrightarrow 2Hg + SO_4^{2-} \qquad (78)$$

$$E^\circ_{30^\circ C} = +611.1 \text{ mV S.H.E.}$$

The sign and polarity conventions used in this work are those of the Stockholm Convention. See Appendix I.

Potentials or currents were applied to the working electrode by a potentiostat Galvanostat (EG and G Princeton Applied Research, Model 363) in conjunction with a universal programmer (EG and G Princeton Applied Research, Model 175). With this configuration various current and potential profiles could be applied to the cell at different rates,

thus allowing standard electrochemical experiments to be performed.

The resultant current and potential profiles were recorded on either an X-Y recorder (RDK Rikadenki) or an X-t recorder (Linseis flat bed series LS4) or both, as appropriate. Measurements of potentials were also made using a digital voltmeter (Schlumberger Solartron 7040).

2.1.3.2 Electrode Fabrication and Preparation

2.1.3.2 (i) Solid UO_2 Electrodes.

(a) Fabrication

The UO_2 slab was cut with a diamond saw, such that the area of the large faces varied from 0.4 - 1.4 cm^2. The piece of UO_2 was placed face down in a mould and set in epoxy resin such that a disc of only slightly greater thickness than the UO_2 was produced. This disc was polished with silicon carbide paper (600 A grade) until the full area of UO_2 on each side of the disc was exposed.

The disc was then replaced in its mould and mercury poured into the mould to act as an electrical contact. This electrode was used as a cathode in an acidified copper sulphate bath. The anode was copper foil. A current of 10 mA cm^{-2} was applied to the cell for one hour, with the result that copper was plated on to the exposed face of the UO_2. This method was found to give an intimate and durable ohmic contact.

Copper wire was then fixed to the copper contact using silver loaded epoxy resin. It was found that soldering the joint caused the contact to peel away from the UO_2.

The electrochemical plating and silver epoxy contact process was repeated to give an ohmic contact on both sides of the UO_2. The resistance of the assembly was then measured by passing currents of 1 μA to 10 mA and measuring the potential. Table 4 shows the resistivities data six electrodes made with the slab UO_2, and measured by the method described above.

TABLE 4: Resistivity data for six electrodes used in this project

Electrode Identity	Resistance 10 μA-10 mA (Ω)	Surface area (cm^2)	Thickness (cm)	Resistivity (Ωcm)
A	290	0.631	0.559	327.3
B	90	0.691	0.559	111.2
C	99	0.740	0.559	131.0
D	70	1.425	0.559	178.4
E	140	1.014	0.559	253.9
F	100	0.777	0.559	138.9

Resistivity comprehends the size as well as the resistance of the object concerned. Resistivity is defined mathematically as:

$$\rho_{T=T} = R_{T=T} \frac{S}{L} \tag{79}$$

$\rho_{T=T}$ = Resistivity at T=T (Ωcm)

$R_{T=T}$ = Resistance at T=T (Ω)

S = uniform cross sectional area (cm^2)

L = constant length through which current is forced (cm)

As the same UO_2 was used in all electrodes, the measured resistivity should be very similar. An explanation for the apparent diversity of values displayed in the data of Table 4 is simply that the copper contacts on the UO_2 faces is better in some cases than others.

Graph 1 shows the measured potential of the electrodes plotted against the current imposed on it. The straight lines lead to two main conclusions. They are:

(a) Although the copper contacts are not equally good, all the joints are ohmic in character.

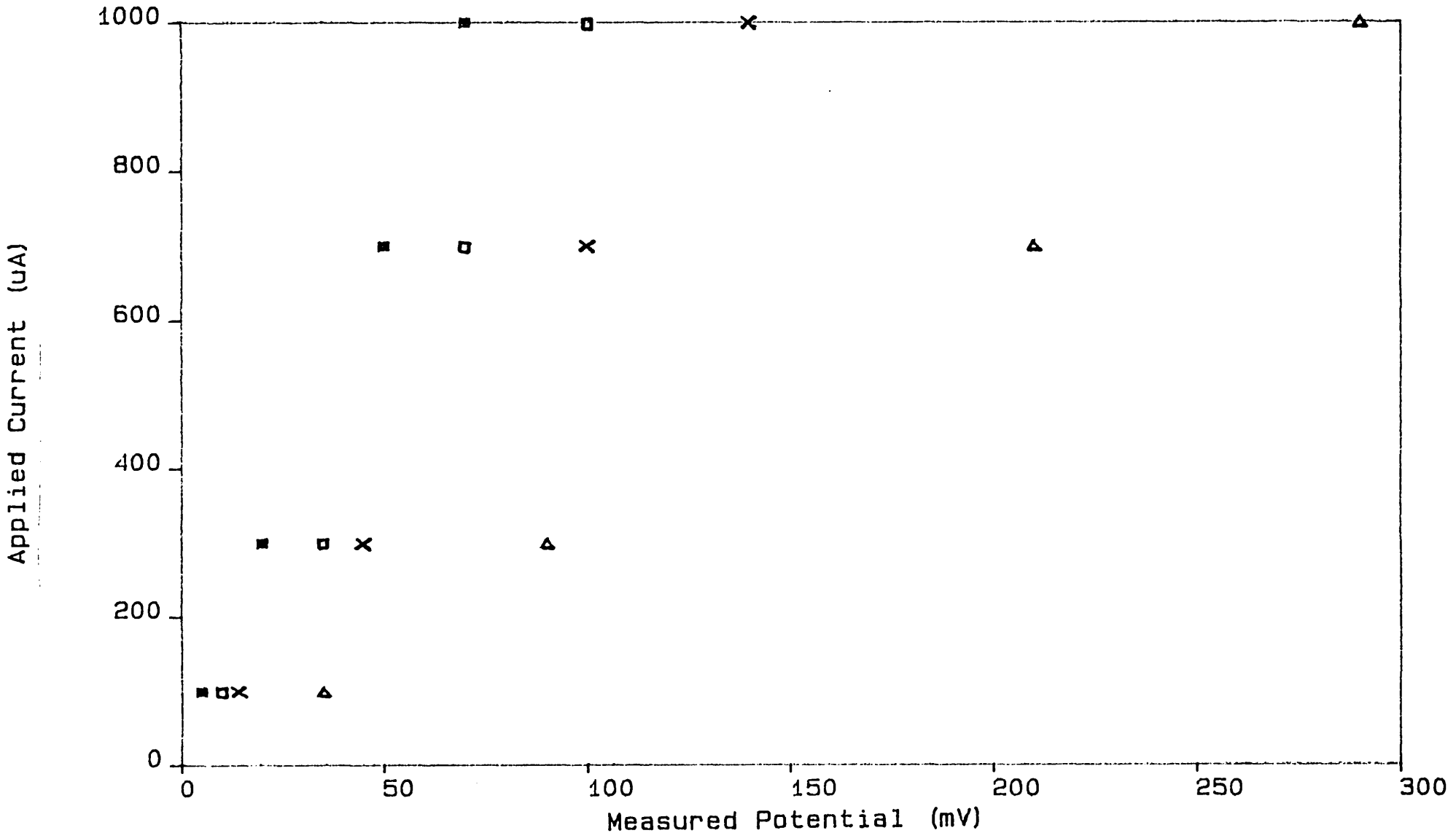
(b) The implications for the electrode behaviour are that the resistance does not change with current.

After the resistivity measurements had been completed, one of the ohmic contacts was removed. A glass tube, which afforded protection to the copper wire, was then fixed to the ohmic contact, and the whole assembly made water tight and secure with epoxy resin (Araldite rapide).

The exposed face of UO_2 was then polished using silicone carbide (600A grade) to totally remove any traces of copper or silver loaded epoxy resin.

Figure 5 shows a schematic diagram of a completed electrode.

Graph 1 The Measured Impedance of some Uranium Dioxide Electrodes



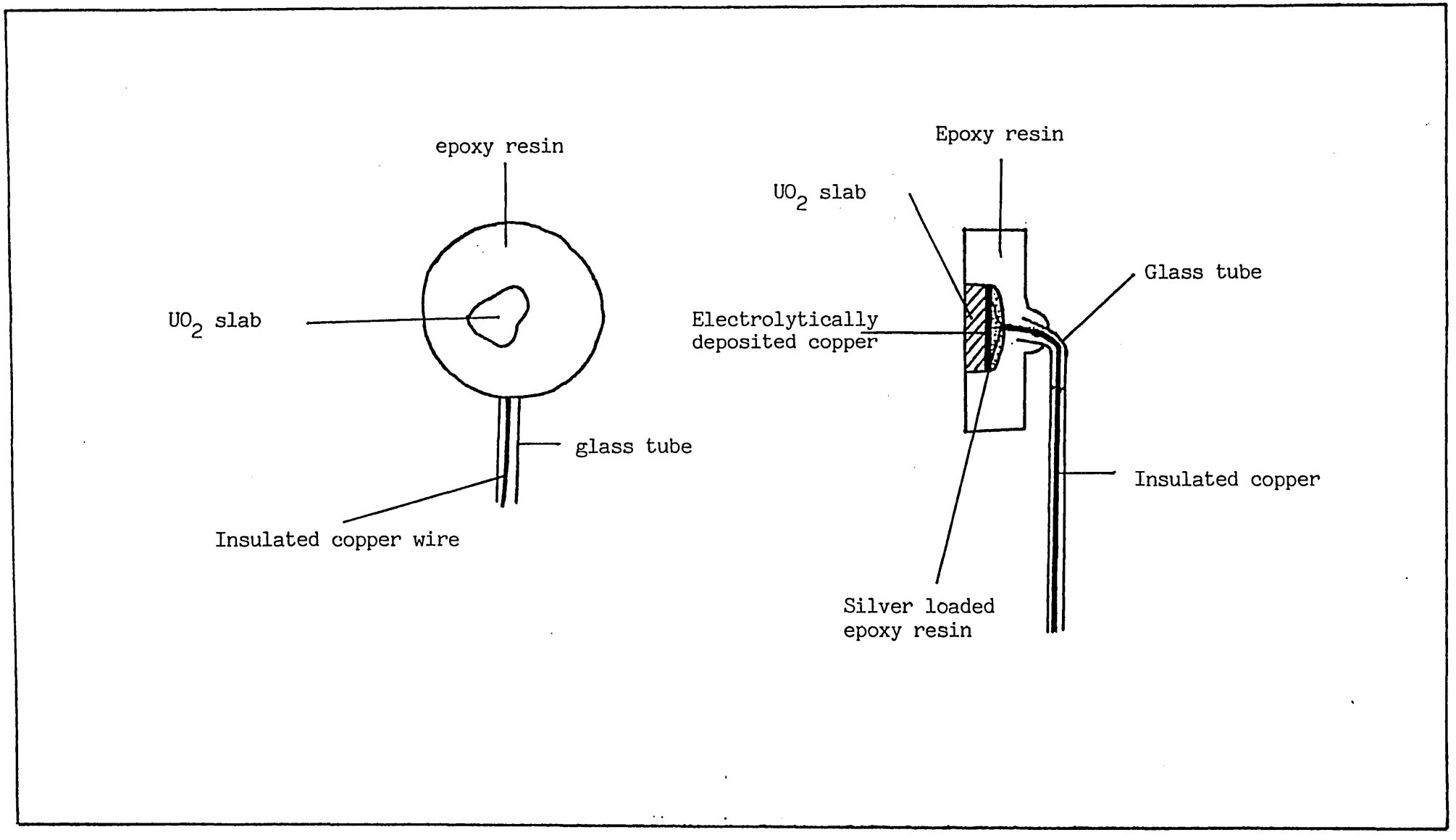


FIG. 5. A schematic diagram of a UO_2 electrode.

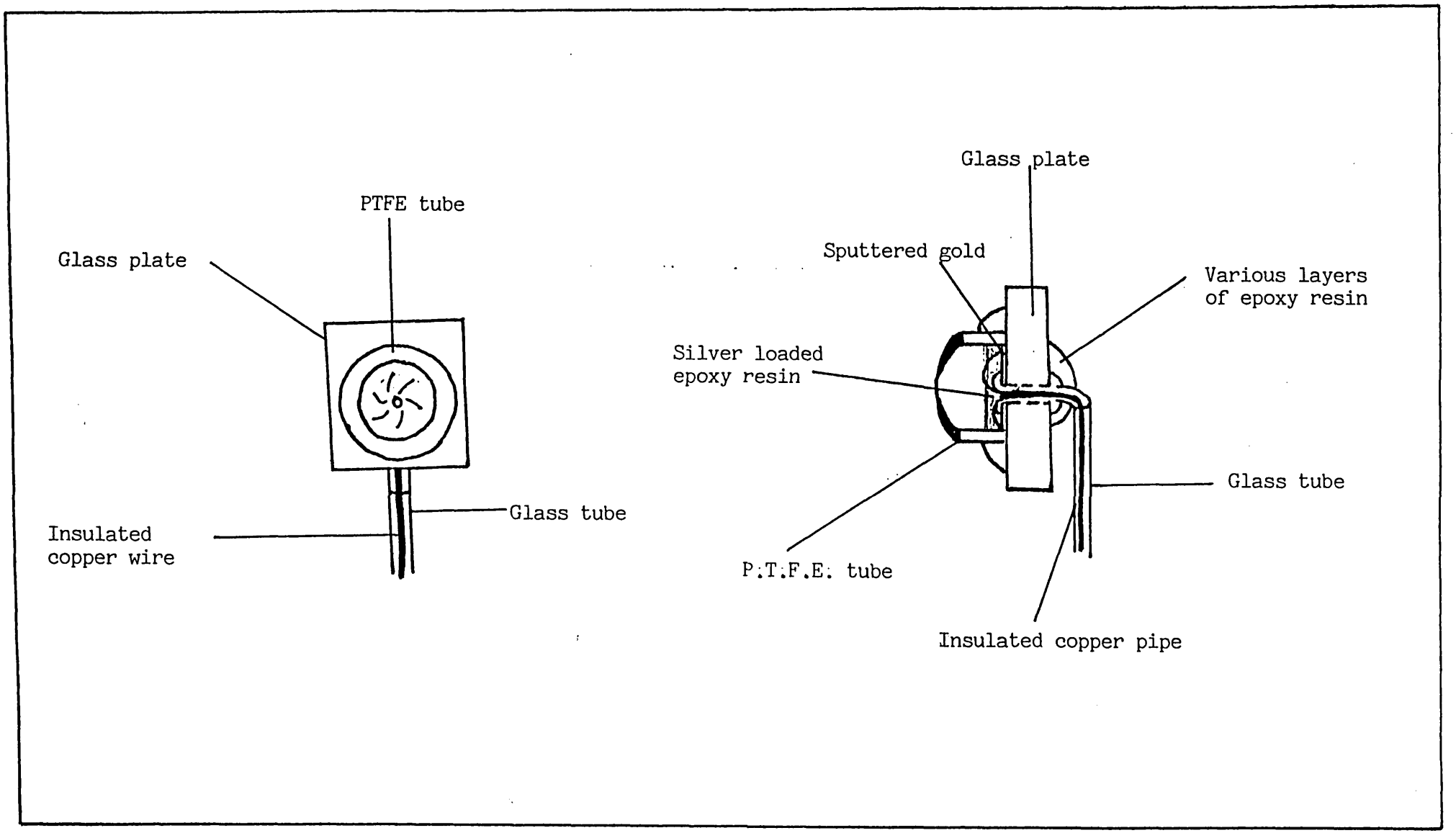


FIG. 6. A schematic diagram of the carbon paste electrode holder.

(b) Preparation

Every electrode was polished with silicone carbide paper (600A-grade) on a metallurgical polishing wheel. This was the standard surface preparation employed throughout this project and was found to give reproducible results. However, in some specific experiments, the surface was polished to 2 μ using a metallurgical polishing wheel and diamond polishing solutions. Wherever this non-standard surface preparation is used, it is noted in the results.

2.1.3.2 (ii) Carbon Paste Electrodes.

2.1.3.2 (ii) (a) Fabrication of Holder.

The carbon paste electrode holder consisted of a rectangular piece of glass (2 x 3 x 0.5 cm) with a small hole (0.25 cm) drilled between and connecting the two large faces. An area of approximately (1 x 1.5 cm) centrally on one face of the glass was sputtered with gold (using a Technics "Hummer"), to a thickness of 100 Å.

A length of insulated copper wire was then threaded through the hole and fixed to the gold contact using silver loaded epoxy resin. A small tube of P.T.F.E. was fixed on top of the contact using epoxy resin (Araldite rapide). The same epoxy resin was also used to cover the exposed epoxy and gold contacts, and to make the whole assembly waterproof.

A piece of glass tubing was fixed centrally to the rear of the assembly with epoxy resin (Araldite rapide).

The copper wire contact was inside this tube. The rear of the assembly was made waterproof using the same resin.

Finally a small amount of liquid epoxy resin was poured into the glass tubing on the rear of the electrode to prevent any ingress of electrolyte into the assembly via the entry hole for the copper wire.

A schematic diagram of the carbon paste electrode holder appears in Figure 6.

2.1.3.2 (ii) (b) Electrode Preparation.

The carbon paste electrodes were prepared by first tightly packing the base of the electrode holder with carbon paste blank, and then packing a thin layer (approximately 3 mm) of uranium oxide paste on top of the carbon paste blank.[70]

The carbon paste blank was prepared by completely mixing lamp black (5 g) with liquid paraffin (2 mls) in an agate mortar and pestle. This mixture was also used as the blank electrode in pilot tests.

The uranium oxide paste was prepared by thoroughly mixing the appropriate Uranium oxide (1.5 g) with lamp black (3.5 g). This mixture was then mixed with liquid paraffin (2 ml) as with the carbon paste blank.

2.1.3.3 Preparation of Electrolyte Solutions

Usually, the electrolyte solutions were prepared as required for each experiment. The major electrolyte in all electrochemical experiments was sodium sulphate (1 M). A large stock (1 L) of sodium sulphate (1 M) was kept.

If any hydrogen peroxide or peroxymonosulphuric acid were required, they were pipetted into a 250 ml beaker containing about 60 mls of sodium sulphate (1 M). The pH was then adjusted to approximately 0.1 pH units lower than the required value, using sulphuric acid (1 M) or sodium hydroxide (1 M). If the additions were such that the total sulphate concentration of the electrolyte in the beaker was less than about 0.9 M, sodium sulphate was added to the beaker so that the total sulphate concentration $\geq$ 1. The pH was readjusted as before. The contents of the beaker were then quantitatively transferred to a 100 cm^3 volumetric flask with a little sodium sulphate (1 M) and made up to the mark with the same. The pH was checked.

In one particular experimental set, the goal was to ascertain the effect of sulphate (at fixed pH) on the anodic half cell reaction (UO_2 to UO_2^{2+}). In these cases the required amount of sulphate (as sulphuric acid (1 M) and/or sodium sulphate as appropriate), was added to the flask, and no more sulphate was added. The volumetric flask was made up to the mark with water.

The other problem with this particular experimental set was adjusting the pH after the required amount of sulphate had been added (as sulphuric acid). This problem only occurred on very few occasions and was circumvented by adjusting the pH with perchloric acid.

Occasionally, a larger volume of electrolyte was prepared for a number of experiments. On these occasions the procedure was the same as that described above, except on a larger scale, typically 1 litre.

2.1.3.4 (i) General Dissolution Procedure

The cell (see Figure 3) was thoroughly dismantled, washed, and dried. Those parts that required it were thoroughly degreased with acetone. The stopcock (between the working and reference compartments) was thoroughly greased and assembled. The Luggin plunger was thoroughly greased. With the stopcock open, the reference cell was filled with electrolyte solution so as to exclude air bubbles from the stopcock and Luggin probe. Some electrolyte was allowed to flow through the Luggin probe, and the stopcock was worked to ensure a thin film of electrolyte was present between the barrel and walls of the stopcock. The stopcock was then closed. The reference and working compartments were then assembled by sliding the greased Luggin plunger into the Luggin barrel. The working compartment was then filled to the mark with electrolyte, and the reference electrode fitted.

The thermometer, condenser holder, counter and previously prepared working electrodes were then fitted into the lid, which was clipped to the top of the working compartment. When the lid was fixed, the working electrode was in a partially retracted position so that at no time was it in contact with the electrolyte. The cell was then clamped into the water bath.

Once in the bath, taking care that the potentiostat was in the disconnected mode, the reference, counter and working electrodes were appropriately connected to it. The gas bubbler was then connected to the cell via the condenser, and the input bubbler was connected. The nitrogen and water supply to the condenser were turned on. The cell was then left for one hour to degas and reach the appropriate temperature.

After this time the potentiostat was set for the electrode pre-treatment (3 minutes at -1.8 V (SHE) for solid UO_2 electrodes and -0.38 V (SHE) for carbon paste electrodes), and put into the connected mode. The working electrode was then lowered into the electrolyte and the Luggin probe was adjusted appropriately.

After the 3 minute pre-treatment, the electrochemical experiment was initiated, usually by connecting the programmer (in the initial mode) to the potentiostat.

In the few cases when the effect of the amount of sulphate in the working cell was the subject of the

experiment, the reference cell and Luggin probe were filled with sodium sulphate (1 M). This presented practical problems because of the diffusion of sulphate into the working cell from the Luggin Probe. This will be discussed more fully in the practical applications section.

2.1.3.4 (ii) Electrochemical and electrolytic experiments

(a) Electrolytic Experiments

The electrolytic experiments performed in this work along with the manner in which the results were collected appears below in summary form. Appendix 1 contains a discussion on the various experimental methods, as well as an explanation of how the various methods were used in this project. The electrolytic experiments carried out in this project are summarised in Figure 7.

(1) Chronoamperometry

A constant potential is imposed on the system, and the current is measured. In this work, chronoamperometry was used to determine steady state currents for the electrode-kinetic order and Tafel slope determinations.

(2) Linear Sweep and Cyclic Voltammetry

A potential ramp is applied to the system at a constant rate. The potential-current transient is recorded. This can yield much qualitative information about the

oxidation mechanism. Cyclic voltammetry was the major type of sweep voltammetry used in this project. It was used with solid UO_2 electrodes and carbon paste uranium oxide electrodes. In all cases the standard scan rate used was 20 mV sec^{-1}.

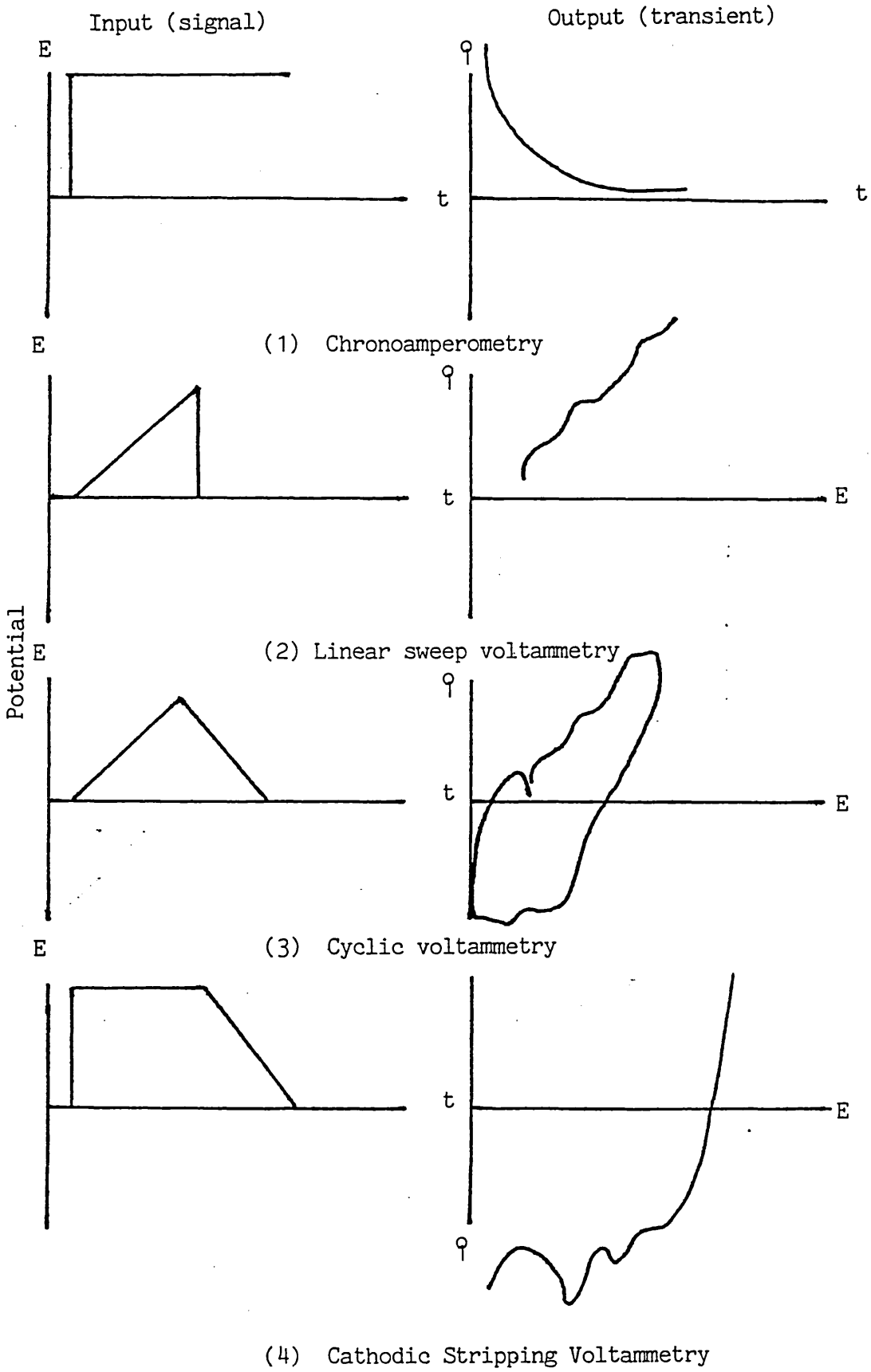
(3) Cathodic stripping voltammetry

A constant anodic potential is imposed on the system for a known time, followed by a constant rate cathodic ramp. The current-time and current-potential transients are simultaneously recorded. By varying the amount of time and potential of the initial polarisation section, information on the identity of the intermediates formed at different potentials can be obtained. By integration of the current-time and current-potential transients, film thicknesses can be calculated. In this work, this technique was used extensively. The polarisation potentials ranged from 111 mV SHE, the times ranged from 10 to 4000 seconds. The scan (strip) rate was 20 mV sec^{-1} in all cases. The charges were calculated by cutting out the paper under the curves and weighing it on an analytical balance. In all cases the cathodic boundary condition was -581 mV SHE.

(b) Electrochemical experiments.

The electrochemical experiments performed in this work were carried out within the chemical leaching studies. They comprised measuring the corrosion potential imposed

FIG. 7. A summary of the electrolytic experiments carried out in this project.



by different concentrations of hydrogen peroxide and peroxymonosulphuric acid under different conditions of temperature. The experimental procedure is identical to that which appears in Section 2.1.2.3., with the following additions:

(a) The uranium dioxide electrode was retracted out of the leaching solution and not allowed to come into contact with it until the uranium dioxide spheres were added to the reactor.

(b) The uranium dioxide electrode and the mercurous sulphate reference electrode were suitably connected to a digital voltmeter.

(c) Sampling was achieved by removal of the mercurous sulphate reference electrode.

The area of the uranium dioxide electrode was taken into account when calculating the equivalent current density.

In a few cases, the corrosion potential was measured in situations with low concentrations of sulphate present. When this was necessary, the electrochemical cell with Luggin probe and magnetic stirring was used. In these cases the experimental procedure which appears in Section 2.1.3.4 (i) was followed, except that no nitrogen was bubbled.

2.1.4 Methods of Analysis

2.1.4.1 Introduction

Analysis has played a major part in this project. All the rate data in the chemical kinetic studies, and the elucidation of the partial anodic currents for hydrogen peroxide and peroxymonosulphuric acid hinge on the analysis for uranium in solution.

The composition data for the chemical kinetic data rely on the atomic absorption spectroscopic analysis for sodium and potassium, as well as analysis for sulphur by inductively coupled plasma spectroscopy.

Obviously, many 'wet' analytical methods were used in this work, but not all those methods will be discussed here, although references to the detailed descriptions of those analyses will be given. Only those methods that have been specifically adapted or repeatedly used in this project will be discussed in any depth.

2.1.4.2 Determination of Uranium in Solution

The method employed for the determination of uranium was a modified version of that developed by Johnson et al.[84,85] This modified method was fully described by Sajik.[26] Interested readers are referred to that work for a full list of reagents. Only the particular format employed in this project will be outlined here, and the method discussed.

The original method was designed to determine the concentration of uranium in the presence of various other ions resulting from the leaching of ores in natural waters and phosphoric acid systems. The analysis is a two stage process consisting of a selective solvent extraction into a tri-octylphosphine oxide (T.O.P.O.) phase, followed by colorimetric analysis for uranium as the 2-(5-Bromo-2-pyridylazo)-5-diethylaminophenol (P.A.D.A.P.) complex.

The format of the method used in this project is as follows:

(a) Solvent extraction.

- into a 50 ml volumetric flask
- add uranium solution to be analysed. The volume chosen should be such that the maximum uranium content $\leq$400 µg ml^{-1}.
- add 10 ml HNO_3 (9 M) solution,
- add 5 ml NaF (20 g/litre) solution,
- add 2 ml ascorbic acid (50 g/litre) freshly prepared solution, mix.
- add 5 ml T.O.P.O. solution (38.6 g/litre in cyclohexane).
- make up to 50 ml with distilled water. Shake thoroughly for at least two minutes, venting the pressure as required. Allow the phases to settle overnight.

(b) Analysis.

- into a 25 ml volumetric flask
-add 2 ml of above separated T.O.P.O. solution.

- add 1 ml of dilute complexing agent, pH = 8.35.

- add 4 ml of bromo-P.A.D.A.P. solution (0.5 g/litre in absolute ethanol)

- add 1 ml buffer, pH = 8.35.

- shake thoroughly and leave overnight for the colour of the complex to develop.

- add 16 ml ethanol (absolute)

- make up to 25 ml with distilled water, mix well and leave for at least 15 minutes.

- measure absorbance at 574 nm, in $\frac{1}{2}$ cm silica cells as appropriate.

Optical density measurements were made on a Unicam SP6-200 spectrophotometer, using the blue photocell. Reagents were not taken directly from stock solutions, but approximate quantities were poured into beakers and the residues discarded.

Most of the reduction and complex reactions were designed to remove interference from specific metal ions, but pilot work determined that due to the presence of oxidizing agents and possibly trace impurities, the additions were necessary to get reproducible results. In the original method the ascorbic acid reduced cerium and vanadium. The fluoride complexed zirconium and thorium, both stages preventing extraction of these metals into the T.O.P.O. phase.

The normal quantity of uranium solution analysed was 1 ml. It was found that the most reproducible way

of delivering this solution was by the use of an automatic pipette (Oxford-macro pipette). This method was compared to the use of a diluter (Hook and Tucker Instruments), and to the use of bulb pipettes (1 ml). The use of the automatic pipette is not a precise method of volume delivery, (to within 1-2%) but it is extremely reproducible and it is this reproducibility that is paramount in an analysis of this nature. Because of this reproducibility, and because of practical considerations, most of the additions in this method were performed using this instrument. The exceptions to this were the additions of ethanol and extractions of T.O.P.O. solution, which were performed with a 15 ml bulb pipette (with a stem, recalibrated at 16 ml), and a grade A 2 ml bulb pipette respectively.

As this analysis is a comparative method, blanks were prepared from the initial leach liquors. Comparison of these blanks with blanks of water, revealed no detectable difference in abosrbance of the final bromo-P.A.D.A.P. solutions.

Normally, four standards (100, 200, 300 and 400 ppm) were employed. Pilot tests showed that the detection limit of the above procedure was 5 ppm, and the sensitivity was 10 ppm.

In a different procedure which involved 25 mls of sample in a 100 ml volumetric flask and which was not used in this project, the detection limit could be lowered to 0.4 ppm, and the sensitivity to 0.7 ppm.

The absorbence scale on the Unicam SP6-200 covers the range from 0 to 2 absorbence units. Using the main procedure above, this corresponds to 0 to 300 ppm uranium. Pilot tests showed that the optical density plotted against the uranium concentration was a straight line over the whole range. However, samples were usually less than 400 ppm and only the very occasional sample was measured outside the calibrated range and this is not a recommended practice.

Pilot tests showed that sulphate concentrations up to 3.0 M, or the presence of hydrogen peroxide and peroxymonosulphuric acid up to 0.5 M had no effect on uranium extraction, except where the concentration of hydrogen peroxide was such to cause precipitation of uranium peroxides ($UO_4.2H_2O$ and $UO_4.4H_2O$). Precipitation of $UO_4.2H_2O$ makes sampling, pipetting and extraction uncertain. No sample was analysed in which any precipitate was observed.

The analysis process tended to be time-consuming. In any five day cycle, the first two days were spent doing runs, and the last three days spent in analysis, including all preparation times, analyses and thorough organic removal from, and washing up of, glassware. The maximum recommended number of samples analysed on this time scale would be 70. This includes standards and blanks.

2.1.4.3 Other Methods

(i) Determination of sodium and potassium in solution.

The determination of the concentrations of sodium and potassium in leaching solutions was achieved by atomic absorption spectroscopy, using a Perkin-Elmer 2380 double beam spectrophotometer. This machine employs deuterium arc background correction and microprocesser controlled sampling procedure.

Because of the very large concentrations of sodium and potassium to be measured (up to 3 M) the burner was turned at an angle of 45° to the detector, and the less sensitive wavelengths were used in the determinations. The sampling pattern chosen for each sample was 10 readings at 1 second intervals. The machine then gave the mean and standard deviation of those observations.

All samples were diluted by a factor of 50 before analysis. The dilution was performed using (0-0.1 ml) automatic pipette and volumetric glassware. Pilot tests showed that the precision of the automatic pipette when delivering 0.500 mls was $\pm$0.002 mls. (This is equivalent to $\pm$0.4%). At least 5 samples were analysed from each run.

All the determinations were carried out in accordance with principles of use of the spectrophotometer,[87] and the methods used were adapted from the Perkin-Elmer 'cookbook'.[88]

The standards for both sodium and potassium were prepared from Analar sodium or potassium sulphate which had been ignited at 600°C for 24 hours.

The determinations for sodium were carried out at a wavelength of 330.2 nm with a slit width of 2.0 nm. The relative sensitivity under these conditions is 185. The determinations for potassium were carried out at a wavelength of 404.4 nm with a slit width of 2.0 nm. The relative sensitivity under these conditions is 500. In all cases the light source was a hollow cathode lamp, and an air/acetylene flame (lean and oxidising) was used. A calibration check was carried out every five samples.

Pilot tests involving thirty dilutions and determinations on identical samples showed the method to be reproducible to within $\pm$2% of the measured quantity (standard deviation = 16.2 ppm).

(ii) Determination of sulphur in solution.

The samples were submitted to the Department of Geology ICP service. ICP is a form of emission spectroscopy. The major difference between ICP and other emission techniques is the much higher temperatures encountered in an argon plasma, typically 10,000 K. ICP is obviously a destructive method of analysis, but this in turn means that the molecular state of the element to be determined does not affect the response. Those readers requiring a fuller guide to ICP are directed to reference 68.

The reason for the analysis for total sulphur in the 10 runs was due to a lack of density data for the peroxymonosulphuric acid used in these runs. Five samples from each run were analysed. The samples were diluted 1000 times in three stages. Each stage represented a dilution of ten times. Grade A volumetric glassware was used throughout. The standards were prepared from Analar sodium sulphate which had been ignited at 600°C for 24 hours.

Pilot tests on standards designed to quantify the total error of the combined dilution and determination yielded a result of $\pm$0.9% on the measured quantity.

(iii) Analysis of peroxymonosulphuric acid and hydrogen peroxide.

The method employed for the determination of peroxymonosulphuric acid and hydrogen peroxide is a modified version of that which appears in Vogel.[89] The modified method appears in a publication of Interox Chemicals Ltd.[74]

The method is based on the fact that hydrogen peroxide does not react with arsenious oxide but will react with Ce IV at room temperature without a catalyst (80), whereas peroxymonosulphuric acid and Ce IV will react with arsenious oxide only in the presence of osmic acid (82). Equation (81) expresses the prior dissolution of arsenious oxide in an alkaline medium.

$$H_2O_2 + H_2SO_4 + 2Ce(SO_4)_2 \longrightarrow Ce_2(SO_4)_3 + 2H_2O \quad (80)$$

$$As_2O_3 + 4OH^- \longrightarrow 2HAsO_3^{2-} + H_2O \quad (81)$$

$$H_2O + 2Ce^{4+} + H_3AsO_3 \longrightarrow H_3AsO_4 + 2Ce^{3+} + 2H^+ \quad (82)$$

Extreme caution was exercised in the handling of arsenious oxide and osmic acid, the latter only being used in a fume cupboard.

The total acidity of Caro's acid was also determined by titration against standardised sodium hydroxide (1 M).

(iv) Other methods.

All the acids used in this project were standardised using Analar sodium carbonate (dried for 24 hours at 105°C), as the primary analytical standard. These standardised acids were then used as secondary analytical standards to standardise the sodium hydroxides used in this project.

Details of these common analyses are described in Vogel.[89] All analytical practice was as far as possible within the conditions laid down for external analysis.[90]

2.1.5 TREATMENT OF KINETIC RESULTS

2.1.5.1 Generation of Rate Curves

The crude experimental results were processed by a computer program called Sarah. This program which appears in Appendix 2, recognised and compensated for the

fact that periodically, when a sample was taken, the total volume of leach liquor was reduced. The programme calculated the fraction of the UO_2 dissolved (α), $1-(1-\alpha)^{\frac{1}{3}}$, and $1-\frac{2}{3}\alpha-(1-\alpha)^{\frac{2}{3}}$ at time = t (minutes). Initially other models were calculated, but it was found that $1-(1-\alpha)^{\frac{1}{3}}$ gave a satisfacory fit to experimental data. The rate plot was then constructed manually, using the $1-(1-\alpha)^{\frac{1}{3}}$ versus time data, as below.

$$\frac{dn}{dt} = \frac{d\alpha}{dt}.\ n_o = \frac{df(\alpha)}{dt}.\ 3n_o = Ak_o k'[A]^x \qquad (83)$$

where: $\alpha = \frac{n}{n_o}$

n = number of moles of UO_2 dissolved

n_o = initial number of moles present

V = the particle molar volume ($cm^3 mole^{-1}$) = $\frac{M}{\rho}$

M = molecular mass

ρ = density ($g\ cm^{-3}$)

t = time (sec)

α = fraction of UO_2 dissolved

k_o = concentration of potentially reactive sites (cm^{-2})

k' = rate constant ($cm^3 sec^{-1}$)

$f(\alpha) = 1-(1-\alpha)^{\frac{1}{3}} = k_L t$

$k_L = \frac{[A]^x V k_o k'}{r_o}$

r_o = initial radius of UO_2 sphere (cm)

The use of $1-(1-\alpha)^{\frac{1}{3}}$ extends the initial linear region of rate plot, so that a reliable initial rate can be measured.

If any point on the plot was obviously in error, it was disregarded. If more than one point was in error, or it was not possible to delineate a unique line through the data, the run was omitted from the kinetic evaluation. Initially linear regression was used to calculate the reaction rates, but it was found to be unnecessary if the above method was used.

2.1.5.2 Calculation of Concentrations

The concentrations of sulphate, bisulphate and hydrogen ion were calculated using the computer programs Nina and Nuna, for the hydrogen peroxide and peroxymonosulphate systems respectively. The programs use both the correlations of Lindstrom et al.[27] and Marshall et al.[28] Both of the computer programs, with the theoretical background appear in Appendix 3. The concentration calculations take account of total ionic strength and temperature.

2.1.5.3 Calculation of Potentials

The potential imposed upon the surface of UO_2 by both hydrogen peroxide and peroxymonosulphuric acid was measured in a number of runs representing the different concentrations of oxidising agents, ranges of pH and temperature encountered in the different kinetic runs. These data were then used in an empirical regression equation to interpolate for the potential. Both of the regression outputs along with the data bases used to generate them

appear in Appendix 2. It is stressed that the derived equations have no theoretical basis, and were used only for the interpolation of potential values. The reason that the potential was not measured as a matter of course in all runs, were twofold:

(1) When sampling involves the removal of electrodes, practical difficulties arise.

(2) In situations of low sulphate concentrations, it is not possible to measure accurately the potential imposed upon the UO_2 surface without the use of a device which performs the same function as a Luggin probe. It is not possible to mount a Luggin probe in a kinetic cell, and maintain comparable conditions within that cell.

2.1.5.4 The Absolute Rate Equation

a) Theoretical Basis of the Absolute Rate Equation

The rate of a complex electrochemical reaction under Tafel conditions of oxidation is described by the Butler-Volmer equation (84).

$$i = nFk_b^o [A]^x \ldots \exp \frac{-\overleftarrow{\alpha} FE}{RT} \qquad (84)$$

$$\text{But,} \quad V = \frac{i}{nF} \qquad (A10)$$

where $V = \frac{dn}{dt}$ = reaction rate (mols $cm^{-2} sec^{-1}$)

and all other symbols retain their usual meanings.

Therefore:

$$V = k_b^o [A]^x \,..\, \exp \frac{-FE\overleftarrow{\alpha}}{RT} \tag{85}$$

But, $$k_b = k_b{}^o \exp \frac{-nFE\overleftarrow{\alpha}}{RT} \tag{A37}$$

After rearrangement,

$$k_b^o = k_b \exp \frac{+\overleftarrow{\alpha}nFE}{RT} = k_b \exp \frac{-\Delta G^{\neq}_{e,cont.}}{RT} \tag{86}$$

and, by Arrhenius Equation,

$$k_b = A \exp \frac{-\Delta G^{\neq}_{o,c}}{RT} \tag{A5}$$

Therefore, by substitution of equation (A5) into equation (86), and then substitution of the resultant into equation (85), one obtains equation (88). (n=2)

$$V = A \exp \frac{-\Delta G^{\neq}_{o,c}}{RT} \; [A]^x \,...\, \exp \frac{+\overleftarrow{\alpha}FE}{RT} \tag{88}$$

Taking logs. of both sides

$$\log V = \log A - \frac{\Delta G^{\neq}_{o,c}}{2.303RT} \pm x\log[A] \,..+ \frac{\overleftarrow{\alpha}FE}{RT.\ 2.303} \tag{89}$$

where A is a complex constant, and all other symbols retain their usual significance. Equation (89) is referred to as the absolute rate equation, and is applicable at E = E, and T = T. By using this type of analysis, the effects of potential on both the rate of reaction and the

activation energy (hence the rate constant), can be differentiated. Equation (89) is a straight line, and multilinear regression analysis can be applied to it. The non-concentration variables are: 1/T, and E/T.

b) The Basis of Choice of Concentration Variables

The concentration variables in the final regression were chosen by using the regression analysis itself as the indicator. All possible combinations of concentration variables (in the context of equation (89)) were used in successive regression analysis, and the minimum number of statistically relevant concentration variables which gave the best fit were chosen.

TABLE 2. Comparison of X.R.D. pattern data A.S.T.M. No. 31-1424 (U_3O_8) with the patterns of the product of the stoichiometry determination of the UO_2 used in the chemical kinetic runs and the UO_2 used in the electrode fabrication.

A.S.T.M. standard pattern No. 31-1424 Orthorhombic U_3O_8 (Theoretical)		Product of the stoichiometry determinations of different UO_2.			
		The UO_2 used in chemical kinetics		The UO_2 used in electrochemical studies	
dÅ	Int. (I/I_{100})	dÅ	Int.	dÅ	Int.
4.15	98	4.17	s	4.13	s
3.43	100	3.40	s	3.41	s
3.36	45	3.32	ms	3.34	ms
2.64	62	2.64	ms	2.62	ms
2.61	29	2.60	m	2.59	m
2.07	13	2.06	m	2.06	mw
1.99	10	1.98	vw	1.97	w
1.95	17	1.94	mw,b	1.94	mw
1.80	10	1.78	vw	1.78	mw
1.77	21	1.76	m,b	1.76	ms,b
1.76	25	1.75	m,b	1.76	ms,b
1.58	10	1.57	mw,d	1.57	mw

TABLE 3. Comparison of X.R.D. powder patterns of uranium oxides used in this work with A.S.T.M. standards.

(a) Comparison of A.S.T.M. pattern 5-0550 (UO_2) with the pattern of the UO_2 (Koch-Light) that was used for synthesis and carbon paste electrodes. The pattern of the UO_2 used in the chemical runs is also given.

A.S.T.M. standard pattern No. 5-0550 Cubic UO_2		UO_2(Koch-Light) used in synthesis and carbon-paste electrodes.		UO_2 (UKAEA) used in chemical kinetic runs.	
dÅ	Int. (I/I_{100})	dÅ	Int.	dÅ	Int.
3.157	100	3.11 - 3.17	vs,b,d	3.11-3.17	vs,b,d
2.735	48	2.72	s	2.72	s
1.934	49	1.93	s,b	1.93	s,b
1.649	47	1.64	s,b	1.65	s,b
1.579	1.57	m,b	1.57	m,b	
1.255	18	1.25	m,b,d	1.25	m,b
1.223	15	1.25	m,b,d	1.23	m,b
1.116	13	1.12	mw	1.12	m
1.052	15	1.06	m	1.06	m
0.9243	15	0.91	m	0.91	m

TABLE 3 (continued)

(b) Comparison of A.S.T.M. pattern 24-1172 (U_3O_8) with the pattern of the U_3O_8 (Koch-Light) that was used for synthesis and carbon paste electrodes.

A.S.T.M. standard pattern no. 24-1172 Orthorhombic U_3O_8		U_3O_8 (Koch-Light) used in synthesis and carbon paste electrodes	
dÅ	Int. (I/I_{100})	dÅ	Int.
4.15	95	4.13	s
3.43	100	3.39	s
3.36	55	3.34	ms
2.64	75	2.62	ms
2.61	35	2.59	m
2.07	20	2.06	mw
1.99	14	1.97	w
1.95	20	1.94	mw
1.80	16	1.78	mw
1.77	25	1.76	s,b,d
1.76	50	1.76	s,b,d
1.71	14	1.70	w
1.58	18	1.57	mw
1.42	18	1.41	mw

TABLE 3 (continued)

(c) Comparison of A.S.T.M. pattern 15-4 (U_3O_7) with the pattern of the U_3O_7 synthesized and used in carbon paste electrodes.

Synthesised U_3O_7		A.S.T.M. 15-4 Tetragonal U_3O_7	
dÅ	Int.	dÅ	Int.
3.13	vs	3.14	100
2.72	ms,b	2.72	30
2.72	ms,b	2.70	20
1.92	s,b	1.93	40
1.92	s,b	1.92	25
1.64	s,b	1.64	20
1.64	s,b	1.63	15
1.57	mw	1.57	15
1.36	vw	1.37	5

TABLE 3 (continued)

(d) Comparison of A.S.T.M. pattern 32-1403 (U_2O_5) with the pattern of the U_2O_5 synthesised and used in carbon paste electrodes.

Synthesised U_2O_5		A.S.T.M. 32-1403 Hexagonal U_2O_5	
dÅ	Int.	dÅ	Int. (I/I_{100})
4.14	s	4.11	90
3.40	s	3.42	95
3.35	m		
3.13	s		
2.70	m		
2.63	m		
2.60	mw		
2.21	s	2.22	100
2.06	mw		
2.06	mw		
1.91	s		
1.78	m	1.78	40
1.76	m	1.77	45
1.75	m	1.71	50
1.63	ms	1.64	70
1.60	mw	1.58	20
1.35	mw	1.37	25
1.35	mw	1.36	30
1.27	w	1.28	16
1.13	mw	1.13	21
1.11	vw	1.10	11
1.06	w	1.07	14
1.02	w	1.03	14
0.93	w	0.94	11

TABLE 3 (continued)

(e) Comparison of A.S.T.M. pattern 16-207 ($UO_4.2H_2O$) and A.S.T.M. pattern 16-206 ($UO_4.4H_2O$) with the pattern of the $UO_4.2H_2O$ that was used for carbon paste electrodes.

$UO_4.2H_2O$ used in carbon paste electrodes.		A.S.T.M. 16-206 $UO_4.4H_2O$ (monoclinic)		A.S.T.M. 16-207 $UO_4.2H_2O$ (orthorhombic)	
dÅ	Int.	dÅ	Int. (I/I_{100})	dÅ	Int. (I/I_{100})
5.90	m,b,d	5.88	100		1
5.20	w,b,d			5.22	100
				4.39	35
4.20	w	4.23	12		
				3.79	35
3.55-3.35	mw,b,d	3.55	10		
				3.53	35
		3.49	18		
		3.40	20		
3.12	vw,b,d	3.39	30		
3.00-2.90	vw,b,d			3.25	16
2.70-2.60	vw,b,d			2.75	20
				2.67	20
				2.61	10
2.5-2.3	bw,b,d			2.47	20
2.23	vw,b,d			2.403	16
2.10	vw,b,d			2.10	12
		2.01	12		
		1.97	10		
		1.96	10		
				1.95	14
				1.93	14
				1.86	14

SECTION 3

RESULTS AND DISCUSSION

3.1 INTRODUCTION

In this project, it is an electrochemical reaction which is being studied. Therefore it seems appropriate to analyse the results for the major anodic half cell reaction first, followed by the full system results. After all of the results have been analysed and discussed, a final section entitled 'The practical applications of electrochemistry to real systems' has been included. The purpose of this section is simply to bring before the readers some of the assumptions employed in the application of electrochemistry to hydrometallurgy, and to evaluate their validity.

3.2 THE ANODIC OXIDATION OF UO_2

3.2.1 Cyclic Voltammetry

Although cyclic voltammetry has been used extensively throughout this work, the major analytical work was performed at pH = 1.5 and pH = 9.5. Voltammograms for other, different pHs are also compared. The interpretation of cyclic voltammetry must, to some extent, be qualitative, and in this work it has been used as a starting point.

(a) Solid UO_2 electrodes

(i) pH = 1.5

Figure 8 shows a number of cyclic voltammograms performed with varying anodic limits. By varying the anodic limit detailed analysis of the interrelation of anodic and cathodic peaks can be carried out. Table 5 contains the analysis of the areas of oxidation and reduction of the voltammograms that appear in Figure 8.

At the least anodic limit (E = 311 mV SHE) the reduction of oxidised products occurs at peaks (7) and (8). Peaks (4) and (6) are absent, and peak (5) is reduced in size. This could suggest that the anodic oxidation products formed at (3) are reduced at peaks (4), (5) and (6). Further, this could also suggest that the oxidation products of (1) and (2) are reduced at (7). The appearance of peak (8) is not fully understood, but could represent a reduction to a lower oxide, e.g. U_4O_7. It is worthy of note that peaks (5) and (6) begin to appear when the anodic limit reaches (E = 361 mV SHE). This indicates substantial and diverse oxidation occurs at potentials more oxidizing than E = 361 mV SHE.

This is a complex voltammogram, but one that shows at least four anodic oxidation products. Comparison with voltammograms produced by Nicol et al.,[38] although showing a similar shape, also show a number of differences. They are:

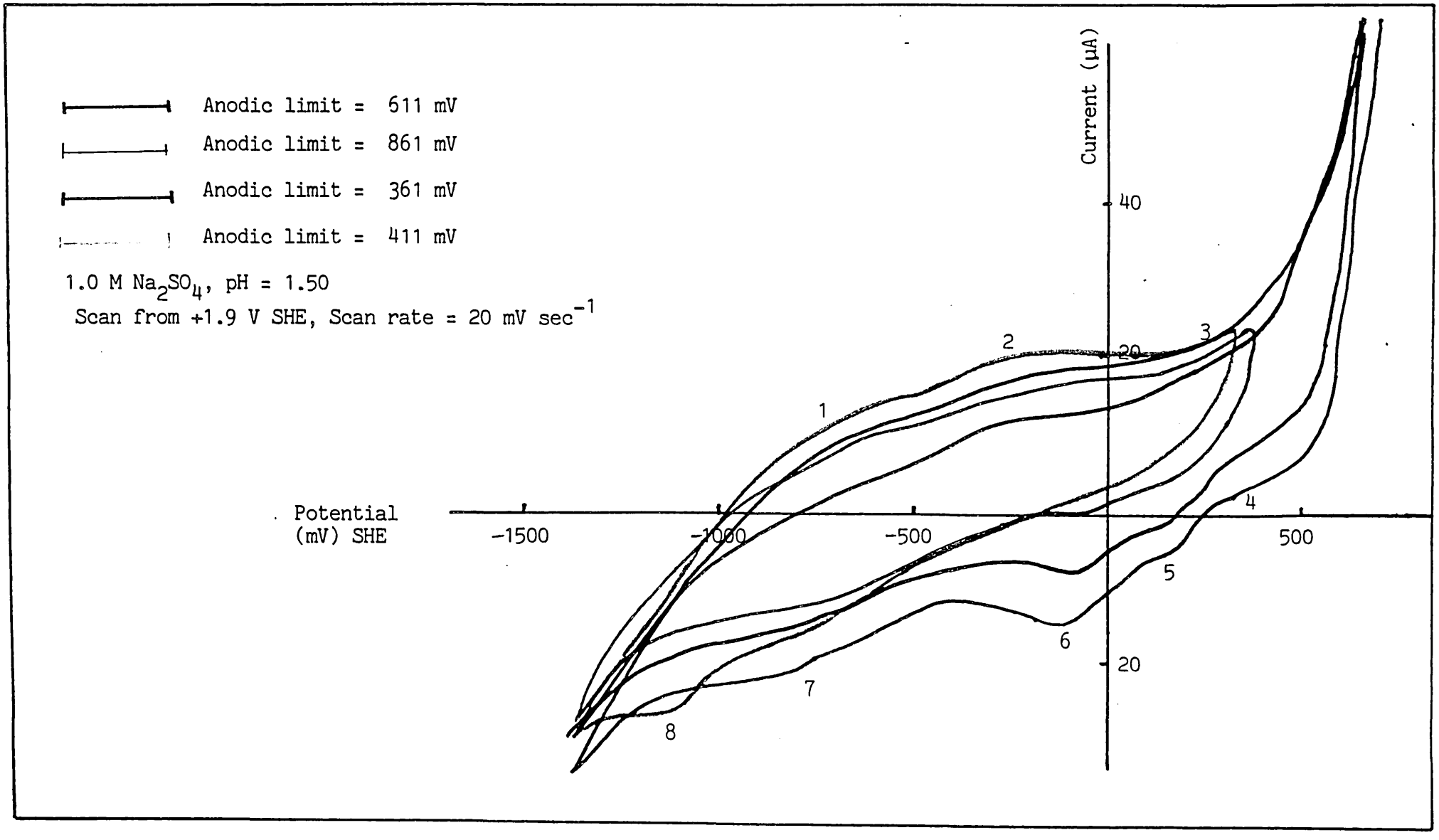


FIG. 8. Cyclic voltammograms with varying anodic limits at pH 1.5 (this work).

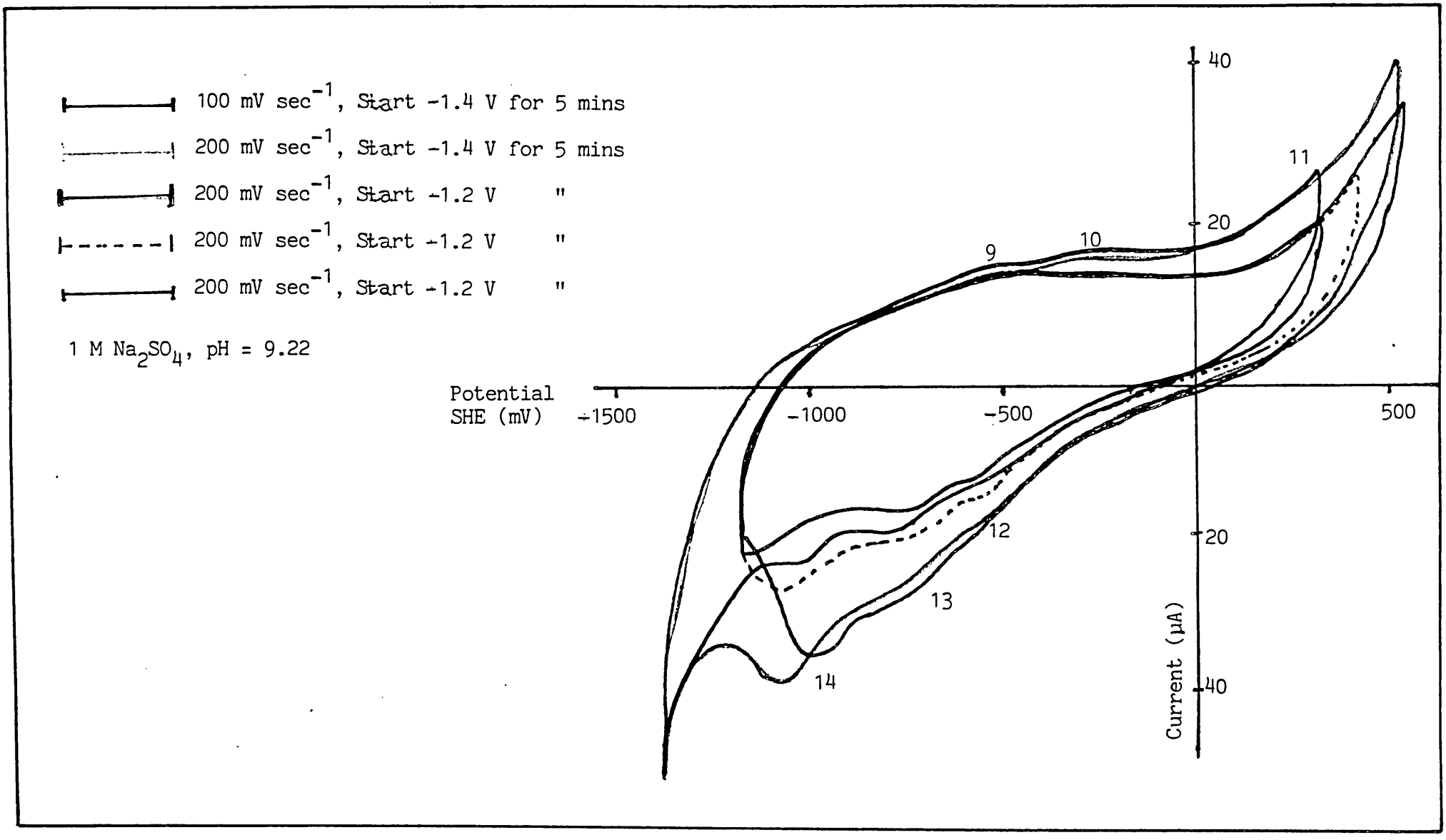


FIG. 9. Cyclic voltammograms with varying anodic and cathodic limits at pH 9.2 (this work).

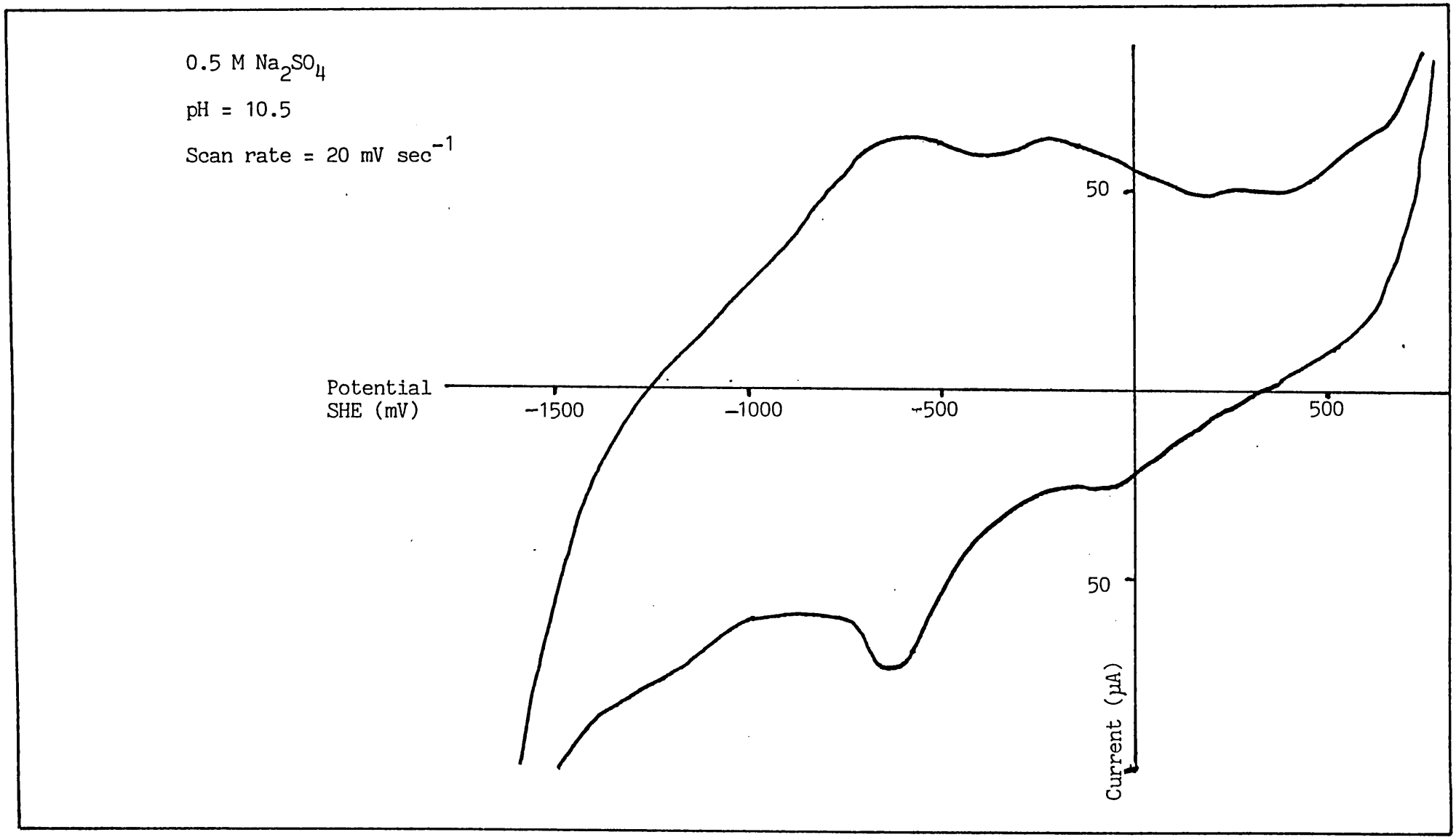


FIG. 10(a) A comparison of cyclic voltammograms from this work (a) and Sunder et al.(b).

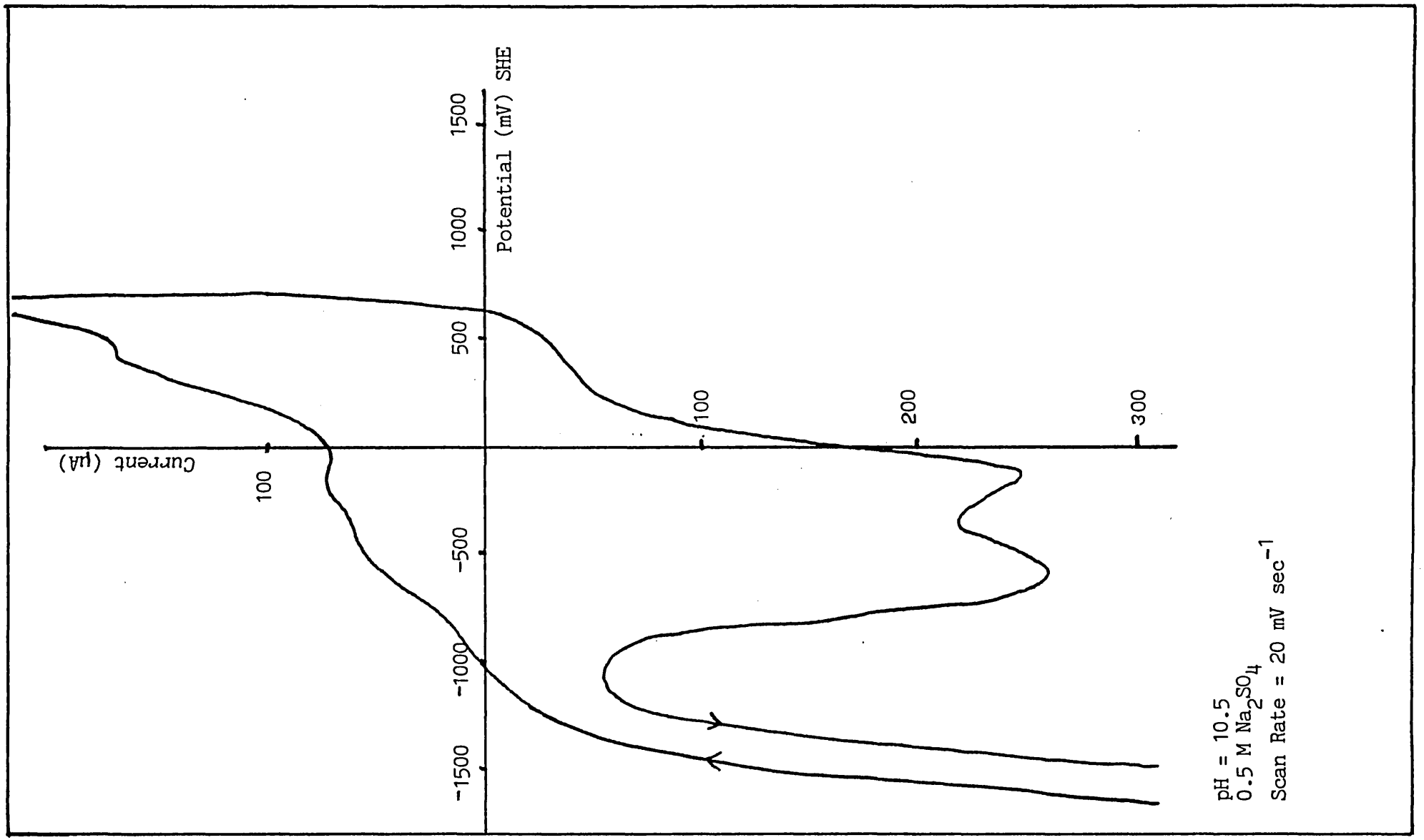


FIG. 10(b). A comparison of cyclic voltammograms from work by Sunder et al.[45]

TABLE 5. Oxidation and reduction area analysis of the voltammograms that appear in Figure 8.

Potential range of peak(s) on voltammogram scale (mV) SHE	Approximate peak current (μA)	Anodic/cathodic and reference number	Comments
-889 to -639	15	anodic 1	A complex series of very weak peaks or one very flat peak.
-489 to -89	20	anodic 2	A complex series of very weak peaks or one very flat peak.
11 to 411	30	anodic 3	A complex series of peaks.
511 to 311 centre 361	5	cathodic 4	A broad shoulder.
11 to 211 centre 111	5	cathodic 5	A well defined peak.
11 to -289 centre -139	15	cathodic 6	A well defined peak.
-889 to - 489 centre -688.9	20	cathodic 7	A flat peak which is present in all voltammograms and is more pronounced when the anodic limit is more anodic than E = 611 mV SHE.
-1139	25	cathodic 8	Well defined single peak, only present when the anodic limit is more anodic than E = 370 mV SHE.

TABLE 6. Oxidation and reduction area analysis of the voltammograms that appear in Figure 9.

Potential range of peak(s) on voltammograms scale (mV) SHE	Approximate peak current (μA)	Anodic/cathodic and reference number	Comments
-688.9 to -488.9 centred -589	·15	anodic 9	A small, flat topped peak. It could be a complex series of very small peaks.
-489 to -139 centred -339	15	anodic 10	A small, flat topped peak. It could be a complex series of very small peaks.
111 to 361 centred 211	·20	anodic 11	A broad peak, which is complex.
-389 to -639 centred -489	·10	cathodic 12	A small shoulder.
-639 to -889 centred -789	·20	cathodic 13	A well defined shoulder.
-889 to -1189 centred -1089	·35(max)	cathodic 14	A well defined peak.

(1) The potential range over which the voltammograms were obtained is different. A very similar discrepancy in potentials was found between the work of Nicol et al.[38] and Sunder et al.,[45] and is fully discussed at that point. (Section 1.5.1).

(2) The voltammograms in this work show more detail than those presented by Nicol et al.[38] This is probably because in this work 1 M sodium sulphate solution was used throughout the cell. This means in effect that all voltammograms were carried out in the reference compartment, hence eliminating liquid junction potentials.

(3) The voltammograms in this work are less flattened with potential. This is for the same reason as (2) and will be fully discussed in the practical applications section.

Finally there is one further aspect of these voltammograms which is worthy of comment. One would expect the anodic part of the voltammograms to concur. This is obviously not the case in these voltammograms. Given that the same pre-treatment was applied to all the voltammograms, a possible cause of this is that the pre-treatment may be initiating some inconsistent surface effect.

(ii) pH = 9.22

Figure 9 shows a number of cyclic voltammograms performed at pH = 9.2 with varying anodic and cathodic limits. Table 6 contains the analysis of the areas of oxidation

and reduction of the voltammograms that appear in Figure 9.

At the least anodic limit, all the cathodic peaks that are present at the greatest anodic limit appear to be present, albeit with lesser intensities. The changing of the pre-treatment conditions does not affect the potentials of the peaks, but changing the scan rate does. Peak (14) may well be complex due to its shape and apparent plurality.

The general range, shape and position of the anodic peaks are not dissimilar to those in the voltammograms at pH 1.5. The discrepancy in the potentials of the cathodic peaks is due to differences in scan rates. The two sets of voltammograms are similar in that both are complex. The high pH voltammograms show a minimum of 3 oxidation products reduced.

Comparison with work by Nicol et al.,[38] is difficult because the voltammograms in that work are performed with different electrolytic solutions and at different pHs.

(iii) $1.5 \leq pH \leq 12.06$

Sunder et al.[45] have recorded cyclic voltammograms at pH = 10.5 in 0.5 M Na_2SO_4 solutions, and comparison of that work with a cyclic voltammogram recorded in this work under similar circumstances is made in Figure 10. The general shape, potential and current ranges of the voltammograms are very similar, the only very minor difference between them is that the voltammograms by Sunder et al. seem to have slightly less detail than those obtained in this work.

A number of voltammograms recorded in this work, under very similar conditions at various pH values ($1.5 \leq pH \leq 12.06$) appear in Figure 11. The potential range is on a much larger scale, and is thus truncated with respect to the previous voltammograms. This comparison is very interesting for the following reasons:

(1) The potential range on these voltammograms is broadly in the area of the common anodic peak present in both the pH = 1.5 and pH = 9.22 voltammograms. It can be seen that a vast variety of intermediates are present in this area over the pH range examined.

(2) In general terms, as the pH is lowered, so too is the current associated with each voltammogram and peak. This indicates that there are less of the intermediates present, and less total current flowing.

(3) At pH = 12.06 there is a major change in the shape of the anodic end of the voltammogram, with much greater currents involved in dissolution.

(4) Relative to the other pH values, pH = 1.5 seems much smoother, but this could be an effect of the smaller current.

(5) In all the voltammograms the positions of the areas of oxidation are approximately similar, whilst the areas of reduction seem more scattered.

Figure 12 compares the different anodic oxidation areas of UO_2 found from cyclic voltammetry at different pHs from this work, and various works by Sunder et al.[44,45,47,49]

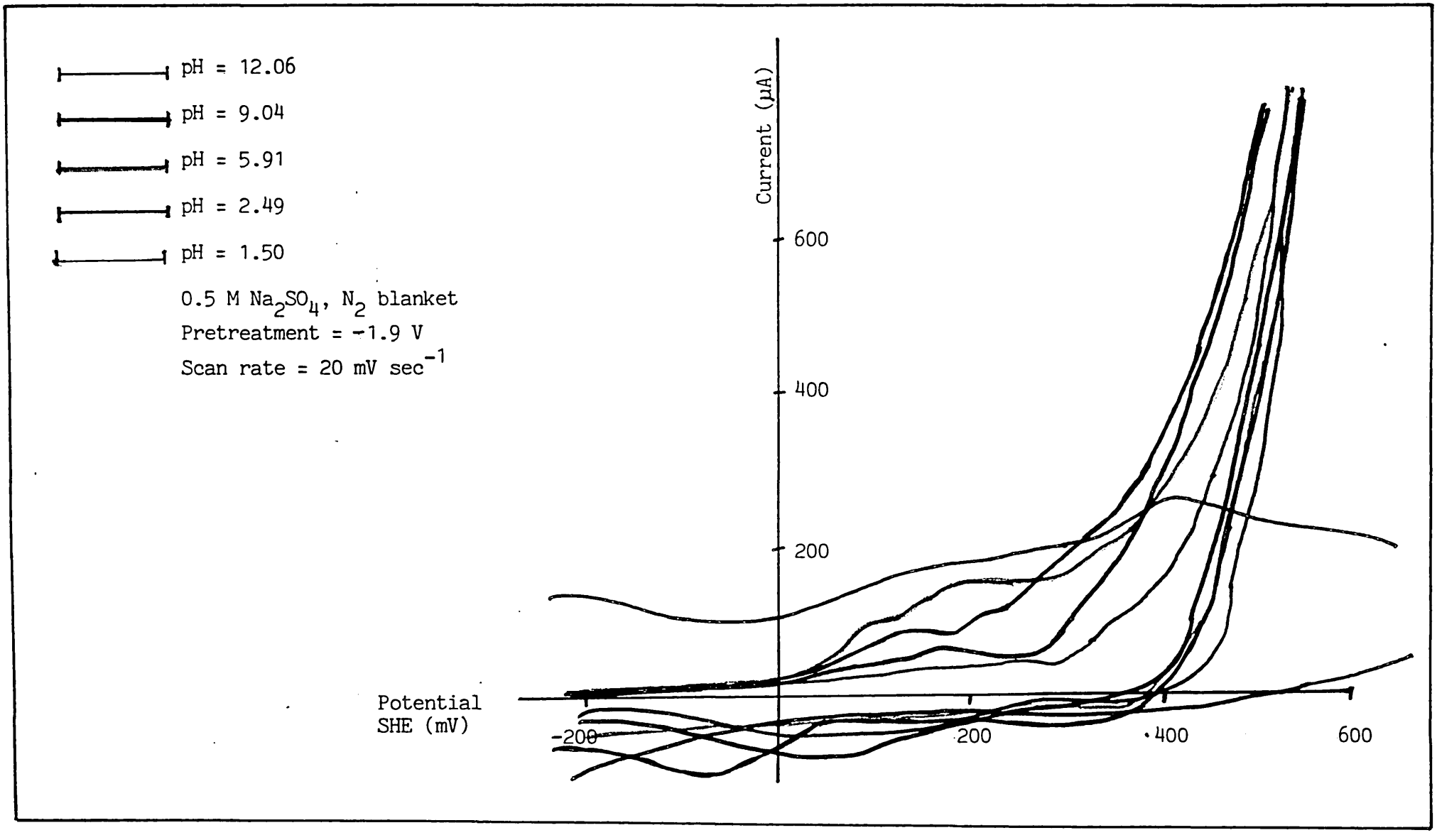


FIG. 11. A comparison of cyclic voltammograms at different pHs (this work).

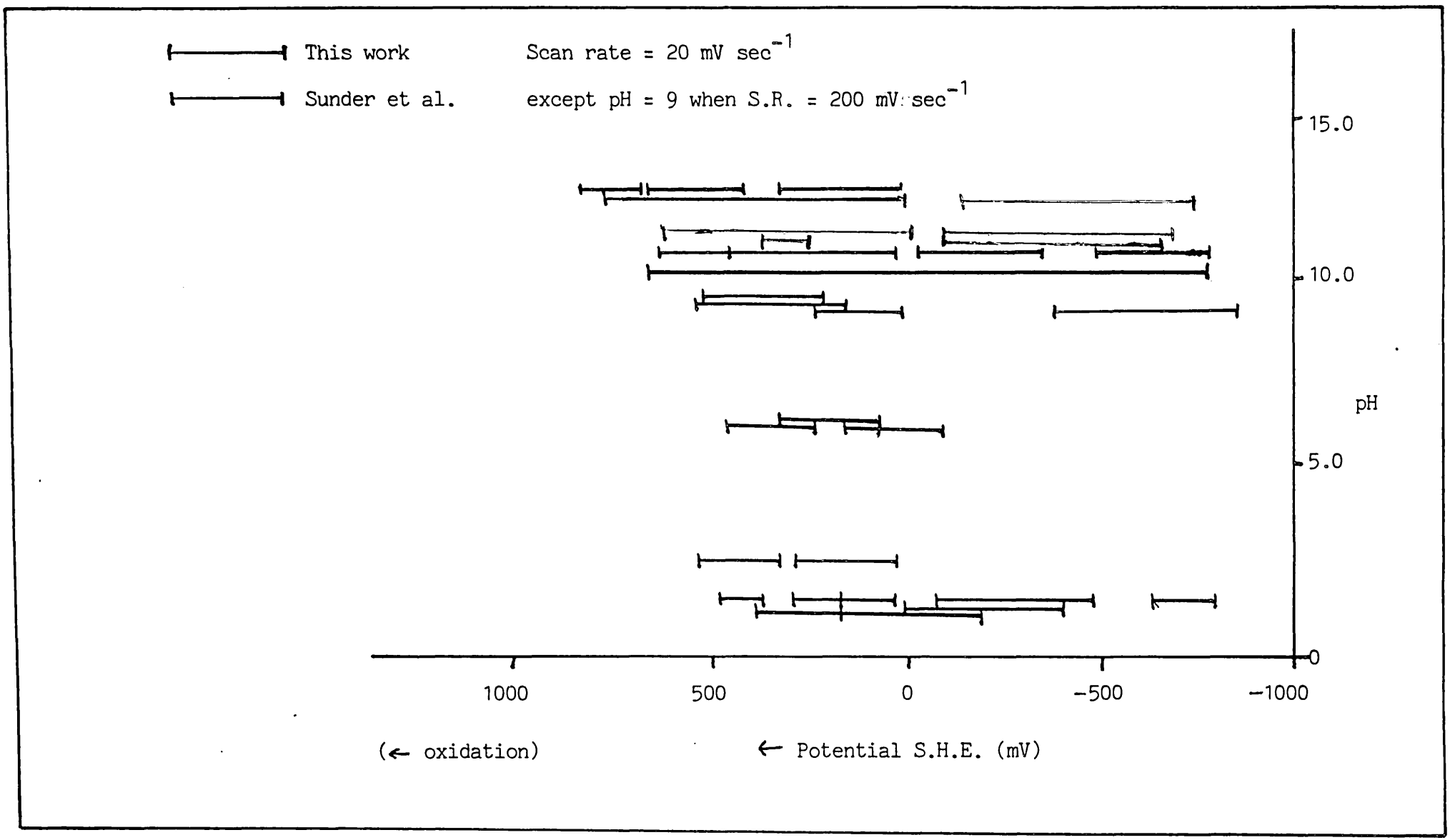


FIG. 12. A comparison of anodic oxidation areas found by cyclic voltammograms at different pHs (this work and Sunder et al.[44,45,47,49]).

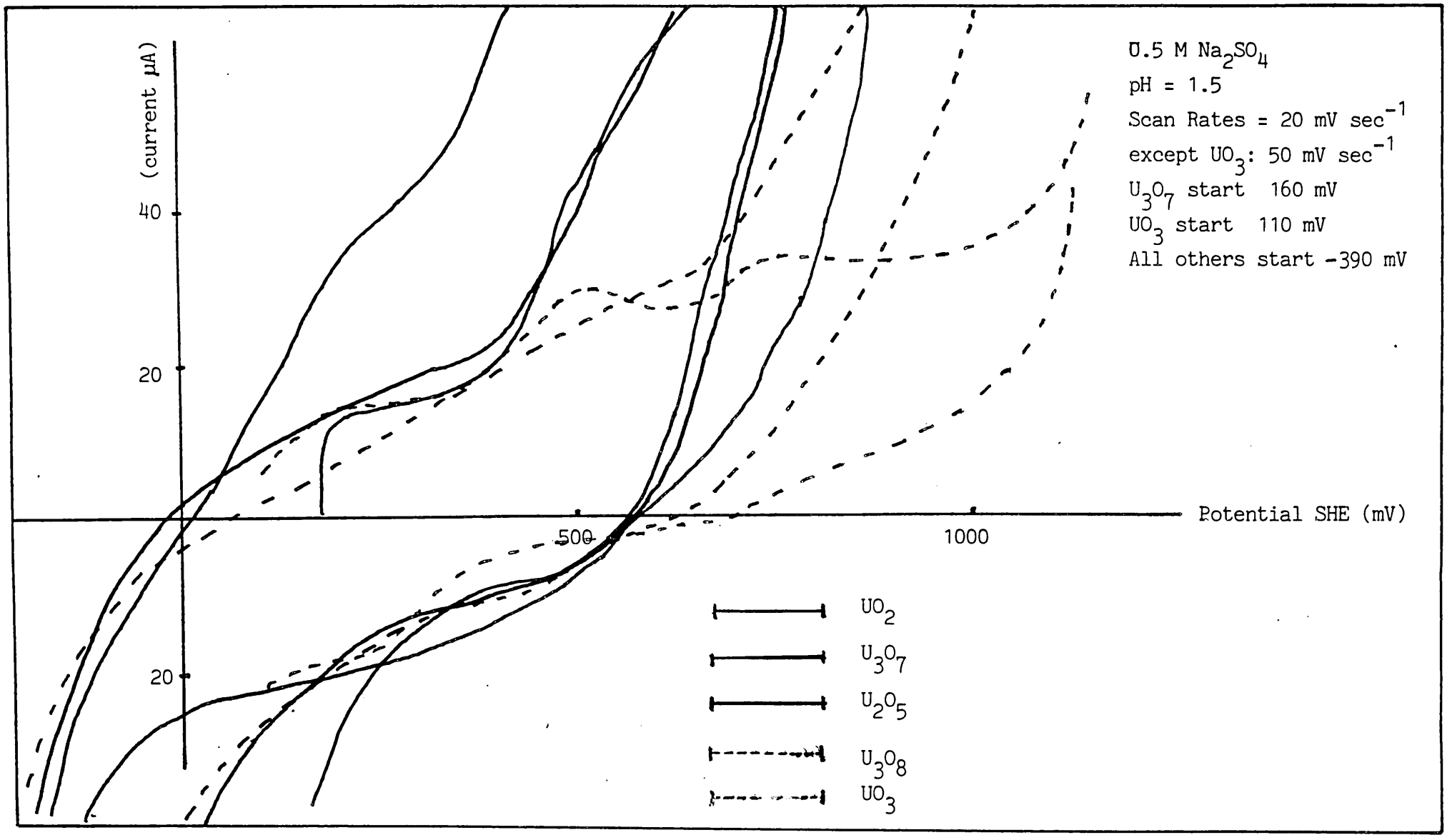


FIG. 13. A comparison of voltammograms obtained using different uranium oxides in carbon paste electrodes (this work).

The purpose of this diagram is simply to show the large number of oxidation areas detected in UO_2 oxidation.

Cyclic voltammograms performed at pH = 1.5 in the presence of hydrogen peroxide and peroxymonosulphuric acid display the same general shape and complexity as those performed without the oxidising agents.

3.2.1.(b) Carbon paste electrodes

Figure 13 compares a number of cyclic voltammograms obtained using different uranium oxides as part of carbon paste electrodes. Figures 14 and 15 show voltammograms of specific uranium oxides recorded on different scales. Comparing the three figures, it can be seen there are three main areas of oxidation over the oxide range employed. These are summarised in Figure 16.

Ideally one would hope to see one or more peaks representing the oxidation of each different oxide. This is not the case. It is worthy of note, that in the case of U_3O_7, the peaks which appear at less oxidising potentials are only apparent when the pre-treatment is carried out at the relatively reducing potential of -388 mV SHE. This may indicate that the pre-treatment has reduced some of the U_3O_7 to a lower oxide. If this was so, one would expect to see a gradual shift from lower to higher potential of the areas of oxidation, as the oxidation index rose. This is fairly well demonstrated up to and including U_3O_8.

Obviously in this series, UO_3 does not conform to this trend. The shape of the UO_3 voltammogram is much flatter, and the peaks, although conforming to the potentials of the oxidation areas of the other oxides are much simpler and more rounded. The positions of the reduction peaks tend to indicate fairly reversible reductions of oxidised products, again contrary to the characteristics of the other oxides. It is proposed that processes other than oxidation are observed occurring in this voltammogram. For comparison purposes, Figure 17 shows a voltammogram obtained using $UO_4.4H_2O$ in a carbon paste electrode. Although the currents involved are about an order of magnitude higher, and the system is different to the other oxides due to the presence of a peroxy oxygen, it is interesting to note that the voltammogram becomes complex only in the second sweep, after it has been exposed to reducing potentials. The general rounded character of the peaks previously observed with UO_3, is also displayed in this voltammogram. The potentials of any oxidation areas will be cathodically shifted due to the differences in current. The three oxidation areas of interest may be contained in the major (complex) peak of the voltammogram (11 mV $<$ E $<$ 311 mV SHE). The presence of a shoulder at (1011 mV $<$ E $<$ 1211 mV SHE) is also unexplained. A possible explanation is the formation of short-lived complex peroxyoxides e.g. Na_4UO_5, but this would not be expected in an acid system.

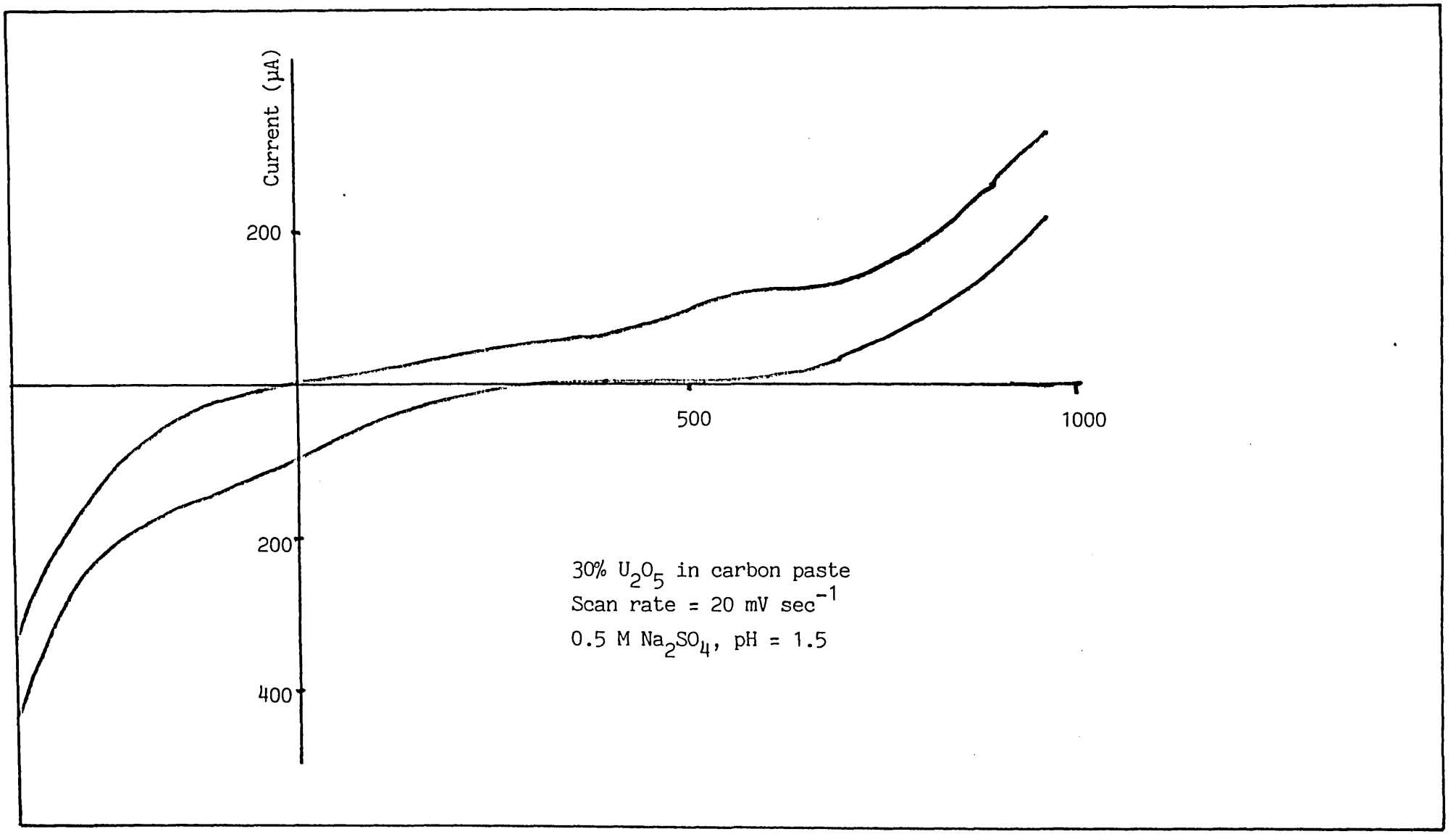


FIG. 14. A single cyclic voltammogram obtained using U_2O_5 in carbon paste electrodes (this work).

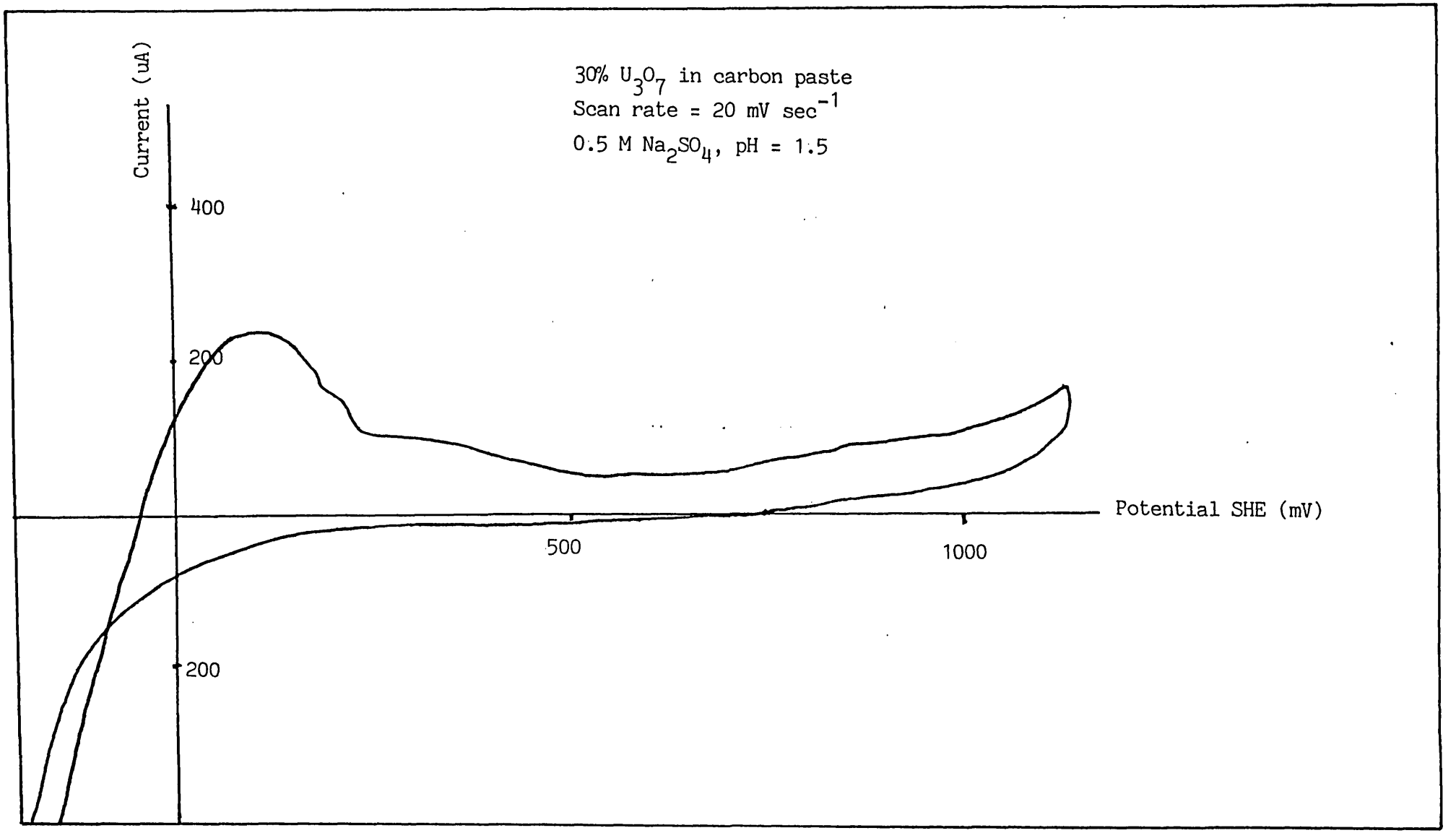
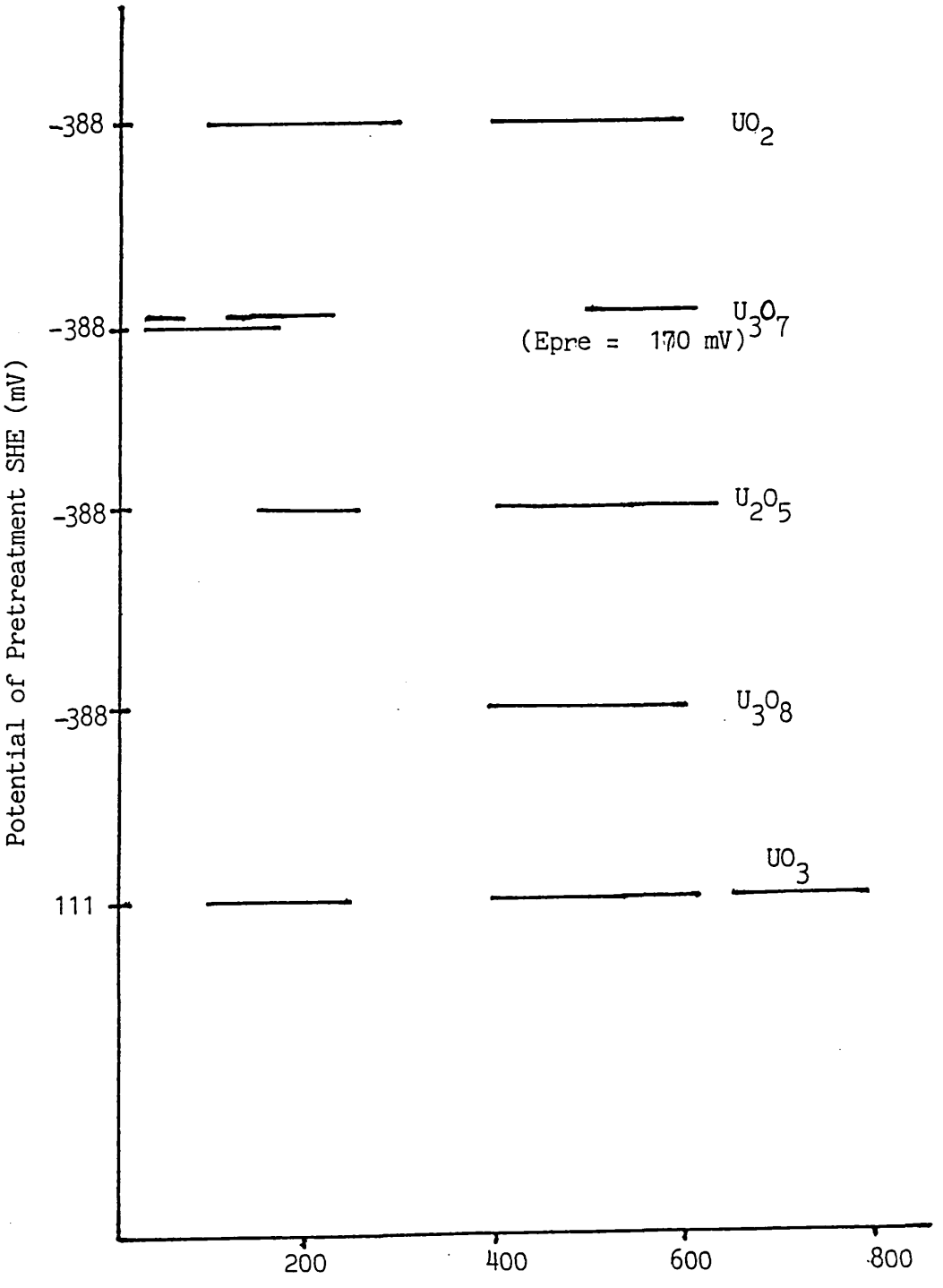


FIG. 15. Single voltammogram obtained using U_3O_7 in carbon paste electrodes (this work).

FIG. 16. A comparison of the oxidation areas shown in Figures 13, 14 and 15.



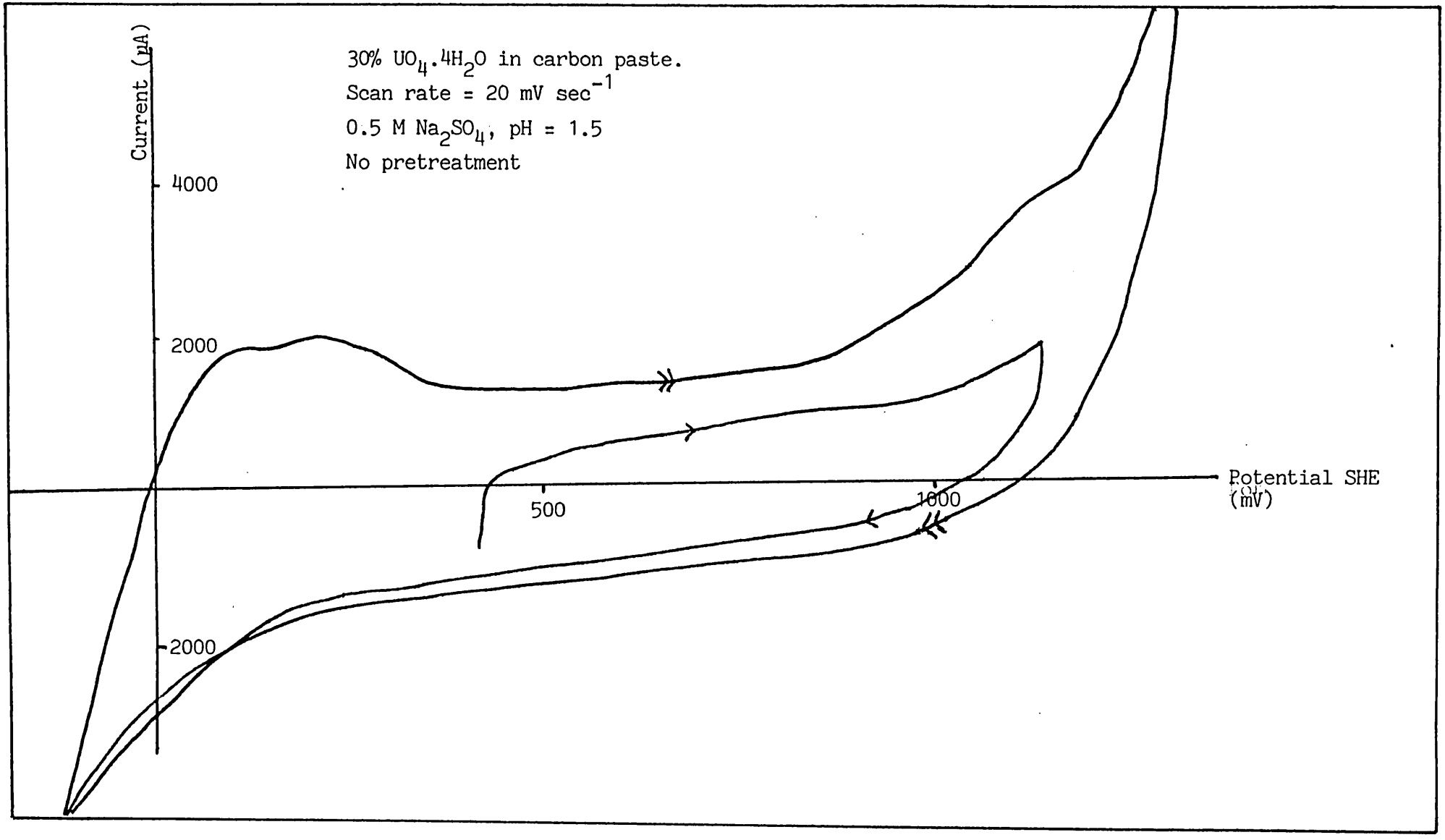


FIG. 17. A single cyclic voltammogram obtained using $UO_4.4H_2O$ in a carbon paste electrode (this work).

3.2.1. (c) Summary of the results of cyclic voltammetry

The cyclic voltammetry, although revealing much qualitative information has been of very little quantitative help.

Examination of the complex solid state UO_2 cyclic voltammograms reveals three main oxidation areas which are present at all pHs. Detailed examination of the most anodic of these areas at ($1.5 \leq pH \leq 12.06$) reveals a complex picture of at least three oxides in all cases except at pH = 12.06. This may imply that the other areas of oxidation are complex. The cathodic reduction curves show at least three oxidation products reduced at high pH, and at least four oxidation products reduced at low pH. The shapes of the solid state voltammograms are generally consistent with previous work.

Examination of the complex cyclic voltammograms obtained with carbon paste electrodes, reveals three main oxidation areas whose presence depends on the oxidation index of the oxide used and the conditions of the pre-treatment. Generally, the higher the oxidation index of the oxide, and the milder the pre-treatment process, then the more anodic the oxidation area(s) displayed. Voltammograms obtained using UO_3 and $UO_4.4H_2O$ do not appear to be of the same form as the voltammograms obtained from the lower oxides. Possible reasons for this are discussed.

At this juncture the identity of the intermediates implied by the presence of the oxidation areas has not been

considered. However, in a system which only contains pH adjusted sodium sulphate and uranium oxide, it is difficult to imagine what these intermediates could be, except uranium oxides. The use of intermediate oxides in the carbon paste cyclic voltammetry yielded results which are similar to those obtained from solid state UO_2 electrodes. Previous work has characterised intermediate uranium oxides at high pH.[44,45,47,49]

Attempts to isolate surface films for X.R.D. analysis were not successful, therefore there is no direct proof of what the identities of these substances may be.

Having stated that there is no proof of the identities of these substances, and in the light of what has been discussed above, it will be assumed from henceforth that the oxidation intermediates are in fact uranium oxides. An assumption on the identities of the intermediates is required for the cathodic stripping voltammetry.

3.2.2 Cathodic Stripping Voltammetry

3.2.2 (a) Introduction

Cathodic stripping voltammetry has been used in two ways in this work. The first involved the comparison and analysis of the stripping voltammograms. The second involved integration of the stripping curves and using the derived charge data to calculate film thickness. To be able to do this, the identity of the intermediates must be known.

Therefore after the initial analysis and comparison stage, the intermediate oxides will be provisionally given identities.

3.2.2 (b) Cathodic stripping voltammogram analysis

Cathodic stripping was performed at five different potentials, for varying times. The cathodic stripping voltammograms appear in Figure 18. Some of the sets of voltammograms show evidence of film destabilisation with time, and all are complex.

At E = 111 mV (SHE) there are two major substances stripped, one of which swamps the other. The scale and resolution of these voltammograms are poor. The cathodic charge only grows slowly with time.

At E = 286 mV (SHE) there are three major substances stripped, all of which appear to be present at the longest time (3690 secs.). These voltammograms have greater clarity than previously. The cathodic charge is greater than previously, but it only grows slowly with time.

At E = 611 mV (SHE) the voltammogram becomes more complex. It is poorly defined and the peaks display plurality. There are four major peaks and one weak shoulder. After approximately 100 secs of film growth, the film decays to about half its previous thickness.

At E = 811 mV (SHE) the voltammograms are much clearer, but complex. There is evidence for destabilisation of at

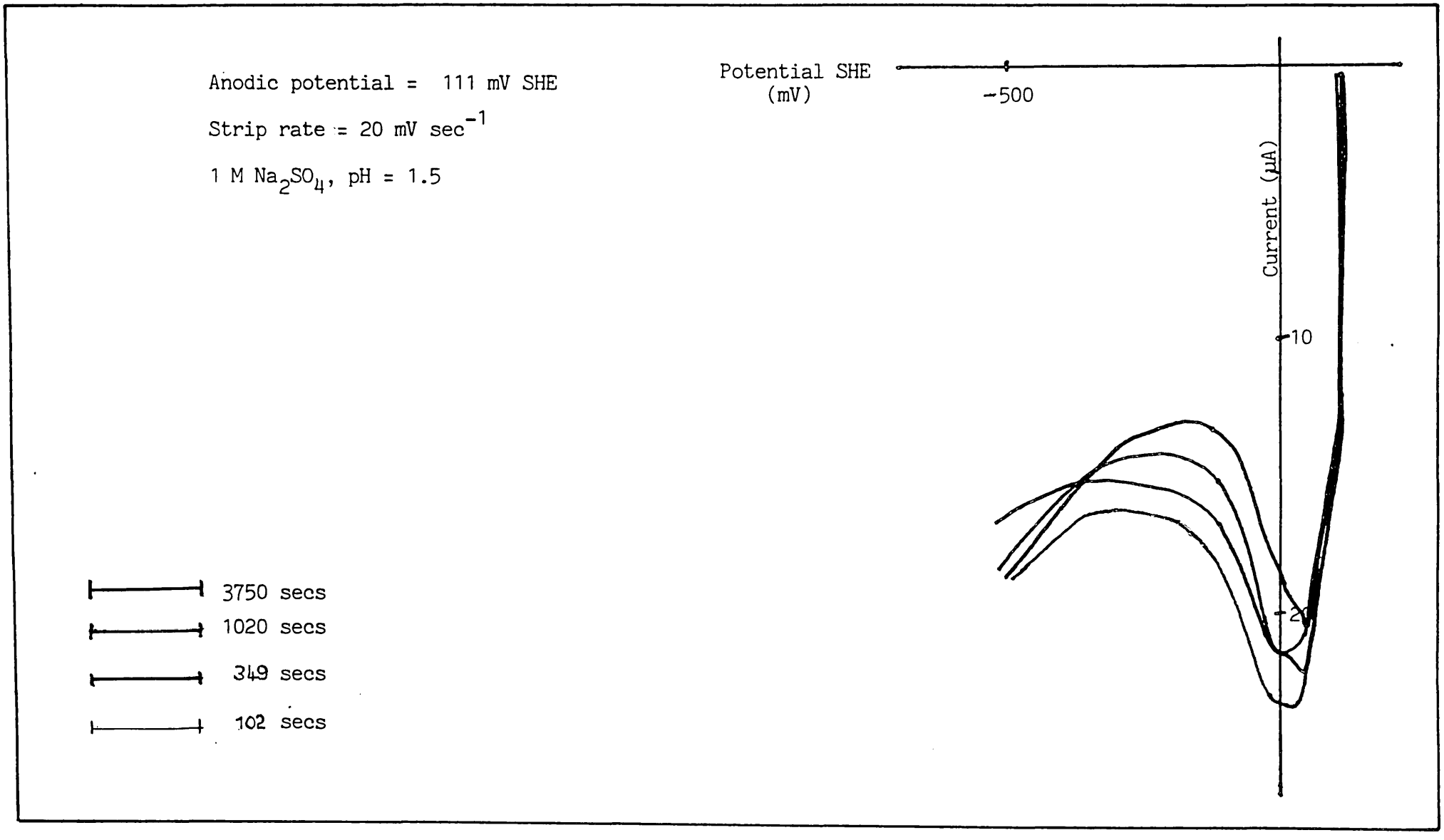


FIG. 18. Cathodic stripping voltammograms at various potentials as shown (this work).

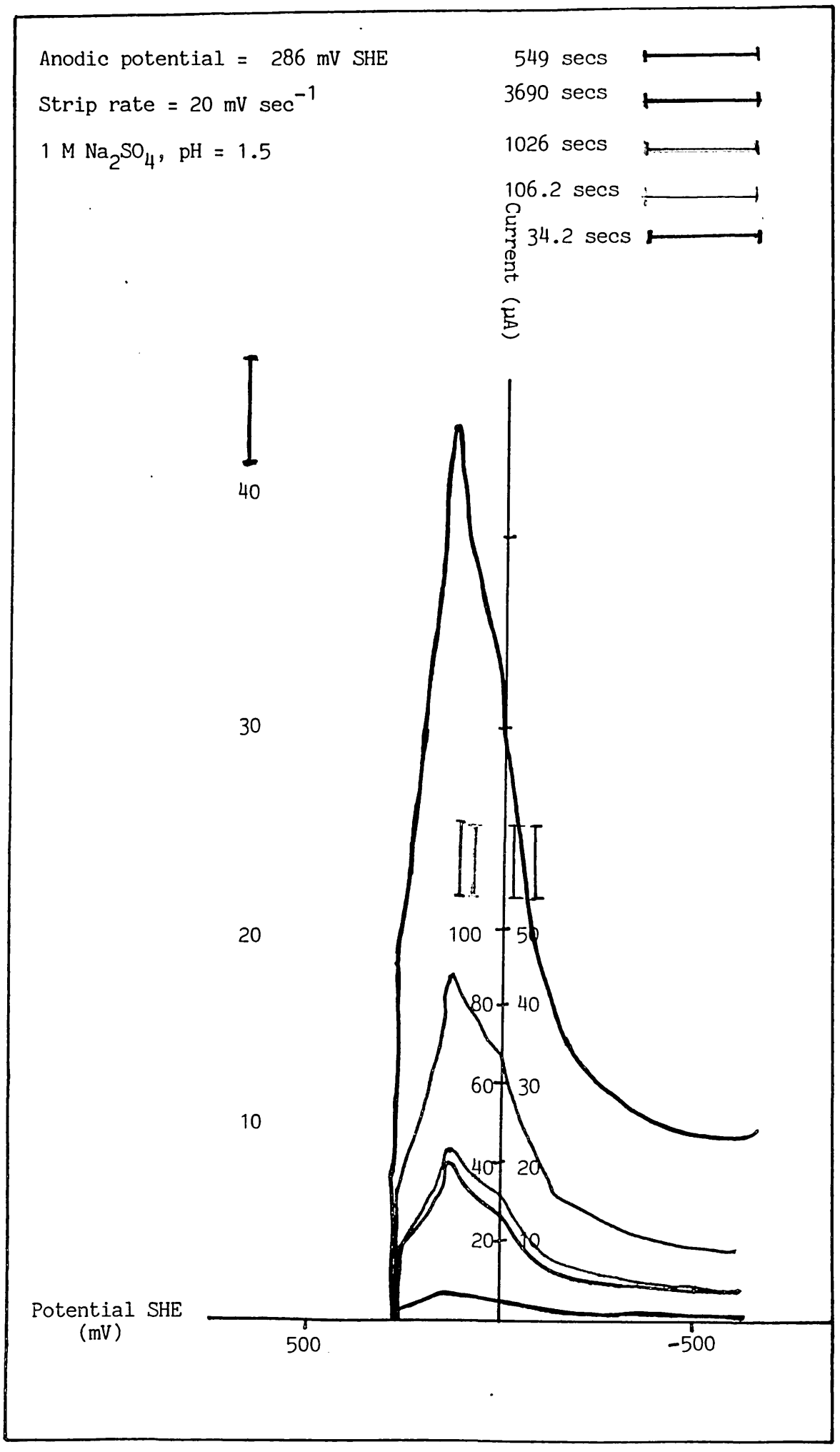

Anodic potential = 286 mV SHE
Strip rate = 20 mV sec^{-1}
1 M Na_2SO_4, pH = 1.5
549 secs
3690 secs
1026 secs
106.2 secs
34.2 secs
Current (μA)
40
30
20
10
100
50
80
40
60
30
40
20
20
10
Potential SHE (mV)
500
-500

FIG. 18. cont.

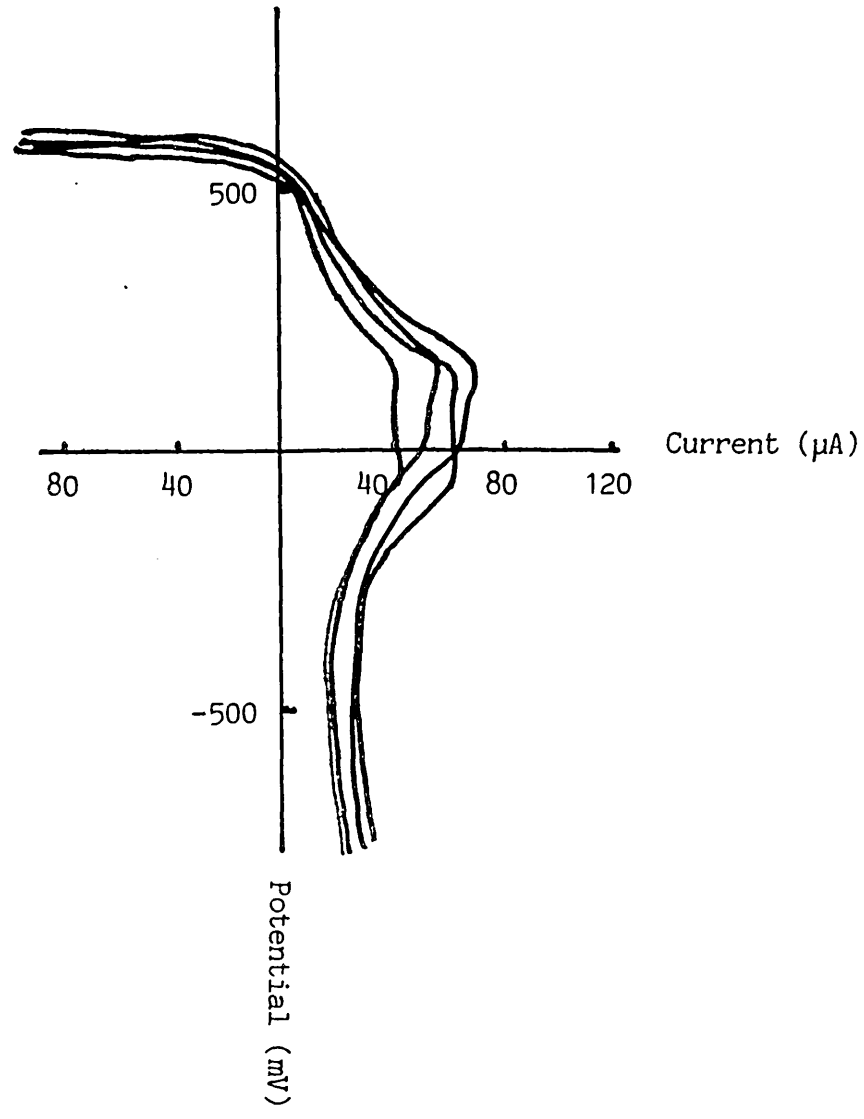


FIG. 18. cont.

Anodic potential = 611 mV SHE

Strip rate = 20 mV sec^{-1}

1 M Na_2SO_4, pH = 1.5

109.2 secs

986.4 secs

566.4 secs

3801 secs

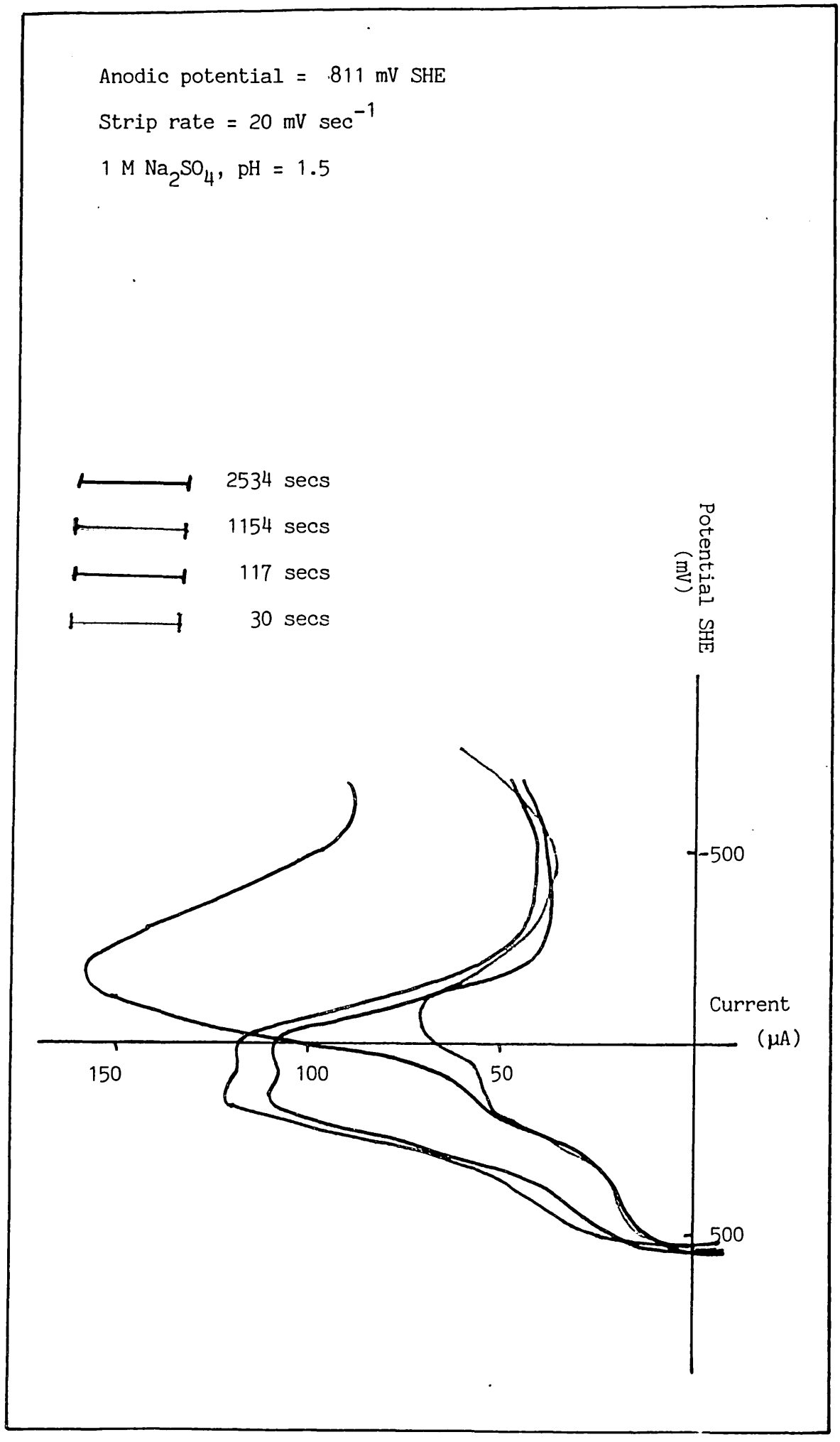

Anodic potential = 811 mV SHE
Strip rate = 20 mV sec^{-1}
1 M Na_2SO_4, pH = 1.5
2534 secs
1154 secs
117 secs
30 secs
Potential SHE (mV)
-500
Current (μA)
150
100
50
500

FIG. 18. cont.

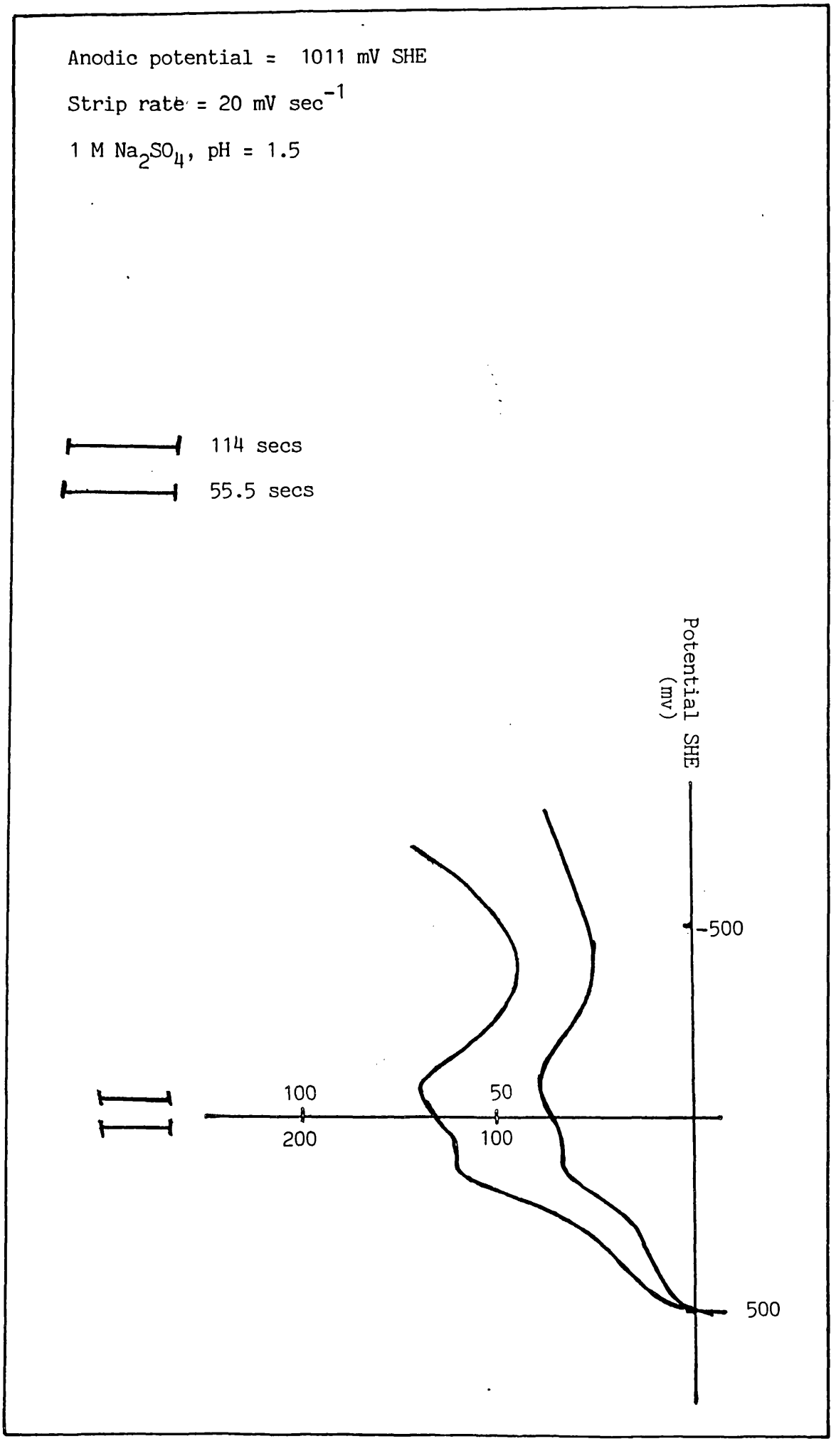

Anodic potential = 1011 mV SHE
Strip rate = 20 mV sec^{-1}
1 M Na_2SO_4, pH = 1.5
114 secs
55.5 secs
Potential SHE (mv)
-500
500
100
200
50
100

FIG. 18. cont.

TABLE 7. A summary of the cathodically stripped intermediates from the voltammograms that appear in Figure 18.

Potential at which phase is stripped (mV) SHE.	Potential of oxidation (mV) SHE					A tentative initial identification	Probable cyclic voltammetry peak reference number
	−111	286	611	811	1011		
			411 to 461	411 to 461	411 to 461	UO_2^{2+}	4
		181	161			U_8O_{19} or orthorhombic U_3O_7	5
		141 to 131	141 to 111	141 to 111	131 to 121	U_2O_5	5
	21	21 to 1	−9	21 to −9	?	U_3O_7	5
	−19 to −39					U_4O_9	6
			−79 to −59	−89	−69 to −79	U_3O_8	6
				−199	?	UO_3	6

least two phases. There are 5 major substances stripped. The total charge behaviour is complex.

At E = 1011 mV (SHE) there are two major peaks and one shoulder. As the time increases the films grow thicker, and the major peak broadens, possibly indicating increased complexity.

Table 7 contains a summary of the potentials of the peaks in the voltammograms. It is not possible to equate the more anodic stripping potentials to those oxides with the higher oxidation index because of differences in reversibility of the reduction mechanism of the individual oxides. Also, there may be a 'sandwich' structure of oxide layers which would 'mask' an underlying oxide layer. Table 7 has been drawn such that those oxides which were stripped at the same potential are in horizontal lines. It is reasonable to assume that those oxides that are stripped at the same potential are the same oxide. From Table 7, it can be seen that intermediateswere stripped at 7 different potentials, thus implying seven uranium oxide species. The cyclic voltammograms showed at least 4 intermediates in the cathodic scans. The difference is due to the increased sensitivity of the cathodic stripping voltammetry stemming from the much greater amount of oxidised product being reduced. The potentials at which these intermediates occur agree well with the reduction areas found in the cyclic voltammetry. Table 7 contains probable cyclic voltammetry peak reference numbers.

Any identification of these oxides can only be tentative, and must be based on the potential of formation, which should be related to the oxidation index of the oxide. Table 8 contains data on the known uranium oxides (in the range UO_2 to UO_3) and their known structures. Table 9 contains an analysis of system structures. The reversibility of a reduction reaction of the sort encountered in the cyclic and cathodic voltammograms depends on how drastically the structure has to change from its initial state (as the oxidised product) to its reduced state (UO_2). Where little modification is required, the reaction is reversible. In practice, this means that the reduction occurs at a potential relatively close to the potential of formation. In cases where major modifications to the structure are required, the reaction will take place at a more cathodic stage in the scan. Using this knowledge, along with the data in Table 8, a provisional, very tentative initial identification can be made, as in Table 7. These identifications cannot be directly proved. They are only made because the next stage of the analysis of results demands that the intermediates have some identity.

The order in which the oxides are formed and the reversibility of their reduction both concur to give the tentative initial identification. The identity of the oxide which was formed in the potential range $286\ mV \leq E \leq 611\ mV$ SHE presents a slight problem. There is no characterised orthorhombic form of U_3O_7, although at some juncture between

$UO_{2.33}$ and $UO_{2.50}$ orthorhombic compounds exist. There is, on the other hand a characterised uranium oxide, the molecular formula of which is U_8O_{19} (A.S.T.M. 15-3). The empirical formula being $UO_{2.375}$. The problem is that it would not seem likely that such a large molecule would form. The closeness of the stripping and formation potentials indicates that the structures of the two compounds are likely to be similar. Indeed U_8O_{19} can be formed by the reaction of eight moles of U_3O_7 and one oxygen atom. There is not sufficient evidence at present to pursue this much further. Therefore it will be provisionally called U_8O_{19}.

This point, however, raises a more fundamental question. Obviously the presence of the various peaks in the voltammograms of Figure 18 indicates that the sensitivity of this method is such so as to be able to discriminate between those different surface phases. If however, only small quantities (e.g. a few monolayers) were present on the surface, the application of bulk crystal phase data (such as that contained in Table 8) is of dubious validity. In the present case, C.S.V. can discriminate between the two proposed oxides U_3O_7 and U_8O_{19}. The actual difference between a few monolayers of each substance however is very small. Indeed one mole of U_8O_{19} can be formed from eight moles of U_3O_7 and one atom of oxygen. This is demonstrated in the closeness of the stoichiometric formulae of the two substances (see Table 8). So although the electrochemical method indicates two very similar substances, it is difficult to imagine

quite what these differences really are in the situation of a few monolayers of each oxide. It is interesting to note that UO_2^{2+} only occurs in detectable amounts when U_3O_8 also appears.

3.2.2 (c) Coulometry calculations

If the total cathodic charge is known, then the equivalent number of mols of substance can be calculated (90):

$$\frac{Qc}{nF} = m \qquad (90)$$

where Qc = the cathodic charge

m = the number of mols of substance

and all other symbols retain their usual significance.

If one knows the underlying (template) area of the electrode, the determination of surface film thickness requires a knowledge of the identity and density of the substance, equation (91).

$$\frac{QC\ M}{nFA\rho\sigma} = d \qquad (91)$$

where M = molecular mass

ρ = density (g cm^{-3}), taken as the density of UO_2 10.26 g cm^{-3}

d = layer thickness in cm

A = area of electrode in cm^2

σ = roughness factor = 3, see below.

TABLE 8. A summary of the characterised structures of some known uranium oxides in the stoichiometric range UO_2 to UO_3.

STRUCTURE					Uranium oxide	Oxidation
Cubic	Tetragonal	Orthorhombic	Hexagonal	Monoclinic	molecular formula	index
√	√				UO_2	2.0
√					U_4O_9	2.25
	√				U_3O_7	2.33
					U_8O_{19}	2.375
		√	√	√	U_2O_5	2.5
		√	√		U_3O_8	2.67
√						2.82
						2.86
		√				2.90
√	√	√	√	√	UO_3	3.0

TABLE 9. An analysis of system structures after Jones.[91]

System	Axis	Angles	Symmetry
triclinic	$a \neq b \neq c$	$\alpha \neq \gamma \neq \beta$	
monoclinic	$a \neq b \neq c$	$\beta \neq 90$, $\alpha = \gamma = 90$	
orthorhombic	$a \neq b \neq c$	$\alpha = \beta = \gamma = 90$	
tetragonal	$a = b \neq c$	$\alpha = \beta = \gamma = 90$	
hexagonal	$a = b \neq c$	$\alpha = \beta = 90$, $\gamma = 120$	
rhombahedral trigonal	$a = b = c$	$\alpha = \beta = \gamma \neq 90$	
cubic	$a = b = c$	$\alpha = \beta = \gamma = 90$	

Assumptions regarding the identities of the intermediate oxide species have been made. The densities of the intermediate uranium oxides are assumed to be equal to that of uranium dioxide. The roughness factor for UO_2 polished with silicon carbide paper (600A) has been determined as 3.[45]

The total anodic charge can be calculated by equation (92):

$$Q_A = It \qquad (92)$$

where all symbols retain their usual significance.

The difference between the anodic charge (Q_A) which is forced through the cell, and the cathodic charge (Q_c) which is represented by the amount of substance on the electrode as oxide films, is the amount of charge used for dissolution. A source of error in this type of work when a coulometer is not used, is the contribution of the non-faradaic current to the total current. A convenient way to estimate the contribution of non-faradaic current is to pass a known amount of charge through the system, and hence calculate the theoretical concentration of, in this case, uranium in solution. The actual concentration of uranium in solution is then measured by analysis. The ratio of analysed uranium concentration over theoretical uranium concentration is called the current efficiency (%). In pilot work, the current efficiency of the system was measured as 93.4%.

Table 10 contains the total anodic and cathodic charge data. Observation of the way that total cathodic charge (i.e. extent of film formation) varies with time can give qualitative information on the mechanism. Observation of the way that the cathodic and anodic charges alter with time can demonstrate at what potential dissolution begins, and whether dissolution occurs via just one mechanism or more than one. Graph 2 shows the total cathodic charge at different potentials plotted against log time. Graph 3 shows the anodic and cathodic charges at potential = 111 mV SHE plotted together against log time.

Graph 2 reveals a complex situation, with total film thickness varying with time and potential. Generally, as would be expected, film formation increases with increased potential. The shapes of the lines are interesting. At low potentials (111 mV $\leq$ E $\leq$ 511 mV SHE) the film thickness levels out after a variable period of time. At the lowest potential (E = 111 mV SHE) the film thickness peaks and begins to drop off slightly. These results indicate that a steady state between the dissolution and film formation has been achieved.

At more oxidizing potentials (611 mV $\leq$ E $\leq$ 1011 mV SHE), the situation is quite different. The lines on the graph are not in any way parallel or similar to each other. This indicates a breakdown in the steady state, which may well indicate a change in the mechanism of either film dissolution or formation, or both. This situation also indicates that

the film is not simple (i.e. does not have just one component).

Graph 3 shows that initially, most of the current is used in film formation, with only a small amount of dissolution occurring. After the film formation has stabilised, the dissolution rate increases. It is possible that during the initial film formation stage some dissolution occurs. If this is the case it accounts for only $\sim$10 μC of charge. If it exists it is not possible to say whether this secondary mechanism is independent of or part of the main mechanism. Independent mechanisms have been suggested before, but their existence has not been proved.[45]

Table 11 contains the estimated individual cathodic peak charge data along with film thickness calculated using molecular formulae. Table 12 contains calculated film thickness using empirical formulae. In some cases a range of values is given indicating that the presence or size of peaks changed to a large degree with time. Ranges have not been used to show normal film growth. Where no range is given, the charge data for the longest times are used.

The first general observation is that all the films are relatively thin, even after long times. The small quantities of film explain the difficulty encountered in obtaining a sample for X.R.D. analysis. A number of facts present themselves:

(1) At less oxidizing potentials (-111 mV $\leq E \leq 611$ mV SHE) the main species present seem to be those labelled as U_3O_7 and U_8O_{19}.

(2) At more oxidizing potentials (-611 mV $\leq 0 \leq$ 1011 mV SHE), the main species present seem to be those labelled as U_3O_8 and U_2O_5. The U_3O_8 present grows and is stabilised by more oxidising conditions.

(3) At E = -811 mV SHE U_3O_7 is destabilised, and U_3O_8 is preferentially formed.

(4) U_4O_9 destabilises U_3O_7 only at very low potentials (E = -111 mV SHE), after which it does not occur.

(5) UO_2^{2+} only occurs in amounts $\leq \frac{1}{2}$ a monolayer. This is in keeping with the fact that it is an absorbed substance, and may point to the fact that it is consumed in ways other than simply representing the dissolution current.

These observations are in accordance with the logical oxidation order of UO_2. The abundance of any oxide in relation to others may indicate that oxidation of that oxide may be rate-determining. Different rate determining steps may exist at different potentials. At low potentials possible rate determining reactions could involve U_3O_7 or U_8O_{19}, or both if their contribution to the rate determining factor is approximately equal. At high potential U_3O_8 seems the most stable and prodigious oxide, and may be the major contribution to the rate determining factor. The small amounts of UO_2^{2+} and its appearance at high potential are both in keeping with known fact. UO_3 may be present at E = 1011 mV, but because no data is available at longer times, this cannot be a certainty.

TABLE 10. The cathodic and anodic total charge data.

Experiment reference number	Potential (mV) (SHE)	Time (secs)	Log time	Cathodic charge Qc (μC)	Anodic charge Q_A (μC)
7a2	-111	34.59	1.539	527.6	-
7c	"	1020	3.009	628.1	964.8
7b	"	102	2.009	554.5	696.72
7a3	"	34.0	1.531	539.0	525.6
7d	"	3750	3.574	563.9	1066.1
7a	"	20.55	1.313	380.0	396.96
1e	286	549	2.739	856.3	1137.2
1d	"	3690	3.567	878.4	2137.7
1c	"	1026	3.011	862.95	1379.5
1b	"	106.2	2.026	780.85	900.19
6b	511	206.4	2.315	1310.3	8521.4
5a1	"	37.2	1.570	1197.3	3006.6
5a2	"	104.4	2.019	1301.8	4341.6
5a3	"	1134	3.055	1272.3	13992.0
6a	"	30.9	1.490	1116.3	2808.9
5a4	"	3312	3.520	1312.3	66312.0
2a	611	34.8	1.541	1729.5	12142.3
2d	"	3801	3.580	1395.1	756723
2e	"	566.4	2.753	2103.7	164087
2c	"	986.4	2.994	1709.9	249161
2b	"	109.2	2.038	2167.9	35457
3a2	811	30	1.477	1647.2	-
3b1	"	117	2.068	1849.7	-
3d1	"	2534	3.404	2301.2	-
3c2	"	1154.3	3.062	1179	-
4a1	1011	55.5	1.744	2518.0	-
4a	"	114	2.057	2774	435600

TABLE 11. Film thickness of proposed intermediates (calculated with molecular formulae) at different potentials.

Proposed Oxide	Potential of Formation (mV) SHE										Thickness of one monolayer of oxide (Å)
	111		286		611		811		1011		
	Charge (μC)	Film Thickness (Å)	Charge (μC)	Film Thickness (Å)	Charge (μC)	Film Thickness (Å)	Charge (μC)	Film Thickness (Å)	Charge (μC)	Film Thickness (Å)	
UO_2^{2+}					171	1.2	185 to 115	1.2 to 0.75	251.8	1.6	3.4
U_4O_9	225 to 338	24 to 36									15.6
U_8O_{19}*				37.8		55.0					32.33
U_3O_7	338 to 145	20.6 to 8.83	264	16.08	427.5	26.0	832 to 0	50.7 to 0			12.0
U_2O_5			352	9.53	384	9.62	832 to 0	22.5 to 0	1007.2	27.3 to 0	8.4
U_3O_8					342	10.70	0 to 713.3	0 to 22.2	1259	39.1	13.1
UO_3							0 to 1472.6	0 to 10.25	?	?	4.8
orthorhombic U_3O_7*			264	16.08	384	23.4					12.0

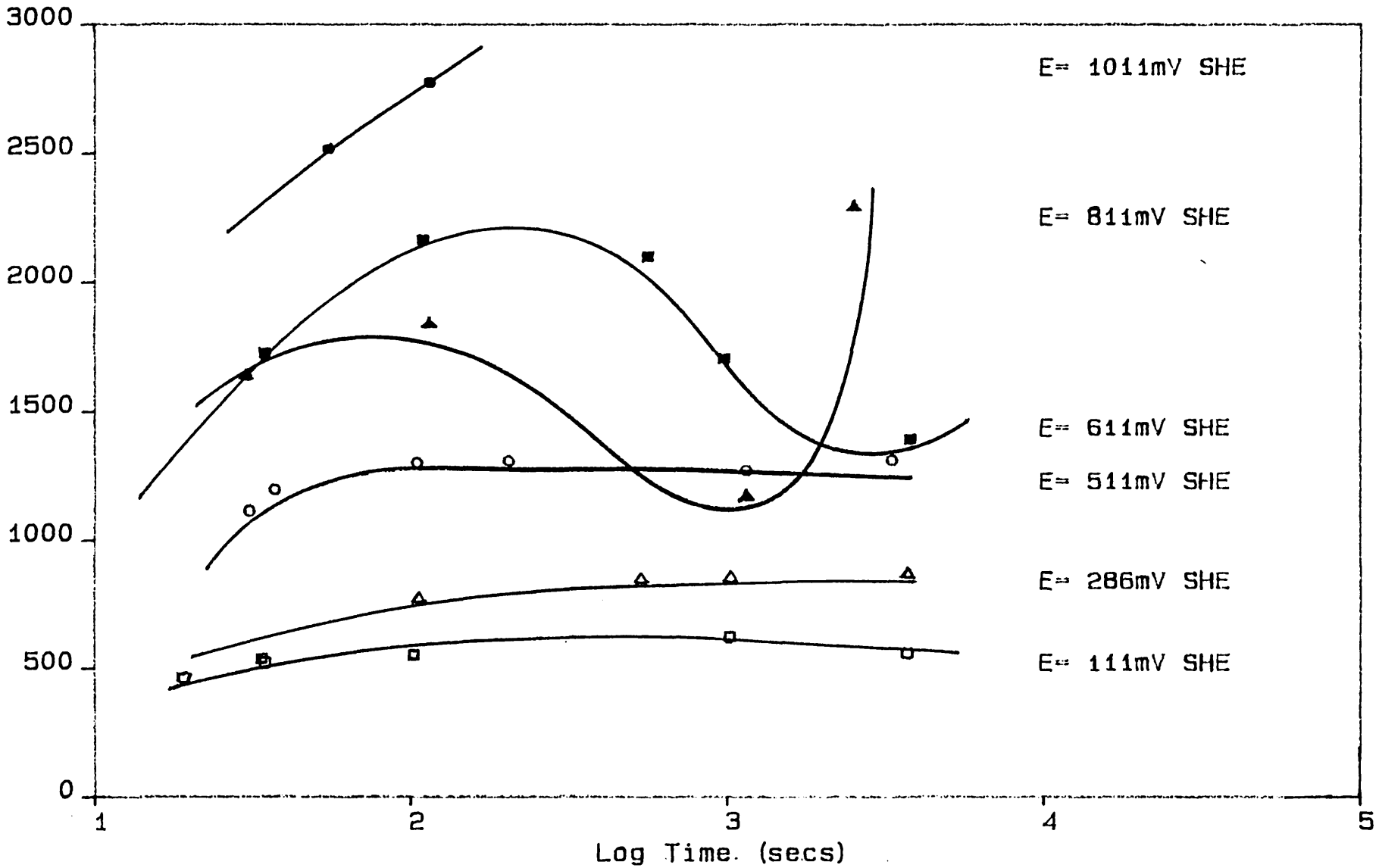
*Although the assignment of an orthorhombic U_3O_7 is thought unlikely, the data for this species is given.

TABLE 12. Film thickness and partial charges for proposed intermediates (calculated using empirical formulae) at different potentials.

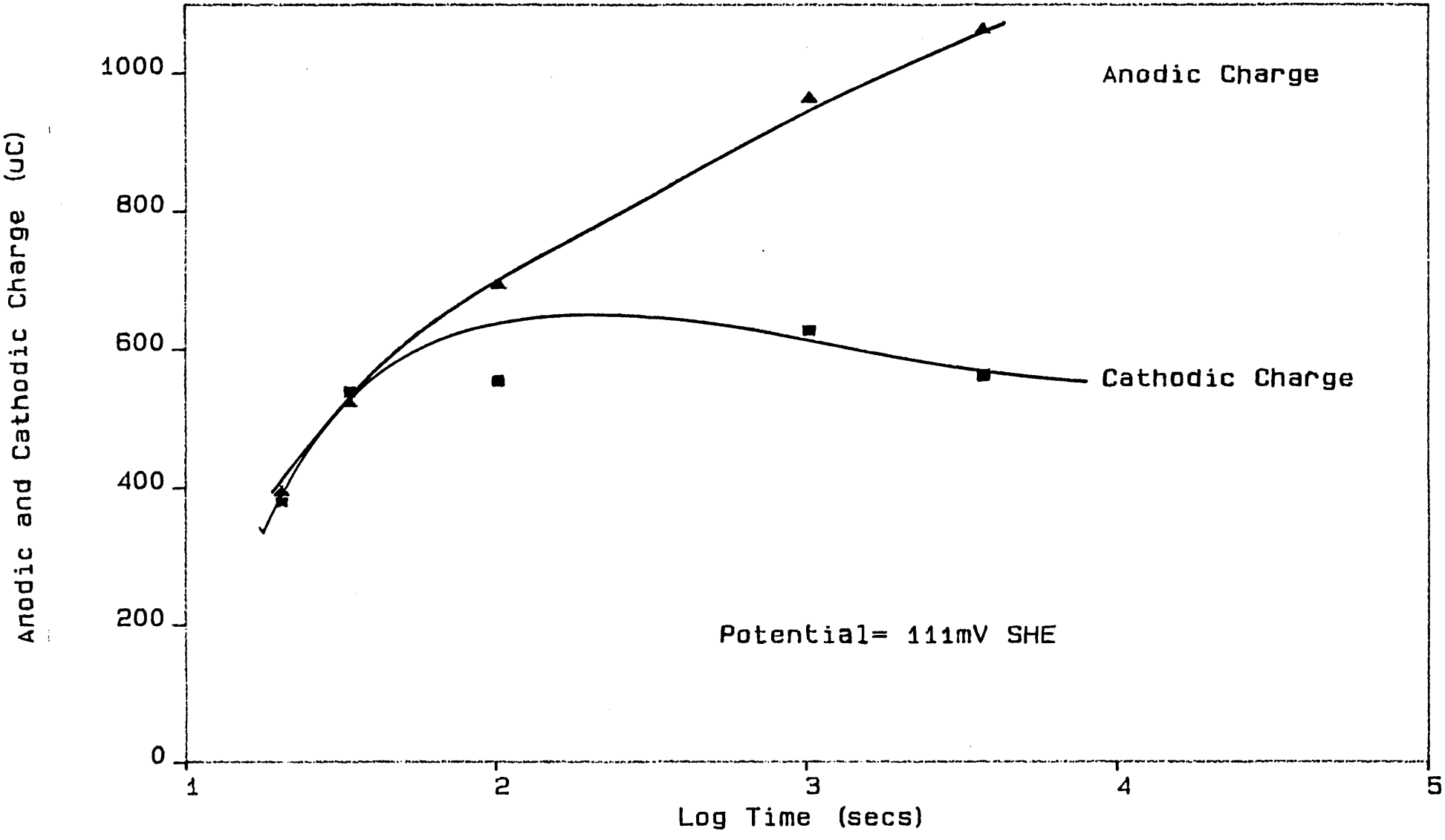
Oxide	Oxides as UO_x	Potential of formation (mV) SHE					Monolayer thickness (Å)
		111	286	611	811	1011	
UO_2^{2+}	$UO_{2.0}^{2+}$			1.2	1.2 0.75	1.6	3.4
U_4O_9	$UO_{2.25}$	6 9					3.9
U_8O_{19}*	$UO_{2.37}$		4.72	6.88			4.04
U_3O_7	$UO_{2.33}$	6.9 2.9	5.36	8.7	16.9 0		4.0
U_2O_5	$UO_{2.50}$		4.76	4.8	11.25 0	13.65 0	4.18
U_3O_8	$UO_{2.67}$			3.6	0 7.4	13.03	4.38
UO_3	$UO_{3.0}$				0 10.25	?	4.76
orthorhombic U_3O_7*	$UO_{2.33}$		5.36	7.8			4.0

*Although assignment of an orthorhombic U_3O_7 is thought unlikely, the data is also given.

Graph 2 The Variation of Cathodic Charge with Time at Different Potentials



Graph 3 A Comparison of the Anodic and Cathodic Charges with Time



Further to the discussion on the applicability of crystal structures to thin films, the results are presented using both molecular and empirical formulae. It is felt that the latter give a better basis for comparisons of film thickness. It is stressed that both methods yield the same relative results.

3.2.3 Summary of the Voltammetry results

At pH = 1.5 the cathodic stripping voltammetry yields results that amplify the cyclic voltammetry. Both sets of results point to a complex mechanism involving many intermediate oxides.

The cathodic stripping voltammetry implies 7 intermediate oxides in the potential range 111 mV < E < 1011 mV SHE. This corresponds to the major area of complex oxidation in the cyclic voltammetry. The cyclic voltammetry also showed 2 further areas of oxidation (peaks 1 and 2). These areas contained very shallow and ill-defined peaks, and were thought to correspond to the similarly disposed peaks in the carbon paste uranium oxide cyclic voltammograms. These peaks were thought to represent reduction products of the uranium oxides UO_2, U_3O_7 and possibly U_2O_5. The identity of those reduction products was thought to be lower uranium oxides, e.g. U_4O_7 etc.

The results obtained from the carbon paste cyclic voltammograms of UO_3 and $UO_4.4H_2O$ were not fully understood,

but comparisons of general shape and peak topography led to the conclusion that they were not of the same series as the voltammograms of the lower oxides.

The reduction patterns observed from the cyclic voltammetry compare well with the stripping potentials of intermediates found in the cathodic stripping voltammetry.

The presence of two cathodic reduction areas indicated by cyclic voltammetry, (peaks 7 and 8) was not confirmed by the cathodic stripping voltammetry. However, it was thought that the oxidation products involved in the reductions presented by peaks (7) and (8) were formed at peaks (1) and (2). The potentials at which peaks (1) and (2) were recorded, were not covered in the cathodic stripping voltammetry.

Cyclic voltammetry results at different pHs ($1.5 < pH < 12.06$) indicate a similar, complex pattern of intermediates. Results at all pHs are consistent with previous work. It was noted that voltammograms recorded at higher pHs had greater clarity than those recorded at low pH. This was thought to be due to the differences in the quantities of intermediates involved in each case.

On the assumption that these intermediates were oxides, tentative identifications were made on the basis of the apparent reversibility of the reductions and the potentials of formation of the intermediates. Good agreement between these two factors and the structures and properties of the

oxides were obtained. An element of uncertainty exists about the identity of one oxide. It was thought to be an orthorhombic form of U_3O_7, or U_8O_{19}. It was noted that U_8O_{19} is very closely related structurally and stoichiometrically to U_3O_7.

The coulometric part of the cathodic stripping voltammetry confirmed the existence of a complex series of surface films. The coulometric determinations also showed that prior to the major uranium dissolution process, a small amount of uranium may be dissolved in a secondary, slow process. Whether this is an entirely different mechanism, or simply a part of the primary mechanism that is only apparent in the initial film building stage is not certain.

Estimations of the charge associated with each stripped intermediate allowed film thicknesses to be estimated. Film thickness can help to identify the rate determining steps. These results may indicate at least two rate determining steps in the potential range of interest. At high potentials ($811 \leq E \leq 1011$ mV SHE) the major, stabilised oxide present was U_3O_8. This indicates that U_3O_8 may be involved in the high potential rate determining step. At low potentials (111 mV $\leq E \leq 611$ mV SHE) the major product was U_3O_7. Large quantities of U_8O_{19} (or orthorhombic U_3O_7) were also present. These two oxides are very closely related stoichiometrically and structurally.

On the basis of these conclusions and observations, a preliminary mechanism consistent with experimental observations will be proposed.

Oxidation:

$$UO_2 \longrightarrow UO_2^{2+} + 2e \quad (93)$$

At less oxidizing potentials (-111 mV $< E <$ 611 mV SHE)

$$4UO_2 + H_2O \longrightarrow [U_4O_8(OH)] + H^+ + e^- \quad (94)$$

$$[U_4O_8(OH)] \longrightarrow U_4O_9 + H^+ + e^- \quad (95)$$

$$3U_4O_9 + H_2O \longrightarrow [U_{12}O_{27}(OH)] + H^+ + e^- \quad (96)$$

$$[U_{12}O_{27}(OH)] \longrightarrow 4U_3O_7 + H^+ + e^- \quad (97)$$

and possibly

$$8U_3O_7 + H_2O \longrightarrow [U_{24}O_{56}(OH)] + H^+ + e^- \quad (98)$$

$$[U_{24}O_{56}(OH)] \longrightarrow 3U_8O_{19} + H^+ + e^- \quad (99)$$

Also occurring very slowly, (these are secondary reactions at this potential) are:

$$UO_2^{2+} + 2U_4O_9 + H_2O \longrightarrow 3U_3O_7 + 2H^+ \quad (100)$$

$$UO_2^{2+} + U_3O_7 + H_2O \longrightarrow 2U_2O_5 + 2H^+ \quad (101)$$

and

$$UO_2^{2+} + U_2O_5 \longrightarrow U_3O_8 + 2H^+ \quad (102)$$

The rate determining step is in the next oxidation step of either U_3O_7 or U_8O_{19}; both of which are very similar, i.e.

either

$$2U_3O_7 + H_2O \longrightarrow [U_6O_{14}(OH)] + H^+ + e^- \quad (103)$$

$$[U_6O_{14}(OH)] \longrightarrow 3U_2O_5 + H^+ + e^- \quad (104)$$

and/or

$$U_8O_{19} + H_2O \longrightarrow [U_8O_{19}(OH)] + H^+ + e^- \quad (105)$$

$$[U_8O_{19}(OH)] \longrightarrow 4U_2O_5 + H^+ + e^- \quad (106)$$

After this the next step is:

$$U_2O_5 + 2H^+ \longrightarrow 2UO_2^{2+} + H_2O + 2e^- \quad (107)$$

and/or

$$3U_2O_5 + H_2O \longrightarrow [U_6O_{15}(OH)] + H^+ + e^- \quad (108)$$

$$[U_6O_{15}(OH)] \longrightarrow 2U_3O_8 + H^+ + e^- \quad (109)$$

followed by dissolution.

At more oxidizing potentials (100), (101), (102) are much faster.
This gives a surface layer of U_3O_8.
The following secondary reactions also occur very slowly.

$$U_3O_8 + 4H^+ \longrightarrow 3UO_2^{2+} + 2H^+ + 2e^- \quad (110)$$

The rate determining step is now the next stage of oxidation:

$$U_3O_8 + H_2O \longrightarrow [U_3O_8(OH)] + H^+ + e^- \quad (111)$$

$$[U_3O_8(OH)] \longrightarrow 3UO_3 + H^+ + e^- \quad (112)$$

After this:

$$UO_3 + 2H^+ \longrightarrow UO_2^{2+} + H_2O \qquad (113)$$

and/or

$$UO_2^{2+} + 3H_2O \longrightarrow UO_3.2H_2O + 2H^+ \qquad (114)$$

followed by dissolution.

Dissolution:

$$UO_2^{2+} \longrightarrow UO_2^{2+}\,(s) \qquad (115)$$

$$UO_2^{2+}(s) + SO_4^{2-} \longrightarrow UO_2SO_4(s) \qquad (116)$$

$$UO_2SO_4\,(s) \longrightarrow UO_2SO_4\,(b) \qquad (117)$$

higher sulphate complexes also form e.g. $UO_2(SO_4)_2^{2-}$...

Notes: (i) all UO_2^{2+} is adsorbed, except when marked with a subscript as below:

s = surface

b = bulk

(ii) Large square brackets indicate transition complexes.

The above tentative mechanism accounts for the experimental observations thus far, and for the next stage of the work an experimental mechanism is required. It is stressed that no oxide has been isolated or identified, which would strengthen evidence for this mechanism. This mechanism is an attempt to quantify the type of oxidation

mechanism proposed. Obviously no direct proof exists for any of the individual steps, although each step is written as a one electron transfer and is theoretically possible. The species that appear as products in for example reactions (94), (96)... are not meant to represent different oxide phases, rather the transition between one oxide phase and another.

3.2.4 Chronoamperometry

3.2.4 (a) Tafel slope determination

When an electrode reaction is performed under irreversible (Tafel) conditions, the assumption that one of the complimentary half cell reactions is producing >98% of the current is valid. In these situations the transfer coefficients of the system can be evaluated, thus assisting mechanistic diagnosis.

As discussed in Appendix 1, the complex Butler-Volmer equation for the anodic half cell reaction rate under Tafel conditions is:

$$i = Fk_a^{o}[A]^{x}\ldots \exp = \frac{\overleftarrow{\alpha} FEa}{RT} \qquad (118)$$

where $\overleftarrow{\alpha} = \frac{n - \vec{\psi}}{\nu} - r\beta$

all symbols retain their normal significance.

The identity of the rate determining step in the reaction sequence is indicated by the magnitude of the transfer coefficient. If there is more than one Tafel region, then there is more than one rate determining step over the potential range being studied. Each rate determining step is valid over the potential range of its Tafel slope.

The Tafel slopes of the system were determined in sodium sulphate (1 M) at pH = 1.5 and a temperature of 30°C. Table 13 contains the steady state current and potential data. Graph 4 is the Tafel plot of the system. The fact that there are two Tafel regions implies that there are two rate determining steps over the potential range studied. This is consistent with previous work,[38,41] and the results of the voltammetry.

Normally in mechanistic studies, the experimentally determined transfer coefficients are compared to the theoretical transfer coefficient of the suspected rate determining step in the proposed mechanism. In this case, although two possible rate determining steps have been proposed from the voltammetry results, the transfer coefficients for all the reactions proposed in this work and others[38-45] will be calculated. The reason for this is that the evidence for the proposed mechanism is rather flimsy. By calculating all possible transfer coefficients, any reaction in the system which gives transfer coefficients of the appropriate magnitude can be examined. Table 14 contains the calculated anodic and cathodic transfer coefficient data for the whole

mechanism. Table 15 contains the experimental Tafel slope analysis. The magnitude of the experimentally determined transfer coefficients agrees well with previous work.[38,41]

Comparing the experimentally determined (570 mV $\leq$ E $\leq$ 700mV SHE) anodic transfer coefficient to theoretical anodic and cathodic transfer coefficients (assuming that a = ν = 1), it becomes obvious that there are three possible reactions which give transfer coefficients of the right magnitude. They are:

$$[U_{24}O_{56}(OH)] \longrightarrow 3U_8O_{19} + H^+ + e^- \qquad \overleftarrow{\alpha}=0.792 \quad (99)$$

$$[U_6O_{14}(OH)] \longrightarrow 3U_2O_5 + H^+ + e^- \qquad \overleftarrow{\alpha}=0.668 \quad (104)$$

$$U_8O_{19} + H_2O \longrightarrow [U_8O_{19}(OH)] + H^+ + e^- \qquad \overleftarrow{\alpha}=0.751 \quad (105)$$

The experimentally determined anodic transfer coefficient is 0.74.

It is immediately apparent that all these reactions are from the area of the mechanism where U_3O_7 or U_8O_{19} is being oxidised. This is consistent with the results of the voltammetry. It is difficult to discriminate further between these steps, but as both U_8O_{19} and U_3O_7 are present in large quantities, it is difficult to imagine the U_3O_7 to U_8O_{19} oxidation as rate limiting. This therefore deletes reaction (99). It has already been mentioned that the structure of U_3O_7 is very similar to U_8O_{19}, and this similarity is reflected in the closeness of the potential at which both these species are reduced (Table 7). It is therefore

possible that the oxidation of both U_8O_{19} and U_3O_7 to U_2O_5 is rate limiting. If this were so, this could be understood in the context of the major changes in the lattice structure which take place at this point in the oxidation. The tetragonal lattices of U_3O_7 and U_8O_{19} become the orthorhombic or hexagonal lattice of U_2O_5.

Comparing the experimentally determined (899 mV $\leq$ E $\leq$ 1700 mV SHE) anodic transfer coefficient to the theoretical anodic and cathodic transfer coefficients (assuming that a = ν = 1), again it is obvious that there are two possible reactions which give transfer coefficients of the right magnitude. They are:

$$U_3O_8 + 4H^+ \longrightarrow 3UO_2^{2+} + 2H_2O + 2e^- \quad \overleftarrow{\alpha}=0.16 \qquad (110)$$

$$U_3O_8 + H_2O \longrightarrow [U_3O_8(OH)] + H^+ + e^- \quad \overleftarrow{\alpha}=0.16 \qquad (111)$$

The experimentally determined anodic transfer coefficient is 0.13.

Again it is apparent that both of these reactions are from the area of the mechanism where U_3O_8 is oxidised. This is consistent with the results of the voltammetry. It is not possible to choose a single rate determining step from these two reactions, but if UO_3 is not present at E = 1011 mV (SHE) in the cathodic stripping voltammetry, this would suggest that reaction (110) is more the rate determining step than reaction (111). In the context of the structure changes at this point it is more likely that reaction (110) is rate determining. This is because in

aqueous systems both U_3O_8 and UO_3 are liable to have orthorhombic structures. The difference between their respective structures is therefore very little.

The proposition of Nicol et al.[38,41] that reaction 91(a) is the rate determining process at low pH is attractive because of its simplicity. However, the theoretical anodic transfer coefficient ($\overleftarrow{\alpha}$) that would be expected if this were so is 1.5. This is in obvious contrast to the results obtained in this work, and their own.

Sunder et al. have not yet published their work on the low pH dissolution of uranium dioxide, and have not, to date, published any steady state current-potential data for uranium dioxide dissolution. In their work on the dissolution of uranium dioxide at neutral pH values ($6 < pH < 10$) they note the change in structure from the tetragonal UO_2 - U_4O_9 - U_3O_7 system to the orthorhombic U_2O_5 system is likely to be highly irreversible, and therefore possibly rate determining. The results in this work, although obtained over a different pH range, are consistent with the mechanism proposed in this work.

3.2.4 (b) Reaction order determinations

The orders of reaction with respect to pH, sulphate, hydrogen peroxide and peroxymonosulphuric acid were determined at two potentials. All determinations were carried out at pH = 1.5 and total sulphate concentration

TABLE 13. The steady state current and potential data for the anodic oxidation of UO_2

Potential SHE (mV)	φ ($\mu A\ cm^{-2}$)	log φ
589.0	34.07	3.53
611.9	73.87	4.30
633.2	139.94	4.94
655.2	191.12	5.25
676.4	259.1	5.56
674.2	298.3	5.70
695.2	367.7	5.91
713.9	479.2	6.17
739.2	474.3	6.16
742.6	413.6	6.02
738.8	744.8	6.61
757.9	847.9	6.74
775.5	979.5	6.89
792.8	1114.9	7.02
807.9	1287.9	7.16
806.4	1319.9	7.18
821.1	1498.2	7.31
854.7	1786.0	7.49
883.4	2160.1	7.68
918.0	2431.1	7.80
942.8	2874.8	7.96
975.0	3188.6	8.07
998.1	3662.4	8.21
1022.6	4110.9	8.32

The potentials are corrected for the dry resistance of the electrode.

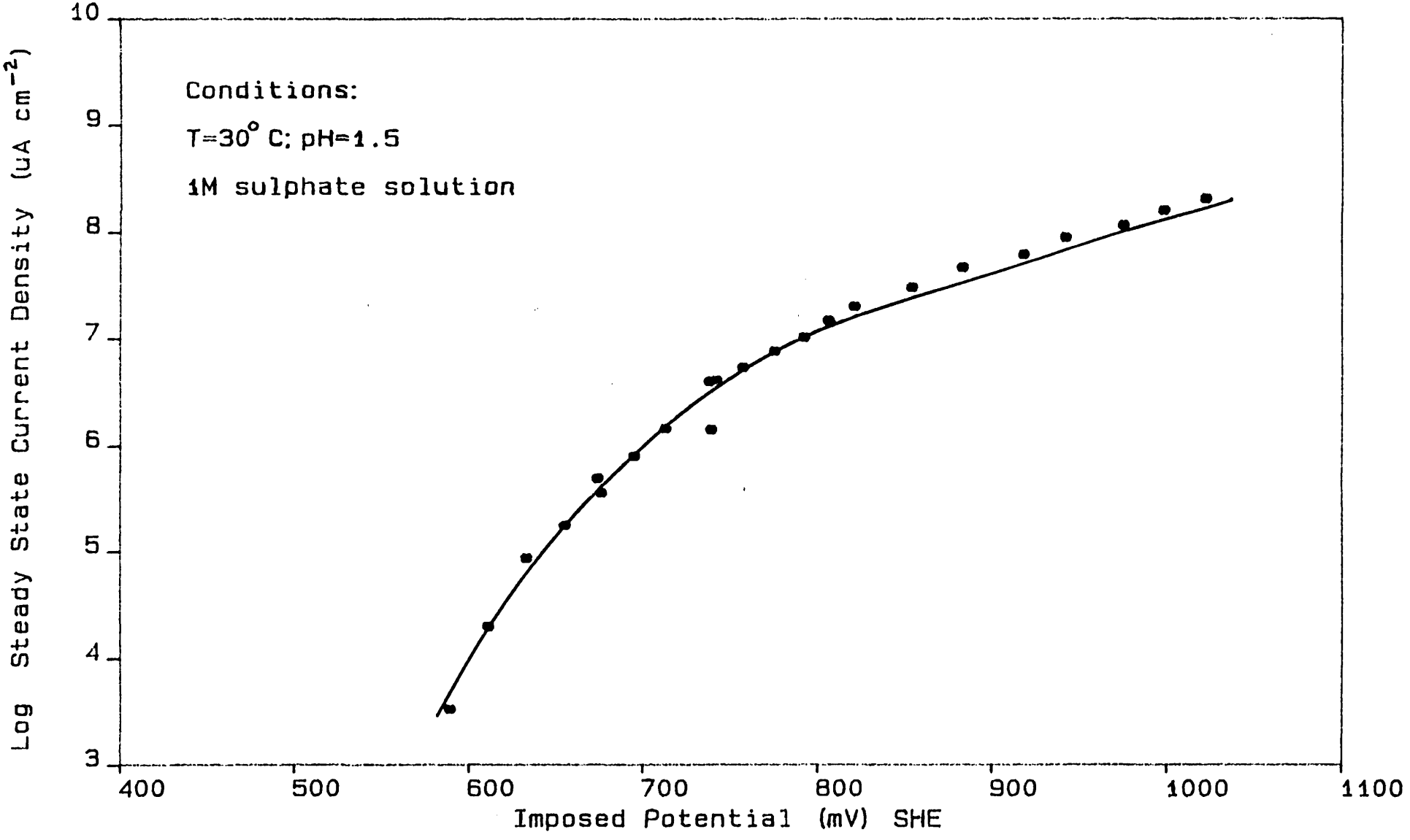
TABLE 14. The calculated anodic and cathodic transfer coefficients for reaction steps in the proposed mechanism.

Reaction number	Reaction	$\vec{\psi}$	$\overleftarrow{\psi}$	r	ν	$\overleftarrow{\alpha}$	$\vec{\alpha}$	No. of electrons in reaction
91	$4UO_2+H_2O \rightarrow U_4O_3(OH)+H^++e^+$	0	1.75	1	1	1.5	0.5	0.25
"	"	0	"	1	2	0.5	0.5	"
92	$U_4O_8(OH) \rightarrow U_4O_9+H^++e^-$	0.25	1.50	1	1	1.25	0.75	0.25
"	"	"	"	1	2	0.375	0.625	"
93	$3U_4O_9+H_2O \rightarrow U_{12}O_{27}(OH)+H^++e^-$	0.50	1.417	1	1	1.0	1.0	0.083
"	"	"	"	1	2	0.25	0.75	"
94	$U_{12}O_{27}(OH) \rightarrow 4U_3O_7+H^++e^-$	0.583	1.334	1	1	0.917	1.08	"
"	"	"	"	1	2	0.209	0.79	"
95	$8U_3O_7+H_2O \rightarrow U_{24}O_{56}(OH)+H^++e^-$	0.666	1.292	1	1	0.833	1.167	0.0416
"	"	"	"	1	2	0.166	0.84	"
96	$U_{24}O_{56}(OH) \rightarrow 3U_8O_{19}+H^++e^-$	0.708	1.251	1	1	0.792	1.21	"
"	"	"	"	1	2	0.146	0.85	"
97	$UO_2^{2+}+2U_4O_9+H_2O \rightarrow 3U_3O_7+2H^+$	0.50	1.333	1	1	1.0	1.0	0.166
"	"	"	"	1	2	0.25	0.75	"
98	$UO_2^{2+}+U_3O_8+H_2O \rightarrow 2U_2O_5+2H^+$	0.666	1.0	1	1	0.833	1.17	0.333
"	"	"	"	1	2	0.166	0.83	"
99	$UO_2^{2+}+U_2O_5+H_2O \rightarrow U_3O_8+2H^+$	1.0	0.666	1	1	0.5	1.5	"
"	"	1.0	"	1	2	-	-	"
100	$2U_3O_7+H_2O \rightarrow U_6O_4(OH)+H^++e^-$	0.666	1.168	1	1	0.834	1.17	0.166
"	"	"	"	1	2	0.167	0.83	"
101	$U_6O_{14}(OH) \rightarrow 3U_2O_5+H^++e^-$	0.832	1.0	1	1	0.668	1.33	"
"	"	"	"	1	2	0.08	0.92	"
102	$U_8O_{19}+H_2O \rightarrow U_8O_{19}(OH)+H^++e^-$	0.749	1.126	1	1	0.751	1.25	0.125
"	"	"	"	1	2	0.125	0.87	"
103	$U_8O_{19}(OH) \rightarrow 4U_2O_5+H^++e^-$	0.874	1.0	1	1	0.613	1.39	"
"	"	"	"	1	2	0.06	0.94	"
104	$U_2O_5+2H^+ \rightarrow 2UO_2^{2+}+H_2O+2e$	1.0	0	1	1	0.50	1.50	1.0
"	"	"	0	1	2	-	-	"
105	$3U_2O_5+H_2O \rightarrow U_6O_{15}(OH)+H^++e^-$	"	0.833	1	1	0.50	1.50	0.166
"	"	"	"	1	2	-	-	"
106	$U_6O_{15}(OH) \rightarrow 2U_3O_8+H^++e^-$	1.166	0.66	1	1	0.374	1.66	"
"	"	"	"	1	2	0.083	0.92	"
107	$U_3O_8+4H^+ \rightarrow 3UO_2^{2+}+2H_2O+2e$	1.333	0	1	1	0.16	1.84	0.667
"	"	"	0	1	2	-	-	"
108	$U_3O_8+H_2O \rightarrow U_3O_8(OH)+H^++e^-$	1.333	0.33	1	1	0.16	1.84	0.333
"	"	"	"	1	2	-	-	"
109	$U_3O_8(OH) \rightarrow 3UO_3+H^++e^-$	1.666	0	1	1	-	-	"
"	"	"	0	1	2	-	-	"
107(a)	$U_3O_8+2H^+ \rightarrow UO_2^{2+}+U_2O_5+H_2O$	1.333	0	0	1	0.66	1.33	0
108(a)	$U_3O_8+H_2O \rightarrow 3UO_3+2H^++2e^-$	"	0	1	1	0.16	1.84	0.66
91(a)	$UO_2+H_2O \rightarrow UO_2OH+H^++e^-$	0	1	1	1	1.5	0.5	1
"	"	0	1	1	2	0.5	0.5	1
92(a)	$UO_2OH \rightarrow UO_3+H^++e^-$	1	0	1	1	0.16	1.84	1
"	"	1	0	1	2	0.5	0.5	1
100(a)	$U_3O_7+H_2O \rightarrow U_3O_7(OH)+H^++e^-$	0.666	1.0	1	1	0.833	1.17	0.33
"	"	0.666	1.0	1	2	0.166	0.84	"
101(a)	$U_3O_7(OH) \rightarrow U_3O_8+H^++e^-$	1.0	0.667	1	1	0.50	1.5	"
"	"	"	"	1	2	-	-	"

TABLE 15. Experimental Tafel Slope Analysis

Potential range of Tafel slope (mV) SHE	$\frac{dE}{d\ln i}$ (mV decade^{-1})	Anodic Transfer Coefficient $\overleftarrow{\alpha}$	Cathodic Transfer Coefficient $\overrightarrow{\alpha}$
$571 \leq E \leq 700$	35.46	0.7366	1.2634
$899 \leq E \leq 1200$	196.0	0.1333	1.8667

Graph 4 The Tafel plot for the Anodic Oxidation of Uranium Dioxide



equal to 1 M. Obviously when these variables were being examined, one of these conditions was not met. All determinations were carried out at a temperature of 25°C, and a potential of 711 mV or 911 mV (SHE). The hydrogen ion variable used was pH, as opposed to hydrogen ion concentration. There are two reasons for this, they are:

(1) Majima et al.[92] have shown that in oxide leaching situations when the ionic strength is high ($\geq$1 M), kinetic data obtained with respect to activities (as opposed to concentrations) of hydrogen ions can often be more meaningfully interpreted. In this case, 1 M sodium sulphate gives high ionic strengths, hence the use of activities. This argument also applied to the interpretation of the kinetic leaching results yet to be discussed.

(2) Although it was possible to calculate the hydrogen ion concentrations for any experiment in this project (see Appendix 2), it was found that in the case of the hydrogen ion concentration, the errors involved in that determination rendered the figures useless. Table 16 contains the steady state current and potential data used for the reaction order determinations. Graphs 5 to 8 show the reaction order plots for the data contained in Table 16.

Graph 5 shows the dependence of the rate of the UO_2 to UO_2^{2+} half cell reaction on pH. In the range $2.5<pH<7.0$ at both potentials, the rate of reaction increases with decreasing pH. The reaction order with respect to the activity of hydrogen ions is -0.07. The reason for this dependence is not fully understood, and the pH region in which it is

displayed is not the central area of interest. However, it is possible that this phenomenon is a non-faradaic effect, and is caused by the changing composition of sulphate solutions with pH. At low pH ($0 < pH < 2$) most of the sulphate is present as the bisulphate ion (HSO_4^-). At high pH ($pH \geq 2$) most of the sulphate is present as sulphate ion (SO_4^{2-}). It is therefore possible that conductance of the electrolyte is different at different pHs. As the pH rises, and more of the bisulphate disassociates to become sulphate, the conductance of the solution should increase. The potentiostat which is in a controlled potential mode senses and compares the potential of the reference electrode to the working electrode through the same 1 M sodium sulphate solution. If the conductance of that solution were to change, in the manner described above, then the potentiostat would respond by imposing a slightly higher potential at low pHs. This would give an apparent (small) negative order of reaction with respect to pH. The other option is simply that a faradaic effect is being observed here, and that the reaction order with respect to pH is significant and indicative of a change in the rate determining step across the pH range being studied. The cyclic voltammetry (see Figure 11) revealed a complex system, the composition of which appeared to vary with pH. This admits the possibility that the rate determining step could also change with pH. However, this latter point can be argued either way. The apparent reaction order is displayed over a large pH range, and at both potentials. The system however, has already been shown to be complex,

the presence of phases being dependent on pH and potential conditions. It is therefore unlikely that one rate determining step would be valid over such a range of conditions.

In conclusion, the apparent reaction order of -0.07 is probably due to non-faradaic effects, but is not fully understood. It has been noted that the apparent reaction order is valid outside the central area of interest of this project.

In the range $0 \leq pH \leq 2.5$, at more oxidizing potential ($E \geq$ 911 mV SHE) the order with respect to the activity of hydrogen ions is 0 whilst at less oxidizing potentials ($E \leq$ 711mV SHE) it is -0.14. This difference in reaction orders is thought to show a different rate determining step at each potential. This conclusion would be consistent with other results obtained in this work. The low potential reaction order of -0.14 with respect to the activity of hydrogen ions could be interpreted as +0.14 with respect to the activity of hydroxyl ions. Further to the discussion in the voltammetry section about the state of oxides on the UO_2 surface, any reaction order must be interpreted in the context of the number of moles of UO_2 involved in the reaction. Therefore, reaction orders with respect to pH can imply either an effect involving hydrogen or hydroxyl ions. The two possible rate determining steps indicated by the transfer coefficients are:

$$[U_6O_{14}(OH)] \longrightarrow 3U_2O_5 + H^+ + e^- \quad (\overleftarrow{\alpha} = 0.668) \quad (104)$$

$$U_8O_{19} + H_2O \longrightarrow [U_8O_{19}(OH)] + H^+ + e^- \quad (\overleftarrow{\alpha} = 0.751) \quad (105)$$

In the cathodic stripping voltammetry U_8O_{19} was found to be present at E = 611 mV (SHE), but not present at E = 811 mV (SHE). If reaction (104) is solely rate determining, then the reaction order with respect to the activity of hydrogen ions (calculated on the number of moles of UO_2 present) is -0.16. If reaction (105) is solely rate determining, then the reaction order with respect to the activity of hydrogen ions (calculated as above) is -0.125. If both steps (104) and (105) were jointly rate determining, then the expected reaction order with respect to the activity of hydrogen ions would be -0.29. It is therefore probable that reaction (104) is rate determining at this potential (E = 711 mV (SHE)), but at less oxidizing potentials, both reactions may be jointly rate determining.

Under oxidising conditions which have been electrolytically imposed, the polarity of the electrode surface would be positive, thus tending to repell hydrogen ions. This in effect means that the local pH adjacent to the electrode surface would be higher than the bulk pH.

At high potential, the reaction order with respect to hydrogen ions is zero. The two rate determining steps indicated by the transfer coefficients are:

$$U_3O_8 + 4H^+ \longrightarrow 3UO_2^{2+} + 2H_2O + 2e^- \quad (\overleftarrow{\alpha}=0.16) \qquad (110)$$

$$U_3O_8 + H_2O \longrightarrow [U_3O_8(OH)] + H^+ + e^- \quad (\overleftarrow{\alpha}=0.16) \qquad (111)$$

Obviously, neither of these reactions has a zero order dependence on the activity of hydrogen ions. Whatever the rate determining step is, because of the magnitude of the anodic transfer coefficient, it must involve U_3O_8. It must also not involve hydrogen ions either in its reactants or products. The possibility of two joint rate determining steps, one which consumes and one which generates hydrogen ions is also possible. An example of such a pair of possible rate determining steps is given below:

$$U_3O_8 + 2H^+ \longrightarrow UO_2^{2+} + U_2O_5 + H_2O \qquad (110a)$$

$$U_3O_8 + H_2O \longrightarrow 3UO_3 + 2H^+ + 2e^- \qquad (111a)$$

Both of these reactions are variants of those proposed above, and both are plausible. Whereas reaction (110) is an oxidative dissolution, reaction (110a) is its non-oxidative counterpart. Reaction (111a) is reaction (111) written as a two electron transfer. Whether this implies an actual two electron transfer, or simply 2 moles of reaction (111) occurring for each mole of reaction (110a) is not clear. If an actual two electron transfer were to occur, this would affect the anodic transfer coefficient. This does not appear to be the case. Two electron transfers have been proposed before for the uranium dioxide dissolution reaction.[38,40,42]

Graph 6 shows the dependence of the rate of the UO_2 to UO_2^{2+} half cell reaction on the concentration of total sulphate at pH = 1.5. The reaction order is zero at both potentials, implying that the sulphate concentration does not affect the UO_2 to UO_2^{2+} half cell reaction in the potential range considered. This is consistent with other results obtained in this work.

Graph 7 shows the dependence of the rate of the UO_2 to UO_2^{2+} half cell reaction on the concentration of hydrogen peroxide at pH = 1.5 and a total sulphate concentration of 1 M. At more oxidizing potential (E = 911 mV (SHE)) and at less oxidizing potential (E = 711 mV (SHE)) when the concentration of hydrogen peroxide is less than 0.03 M the reaction order is zero. At less oxidizing potential when the concentration of hydrogen peroxide is greater than 0.03 M, the reaction order is equal to -0.40. At both these potentials, hydrogen peroxide is unstable with respect to oxidation, reaction (A19).

$$H_2O_2 \longrightarrow O_2 + 2H^+ + 2e^- \qquad \text{(A19)}$$

It is proposed that the rate of the anodic oxidation of UO_2 is unaffected by the concentration of hydrogen peroxide at the potentials studied. Rather, it is sensitive to the hydrogen ions that are produced by the decomposition of the hydrogen peroxide. In this context, the zero order dependence at high potential is consistent with other results obtained in this work. The low potential zero order reaction with respect to H_2O_2 is only maintained

when the concentration of hydrogen peroxide is less than 0.03 M. This compares favourably with the pH derived value ($\sim$0.01 M) at which the reaction order with respect to the activity of hydrogen ions of -0.14 also changes. If the apparent effect of hydrogen peroxide is in fact a hydrogen ion dependence, then from equation (A19), the order with respect to hydrogen peroxide should be twice the order with respect to the activity of hydrogen ions. A value of -0.20 is comparable to -0.14 if it is recalled that the hydrogen peroxide data is based on concentrations, whereas the hydrogen ion data is based on activities. One would expect the activity derived data to be of a lower magnitude due to the activity coefficients of the system.

Graph 8 shows the dependence of the rate of the UO_2 to UO_2^{2+} half cell reaction on the concentration of peroxymonosulphuric acid at pH = 1.5 and a total sulphate concentration of 1 M. The reaction order is zero over the potential range considered, implying that the peroxymonosulphuric acid concentration does not affect the rate of the UO_2 to UO_2^{2+} half cell reaction over the potential range under consideration. There is however, a further point to be noted with respect to Graphs 7 and 8. When a specific potential is potentiostatically imposed, in the absence of any other chemical effect, the rate of the anodic reaction is also set. However, when an oxidising agent is added to this constant potential situation, the observed current is the difference between the partial anodic and

cathodic currents of the system. Graphs 7 and 8 imply that there is no change in the difference between the total anodic and total cathodic currents over the concentration range studied. This can only be so if the order of reduction of each oxidising agent at a UO_2 surface is zero. This order of reduction is not necessarily the same as the order of reaction in the leaching system. This fact is well demonstrated by comparisons of the results of Nicol et al.[43] who reported a reaction order of 1 with respect to the reduction of oxygen at a UO_2 surface, and the results of Wadsworth et al.[56] who report an order of 0.5 with respect to oxygen in the acid leaching of UO_2. The conclusion is that the apparent zero order dependence of the rate of hydrogen peroxide and peroxymonosulphuric acid may not be as straightforward as it appears. In this case however, these apparent zero order dependencies concur with other results to be presented in the chemical leaching section, and lead to the conclusion there is a zero order of reaction with respect to hydrogen peroxide and peroxymonosulphuric acid in the low pH dissolution of UO_2.

By examination of the order plots for hydrogen peroxide and peroxymonosulphuric acid, it is apparent that the current densities at equal potentials are very similar. This implies that the oxidising agents do not modify the rate or mechanism of the anodic half cell reaction (i.e. chemically).

Comparison of these results with those of previous work[41] shows very similar initial results, but the interpretation of these is different in this work. The main problems of the previous work[41] have already been described in Section 1.5.1. The mechanism proposed in this work would give rise to complex cyclic voltammograms, which the mechanism presented previously does not, and also gives a much better correlation of theoretical transfer coefficients to experimentally determined transfer coefficients. This is especially true of the higher potential transfer coefficient.

3.2.5. Summary

The preliminary mechanism suggested by the voltammetry section of this work has been examined to determine the identity of the rate determining steps. Two Tafel areas were found, implying that there are two potential dependent rate determining steps. This confirmed results from the voltammetry section. The magnitudes of the two anodic transfer coefficients were determined, and hence the complimentary cathodic transfer coefficients were calculated. These were compared to theoretical transfer coefficients calculated from the proposed mechanism. The possible rate determining steps were similar to those implied by the voltammetry.

The reaction orders with respect to pH and the concentrations of total sulphate, hydrogen peroxide, and

TABLE 16. The steady state current and potential data for the reaction order determination.

(a) The effect of pH on the $UO_2 \rightarrow UO_2^{2+}$ half cell reaction, [TS] = 1 M.

Potential (mV)SHE Imposed	Current Density (ϙ) μA cm^{-2}	log ϙ	pH
711	445.8	2.65	6.20
"	657.8	2.82	3.85
"	713.2	2.85	1.50
"	471.4	2.67	0.80
"	493.3	2.69	0.40
"	974.3	2.99	2.50
911	1946.5	3.29	6.20
"	1954.6	3.29	3.85
"	2870.5	3.46	1.50
"	2725.6	3.43	0.80
"	2806.5	3.45	0.40
"	3042.2	3.48	2.50

(b) The effect of sulphate on the $UO_2 \rightarrow UO_2^{2+}$ half cell reaction, pH = 1.5

Potential (mV) SHE Imposed	log[TS]	Current Density (ϙ) μA cm^{-2}	log ϙ	Total sulphate
711	-1.00	910.0	2.96	0.1
"	-3.00	994.2	3.00	0.001
"	-2.30	1013.1	3.00	0.005
"	0.0	713.2	2.85	1.0
"		817.2	2.91	0
"	-1.147	575.5	2.76	0.07
911	-1.00	2756.9	3.44	0.1
"	-3.00	3255.4	3.51	0.001
"	-2.30	3352.7	3.52	0.005
"	0.0	2870.4	3.46	1.0
"	-	3187.9	3.50	0
"	-1.147	2891.8	3.46	0.07

TABLE 16. (continued)

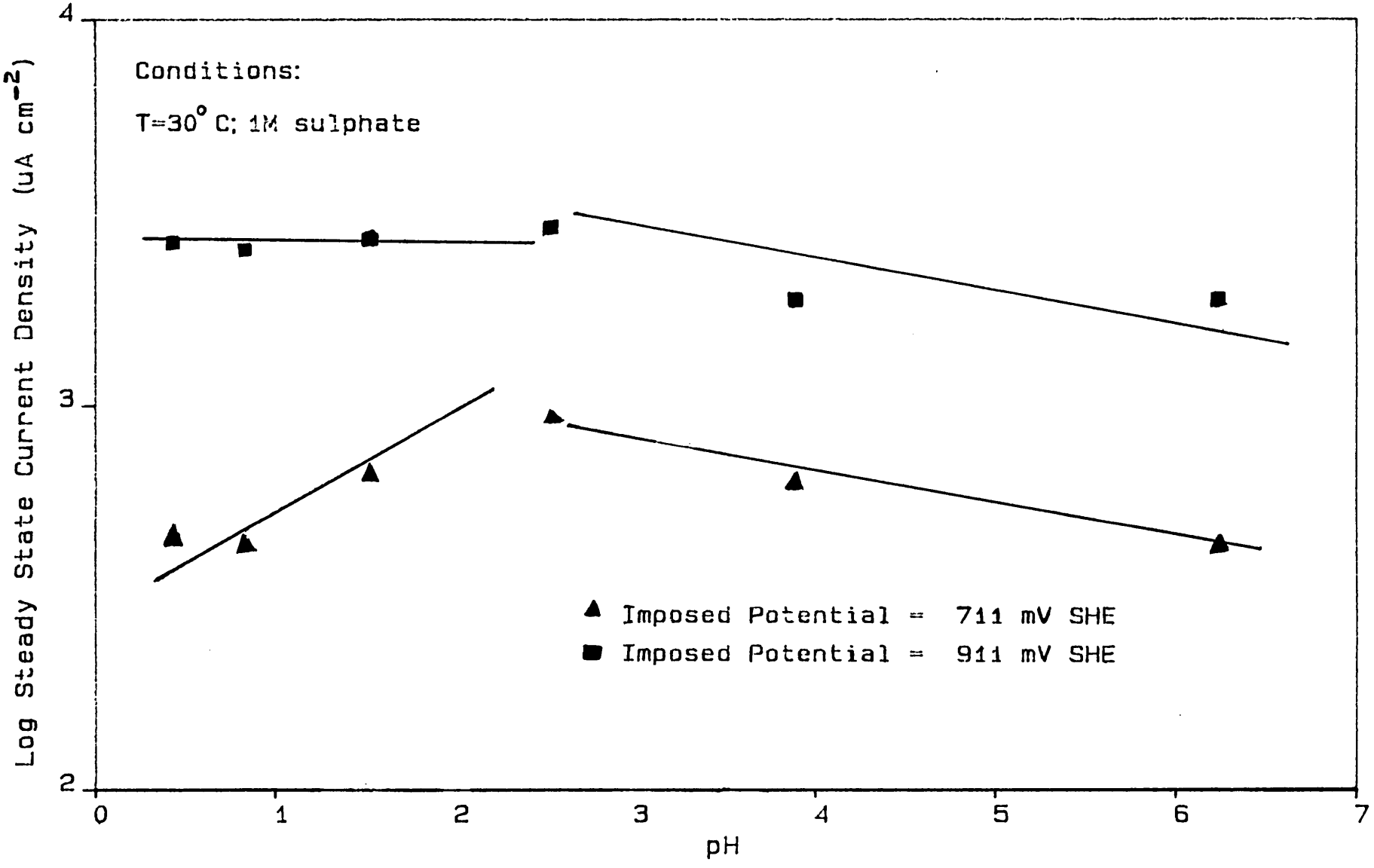
(c) The effect of hydrogen peroxide on the $UO_2 \rightarrow UO_2^{2+}$ half cell reaction, pH = 1.5; [TS] = 1 M.

Potential (mV) SHE	Current Density φ ($\mu A\ cm^{-2}$)	log φ	Concentration of hydrogen peroxide	log[H_2O_2]
711	575.5	2.760	0.07	-1.155
"	334.4	2.524	0.30	-0.523
"	535.6	2.728	0.005	-2.301
"	713.2	2.853	0.0	-
"	630.96	2.80	0.02	-1.699
"	648.4	2.81	0.0001	-4.0
911	2891.8	3.461	0.07	-1.155
"	2847.0	3.454	0.30	-0.523
"	2350.9	3.371	0.005	-2.301
"	2870.4	3.458	0.0	-
"	2818.4	3.450	0.02	-1.699
"	2897.3	3.462	0.0001	-4.0

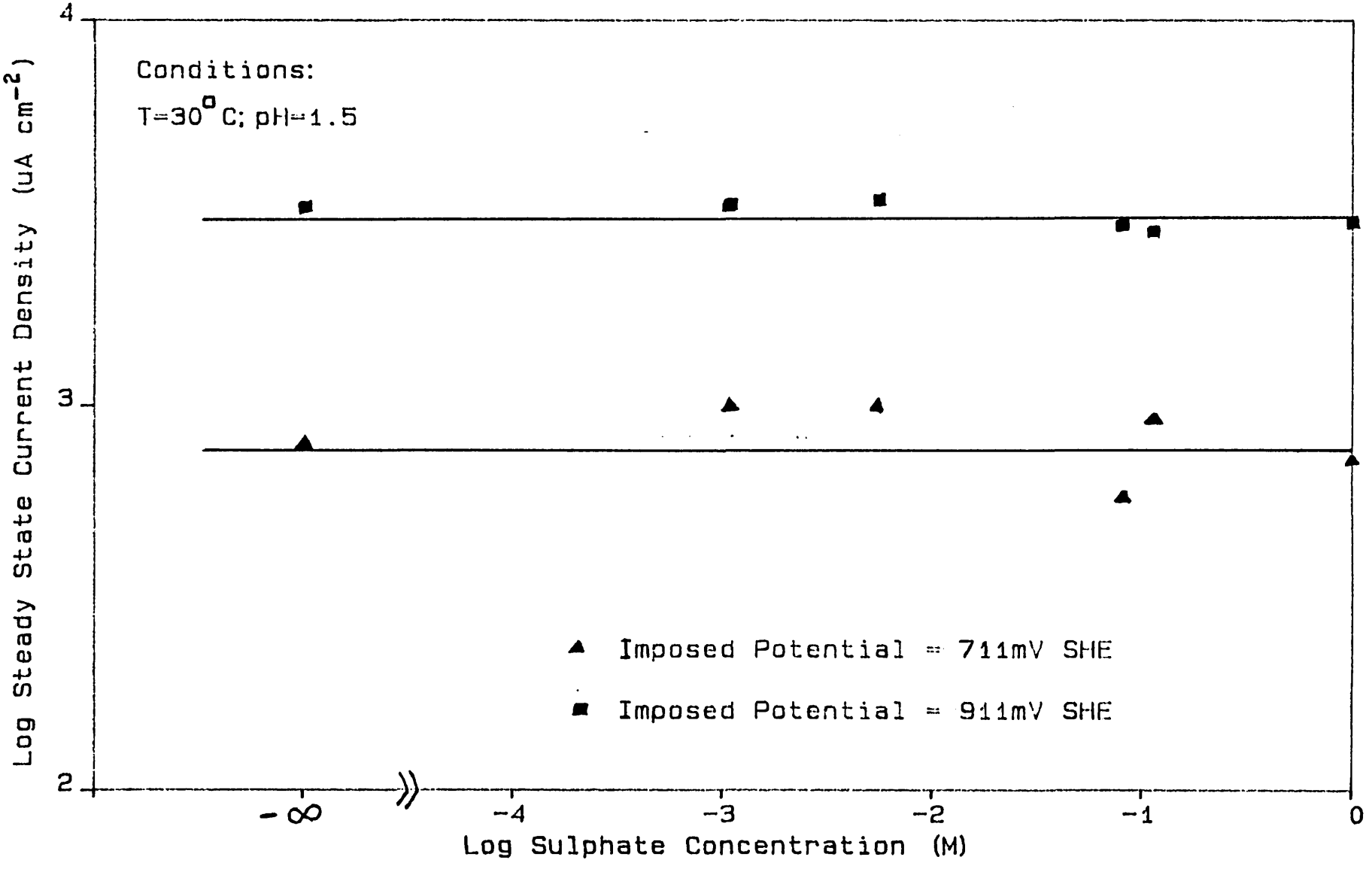
(d) The effect of peroxymonosulphuric acid on the $UO_2 \rightarrow UO_2^{2+}$ half cell reaction, pH = 1.5, [TS] = 1 M.

Potential (mV) SHE	Current Density φ ($\mu A\ cm^{-2}$)	log φ	Concentration of peroxymonosulphuric acid	log[HSO_5]
711	713.2	2.853	0	-
"	724.9	2.86	0.005	-2.30
"	623.8	2.79	0.05	-1.30
"	489.0	2.69	0.50	-0.30
"	707.9	2.85	0.0001	-4.0
911	2870	3.458	0	-
"	2457	3.39	0.005	-2.30
"	2578	3.41	0.05	-1.30
"	2421	3.38	0.50	-0.30
"	2630.3	3.42	0.0001	-4.0

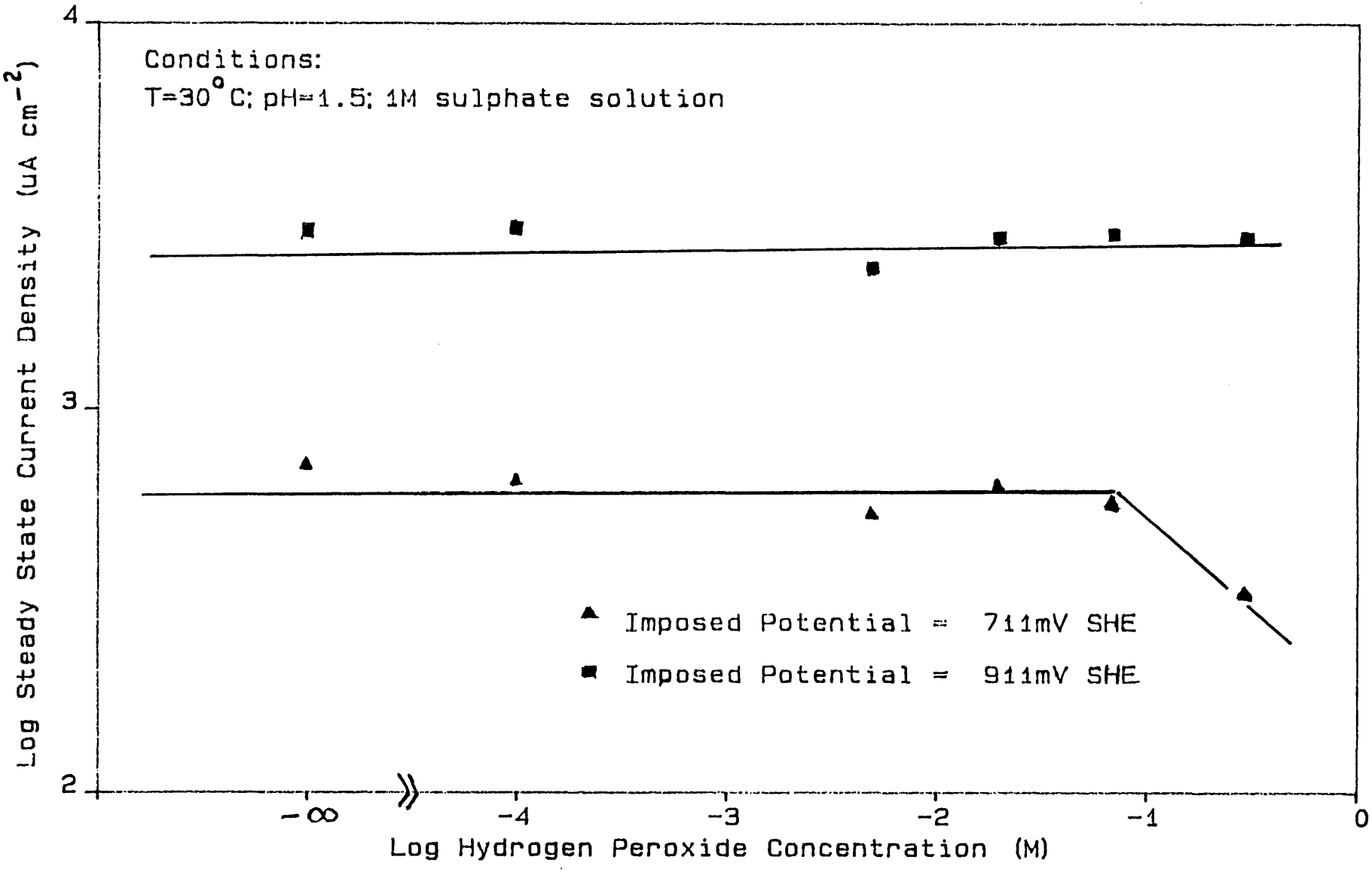
Graph 5 The Effect of pH on the Anodic Oxidation of Uranium Dioxide



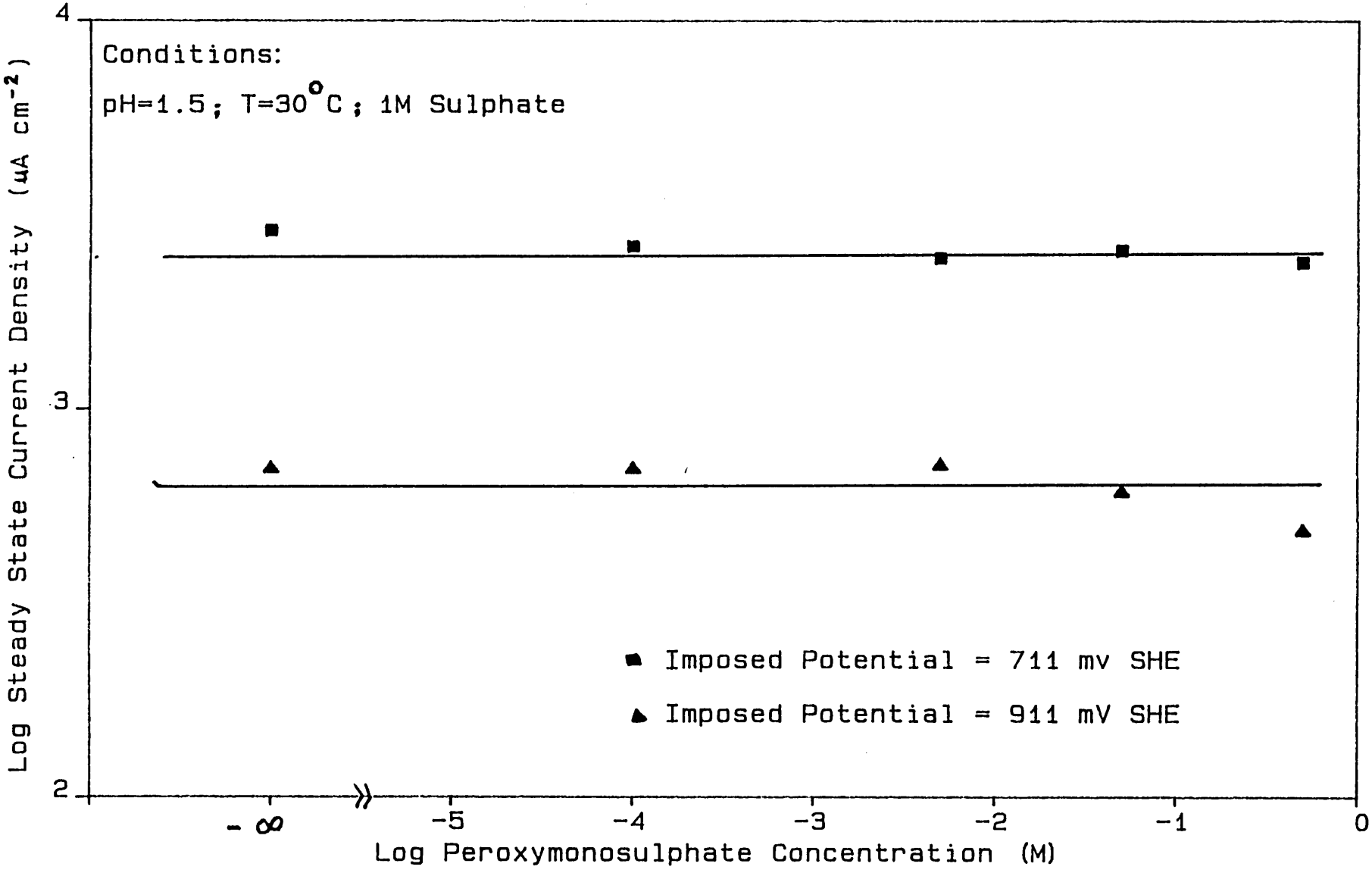
Graph 6 The Effect of Sulphate on the Oxidation of Uranium Dioxide



Graph 7 The Effect of Hydrogen Peroxide on the Oxidation of Uranium Dioxide



Graph 8. The Effect of Peroxymonosulphate on the Oxidation of UO_2



peroxymonosulphuric acid were determined at two potentials. These results further refined the knowledge of the rate determining steps of the process, and were consistent with all previous results in this work.

There are two inconsistencies left unanswered in this section. They are:

(1) The voltammetry section indicates large quantities of U_8O_{19} present with U_3O_7 at E = 611 mV (SHE) but no U_8O_{19} present at E = 811 mV (SHE). The reaction order analysis precludes the involvement of U_8O_{19} in the rate determining step at E = 711 mV (SHE). This may imply that although at E = 611 mV (SHE) there are two very similar rate determining steps occurring concurrently, involving both U_3O_7 and U_9O_{18}, at E = 711 mV (SHE), only oxidation of U_3O_7 is rate limiting.

(2) The reaction order analysis indicates a rate dependency on pH at high pH values. This is not understood.

It must be apparent at this point that unless the surface oxides can be unequivocably identified, the mechanism cannot be said to be proven. However, all the results of this work point to a mechanism of this nature, and although uncertainties over the identification of individual oxides remain, it is difficult to imagine any other type of mechanism that would explain the results of the chronoamperometric and voltammometric studies.

The mechanism proposed in this work also ameliorates difficulties in the mechanism of UO_2 dissolution proposed by Nicol et al.[41]

It appears that hydrogen peroxide and peroxymonosulphuric acid do not, in a chemical sense, modify the rate of the anodic oxidation of UO_2. It is proposed that the oxidation of UO_2 under acidic conditions proceeds via a number of surface oxide species and the rate determining stages coincide with major changes in the lattice structure. A mechanism consistent with the experimental results is summarised below. Every step in the proposed mechanism is a single electron transfer. The individual steps appear at the end of the voltammetry section.

Oxidation:

At less oxidizing potentials $111\ mV \leq E \leq 611\ mV$ (SHE)

$$4UO_2 + H_2O \longrightarrow U_4O_9 + 2H^+ + 2e^- \qquad (94\text{-}95)$$

$$3U_4O_9 + H_2O \longrightarrow 4U_3O_7 + 2H^+ + 2e^- \qquad (96\text{-}97)$$

$$8U_3O_7 + H_2O \longrightarrow 3U_8O_{19} + 2H^+ + 2e^- \qquad (98\text{-}99)$$

$$2U_3O_7 + H_2O \longrightarrow 3U_2O_5 + 2H^+ + 2e^- \qquad (103\text{-}104)$$

$$U_8O_{19} + H_2O \longrightarrow 4U_2O_5 + 2H^+ + 2e^- \qquad (105\text{-}106)$$

$$[U_6O_{14}(OH)] \longrightarrow 3U_2O_5 + H^+ + e^- \qquad (104)$$

$$U_8O_{19} + H_2O \longrightarrow [U_8O_{19}(OH)] + H^+ + e^- \qquad (105)$$

where reactions (104) and (105) are jointly rate determining. When $E \geq 761\ mV$ (SHE) reactions (98-99) and (105-106) do not occur.

Then

$$U_2O_5 + 2H^+ \longrightarrow 2UO_2^{2+} + H_2O + 2e^- \qquad (107)$$

Followed by dissolution:

At more oxidizing potentials $761\ mV \leq E \leq 1011\ mV$ (SHE), the following reactions also occur at appreciable rates.

$$UO_2 \longrightarrow UO_2^{2+} + 2e^- \qquad (93)$$

$$UO_2^{2+} + U_3O_7 + H_2O \longrightarrow 2U_2O_5 + 2H^+ \qquad (101)$$

$$UO_2^{2+} + U_2O_5 + H_2O \longrightarrow U_3O_8 + 2H^+ \qquad (102)$$

$$3U_2O_5 + H_2O \longrightarrow 2U_3O_8 + 2H^+ + 2e^- \qquad (108\text{-}109)$$

$$U_3O_8 + 2H^+ \longrightarrow UO_2^{2+} + U_2O_5 + H_2O \qquad (110a)$$

$$U_3O_8 + H_2O \longrightarrow 3UO_3 + 2H^+ + 2e^- \qquad (111a)$$

When the original layer of U_2O_5 is covered by a layer of U_3O_8, the oxidation of U_3O_8 (reactions (110a) and (111a)) is rate determining.

Then

$$UO_3 + 2H^+ \longrightarrow UO_2^{2+} + H_2O \qquad (113)$$

$$UO_2^{2+} + 3H_2O \longrightarrow UO_3.2H_2O + 2H^+ \qquad (114)$$

Followed by dissolution

Dissolution

$$UO_2^{2+} \longrightarrow UO_2^{2+}\ (s) \qquad (115)$$

$$UO_2^{2+} + SO_4^{2-} \longrightarrow UO_2SO_4\ (s) \qquad (116)$$

$$UO_2SO_4\ (s) \longrightarrow UO_2SO_4\ (b) \qquad (117)$$

Higher sulphate complexes form according to pH e.g. $UO_2(SO_4)_2^{2-}$ ...

Note: all UO_2^{2+} is adsorbed, except when marked with a subscript:

s = surface

b = bulk.

3.3 THE MECHANISM OF THE FULL LEACHING SYSTEM

3.3.1 Introduction

In the last section, the mechanism of the anodic oxidation of UO_2 was studied. The aim of this section is to gain an insight into the mechanism of the overall leaching process, and to determine whether the rate determining step is contained in the anodic or cathodic half cell reaction. The work reported in this section was the major part of the project. The experiments consisted of chemical leaching runs, which have already been described. The experimental data for all the kinetic runs appears in Appendix 3. The composition of each run was calculated using a computer program, as described in Appendix 2. Only those runs for

which a unique rate could be determined, and which were amenable to composition analysis, as described in Appendix 2, were included in the statistical regression analysis. It was found that those runs which contained potassium were not amenable to composition analysis. The reason for this is that the only sulphate/bisulphate equilibrium data available were for the sulphuric acid and sodium bisulphate systems. Initially, it was assumed that this data could be applied to the potassium sulphate/bisulphate system. This was shown not to be the case.

3.3.2 Peroxymonosulphuric Acid

The fact that the initial rate data can be fitted to the shrinking particle model (119) indicates that diffusion of reactants or products through a growing product layer is not rate limiting. This model does not, of itself allow discrimination between chemical or diffusion control of reaction rate.

$$1 - (1 - \alpha)^{\frac{1}{3}} = kt \qquad (119)$$

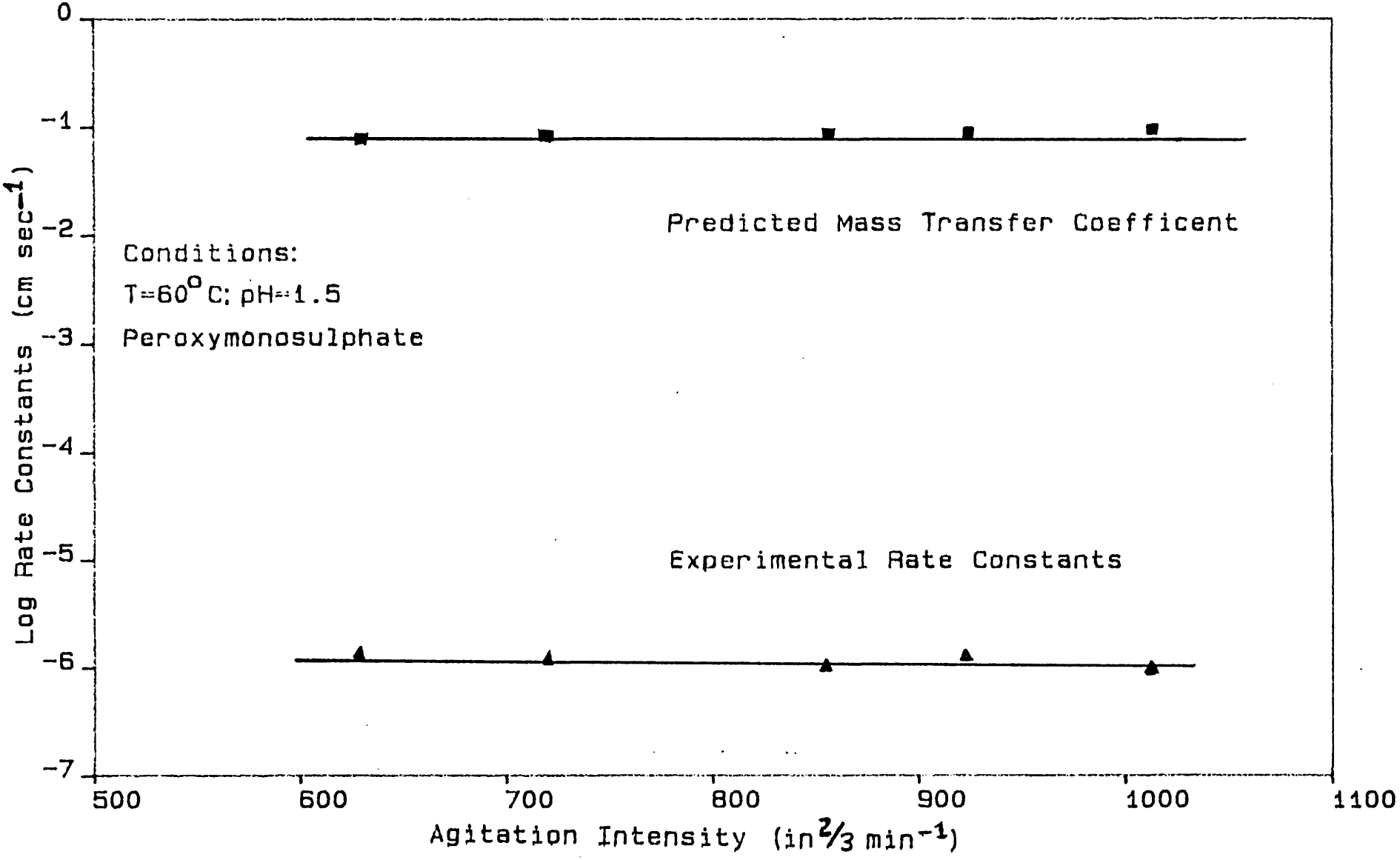
where all symbols have their usual meaning.

One method of deciding whether a reaction is chemically or diffusion controlled is by the calculation of the mass transfer coefficients for the diffusing species. Comparison of these with experimentally determined rate constants can indicate if diffusion of any of these species could be rate

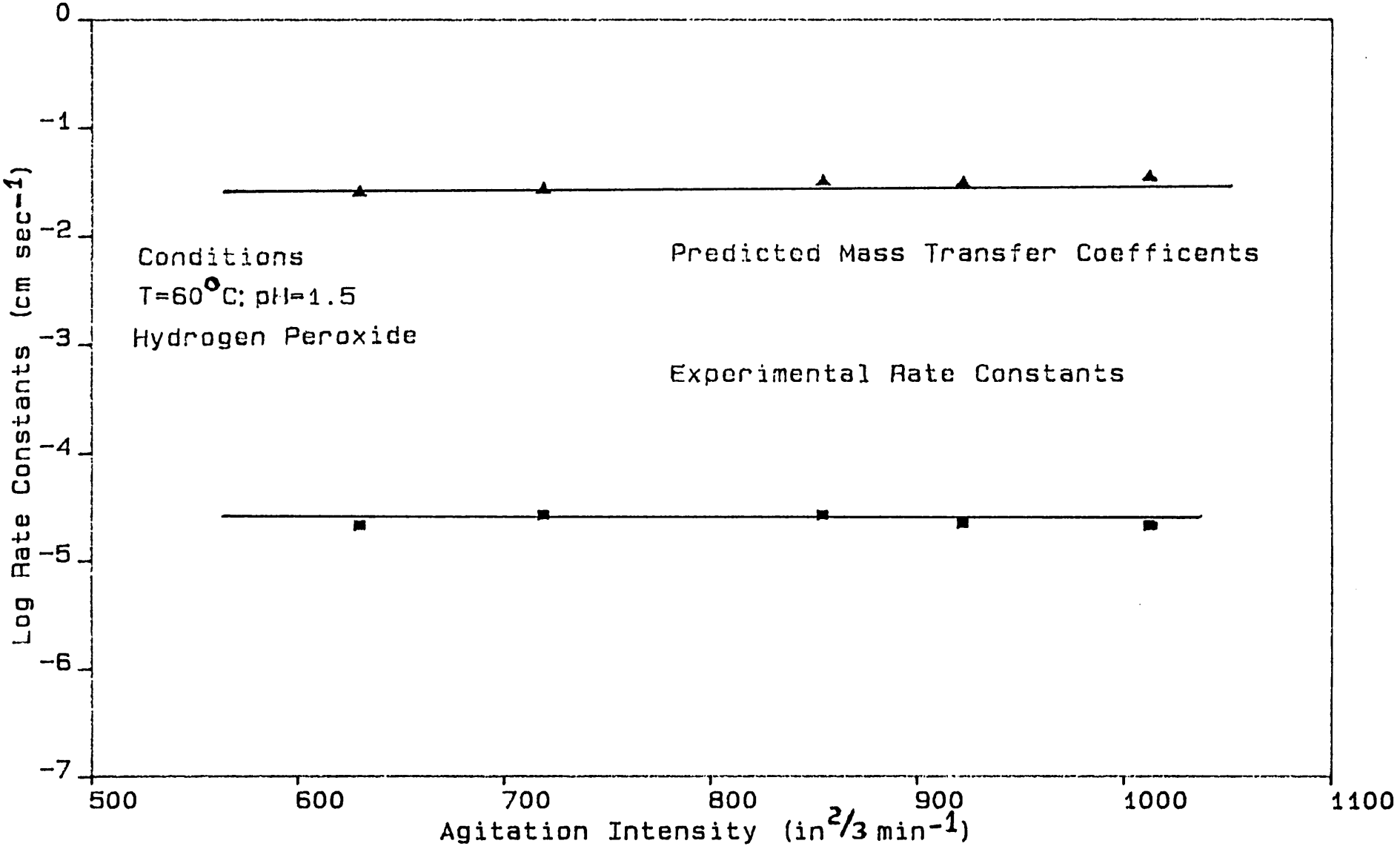
TABLE 17. Experimental rate constants and theoretical mass transfer coefficients for the hydrogen peroxide and peroxymonosulphuric acid systems.

Run	Stirrer speed (rpm)	Agitation Intensity	Predicted mass transfer coeff.		df(∝)/dt		dn/dt		$k_o k'$		Initial amount of UO_2		Area	Conc. H_2SO_5
			$cmsec^{-1}$ x 10^2	log $cmsec^{-1}$	min^{-1} x10^{+4}	sec^{-1} x10^{+6}	mols sec^{-1} x10^9	mols $cm^{-2}sec^{-1}$ x10^{10}	$cmsec^{-1}$ x10^{+6}	log $cmsec^{-1}$	moles x10^{+3}	grams	cm^2	mols km^{-3} x 10^{+4}
118	560	629.8	7.7	-1.113	2.22	3.70	8.46	1.84	1.38	-5.86	2.287	0.6175	45.91	1.33
119	760	854.7	9.0	-1.046	1.71	2.85	5.52	1.42	1.09	-5.96	1.938	0.5232	38.90	1.30
120	900	1012.1	10.0	-1.00	1.71	2.85	5.12	1.42	1.08	-5.97	1.798	0.4855	36.10	1.32
121	820	922.2	9.2	-1.036	2.20	3.67	6.99	1.83	1.37	-5.86	1.905	0.5145	38.26	1.33
122	640	719.7	8.3	-1.081	2.07	3.45	5.88	1.72	1.30	-5.89	1.706	0.4606	34.25	1.32
					min^{-1} x10^3	sec^{-1} 10^5	mols sec^{-1} x10^7	mols $cm^{-2}sec^{-1}$ x10^9	$cmsec^{-1}$ x10^{+5}					Conc. of hydrogen peroxide
140	560	629.8	2.6	-1.58	4.39	7.32	1.44	3.63	2.187	-4.66	1.975	0.5334	39.66	1.66
141	660	719.7	2.8	-1.55	5.03	8.38	1.56	4.16	2.737	-4.56	1.868	0.5045	37.51	1.52
143	820	922.2	3.2	-1.49	4.70	7.83	1.27	3.81	2.295	-4.64	1.662	0.4487	33.36	1.66
144	900	1012.1	3.6	-1.44	4.34	7.23	1.21	3.61	2.175	-4.66	1.669	0.4506	33.50	1.66
142	760	854.7	3.3	-1.48	5.18	8.63	1.52	4.54	2.735	-4.56	1.757	0.4744	35.27	1.66

Graph 9 A Comparison of Predicted and Experimental Rate Constants



Graph 10 A Comparison of Predicted and Experimental Rate Constants



limiting. The mass transfer coefficients of HSO_5^- were calculated using the semi-empirical correlations of Harriot.[4] The calculation procedure is fully described by Sohn.[2] To calculate the Reynolds, Sherwood and Schmidt numbers which are required in the method, it was assumed that the diffusion coefficient of HSO_5^- was similar to that of HSO_4^-.

Table 17 contains experimental rate constants and the calculated mass transfer coefficients for HSO_5^-. Other data needed for the calculations is also included. Graph 9 compares the calculated mass transfer coefficients to the experimentally determined rate constants. It is apparent that the experimental rate constants are approximately four orders of magnitude slower than the calculated mass transfer coefficients. Therefore, mass transfer of HSO_5^- is not the rate controlling process in this reaction. As the value of the diffusion coefficient for HSO_5^- was assumed to be similar to that for HSO_4^-, it can also be concluded that diffusion of HSO_4^- to the surface is not rate limiting. As diffusion of hydrogen ions occurs via a very fast chain mechanism, it is unlikely that diffusion of hydrogen ions is rate limiting. Diffusion of hydroxyl ions can be viewed as reverse diffusion of hydrogen ions, and therefore is unlikely to be rate determining. It can therefore be concluded that diffusion of species to the surface is not rate limiting. This implies that the rate determining process is either diffusion of products away from the surface, or a chemically controlled step in either the anodic or cathodic half cell mechanisms. If diffusion of products away from the surface

FIG. 19. Extracts of the Minitab multilinear regression output. (a) The Peroxymonosulphuric acid system.

```
THE REGRESSION EQUATION IS
Y =    18.6 -  .580 X1 +  .333 X2
    -11719. X3 +  8.00 X4

                                          ST. DEV.      T-RATIO =
       COLUMN      COEFFICIENT          OF COEF.      COEF/S.D.
       --                18.5502            0.7651          24.25
X1     LS04             -0.57987         0.06058          -9.57
X2     PH                0.33328         0.04375           7.62
X3     1/TK          -11718.5             429.0          -27.32
X4     E/T               7.9991           0.4061          19.70

THE ST. DEV. OF Y ABOUT REGRESSION LINE IS
S = 0.1663
WITH (   66-  5) =   61 DEGREES OF FREEDOM

R-SQUARED =  95.3 PERCENT
R-SQUARED =  94.9 PERCENT, ADJUSTED FOR D.F.

ANALYSIS OF VARIANCE

  DUE TO      DF                SS          MS=SS/DF
REGRESSION     4          33.82929           8.45732
RESIDUAL      61           1.68680           0.02765
TOTAL         65          35.51609

FURTHER ANALYSIS OF VARIANCE
SS EXPLAINED BY EACH VARIABLE WHEN ENTERED IN THE ORDER GIVEN

  DUE TO      DF                SS
REGRESSION     4          33.82929
LS04           1           5.38059
PH             1           1.28034
1/TK           1          16.43705
E/T            1          10.73131
```

FIG. 19. Extracts of the Minitab Multilinear regression output. (b) The hydrogen peroxide system

```
THE REGRESSION EQUATION IS
Y =     18.3 -10647. X1 -  .0064 X2
    +  6.42 X3

                                                ST. DEV.      T-RATIO =
        COLUMN      COEFFICIENT                 OF COEF.      COEF/S.D.
        --
                        18.321                    1.120          16.36
X1      1/TK          -10647.1                    530.2         -20.08
X2      LSO4          -0.00642                  0.05325          -1.62
X3      E/T             6.4204                   0.4094          15.68

THE ST. DEV. OF Y ABOUT REGRESSION LINE IS
S = 0.2111
WITH (  46- 4) =  42 DEGREES OF FREEDOM

R-SQUARED = 92.4 PERCENT
R-SQUARED = 91.8 PERCENT, ADJUSTED FOR D.F.

ANALYSIS OF VARIANCE

 DUE TO      DF            SS          MS=SS/DF
REGRESSION    3      22.59170           7.53057
RESIDUAL     42       1.87091           0.04455
TOTAL        45      24.46261

1
FURTHER ANALYSIS OF VARIANCE
SS EXPLAINED BY EACH VARIABLE WHEN ENTERED IN THE ORDER GIVEN

 DUE TO      DF            SS
REGRESSION    3      22.59170
1/TK          1      11.38165
LSO4          1       0.25445
E/T           1      10.95560
```

is rate limiting, and a diffusion layer thickness of 1×10^{-3} cm is assumed, the magnitudes of the rate constants in Table 17 imply diffusion coefficients of $\sim 10^{-8}$ cm^2 sec^{-1}. Diffusion coefficients in aqueous systems are usually in the order of 10^{-5}. It is therefore unlikely that diffusion of species away from the surface is rate limiting.

The chemical kinetic results were treated using multilinear regression analysis in the context of the absolute rate equation (89). The theoretical background of this was described in Section 2. The full Minitab multilinear regression output appears in Appendix 4, but Figure 19(a) contains the first part of that output. Table 18 contains a summary of the data in Figure 19(a). The first observation is that only two concentration variables, pH and $\log_{10}[SO_4]$ were found to be relevant. Peroxymonosulphuric acid concentration was not found to be a relevant variable. This indicates that peroxymonosulphuric acid only affects the rate of reaction in as much as it generates a potential. This in effect is indicative of a zero order of reaction with respect to peroxymonosulphuric acid and indicates that it has no chemical effect on the rate of reaction. This may also indicate that the cathodic half cell reaction is not rate limiting. It would be expected that the concentration of oxidising agent would be in the rate equation for the cathodic half cell reaction, were that half cell reaction rate limiting.

It is also apparent, that all the variables (pH, $\log_{10}[SO_4]$, E/T and 1/T) are very significant with high T - ratios, ($7 \leq T \leq 28$). The Pearson correlation coefficient (R^2) is 95.3%, indicating that 95.3% of the variance of the data is accounted for by the regression equation.

From Figure 19(a), the order of reaction with respect to the activity of hydrogen ions is -0.33. It will be recalled from the previous section, that is was proposed that at less oxidising potentials ($E \leq$ 750 mV (SHE)) reactions (104) and (105) were jointly rate determining, whereas at more oxidising potentials only reaction (104) was rate determining.

$$[U_6O_{14}(OH)] \longrightarrow 3U_2O_5 + H^+ + e^- \qquad (104)$$

$$U_8O_{19} + H_2O \longrightarrow [U_8O_{19}(OH)] + H^+ + e^- \qquad (105)$$

This conclusion was based on the results of the cathodic stripping voltammetry, and a reaction order with respect to pH of -0.14 at a potential of 711 mV (SHE). It will be shown in Section 3.3.4 that peroxymonosulphuric acid imposes a relatively weak oxidising potential on the UO_2 surface, (484 mV $\leq E \leq$ 585 mV (SHE)). If the anodic half cell reaction is rate limiting, and proceeds by the mechanism proposed in the previous section, one would expect the reactions (104) and (105) to be jointly rate limiting. If this were the case, the overall reaction order with respect to pH (calculated on the basis of the number of

moles of UO_2 present would be -0.29. This value is the sum of the reaction orders (with respect to pH) for each of the steps (104) and (105). This value compares favourably with the value of -0.33 found in this section.

The reaction order -0.58 with respect to the concentration of sulphate ions implies that sulphate is involved in the rate determining step of the reaction. Results presented in the previous section indicate that sulphate does not affect the rate of the anodic half cell reaction. The reaction order data for peroxymonosulphuric acid and hydrogen ion both imply that the anodic oxidation of UO_2, and not the cathodic reduction of peroxymonosulphuric acid, is rate limiting. In this work the actual concentrations of species were determined, and those concentration data treated by multilinear regression. Multilinear regression works by correlating the variables (in this case pH and $\log_{10}$ sulphate concentration) with the response ($\log_{10}$rate). If one variable is significant and meaningful, but is strongly correlated to a second, insignificant variable, the regression may correlate both variables to the response. It is proposed that in this case, the pH is the relevant variable, and the sulphate dependence is caused by the strong correlation of sulphate concentration with pH. If this were so, the expected sulphate correlation would be twice that of the pH correlation (A39-A40):

$$H_2SO_4 \longrightarrow 2H^+ + SO_4 \qquad \text{(A39-A40)}$$

The value of -0.58 for the sulphate dependence compares well with -0.66, (this value is twice the reaction order with respect to pH). As the pH value is based on concentrations, one would expect the concentration derived reaction orders to be less than the activity derived reaction order. This is displayed in the two values above.

The coefficient of the 1/T term is -11718.5, see Figure 19(a) and Table 18. The derived chemical activation energy value ($\Delta G^{\neq}_{o,c}$) is +244.4 kJ mol^{-1}. This quantity is termed the activation energy at E = 0 on the scale of use (see Appendix 1). It represents the value of the activation energy without any potential contribution. In effect it is the activation energy for the reaction that would be measured, if the reaction was not an electrochemical reaction. The very high value implies that the reaction is chemically controlled and would be very slow without any potential contribution. It is a well documented fact that UO_2 does not dissolve in acid systems unless oxidising potentials are imposed on the UO_2 surface. The measured activation energy ($\Delta G^{\neq}_{E=E}$) at any given potential is the sum of the chemical activation energy ($\Delta G^{\neq}_{o,c}$) and the electrochemical contribution to the activation energy ($\Delta G^{\neq}_{e,cont.}$). This situation is described by equation (A34) and is fully discussed in Appendix 1.

$$\Delta G^{\neq}_{E=E} = \Delta G^{\neq}_{o,c} + \Delta G^{\neq}_{e,cont.} \qquad (A34)$$

The chemical activation energy ($\Delta G^{\neq}_{o,c}$) is constant and is potential independent. The electrochemical contribution to the activation energy ($\Delta G^{\neq}_{e,cont.}$) is dependent on potential and becomes increasingly larger as the applied potential becomes more oxidising (A33). Hence the measured activation energy ($\Delta G^{\neq}_{E=E}$) becomes smaller as the potential becomes more oxidising. Carried to the extreme, at very oxidising potentials the measured activation energy becomes very small, the reaction rate becomes very fast, and the reaction becomes mass transport limited.

From Figure 19(a) and Table 18, the coefficient of the electrochemical contribution to the activation energy term is 7.9991. The same term in the absolute rate equation (89) is used to derive both the transfer coefficients, and the electrochemical contribution to the activation energy.

$$V = A \exp \frac{-\Delta G^{\neq}_{o,c}}{RT} \exp \frac{+\overleftarrow{\alpha} FE}{RT} \cdot [A]^{x} \ldots \qquad (89)$$

where the term of interest is:

$$\frac{+\overleftarrow{\alpha} FE}{2.303RT}$$

and $$\frac{d \ln \overrightarrow{i}}{d(E/T)} = \frac{\overleftarrow{\alpha} F}{2.303R} = 7.9991 \qquad (89(a))$$

But:

$$\Delta G^{\neq}_{e,cont.} = -n\overleftarrow{\alpha}FE \qquad (A33)$$

where all symbols retain their usual significance.

Obviously the magnitude of $\Delta G^{\neq}_{e,cont.}$ varies with potential, and this is expressed in Graph 11(a). The measured activation energies ($\Delta G^{\neq}_{E=E}$) are calculated by equation (A34). The results of this calculation appear in Graph 11(b). The first observation is that in the potential area of interest (484 mV $\leq$ E $\leq$ 585 mV (SHE)) the reaction is chemically controlled with measured activation energies ($\Delta G^{\neq}_{E=E}$) $\geq$ 70 kJ mol^{-1}. These results support the conclusions reached earlier in this work. Comparisons with previous work are difficult. In the voltammetry section it was found that comparison of the work of Nicol et al.[39] with this work on a potential basis was difficult because there was a difference in potential of $\sim$100 mV between the two works. Assuming that the difference is due to properties and design of the cell, comparisons of the activation energy data from that project with those of this work 'corrected' for this potential difference should give a basis for qualitative comparisons.

A figure of 61 kJ mol^{-1} at E $\sim$ 570 mV (SHE)[39] compares favourably with 55.9 kJ mol^{-1} at E = 570 mV (SHE) obtained in this work, as described above. As all activation energies measured in electrochemical leaching studies are means of the anodic and cathodic activation energies, exact agreement between activation energy data obtained with

two different cathodic half cell reactions would not be expected.

The anodic transfer coefficient is calculated from the same term in the absolute rate equation as the electrochemical contribution to the activation energy. As discussed in Appendix 1, the magnitudes of the transfer coefficients are related in a very intimate way to the chemistry of the rate determining step (rds) of the overall process.

Comparisons of theoretical anodic transfer coefficients with those measured both electrolytically and in the full leaching system enables the rds of each system to be identified. However, before meaningful comparison between the various transfer coefficients can be made, the conditions under which they were determined or the assumptions under which they were calculated must be examined.

Table 14 contains a full list of possible rate determining reactions with their respective theoretical anodic transfer coefficients. Previous results obtained in this work indicate that for the anodic oxidation of UO_2 under less oxidising conditions ($E \leq 611$ mV (SHE)) the anodic transfer coefficient ($\overleftarrow{\alpha}$) is 0.74. This corresponds to reactions (104) and (105) being jointly rate controlling. These previously determined transfer coefficients were determined under electrolytic conditions with no oxidising agent present. Both these and the calculated theoretical transfer coefficients are based

on the assumption that all electron transfers (including the rds) were single electron transfers. Therefore a (the number of electrons in the rds), was assumed to be unity. The magnitude of a profoundly affects the value of the anodic transfer coefficient (A29(b)).

$$\left(\frac{n-\vec{\psi}}{\nu} - r\beta \right) a = \overleftarrow{\alpha} \qquad \text{(A29(b))}$$

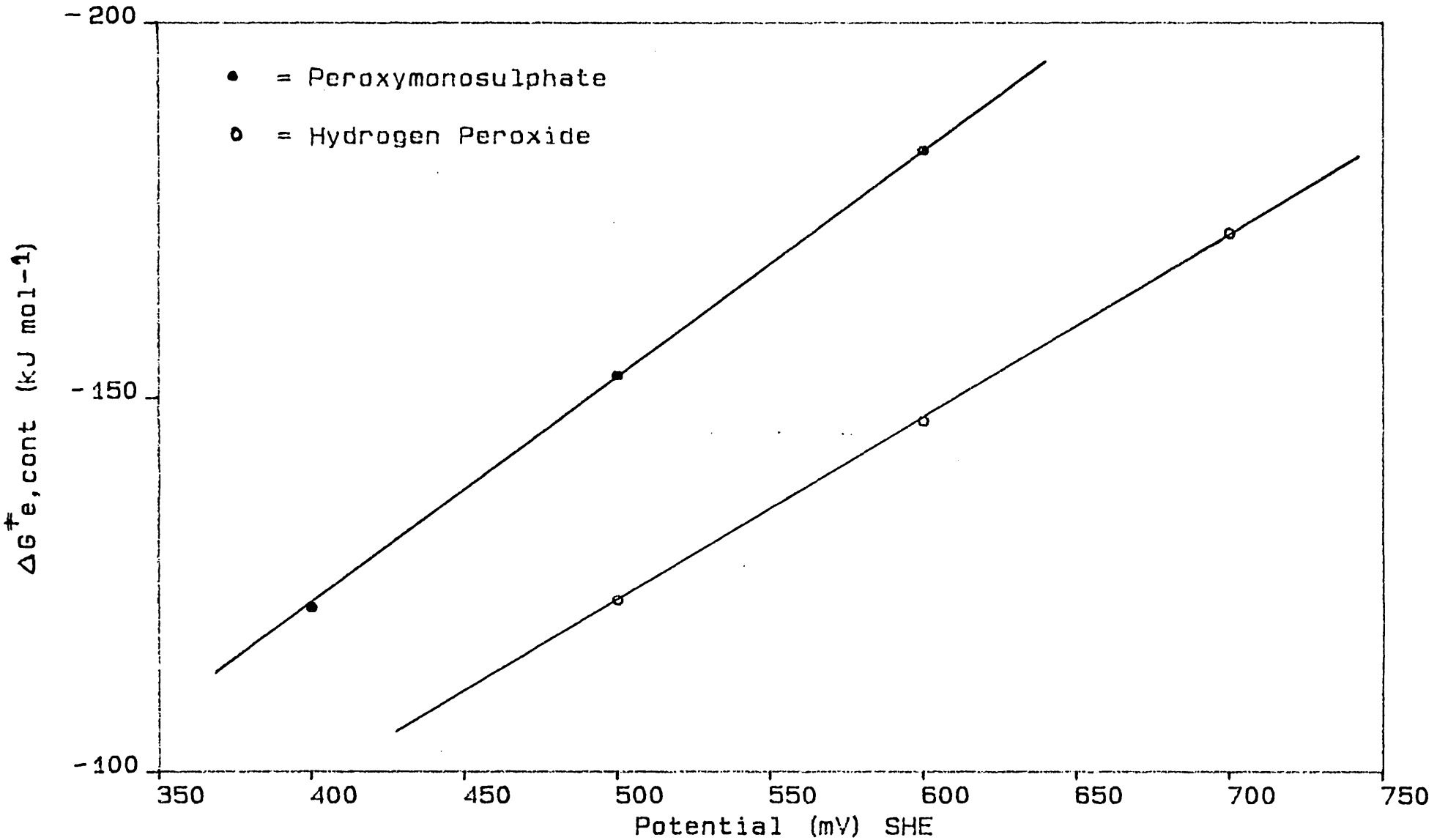
In contrast to the electrolytically determined transfer coefficients, the anodic transfer coefficient determined in the full leaching system were obtained by the use of an oxidising agent which was used to impose the potential. Peroxymonosulphuric acid is reduced with the capture of two electrons. The rds of the anodic oxidation (105) is a single electron transfer. Therefore, on a simple number of electrons (molar) basis, for every mole of peroxymonosulphate that is reduced, two moles of rds are driven.

It should be noted at this point, that the overall anodic half cell process (A15) involves two electrons, but transfer coefficients only relate to the rate determining step(s).

$$UO_2 \longrightarrow UO_2^{2+} + 2e^- \qquad \text{(A15)}$$

This inequality (on the molar scale) means that although the same reaction may underlie both systems,

Graph 11 (a) The Variation of $\Delta G^{\ddagger}_{e,cont}$ with Potential



Graph 11 (b) The Variation of $\Delta G^{\neq}$ E=E with Potential

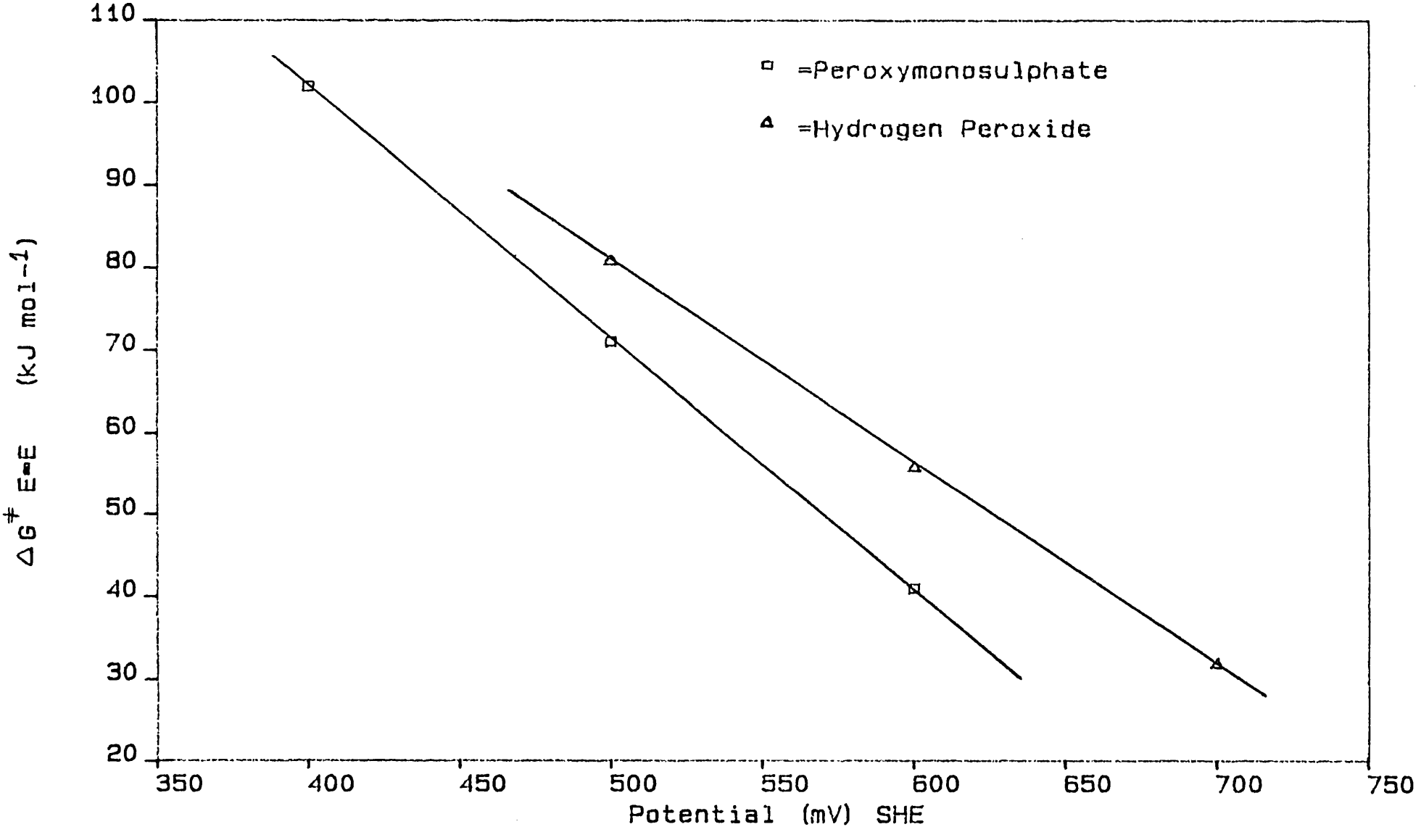


TABLE 18. An analysis of the results of the multilinear regression analysis of the kinetic runs containing peroxymonosulphuric acid and hydrogen peroxide respectively.

Absolute Rate Equation Term	Name of Quantity to be determined	Regression Variable	Regression Coefficient	Value of Determined Quantity
$-\frac{\Delta G^{\neq}_{o,c}}{2.303RT}$	The chemical activation energy at E=0 on the scale of use ($\Delta G^{\neq}_{o,c}$)	1/T(K)	-11718.50	+224.38 $kJmol^{-1}$
$+\frac{\overleftarrow{\alpha}EF}{2.303RT}$	The electrochemical contribution to the activation energy ($\Delta G^{\neq}_{e,cont}$)	E/T(K)	7.99	See text
$+\frac{\overleftarrow{\alpha}EF}{2.303RT}$	The anodic transfer coefficient ($\overleftarrow{\alpha}$)	E/T(K)	7.99	27.2 mV $decade^{-1}$ ≡ 1.59(a=1) ≡ 0.79 (a=2)
x log[A]	The order of reaction w.r.t. (pH)	pH	+0.33	+0.33
x log [B]	The order of reaction w.r.t.[SO_4]	$\log_{10}[SO_4]$	-0.5	-0.58

... continued ...

TABLE 18. (Continued)

Absolute rate equation term	Name of quantity to be determined	Regression Variable	Regression Coefficient	Value of determined quantity
$-\frac{\Delta G^{\neq}_{o,c}}{2.303RT}$	The chemical activation energy at E=0 on the scale of use ($\Delta G^{\neq}_{o,c}$)	1/T(K)	-10647.10	+203.86 $kJmol^{-1}$
$+\frac{\overleftarrow{\alpha}EF}{2.303RT}$	The electrochemical contribution to the activation energy ($\Delta G^{\neq}_{e,cont}$)	E/T(K)	-6.42	See text
$+\frac{\overleftarrow{\alpha}EF}{2.303RT}$	The anodic transfer coefficient ($\overleftarrow{\alpha}$)	E/T(K)	-6.42	33.9 mV $decade^{-1}$ ≡ 1.27 (a=1) ≡ 0.64 (a=2)
x log [A]	The order of reaction w.r.t.[SO_4]	$\log_{10}[SO_4]$	0.08	0

different transfer coefficients could be obtained for each system. The basis of that difference would be entirely dependent on the oxidising agent used. Therefore anodic transfer coefficients obtained in these two ways cannot be directly compared.

To enable comparison between the two sets of transfer coefficients, in those systems where the molar concentration of electrons is not equal to the equivalent concentration of electrons (as in the present case), it is necessary to interpret the transfer coefficients on an equivalent, as opposed to a molar basis.

The simplest way of achieving this is to redefine a in terms of the number of moles of anodic rds per mole of cathodic reaction. This converts a from a molar to an equivalent quantity. Anodic transfer coefficients from the full leaching system can now be compared to the theoretical anodic transfer coefficients (recalculated using the equivalent value of a) and electrolytically determined anodic transfer coefficients (compensated for the equivalent value of a).

$$\frac{\overleftarrow{\alpha}F}{2.303RT} = 7.9991 \qquad (89(a))$$

$$\Delta G^{\neq}_{e,cont} = -n\overleftarrow{\alpha}FE \qquad (A33)$$

where all symbols retain their usual significance.

By application of equation(A33) to the appropriate term in the absolute rate equation (see Figure 19(a) and Table 18), the anodic transfer coefficient is found to be 1.58. Recalculation of the theoretical anodic transfer coefficients in Table 14 with an equivalent a value of two, as discussed above, yields anodic transfer coefficients of 1.50 for reaction (105) and 1.35 for reaction (104). These values are in good agreement with each other. If the previously determined anodic transfer coefficient for the anodic half cell reaction is adjusted for an a value of two, it yields a value of 1.48. This latter value agrees very well with those values reported above.

When it is considered that the anodic transfer coefficient for the full leaching system has (statistically) 61 degrees of freedom, the agreement with theoretical and electrolytically derived anodic transfer coefficients is extraordinary.

In conclusion, the results presented are consistent with reactions (104) and (105) being jointly rate determining in the full leaching system. Mass transfer coefficients, reaction order indices, anodic transfer coefficients, and activation energies are consistent with these reactions being rate determining in the full system.

$$[U_6O_{14}(OH)] \rightarrow 3U_2O_5 + H^+ + e^- \qquad (104)$$

$$U_8O_{19} + H_2O \rightarrow [U_8O_{19}(OH)] + H^+ + e^- \qquad (105)$$

Readers are reminded that species in square brackets indicate transition complexes.

SUMMARY

The calculated mass transfer coefficients of the peroxymonosulphate ion were compared to experimental rate constants. It was found that the rate of reaction is not controlled by the diffusion of this species to the surface. On the basis of the likely magnitudes of the diffusion coefficients of the system, it was shown that diffusion of any species present to or from the surface is not likely to be rate controlling.

Analysis of the multilinear regression results yielded activation energies which were consistent with a chemical or electrochemical step being rate controlling. These same results yielded a zero order dependence of the rate of reaction on peroxymonosulphuric acid concentrations, implying that the rate controlling process is not contained in the cathodic half cell reaction.

Reaction order data with respect to pH is consistent with previous results from this work, and with reactions (104) and (105) being jointly rate determining.

A reaction order of -0.58 with respect to sulphate was revealed. It is proposed that this reaction order is the result of strong statistical correlation of the pH and sulphate concentrations.

The anodic transfer coefficient was found to 1.58. This value agrees very well with theoretical and electrolytically determined anodic transfer coefficients, and indicates that the oxidation of U_3O_7 and U_8O_{19} is the rate determining process.

All the available experimental data on the peroxymonosulphate leaching system are consistent with each other and point to the rate limiting process being in the anodic half cell reaction.

3.3.3. Hydrogen Peroxide

The results of both peroxymonosulphuric acid and hydrogen peroxide leaching of UO_2 were treated in a very similar manner. Therefore, less explanation of the methods will be given in this section, as full explanation has already been given in the last section.

The experimental rate data were successfully fitted to a shrinking particle model (141). This implies that diffusion through growing product layers is not rate controlling.

The mass transfer coefficients for hydrogen peroxide were determined as previously. The diffusion coefficient of hydrogen peroxide was taken as 2×10^{-5} cm^2 sec^{-1}.[63] Table 17 contains the experimental rate constants and the calculated mass transfer coefficients for H_2O_2. Other data needed for the calculations is also included. Graph 10 compares the calculated mass transfer coefficients to the experimentally determined rate constants. It is apparent that mass transfer of hydrogen peroxide to the surface is not rate limiting. By similar reasoning as was applied

in the last section, it is also unlikely that the diffusion of any other species, to or from the surface is rate limiting.

The chemical kinetic results were treated as previously, using multilinear regression analysis in the context of the absolute rate equation (89). The full Minitab multilinear regression output appears in Appendix 4, but Figure 19(b) contains the first part of that output. Table 18 contains a summary of the data in Figure 19(b). The first observation is that all the variables (except sulphate) are very significant with very high t-ratios ($15 \leq$ t-ratio ≤ 21). The t-ratio for sulphate is 1.62 which is not statistically significant. This variable was only included for comparison. The Pearson correlation coefficient (R^2) is 92.4%, indicating that 92.4% of the variance of the data is accounted for by the regression analysis.

From Figure 19(b) it can be seen that no concentration terms were found to be significant. This indicates a zero order with respect to hydrogen peroxide, and that hydrogen peroxide only affects the rate in as much as it imposes a potential on the UO_2 surface. This result may also imply that the cathodic half cell reaction is not rate determining. The fact that no concentration terms were found significant implies a zero order dependence of the rate on the pH. This is consistent with results obtained by Eary et al.[63] who found that the rate of UO_2 dissolution with acidic hydrogen peroxide was pH independent, except under conditions when precipitation of $UO_4.2H_2O$ took place. A zero order with

respect to pH is in contrast with the order of 0.33 found in the peroxymonosulphuric acid section. This will be fully discussed at a later point in this section.

It was proposed in the last section that the reaction order with respect to sulphate was in reality a manifestation of the strong correlation between the pH and sulphate concentration. If this is the case, because the reaction order with respect to pH is zero, the reaction order with respect to sulphate would also be expected to be zero. This is well demonstrated in this case.

The coefficient of the 1/T term is -10647.1. See Figure 19(a) and Table 18. The derived chemical activation energy value ($\Delta G^{\neq}_{o,c}$) is +203.86 kJ mol^{-1}. This quantity is termed the activation energy at E=0 on the scale of use (see Appendix 1). This value is slightly less than that for peroxymonosulphuric acid, but is of similar magnitude. The very high value implies that the reaction is chemically controlled and would be very slow without any potential contribution.

From Figure 19(a) and Table 18, the coefficient of the electrochemical contribution to the activation energy term is 6.420. The same term in the absolute rate equation (89) is used to derive both the transfer coefficients and the electrochemical contribution to the activation energy. The term of interest in the absolute rate equation is

$$+\frac{\overleftarrow{\alpha}FE}{2.303RT}$$

and $$\frac{d \ln \overleftarrow{\rho}}{d(E/T)} = \frac{\overleftarrow{\alpha} F}{2.303R} = 6.4204 \qquad (89(b))$$

and $$\Delta G^{\neq}_{e,cont} = -n\overleftarrow{\alpha}FE \qquad (A33)$$

where all symbols retain their usual significance. The electrochemical contribution to the activation energy ($\Delta G^{\neq}_{e,cont}$) varies with potential, and this is expressed in Graph 11(a). The measured activation energies ($\Delta G^{\neq}_{E=E}$) are calculated by equation (A34). The results of this calculation appear in Graph 11(b). The first observation is that in the potential area of interest (561 mV $\leq$ E $\leq$ 681 mV (SHE)) the reaction is chemically controlled with measured activation energies ($\Delta G^{\neq}_{E=E}$) $\geq$ 50 kJ mol^{-1}. These results support the conclusions reached earlier in this work. Comparison of the data for the hydrogen peroxide and peroxymonosulphuric acid system reveals major differences between them. In Graph 11(a), it can be seen that the electrochemical contribution to the activation energy ($\Delta G^{\neq}_{e,cont}$) is smaller in the hydrogen peroxide system than in the peroxymonosulphuric acid system. This means that for a given potential, the rate accelerating effect of that potential is less in the hydrogen peroxide system than for the peroxymonosulphuric acid system.

Also in Graph 11(a) it can be seen that although the electrochemical contribution to the activation energy ($\Delta G^{\neq}_{e,cont}$) becomes larger with more oxidising potentials for both hydrogen peroxide and peroxymonosulphuric acid,

the peroxymonosulphuric acid system responds to changes in potential more than does the hydrogen peroxide system. This latter point is more clearly displayed in Graph 11(b).

This implies two things:

(a) The electrochemical contribution to the activation energy at a given potential is less for hydrogen peroxide than for peroxymonosulphuric acid. It is therefore probable that if the same rate determining step underlies both systems, some other cathodic electrode reaction is being driven along with the reduction of hydrogen peroxide. If a different rate determining step underlies both systems, results such as those in Graph 11(a) and (b) would be expected.

(b) Similar increases in potential in both systems affect the measured activation energies ($\Delta G^{\neq}_{E=E}$) hence the rates, differently. This implies that either different rate determining steps underlie each system, or if this is not the case, then a second major anodic process is occurring alongside the reduction of hydrogen peroxide. At the potentials in question, the oxidation of hydrogen peroxide is more reversible than its reduction.[43] This means that on the surface of the UO_2, the hydrogen peroxide is being both oxidised and reduced. In effect not all of the electrical energy being inputted into the system (by the hydrogen peroxide) is being used to oxidise the UO_2. This would explain the differences in the electrochemical contribution to the activation energies ($\Delta G^{\neq}_{e,cont}$) between the two systems. The nub of all this is that although

hydrogen peroxide is a good oxidising agent, if it were not itself continuously being oxidised, it would be very much better. The potential it generates on the UO_2 surface is being constantly 'bled off' to maintain the hydrogen peroxide oxidation reaction.

Another difference between the two systems is the magnitude of the chemical activation energies ($\Delta G^{\neq}_{o,c}$). The chemical activation energy in the peroxymonosulphuric acid system is $\sim$20 kJ mol^{-1} larger than that from the hydrogen peroxide system. This implies that the changes required to bring about the 'activated complex' state are less with the hydrogen peroxide system than with the peroxymonosulphuric acid system. (This is consistent with the fact that peroxymonobisulphate is a more complex molecule than hydrogen peroxide, and therefore more bonds and quasi-bonds have to be broken and made).

The anodic transfer coefficient ($\overleftarrow{\alpha}$) is calculated from the same term in the absolute rate equation as the electrochemical contribution to the activation energy (see Figure 19(a) and Table 18). By the application of equation (A33) the anodic transfer coefficient is found to be 1.274. Hydrogen peroxide, although having a very different chemistry to peroxymonosulphuric acid is reduced in the same way, with the capture of two electrons. Therefore, as in the peroxymonosulphuric acid system, for every mole of cathodic reaction, two moles of anodic rods are driven. As discussed previously this makes direct comparison of

theoretical transfer coefficients and electrolytically obtained transfer coefficients with full system transfer coefficients impossible.

Comparisons can be made however, if the theoretical, electrolytic and full system transfer coefficients are all put on the same equivalent scale. This is analogous to the treatment applied to the peroxymonosulphuric acid results.

If the previously determined anodic transfer coefficients for the anodic half cell reaction are adjusted for a value of two, they yield values of 1.48 ($E \leq 611$ mV (SHE)) and 0.26 ($E \leq 761$ mV (SHE)). Although the full system anodic transfer coefficient is of the same order as the latter two values, it is obvious that there is considerable difference between the full system anodic transfer coefficient and either of the electrolytically determined anodic transfer coefficients. This will be pursued in the next section. To avoid confusion, all the theoretical and electrolytic anodic transfer coefficients referred to will be those calculated with an equivalent value of two.

This proposal implies, as in the peroxymonosulphuric acid system, that the underlying rate determining process in both the electrolytic and electrochemical systems is the anodic oxidation of UO_2.

There is however, a further complication in this system. It will be shown in the next section that the potentials imposed on the UO_2 surface by hydrogen peroxide are more oxidising (561 mV $\leq E \leq 681$ mV (SHE)) than those

imposed by peroxymonosulphuric acid (484 mV $\leq$ E $\leq$ 585 mV (SHE)). The values of anodic transfer coefficients are potential dependent i.e. if the rate determining step changes with potential, the value of the transfer coefficients of the system will also change. For the electrolytic system, it was found that at oxidising potentials (E $\geq$ 761 mV (SHE)) the anodic transfer coefficient was 0.26. At less oxidising potentials (E $\leq$ 611 mV (SHE)) the anodic transfer coefficient was 1.48. Although the potentials imposed on the UO_2 surface by peroxymonosulphuric acid all fall within the potential range of one of the rate determining steps above, those imposed by hydrogen peroxide do not. It is highly likely therefore, that the rate determining process(es) in the hydrogen peroxide system are not solely those represented by either of the anodic transfer coefficients measured in the electrolytic system. A value somewhere between 0.13 and 0.74 would be expected. Thoughtful inspection of the Tafel plot of the electrolytic system (Graph 4) reveals the possible existence of small areas of constant slope between the two major Tafel areas. This supports the theory that intermediate rate determining processes exist in the potential range between the two major Tafel regions.

The value of the anodic transfer coefficient derived from the hydrogen peroxide system is 1.27 (561 $\leq$ E $\leq$ 681 mV (SHE)). This value falls between 0.26 (E $\geq$ 761 mV (SHE)) and 1.48 (E $\leq$ 611 mV (SHE)). These are the equivalent values found in the electrolytic system. This also explains the better T-ratios for the E/T term and correlation coefficients (R^2) in the peroxymonosulphuric acid system

(19.7 and 95.3) as compared to those found in the hydrogen peroxide system (15.68 and 92.4), (see Figure 19 and Table 18). Also there is one further point that must be made regarding this system. It has already been shown from the magnitudes of the various components of the activation energy and the way they vary with potential that there are two anodic reactions occurring in this system (both UO_2 and H_2O_2 are oxidised). This also affects the magnitude of the anodic transfer coefficient. If total current was being measured, the overall transfer coefficient would be a weighted mean of the transfer coefficients of the two processes, weighted on the basis of the partial currents associated with each process. In this case however, the 'current' is calculated from the rate of reaction. The rate of reaction is only based on the concentration of uranium in solution, and therefore only represents a partial anodic current. Without knowledge of the magnitude of the other partial anodic current, it is difficult to draw any further conclusions about the magnitude of the expected transfer coefficient.

Finally, the zero order of reaction with respect to pH must be discussed. It has been shown above that it is highly likely that the rate controlling process(es) at the potentials encountered in hydrogen peroxide leaching of UO_2 are different from those represented by the anodic transfer coefficients of 0.26 and 1.48. It is therefore not surprising that the kinetics suggested by the reaction

order with respect to pH are not those that were found in the peroxymonosulphuric acid system, when the anodic transfer coefficient was 1.58.

SUMMARY

The calculated mass transfer coefficients of hydrogen peroxide were compared to experimental rate constants. It was found that the rate of reaction is not controlled by the diffusion of this species to the surface. On the basis of the likely magnitudes of the diffusion coefficients of the system, it was shown that diffusion of any species to or from the surface is not likely to be rate limiting.

Analysis of the multilinear regression results yielded activation energies which were consistent with a chemical or electrochemical step being rate controlling.

Comparisons of various activation energy data from this section with those from the peroxymonosulphuric acid section revealed that the hydrogen peroxide system is more complex than the peroxymonosulphuric acid system, and that some other anodic reaction (apart from UO_2 oxidation) was occurring. This was thought to be the oxidation of hydrogen peroxide.

The same multilinear regression results yielded a zero order with respect to hydrogen peroxide concentration,

implying that the rate controlling process is not contained in the cathodic half cell reaction.

The magnitude of the anodic transfer coefficient indicates that the rate determining process is intermediate between the high and low potential rate determining steps (found in the electrolytic section of the work), and the zero order with respect to pH may confirm this.

The results presented in this section indicate that the rate controlling process of the dissolution of UO_2 with hydrogen peroxide is within the UO_2 to UO_2^{2+} anodic half cell reaction.

3.3.4 Microscopy and Steady State Electrochemistry

3.3.4.1 Steady State Electrochemistry

The purpose of this section is to give information of a more qualitative nature to help in further elucidation of the mechanism(s) of the mixed system. Comparisons of the two different oxidising agents used in this project are also made.

Table 19 contains the corrosion potential data for both the hydrogen peroxide and peroxymonosulphate systems. The current density data are calculated from the absolute rate data. Graph 12 compares the potential imposed by different concentrations of each oxidising agent on the UO_2 surface. It is obvious that hydrogen peroxide is able to impose a more oxidising potential at a given concentration than

peroxymonosulphate. The difference in concentrations required to impose equivalent potentials on the UO_2 surface is approximately 2 orders of magnitude. What is surprising about these results is the fact that if anything, peroxymonosulphuric acid would have been expected to impose the more oxidising potentials as it is a so much more powerful oxidising agent than hydrogen peroxide. It is possible that peroxymonosulphuric acid does initially impose a very oxidising potential on the UO_2 surface, but this causes the formation of an insulating film of oxide. This process has been proposed before,[37] and although in that work the film was not identified, it was thought to be UO_3 or some related compound. The identification of the film as UO_3 is not unreasonable given the initial strongly oxidising potentials ($E > 1500$ mV (SHE)) experienced by the UO_2. It is possible that the insulating film observed by Nicol et al.[37] was part of the oxide layer structure found in this work. Potentials imposed on a platinum electrode by peroxymonosulphuric acid were difficult to interpret. When the reaction was stirred, the observed potential was very unstable and the reading could not be taken. These unstable potentials were of the order of 900 mV (SHE). When stirring was stopped however, the potentials settled at approximately 1200 mV (SHE) and became much more stable. Although this effect is not understood, and seems confined to the peroxymonosulphuric acid system on platinum, this does show that peroxymonosulphuric acid can impose a very oxidising potential in situ.

Graph 13 compares the leaching rate of UO_2, (as a current density) at different electrochemical potentials, imposed by hydrogen peroxide and peroxymonosulphuric acid. It is possible (Graph 13) that peroxymonosulphuric acid achieves a greater dissolution at less oxidising potentials (480 mV $\leq$ E $\leq$ 550 mV (SHE)) than does hydrogen peroxide. If this is so, it would imply that peroxymonosulphuric acid is a more efficient oxidising agent that hydrogen peroxide. This may be a reflection of the fact that the hydrogen peroxide system expends some of the anodic current in hydrogen peroxide oxidation. This effect seems to diminish at more oxidising potentials however, and the hydrogen peroxide dissolution line follows the steady state current potential line. The main point however is that all three lines follow a similar track. This indicates that the mechanism is similar in all cases.

Graph 14 compares the absolute UO_2 leaching rates produced by a number of oxidising agents. The data for this graph appear in Table 20. The results for ferric ions were taken from work by Amill et al.[69] They were obtained under chemical leaching conditions at temperatures of 25 and 35°C. Data obtained at both temperatures are included in Graph 14, and a probable 31°C line is interpolated between them. The results for peroxymonosulphuric acid and hydrogen peroxide were obtained in this work.

It can be seen that the most sluggish leaching rates are produced by ferric ions. For the leaching of synthetic

UO_2 under the conditions employed, it appears that hydrogen peroxide is approximately 100 times faster than ferric ions and approximately 15 times faster than peroxymonosulphuric acid.

It should be noted that the results from Amill et al.[69] refer to sintered UO_2 pellets which were not treated in any way between runs. This implies that the surface area for such pellets would increase with time over a period of time (and runs), and may indicate that the leaching rates are an over-estimation of the true rate.

SUMMARY

Hydrogen peroxide imposes a much more oxidising potential on the UO_2 surface than peroxymonosulphuric acid. The less oxidising potential imposed by peroxymonosulphuric acid was attributed to the presence of an insulating film formation which is probably part of the normal film formation and may be the result of the very high potentials which are thought to be initially imposed by peroxymonosulphuric acid. It is possible that at equal potentials, peroxymonosulphuric acid produced greater dissolution of uranium than hydrogen peroxide. This was attributed to the inefficiency of hydrogen peroxide as an oxidising agent. Comparisons on the basis of equal molar concentrations of hydrogen peroxide and peroxymonosulphuric acid and ferric ions as oxidising

agents for UO_2 revealed that hydrogen peroxide produced the greatest dissolution of UO_2 followed by peroxymonosulphuric acid and finally ferric ions. Hydrogen peroxide was found to be approximately 100 times as fast as ferric ions and 15 times as fast as peroxymonosulphuric acid. It was noted that due to differences in starting materials and treatments between runs, the absolute rate of uranium dissolution with ferric ions may be an over-estimation.

TABLE 19. The corrosion potential and rate data for both systems at T = 30°C.

(a) Hydrogen peroxide system

Run no.	Concentration of H_2O_2 (m)	Corrosion Potential (mV) SHE	Reaction Rates			Equivalent current density (φ) μAcm^{-2}	$\log_e \varphi$
			$\frac{df(\alpha)}{dt}$ (min^{-1})	$d\alpha/dt$ (sec^{-1})	dn/dt (mols $cm^{-2}sec^{-1}$)		
201	3.99×10^{-3}	570	1.87×10^{-5}	5.61×10^{-5}	4.68×10^{-11}	9.05	2.20
202	8.09×10^{-3}	581	2.42×10^{-5}	7.27×10^{-5}	6.06×10^{-11}	11.69	2.46
203	5.68×10^{-2}	613	1.19×10^{-4}	3.57×10^{-4}	2.98×10^{-10}	57.51	4.05
204	1.21×10^{-1}	618	8.64×10^{-4}	2.59×10^{-3}	2.16×10^{-9}	416.82	6.03
205	6.01×10^{-1}	671	1.12×10^{-3}	3.37×10^{-3}	2.81×10^{-9}	542.25	6.30
206	1.21×10^{-2}	581	5.76×10^{-5}	1.73×10^{-4}	1.44×10^{-10}	27.8	3.32
200	7.48×10^{-4}	549	2.42×10^{-6}	7.27×10^{-6}	6.06×10^{-12}	1.17	1.57

TABLE 19. (b) Peroxymonosulphuric acid system

Run no.	Concentration of H_2SO_5 (M)	Corrosion Potential (mV) SHE	Reaction Rates			Equivalent Current Density i_2 (μAcm^{-2})	$\log_e i_2$
			$\frac{df(\alpha)}{dt}$ (min^{-1})	$d\alpha/dt$ (sec^{-1})	dn/dt (mols $cm^{-2}sec^{-1}$		
207	$1.78x10^{-3}$	484	$1.82x10^{-7}$	$5.47x10^{-7}$	$4.56x10^{-13}$	0.09	-2.43
208	$5.34x10^{-3}$	500	$7.76x10^{-7}$	$2.33x10^{-6}$	$1.94x10^{-12}$	0.37	-0.99
209	$1.05x10^{-2}$	512	$1.01x10^{-6}$	$3.02x10^{-6}$	$2.51x10^{-12}$	0.49	-0.72
210	$5.26x10^{-2}$	541	$3.78x10^{-6}$	$1.13x10^{-5}$	$9.45x10^{-12}$	1.82	0.60
211	$9.81x10^{-2}$	553	$1.11x10^{-5}$	$3.32x10^{-5}$	$2.77x10^{-11}$	5.34	1.67
212	$6.2x10^{-1}$	586	$7.16x10^{-5}$	$2.15x10^{-4}$	$1.79x10^{-10}$	34.56	3.54

TABLE 20. Comparisons of the absolute leaching rates of UO_2 with different oxidising agents.

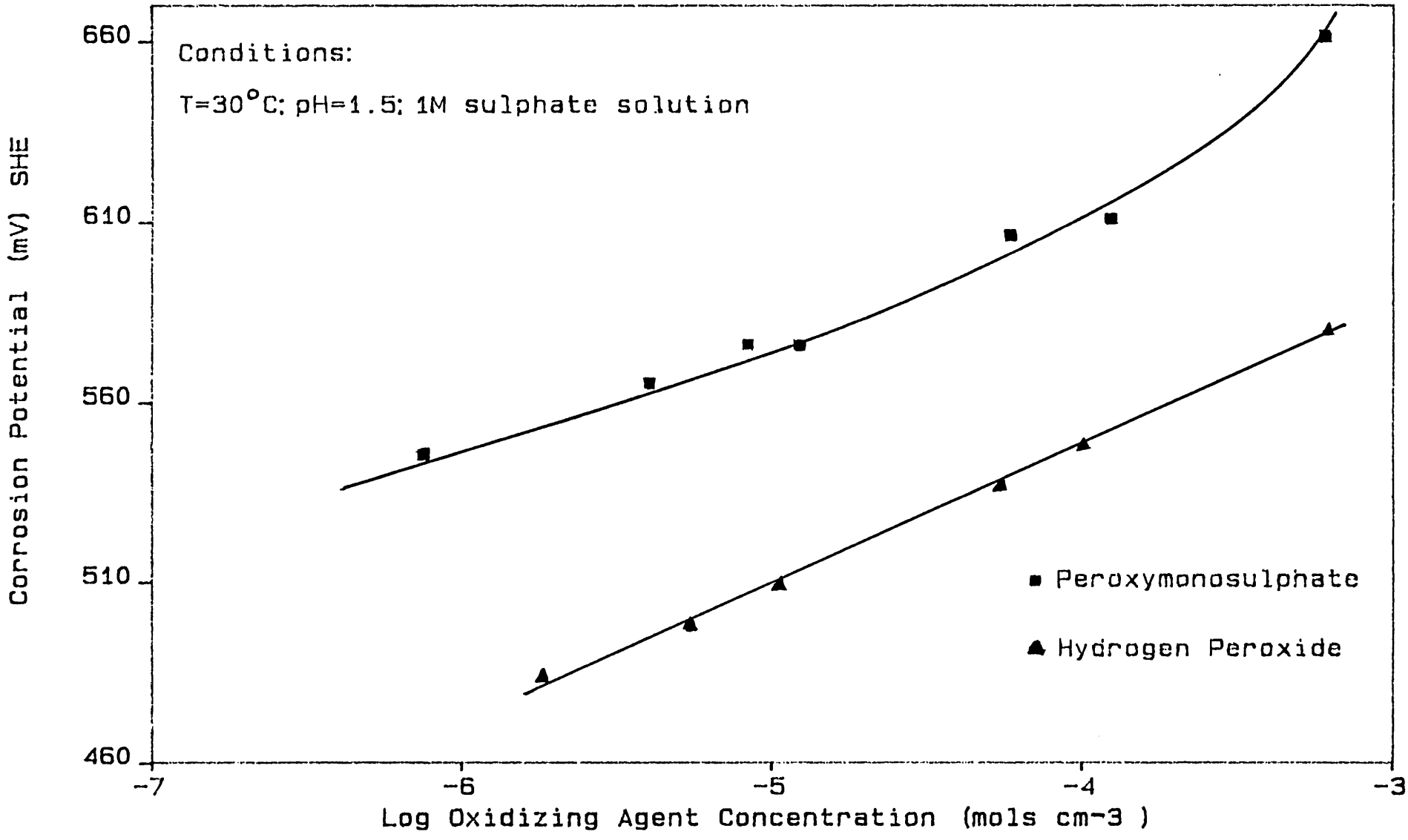
Source of Data		Oxidizing Agent	Relevant reaction parameters.	Absolute rate (mols cm^{-2} sec^{-1})		Concentration of oxidizing agent (mols cm^{-3})		Comments
Work	Run, Graph or Figure etc.			dn/dt	$\log_{10}$dn/dt	[A]	$\log_{10}$[A]	
This work	207	H_2SO_5	T=30°C, pH=1.5, sulphate system	4.56×10^{-13}	-12.34	1.78×10^{-6}	-5.75	
"	208	"	"	1.94×10^{-12}	-11.71	5.34×10^{-6}	-5.27	
"	209	"	"	2.51×10^{-12}	-11.60	1.05×10^{-5}	-4.98	
"	210	"	"	9.45×10^{-12}	-11.03	5.26×10^{-5}	-4.28	
"	211	"	"	2.77×10^{-11}	-10.56	9.81×10^{-5}	-4.01	
"	212	"	"	1.79×10^{-10}	- 9.75	6.20×10^{-4}	-3.21	
"	201	H_2O_2	"	4.68×10^{-11}	-10.33	3.99×10^{-5}	-5.40	
"	202	"	"	6.06×10^{-11}	-10.22	8.09×10^{-5}	-5.09	
"	203	"	"	2.98×10^{-10}	- 9.53	5.68×10^{-5}	-4.24	
"	204	"	"	2.16×10^{-9}	- 8.67	1.21×10^{-4}	-3.92	
"	205	"	"	2.81×10^{-9}	- 8.55	6.01×10^{-4}	-3.22	
"	206	"	"	1.44×10^{-10}	- 9.84	1.21×10^{-5}	-4.92	
"	200	"	"	6.06×10^{-12}	-11.22	7.48×10^{-7}	-6.13	

... continued ...

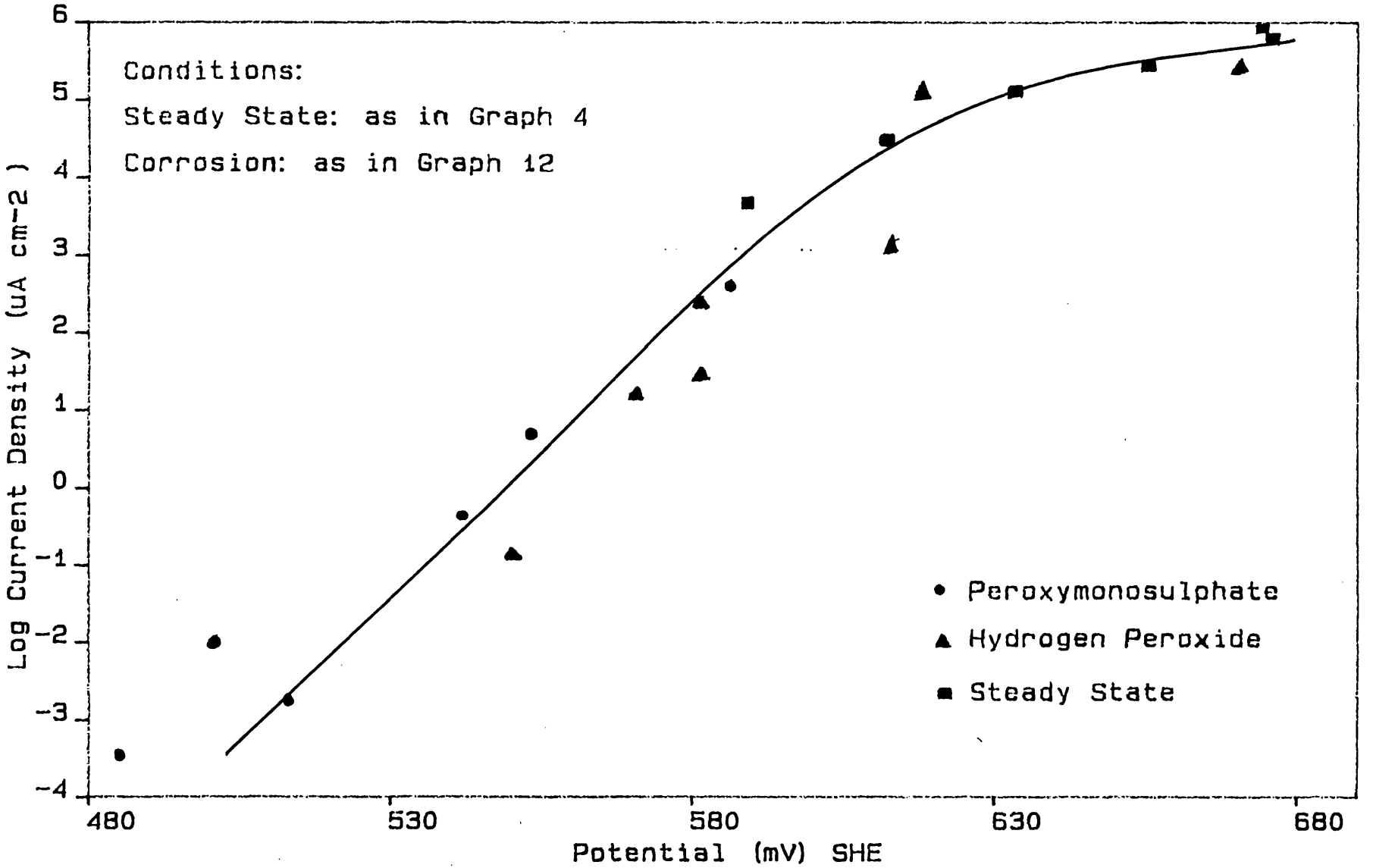
TABLE 20. (continued)

Source of Data		Oxidizing Agent	Relevant reaction parameters	Absolute rate (mols cm^{-2} sec^{-1})		Concentration of oxidizing agent (mols cm^{-3})		Comments
Work	Run, Graph or Figure etc.			dn/dt	$\log_{10}$dn/dt	[A]	$\log_{10}$[A]	
Ref.69	17	FeIII	T=25°C, pH=1.67, sulphate system	2.18×10^{-11}	-10.66	1.99×10^{-3}	-2.70	
"	23	"	" pH=1.85 "	3.81×10^{-11}	-10.42	2.99×10^{-3}	-2.52	
"	25	"	" pH=2.09 "	1.46×10^{-11}	-10.84	3.39×10^{-3}	-2.47	
"	36	"	" pH=1.92 "	5.86×10^{-11}	-10.23	1.99×10^{-3}	-2.70	
"	37	"	" pH=1.99 "	6.13×10^{-11}	-10.21	"	"	
"	42	"	" pH=1.99 "	5.60×10^{-11}	-10.25	"	"	
"	45	"	T=35°C, pH=1.93, SO_4 system	5.60×10^{-10}	- 9.25	"	"	

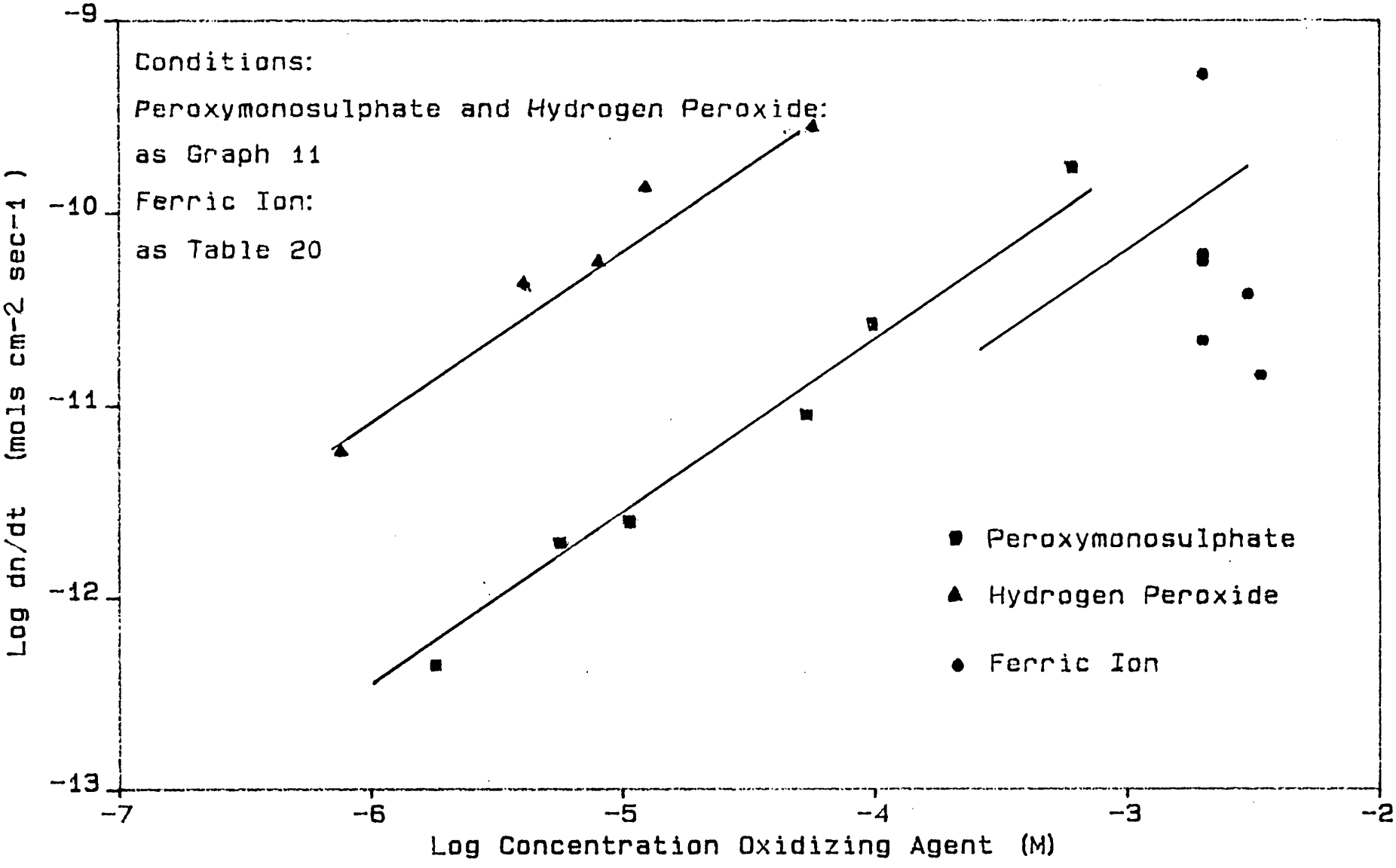
Graph 12 The Potential Imposed on a UO_2 Surface by Different Oxidizing Agents



Graph 13 Comparison of Steady State Current and Corrosion Current Data



Graph 14 The Absolute Leaching Rate of UO_2 with Different Oxidizing Agents



3.3.4.2 Microscopy

Although microscopy did not play a major part in this project, leaching residues and various electrodes were photographed.

Plate 2 contains photographs of the leached UO_2 spheres from run 212. Run 212 was a fairly typical peroxymonosulphuric acid leaching run. Photographs (a) and (b) show that the spheres have retained their characteristic uniformity, and integrity under the conditions employed. Photographs (c) and (d) show the etch pattern on the surface of the spheres. A polyhedral etch pattern is visible, indicating that reaction is occurring at the grain boundaries of the sintered UO_2. The sizes of the individual polyhedra vary, but an area of approximately 1 square micron is not atypical. These patterns have been observed by Eary et al.[63] in their study of UO_2 leaching with hydrogen peroxide. The fact that this detail can be observed indicates that a mechanism involving precipitation on the reacting particles is not occurring to any degree in this case.

These photographs were taken with a 'Vickers' light microscope. Hence because of the limits on the depth of field, only a small part of the sphere can be focussed on at any one time. This is the cause of the apparently smooth areas in some photographs.

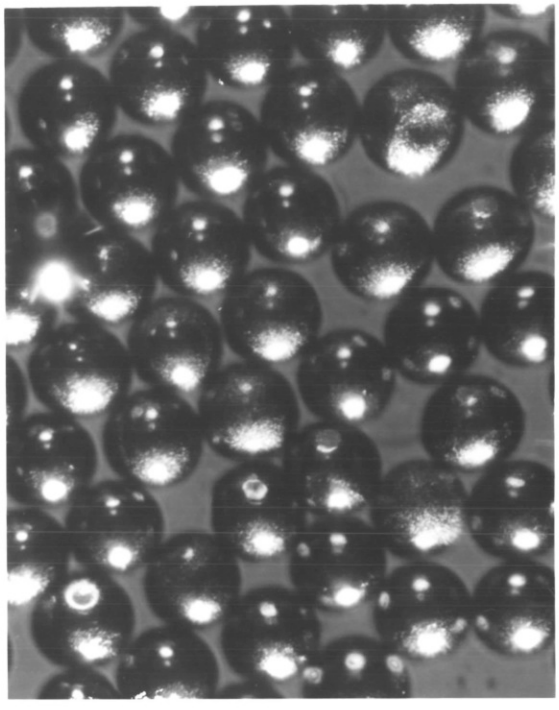
Plate 3 contains photographs of the leached UO_2 spheres from run 203. Run 203 was a fairly typical hydrogen peroxide

run. Photographs (a) and (b) show that the spheres retain their uniformity and integrity under the conditions employed. Photographs (c) and (d) show a similar etch pattern to those from the peroxymonosulphuric acid system. The etch pattern with hydrogen peroxide does however appear to be deeper, and more coarse than those obtained with peroxymonosulphuric acid.

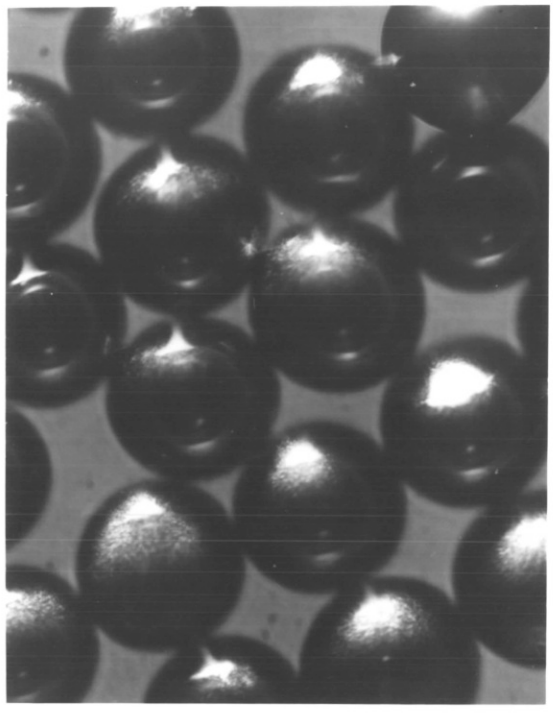
Plate 4 contains photographs of UO_2 electrodes before and after leaching. Very little difference can be observed between photographs (a) (an unleached electrode) and others in the plate.

Although very interesting, this photographic data yields very little further information on the dissolution mechanism of UO_2. The observation of etch patterns in the hydrogen peroxide and peroxymonosulphuric acid systems does indicate that leaching occurs at the grain boundaries. Comparisons of the etch patterns of the two systems reveal that although both are similar, the hydrogen peroxide patterns seem more severe and coarse. It is worthy of note that the hydrogen peroxide concentration which caused the etching apparent in Plate 3 is approximately an order of magnitude less than the peroxymonosulphuric acid concentration which caused the etching apparent in Plate 2. This implies that the amount of uranium leached with the (low) concentration of hydrogen peroxide is greater than that leached with the (higher) concentration of peroxymonosulphuric acid. This supports other results from this work.

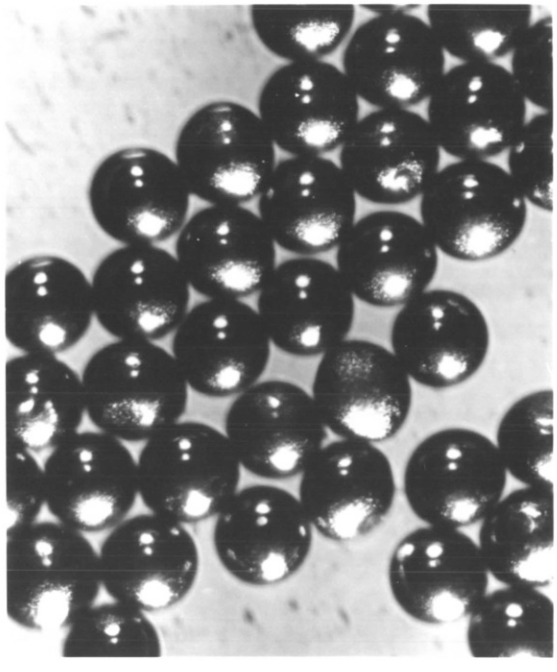
PLATE 1. Unleached uranium dioxide spheres at various magnifications



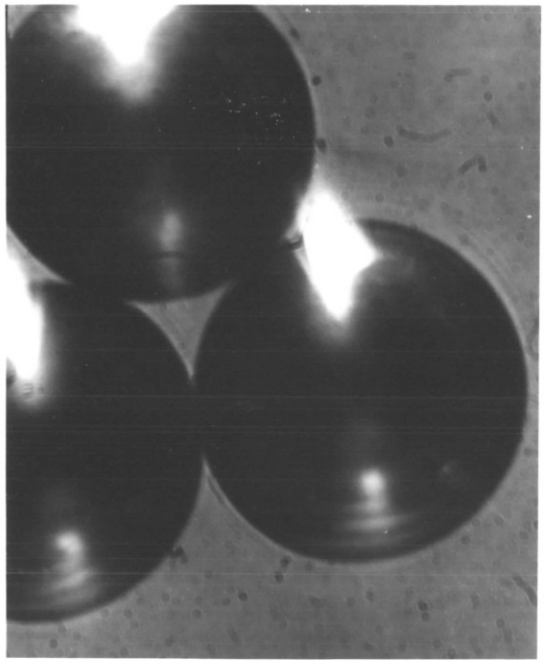
a) Magnification 100x



b) Magnification 200x

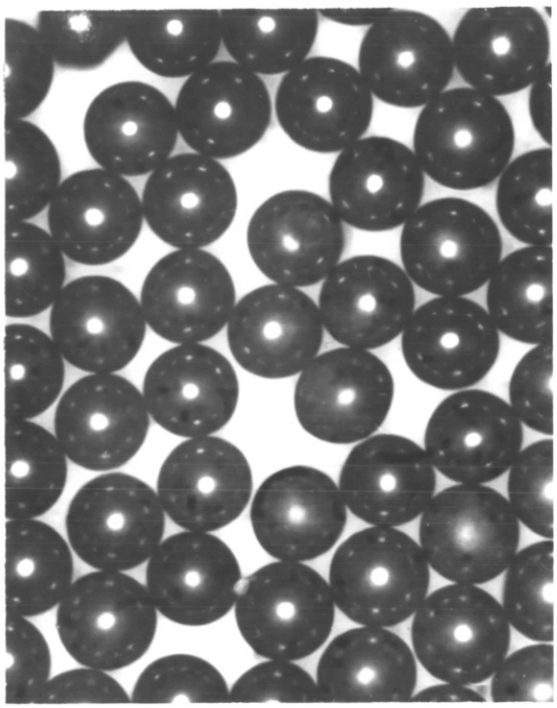


c) Magnification 100x

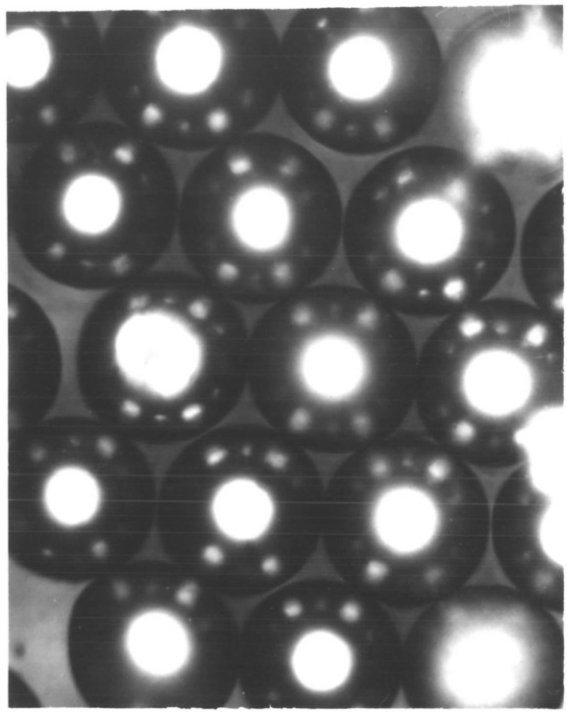


d) Magnification 400x

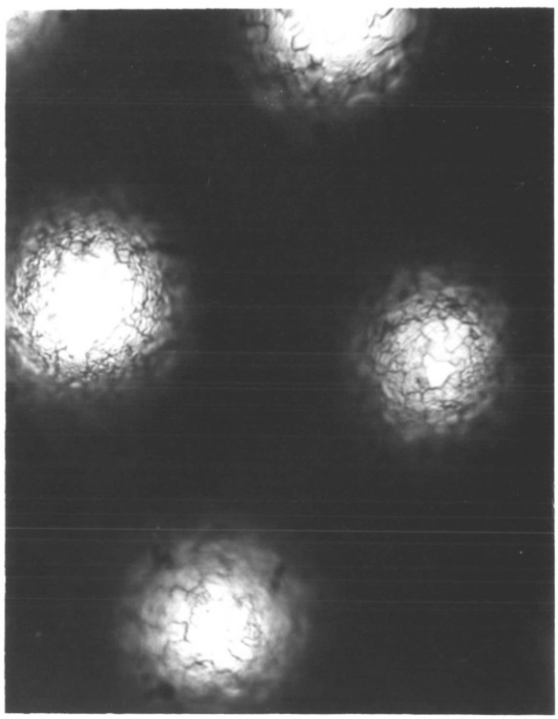
PLATE 2. Leached uranium dioxide spheres from run 212



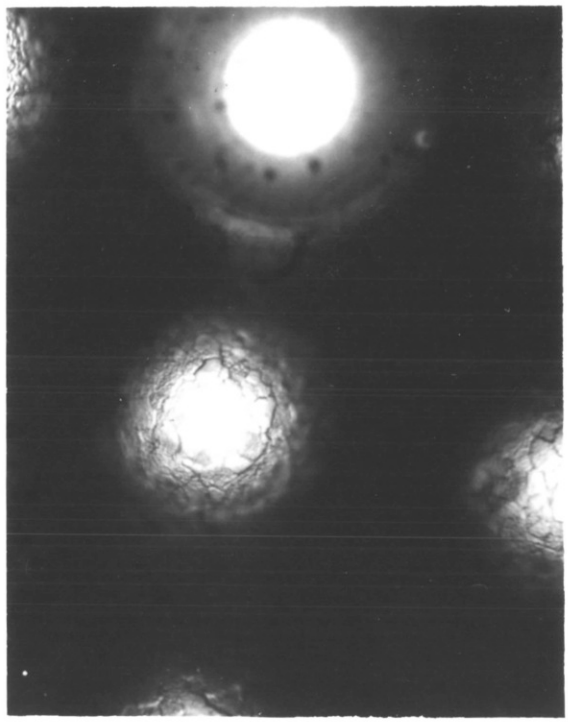
a) Magnification 100x



b) Magnification 200x



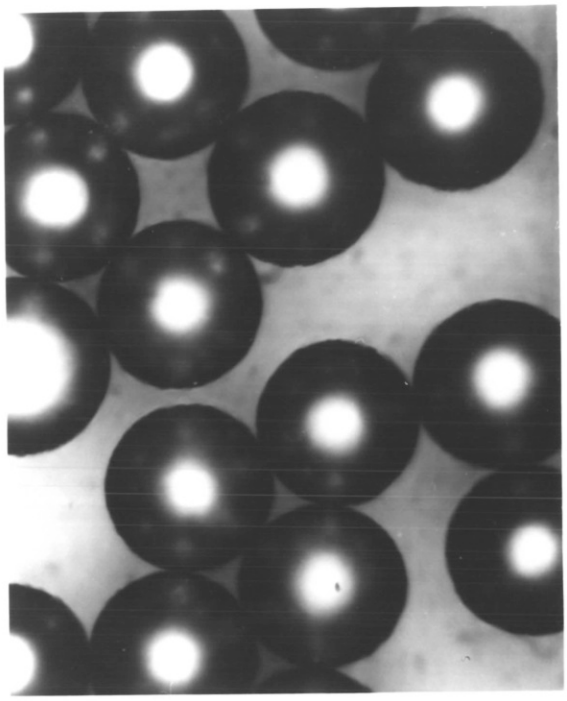
c) Magnification 400x



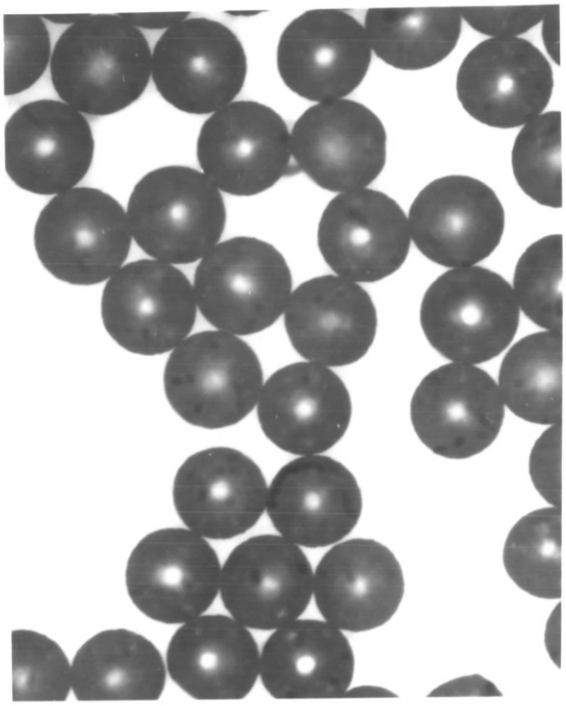
d) Magnification 400x

Leaching conditions: Temperature = 30°C, leached for 60 minutes at a pH of 1.48. [TS] ~ 1 M, $[H_2SO_5]$ = 0.44 M.

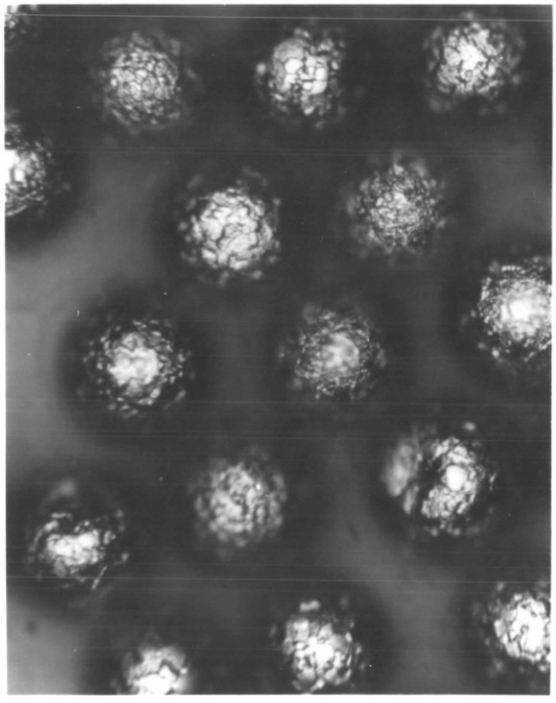
PLATE 3. Leached uranium dioxide spheres from run 203.



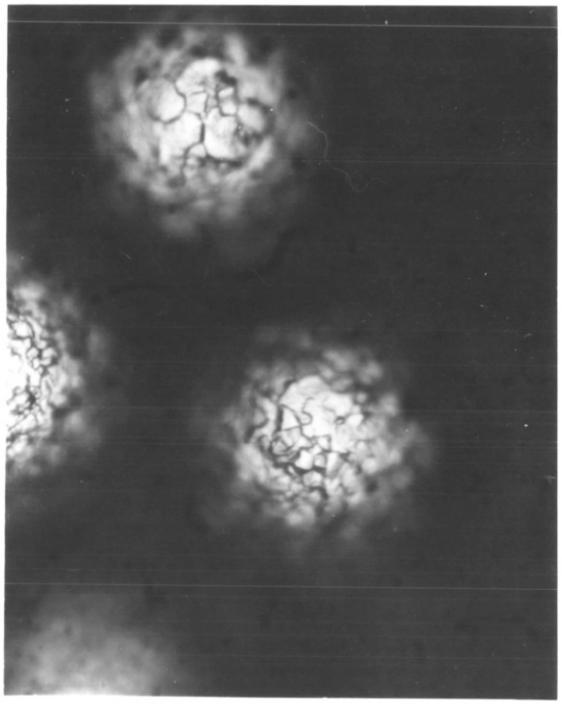
a) Magnification 200x



b) Magnification 100x



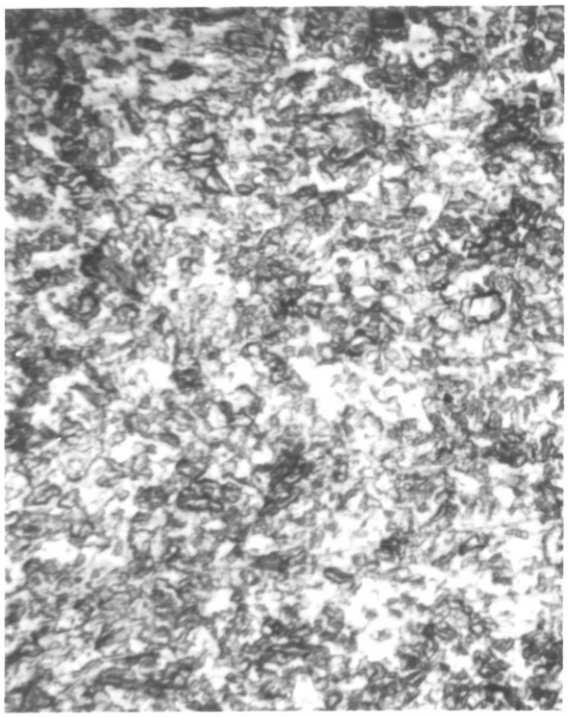
c) Magnification 200x



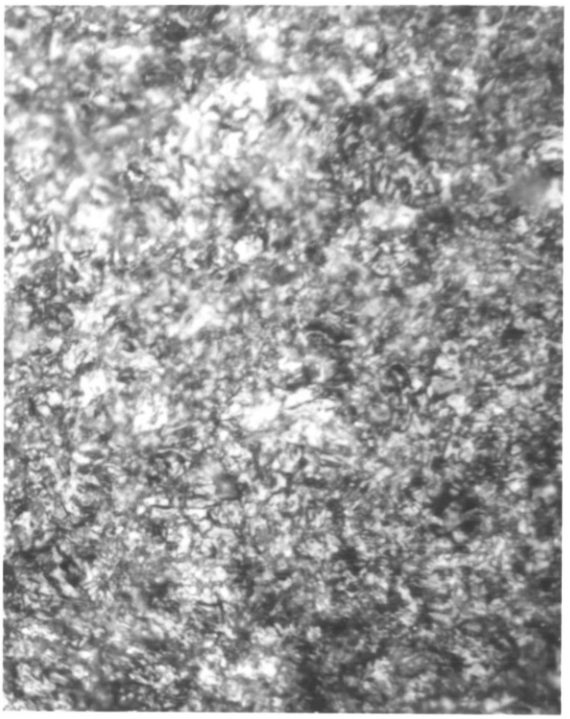
d) Magnification 400x

Leaching conditions: Temperature = 30°C, leached for 60 mins at a pH of 1.48; [TS] ~ 1 M, $[H_2O_2]$ = 0.04 M

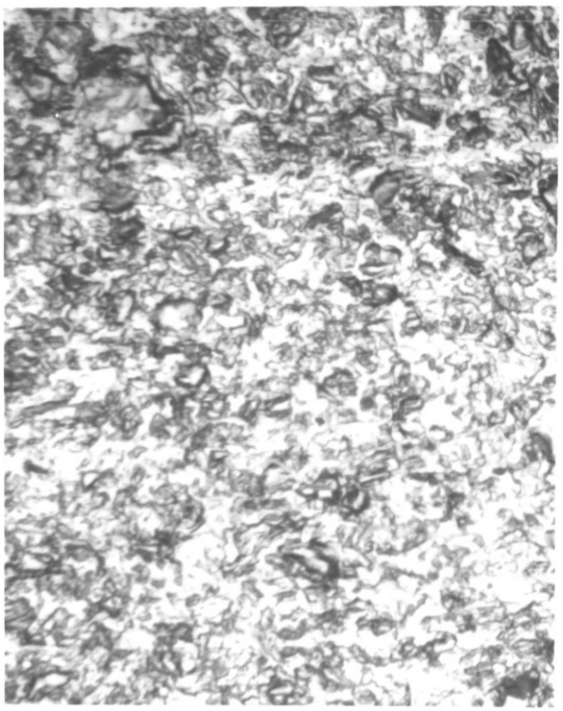
PLATE 4. Uranium dioxide electrodes under various conditions.



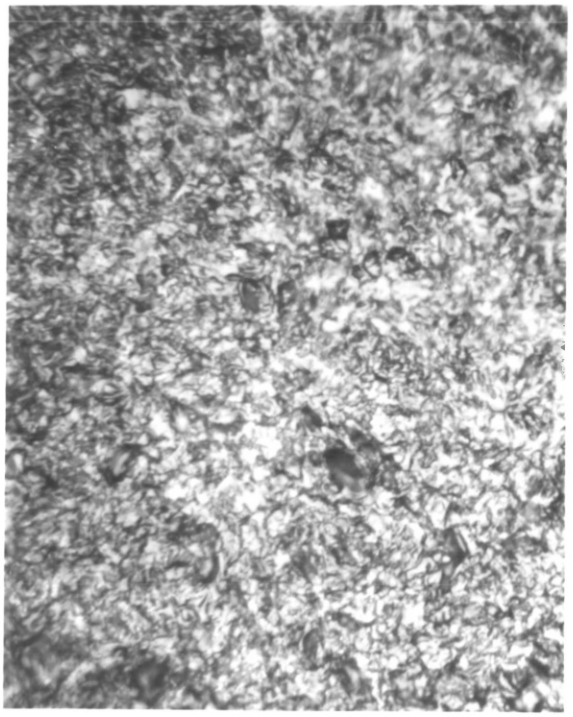
a) Magnification 400x
Unleached UO_2 electrode



b) Magnification 400x
Electrolytically leached for 40 minutes at 30°C with a current of 200 uA [TS]=1.03, pH = 1.50



c) Magnification 400x
Leached for 1 hour at 30°C
[TS] = 0.53, $[H_2O_2]$ = 0.68, pH=1.50



d) Magnification 400x
Leached for 1 hour at 30°C
[TS] = 1.57 M, $[H_2SO_5]$ = 0.72, pH = 1.50

3.4 THE PRACTICAL APPLICATION OF ELECTROCHEMISTRY TO REAL SYSTEMS.

3.4.1 Introduction

Some readers may feel that it is strange to put a section such as this at the end of the results chapter. However, this section does express results, although possibly not of the same species as those reported thus far.

Electrode kinetics have been applied to hydrometallurgical systems for approximately 20 years. In that time the equipment and technical sophistication has grown tremendously. Although very complex waveforms may now be applied to experimental cells, the fundamental problem of practical electrode kinetics has remained largely unanswered. This has resulted in massive technological expertise and very little growth of interpretive knowledge. The aim of this small section is to examine some of the problems as encountered in this work caused by the electrical double layer and the so-called Ir drop.

3.4.2 The Problems

The first major problem is the so-called electrical double layer. The surface of a particle is the largest structural defect that the particle possesses and has many imperfections and unsatisfied valence bonds. When a particle is immersed in a solution ions from the solution adsorb onto the surface of the particle to satisfy the unsatisfied

valence bonds. This adsorption initiates a charge separation effect between various anions and cations in the solution. This charge separation is called the double layer, and the ions whose adsorption cause the double layer are known as potential determining ions (P.D.I.). The formation of the double layer is a spontaneous process and cannot be prevented or avoided. The practical result is two sheets of opposed charge at, and very close to the surface of the particle. In normal chemical leaching studies the double layer is usually only relevant when it affects the diffusion of certain (rate determining) species or in point of zero potential charge determinations. In electrochemical studies however, the double layer acts as a complex capacitor and its effects must be recognised.

The capacitance of a real capacitor is independent of the potential across it. In this case however, because the 'plates' of the capacitor are composed of charged ions which are mobile, the composition of the 'plates' can and does change with potential. The composition of these 'plates' is also susceptible to changes in the concentration or composition of the solution. As the capacitance depends on the nature of the two 'plates', any change in the composition of these plates affects the capacitance of the system. The effect of passing current across the interface is two-fold. Of the current passed across the double layer one part is faradaic (of the electrode reaction), and the other part is non-faradaic. In a normal capacitor the initial current passed is used to charge the plates of the capacitor

according to equation (118). After the plates are charged the non-faradaic contribution to the overall current would be very small.

$$q = C_d E_c \qquad (118)$$

where q = the charge on the capacitor (Coulombs)

E_c = the potential difference across the capacitor (Volts)

C_d = the capacitance of the capacitor (Farads)

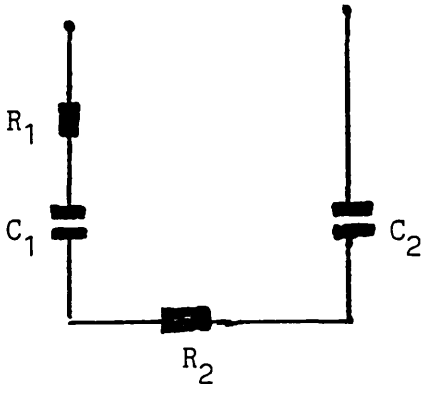
In this case however, this process in itself affects the composition of the 'plates' and hence the potential difference across the capacitor. The charging of the plates is therefore a continuous process because the capacitance of the plates is changing. In chronoamperometric work, this effect soon stabilises, but when any sweep technique is being employed the magnitude of the non-faradaic current depends on the sweep rate. Obviously the higher the sweep rate, the higher the non-faradaic current.

The second part of the problem of how current affects the capacitance of the system hinges around the effect of faradaic current. When faradaic current is passed, charge and mass transport normally also occur. This then affects the composition of the 'plates' and hence alters the capacitance of the double layer.

Briefly then, the capacitance of the double layer (hence the potential drop across it) varies with potential,

current and the concentration and composition of electrolyte. It is also worthy of note that in any electrochemical cell there must be at least two electrodes, therefore two interfaces and two double layers.

The second major problem is the solution and electrode resistance. In this work, the electrode resistance does not change appreciably, but in some work e.g. the dissolution of copper-iron sulphides, this is a problem. Providing the resistance does not change and ohmic contacts are maintained throughout, the potential drop across the electrode can be calculated by Ohms law, for any given current. The solution resistance is only relevant in comparisons between the reference and working electrodes, and will be covered in the next section. An electronic model of an electrochemical cell would therefore involve two capacitors and two resistors, as below:



where R_1 = the electrode resistance

R_2 = the solution resistance

C_1 and C_2 = the double layer capacitances.

If it is assumed that the capacitance of an average double layer is ∿30 μF cm^{-2} and the total charge on the capacitor is ∿20 μC, then the potential drop across the double layer is ∿700 mV. During the charging of this capacitor the magnitude of the non-faradaic charging current flowing would depend on the total resistance in the circuit. If it is assumed that the solution resistance is negligible (this is only valid for strong electrolytes at high concentrations e.g. 1 M KCl or Na_2SO_4) and that the electrode resistance is ∿0.1 KΩ; than taking a typical time constant of 30 μsecs., a charging current of 220 mA would flow for 90 μseconds. In practice UO_2 has very slow double layer charging characteristics,[43] therefore the charging time is much larger.

The third major problem are the liquid junction potentials. When two different ionic solutions, or two solutions containing different concentrations of the same ionic solute are placed in contact with each other, a potential difference between the two solutions is set up. This is caused by the different rates of diffusion of the different constituents of the solution(s). Normally, liquid junction potentials are eliminated by cell design, because it is very difficult to measure them. In the three compartment electrochemical cell however, liquid junction potentials exist at the tip of the Luggin probe and are usually totally uncompensated for.

Until recently, instead of evaluating each effect individually, the total overall effect was compensated for by using an A.C. Fluke impedance bridge. This device is an A.C. version of a Wheatstone bridge. However, recent work has shown that this method is not appropriate. What is required now is a method which allows the generation of a current-potential curve under steady state and non-steady state conditions, the current component of which contains no faradaic contribution at all. This could then be used to correct experimental data. Raffia et al.[93] and Imbeaux et al.[94] have presented intensely mathematical treatments involving non-linear integral equations. Both treatments assume diffusion control. The latter group give a correction procedure for cases when the ohmic drop is $\leq$50 mV. Both groups conclude that although often unconsidered, uncompensated ohmic drop and double layer charging phenomena can alter voltammograms in such a way as to mislead casual analysis. Qualitative effects of these effects include a flattening of faradaic peaks, anodic and cathodic shifting of peaks, a skewing of the voltammograms.

Most modern workers in electrochemistry have either used the A.C. Fluke impedance bridge to compensate for Ir drop or have not compensated at all. The interpretation of results, which with voltammetry means interpreting the shapes and positions of the peaks, is thus made more precarious than it already is.

There is one other assumption which must be explored. For a system to be defined as an electrochemical cell it must contain two electrodes in an electrolyte. It must therefore contain two double layers, and hence it is never possible to measure the properties of a single double layer in isolation.

As mentioned earlier, reaction orders must be determined at constant potential difference ($\Delta\Phi_e$), not constant overpotential. The problem is, because the potentiostat interprets the potential difference applied as that between its two output sockets, the actual potential difference depends on the relative magnitudes of the capacitance of the working and counter electrode double layers. If they are approximately equal, then the assumption that imposed and actual potential differences are approximately equal is valid. If however this is not true, (it is left for the reader to judge whether the double layer capacitance at a UO_2 anode with its associated flux of material is approximately equal to that at a reference electrode with its associated (small) flux of different material), then the 'reaction order' obtained from such a determination is not valid, because it contains a potential dependent term within it. Yet previous workers in the field have usually interpreted reaction orders with respect to constant overpotential.

This work has been carried out in the accepted fashion of previous work in the field. This final section is here

simply to put the results obtained into perspective with the complexities of the non-faradaic processes also occurring at the electrodes.

3.4.3 The Electrochemical Cell

In a normal two or three compartment cell, the reference cell contains a high ionic strength salt bridge solution, e.g. 1 M Na_2SO_4 or 1 M KCl. The working cell contains the working solution. Normally the reference cell is connected to the working cell by the use of a Luggin probe (or capillary) which is filled with the reference electrolyte. The function of the Luggin probe is to extend the reference cell as close to the working electrode as possible, hence minimising the Ir drop between the end of the Luggin probe and the surface of the working electrode. The potentiostat can then accurately compare the potential from the reference electrode to that of the working electrode. A number of major practical problems were encountered by the use of the Luggin probe. They were:

(a) Relatively tiny movements of the Luggin probe produced large differences in potential readings.

(b) The Luggin probe is the path of a small amount of charge transfer. (It is generally recognised that in order to generate a reference potential, a small amount of current (pA to nA) flows between the reference and working electrodes). This in turn stimualtes mass transfer. The Luggin probe therefore relies for its function on

diffusion, which implies that some mixing must occur. In this connection, during experimental runs reference solution could be seen to be mixing with the less dense working solution. This produces two problems:

(1) The ohmic drop was increased because the 1 M Na_2SO_4 in the Luggin probe was diluted by the working cell liquor.

(2) The working cell liquor was contaminated by reference electrolyte. This problem became acute when attempts were made to determine reaction orders with respect to sulphate.

(c) In an attempt to slow down or stop the mixing of the two electrolytes, Luggin probes of smaller internal dimensions were used. These were found to be constantly blocked by air bubbles.

The solution to these problems and the problem of the unknown liquid junction potentials was to carry out all the experiments in 1 M Na_2SO_4 solution, thus in effect carrying out all experiments in the reference compartment. This procedure however, is not usual and begs a question on the precision of potential measurements in other work. In this work the estimated error of measured potentials has been found to be $\pm$25 mV.

SECTION 4

SUMMARY OF RESULTS AND CONCLUSIONS

4.1 ANODIC OXIDATION OF UO_2

The solid state cyclic voltammetry revealed three main oxidation areas at all pHs studied, ($1.50 < pH < 12.06$). The most anodic of these oxidation areas was found to be complex, containing at least three different oxidised products. The position, shape and number of peaks in this oxidation area were found to depend on pH. At pH = 1.5, the cathodic reduction curves indicated that at least four oxidation products were reduced. At pH = 9.22 the cathodic reduction curves indicated that at least three oxidation products were reduced. All the cyclic voltammograms were complex, and were consistent with those reported in previous works.[38,45]

The carbon paste cyclic voltammetry carried out at pH = 1.5, revealed three major areas of anodic oxidation all within the potential range of the most anodic oxidation area found in the solid state cyclic voltammetry. The presence of these oxidation areas depended on the oxidation index of the oxide being used and the severity of the pretreatment. Cyclic voltammograms recorded using UO_3 and $UO_4.4H_2O$ were similar to each other and were distinctly different from the cyclic voltammograms of lower oxides. It was not possible to obtain a sample of the intermediates implied by the peaks of the cyclic voltammetry, therefore

it was not possible to formally identify them. The fact that intermediate uranium oxides have been detected at higher pHs by other workers,[45] and that the results of the carbon paste cyclic voltammetry were similar to those yielded by the solid state cyclic voltammograms led to the assumption that the intermediates were in fact uranium oxides.

Cathodic stripping analysis at pH = 1.5 revealed seven different uranium oxides on the surface of the UO_2, whose presence was potential dependent. Comparisons of the potentials of formation and reversability of the reduction reactions of these oxides with the structures of characterised uranium oxides allowed tentative identification of the individual uranium oxides. The stripping potentials of the intermediates were consistent with the areas of reduction found in the cyclic voltammetry.

Coulometric data obtained by integrating the cathodic stripping voltammograms enabled film thickness to be estimated. The nature of the variation of total film thickness with time at different potentials indicated a complex system. Comparison of total cathodic charge (representing the film thickness) and total anodic charge passed showed that although a small amount of uranium was dissolved during film formation, the dissolution process only began after considerable film formation. Inspection of the thickness of individual oxide films revealed that U_3O_7 and U_8O_{19} (which are very closely structurally and stoichiometrically related) were the

predominant films in the potential range (111 mV $\leq$ E $\leq$ 611 mV (SHE)). The U_8O_{19} was destabilised at E = 711 mV (SHE). At more oxidizing potentials (811 mV $\leq$ E $\leq$ 1011 mV (SHE)) the predominant film was found to be U_3O_8.

The Tafel plot of the system revealed two steady state areas indicating two rate determining steps valid over different potential ranges. At less oxidizing potentials (570 mV $\leq$ E $\leq$ 711 mV (SHE)), the anodic transfer coefficient was found to be 0.74 (dE/dlni= 35.5 mV decade^{-1}). Comparison of the experimental anodic transfer coefficients with theoretical transfer coefficients showed that the less oxidizing potential rate determining step involved the oxidation of U_3O_7 and/or U_8O_{19}. At more oxidizing potentials (750 mV $\leq$ E $\leq$ 1000 mV (SHE)), the anodic transfer coefficient was found to be 0.13 (dE/dlni= 196 mV decade^{-1}). Comparison of the experimental anodic transfer coefficients with theoretical transfer coefficients showed that the more oxidizing potential rate determining step involved the oxidation of U_3O_8.

The reaction order with respect to the activity of hydrogen ions was determined at two potentials, E = 711 mV and 911 mV (SHE). In the pH range (2.5 < pH < 7.0), at both potentials a reaction order of -0.07 with respect to pH was obtained. This was not fully understood, but it was proposed that this is not a mechanistic effect. In the pH range (0 < pH < 2.5) the order with respect to pH at E = 711 mV SHE was found to be -0.14.

This is consistent with reaction (104) being rate limiting. At more oxidizing potentials (E = 911 mV (SHE)) the order with respect to pH was found to be 0. This is consistent with reactions (110a) and (111a) being jointly rate determining. The reaction order with respect to sulphate at pH = 1.5 was found to be zero, and the apparent reaction order with respect to hydrogen peroxide was found to be a pH effect. The reaction order with respect to peroxymonosulphuric acid was found to be zero. These reaction order data support the mechanism proposed. Examination of the current densities of the reaction order analysis reveal that hydrogen peroxide and peroxymonosulphuric acid do not chemically affect the rate of UO_2 dissolution.

It was noted that until the intermediates in this reaction have been formally identified, the mechanism is not proven. The proposed mechanism is however, consistent with the complex kinetic, electrokinetic and electrolytic data. It also ameliorates difficulties in the proposed mechanism of Nicol et al.[41]

4.2 THE LEACHING OF UO_2 WITH OXIDISING AGENTS

4.2.1 Peroxymonosulphuric Acid

Comparison of theoretical mass transfer coefficients of the system to experimentally determined rate constants indicated that diffusion to the surface was not the rate limiting process in the leaching reaction. The magnitudes of the experimentally determined activation energies are

consistent with this conclusion. The fact that the experimental data can be fitted to a shrinking particle model implies that diffusion through a growing product layer is not rate limiting.

The anodic transfer coefficient was calculated as 1.58 ($dE/d\ln i$ = 27.2 mV decade^{-1}), this is consistent with the anodic transfer coefficient calculated for the rate determining step of the anodic oxidation. The agreement between the electrolytic and full system anodic transfer coefficients is extraordinary.

A reaction order with respect to pH of 0.33 is consistent with reactions (104) and (105) being jointly rate limiting. This is further strengthened by the electrochemical results which show that peroxymonosulphuric acid imposes a relatively less oxidizing potential on the UO_2 surface, thus stabilising U_8O_{19}.

A reaction order with respect to peroxymonosulphuric acid of zero implies that peroxymonosulphuric acid is only relevant in as much as the potential it applies to the UO_2 surface. This also implies that the cathodic half cell reaction is not rate limiting.

A reaction order of 0.58 with respect to sulphate was thought to be the result of strong statistical correlation between pH and sulphate concentration, and was not thought to have mechanistic significance.

Comparisons of peroxymonosulphuric acid under the experimental conditions employed in this project with other

oxidising agents on a concentration basis reveal that peroxymonosulphuric acid is approximately seven times faster than ferric ion and fifteen times slower than hydrogen peroxide for oxidising UO_2. Comparisons of peroxymonosulphuric acid with hydrogen peroxide on a potential basis reveal peroxymonosulphuric acid to be the more efficient oxidising agent.

Comparisons of the potential imposed on UO_2 by different oxidising agents on a concentration basis indicate that to impose a similar potential to hydrogen peroxide, peroxymonosulphuric acid must be present at concentrations of approximately two orders of magnitude greater than hydrogen peroxide. This is thought to be due to the generation of an insulating film caused by the initial very high potential imposed on the UO_2 surface by the peroxymonosulphuric acid.

It is concluded that the rate determining step of peroxymonosulphuric acid leaching of UO_2 is in the anodic half cell reaction, and all available data are consistent with this. The results may also indicate that multilinear regression analysis is not the best way of analysing very complex systems.

4.2.2 Hydrogen Peroxide

Comparison of theoretical mass transfer coefficients of the system to experimentally determined rate constants indicated that diffusion to the surface was not the rate limiting process in the leaching reaction. The magnitudes of the experimentally determined activation energies are consistent with this conclusion. The fact that the experimental data can be fitted to a shrinking particle model implies that diffusion through a growing product layer is not rate limiting.

The anodic transfer coefficient was calculated as 1.28 ($dE/d\ln i$ = 33.9 mV decade^{-1}). This is consistent with a rate determining process intermediate between the high and low potential rate determining steps found in the anodic oxidation of UO_2. This is consistent with the potentials imposed on the UO_2 surface by hydrogen peroxide relative to the potentials at which the electrolytic determinations were performed.

A reaction order with respect to hydrogen peroxide of zero implies that hydrogen peroxide is only relevant in as much as the potential it applies to the UO_2 surface. This also implies that the cathodic half cell reaction is not rate limiting.

A reaction order of zero with respect to pH is consistent with the fact that the rate determining process is intermediate between the high and low potential rate determining steps found in the anodic oxidation of UO_2.

A reaction order of zero with respect to sulphate concentration is also consistent with this. Cursory examination of the statistics reveals that this system is not as well described by the treatment given to it as the peroxymonosulphuric acid system.

Comparisons of hydrogen peroxide under the experimental conditions employed in this project with other oxidising agents on a concentration basis reveal that hydrogen peroxide is approximately 15 times better than peroxymonosulphuric acid and 100 times as good as ferric ion for oxidising UO_2. Comparisons of hydrogen peroxide with peroxymonosulphuric acid on a potential basis reveal hydrogen peroxide to be the less efficient oxidising agent. This is consistent with the activation energy data, which also indicate that as the potential increases, the rate of uranium dissolution does not increase as much as would be expected. This was thought to be due to the oxidation of hydrogen peroxide taking place as a side reaction.

It is concluded that this system is less well understood than the peroxymonosulphuric acid system. The rate determining step of the overall process is in the anodic half cell reaction.

Comparisons of the potential imposed on UO_2 by different oxidising agents on a concentration basis indicates that hydrogen peroxide can impose the same potential as peroxymonosulphuric acid at a concentration of approximately two orders of magnitude less.

Comparisons of hydrogen peroxide, peroxymonosulphuric acid and ferric ion as oxidising agents for UO_2 reveal that hydrogen peroxide can leach synthetic UO_2 approximately 100 times as fast as ferric ions and approximately 15 times as fast as peroxymonosulphuric acid.

Microscopy results reveal a similar etch pattern for both the hydrogen peroxide and peroxymonosulphuric acid leaching of UO_2. The hydrogen peroxide etch pattern seems more coarse and largely spaced than the peroxymonosulphuric acid etch pattern. The hydrogen peroxide pattern is also deeper than the peroxymonosulphuric acid pattern even though it was produced over a similar time scale and temperature by approximately ten times less oxidant.

4.3 THE MAJOR WEAKNESSES OF THIS WORK

The mechanism for the anodic oxidation of uranium dioxide is weak without any identification of the intermediate oxides. This major assumption, though not without foundation lies at the heart of all three sections of this work.

The interpretation of the electrode kinetic and electrolytic data, although consistent with the way similar data has been interpreted in the past, is fundamentally weak due to the non-faradaic contribution to the current and potential drops across the double layer.

The distribution of runs in the statistical analysis section is very poor. Inspection of both the hydrogen peroxide and peroxymonosulphuric acid Minitab outputs reveal that the majority of runs appear in the high concentration range.

No leaching of UO_2 with ferric ion (with and without typical ore impurities) was included in this project, hence its practical application to uranium ore leaching is limited.

4.4 THE COURSE OF FUTURE WORK

If any further work on the uranium dioxide system is contemplated, such work should include characterisation of the oxide intermediates, possibly using increased sensitivity X-ray photoelectron spectroscopy, or some similar enhanced method. This work could be extended by the examination of the leaching kinetics of uranium ore, and the leaching of UO_2 with ferric ion.

The most important work however, is not necessarily concerned with uranium oxides. A comprehensive method of compensation for non-faradaic effects not based on A.C. methods must be evolved. This would then allow more correct interpretation of electrode kinetic and electrolytic data.

APPENDIX 1. THE FUNDAMENTAL ELECTROCHEMISTRY

A1.1 The Stockholm electrode convention

A1.2 Fundamental Electrochemistry

A1.2.1 Introduction

A1.2.2 Electrochemical Reactions

A1.3 Electrolytic Methods

APPENDIX 1

A1.1 STOCKHOLM ELECTRODE CONVENTION

Controlling the potential of an electrode is equivalent to controlling the free energy of the electrons in that electrode. By imposing a negative potential on the electrode, (i.e. increasing the 'electron pressure'), the free energy of the electrons within the electrode is raised. They will eventually reach energy levels high enough to be able to move out of the electrode and occupy vacant levels on species in the electrolyte. Electrons will flow from the electrode to the electrolyte and reduction of electrolyte species will occur. Similarly, imposing a high enough positive potential (i.e. a low enough 'electron pressure') results in a flow of electrons from the electrolyte to the electrode, and oxidation of electrolyte species. In reversible systems the critical potential at which these processes occur is related to the Standard Potential (E^{o}) of the species in the system.

The thermodynamic assumption underlying this work is that reduction is spontaneous, and therefore by equation (A1) has a negative free energy and will occur when the Standard Reduction Potential is positive.

$$\Delta G^{o} = -nFE^{o} \qquad (A1)$$

When two half cell reactions are written together, then the half cell reaction with the most positive Standard

Reduction Potential will be the cathodic reaction in that cell. The magnitudes of Standard Potentials can be quoted with reference to any standard electrode. Standard Reduction Potentials (SRP) have been quoted with respect to the Standard Hydrogen Electrode (A2), whose Standard Potential is arbitrarily zero.

$$2H^+ + 2e^- \rightleftharpoons H_2 \qquad (A2)$$

$$E_{cell} = E_R - E_L \qquad (A3)$$

The Standard Reduction Potential of any half cell reaction can be determined by measuring it in a whole cell against the SHE. If the SHE is always written as the left electrode, the cell potential will yield the SRP of the unknown half cell reaction according to equation (A3).

For example, if the measured potential for the cell described below is 0.34 V, the copper terminal being positive, the SRP of the Cu^{2+}/Cu half cell reaction would equal +0.34 V. This convention is sign invariant, as can be seen from this example.

$$2H^+ + 2e^- \leftarrow H_2 \;\|\; Cu^{2+} + 2e^- \rightarrow Cu$$

When a potential is electrolytically imposed the anodic and cathodic polarities are reversed. Figure A1 summarises the situation.

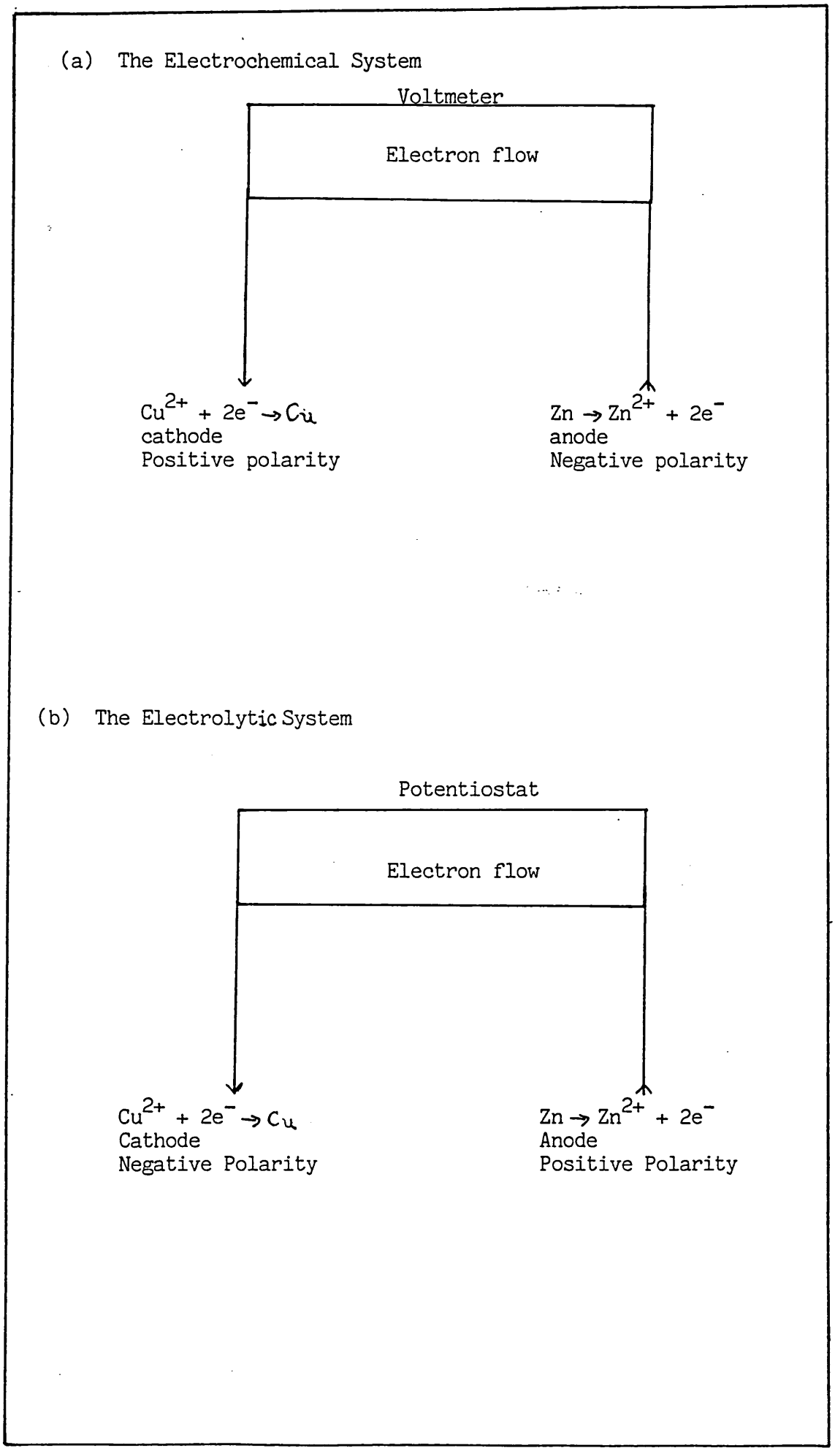


FIG. A1: The differences of polarity in the electrochemical and electrolytic systems.

A1.2 FUNDAMENTAL ELECTROCHEMISTRY

A1.2.1 Introduction

Homogeneous reactions

The rate of a general single step homogeneous reaction (A4) can be described in terms of the concentrations of reactants and rate constants, as below:

$$xA \underset{k_b}{\overset{k_f}{\rightleftharpoons}} yC \qquad (A4)$$

Forward rate $= k_f[A]^x$

Backward rate $= k_b[C]^y$

where k_f = forward rate constant

k_b = backward rate constant

y,x = orders of reactions i.e. the stoichiometry of the rate determining steps.

Obviously, constant temperature and pressure are assumed.

Heterogeneous reactions

In a heterogeneous system, the same basic format applies, except that the constant becomes more complex, depending on the nature of the rate determining step, as below.

Forward rate $= k_f[A]^x$

where chemical control $k_f = A.\ k_o k'$

where diffusion control $k_f = A.\ \frac{D}{\delta\sigma}$

where D = diffusion coefficient of the diffusing species

δ = thickness of diffusion layer (cm)

A = area (cm^2)

σ = a stoichiometry factor which represents the number of moles of the diffusing species required for each mole of metal value released by the reaction.

k_f = apparent forward rate constant

k' = rate constant ($cm^3\ sec^{-1}$)

k_o = concentration of potentially reactive sites (cm^{-2})

Both homogeneous and heterogeneous reactions vary with temperature in accordance with the Arrhenius equation (A5), which is normally quoted in its logarithmic form (A6)

$$k_f = A \exp \frac{-\Delta G^{\neq}}{RT} \qquad (A5)$$

$$\ln k_f = \ln A - \frac{\Delta G^{\neq}}{RT} \qquad (A6)$$

The Arrhenius equation was developed from collision theory, and its derivation appears in many standard textbooks. The rate of any non-electrochemical reaction is primarily unaffected by electrode potential and is entirely dependent on the temperature, light intensity and concentrations of the various components of the system.

If the rate instead of the rate constant is plotted against the reciprocal of the temperature, the left hand side is modified to include concentration terms, but the derived activation energy remains the same.

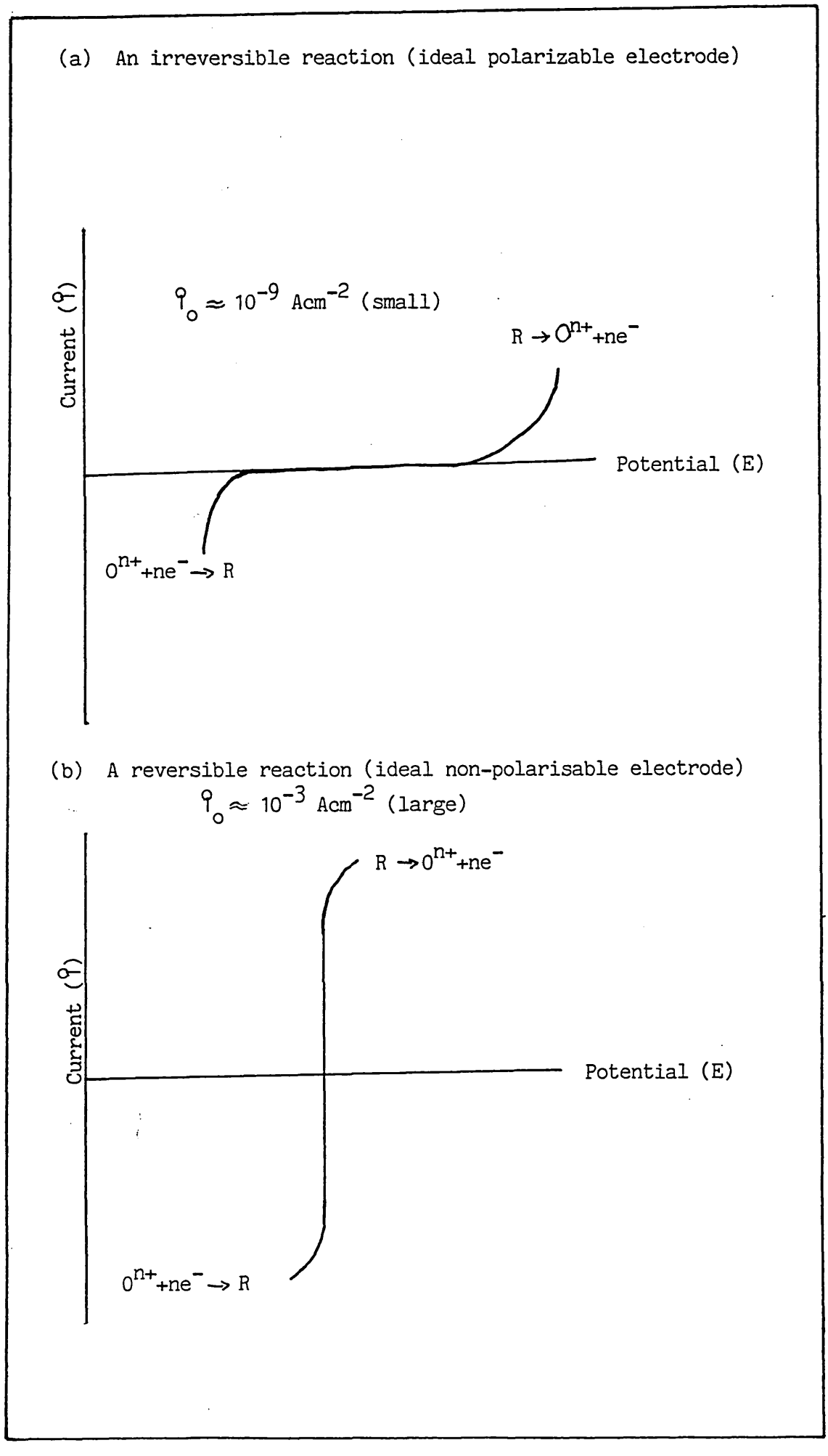


FIG. A2: A comparison of reversible and irreversible reactions.

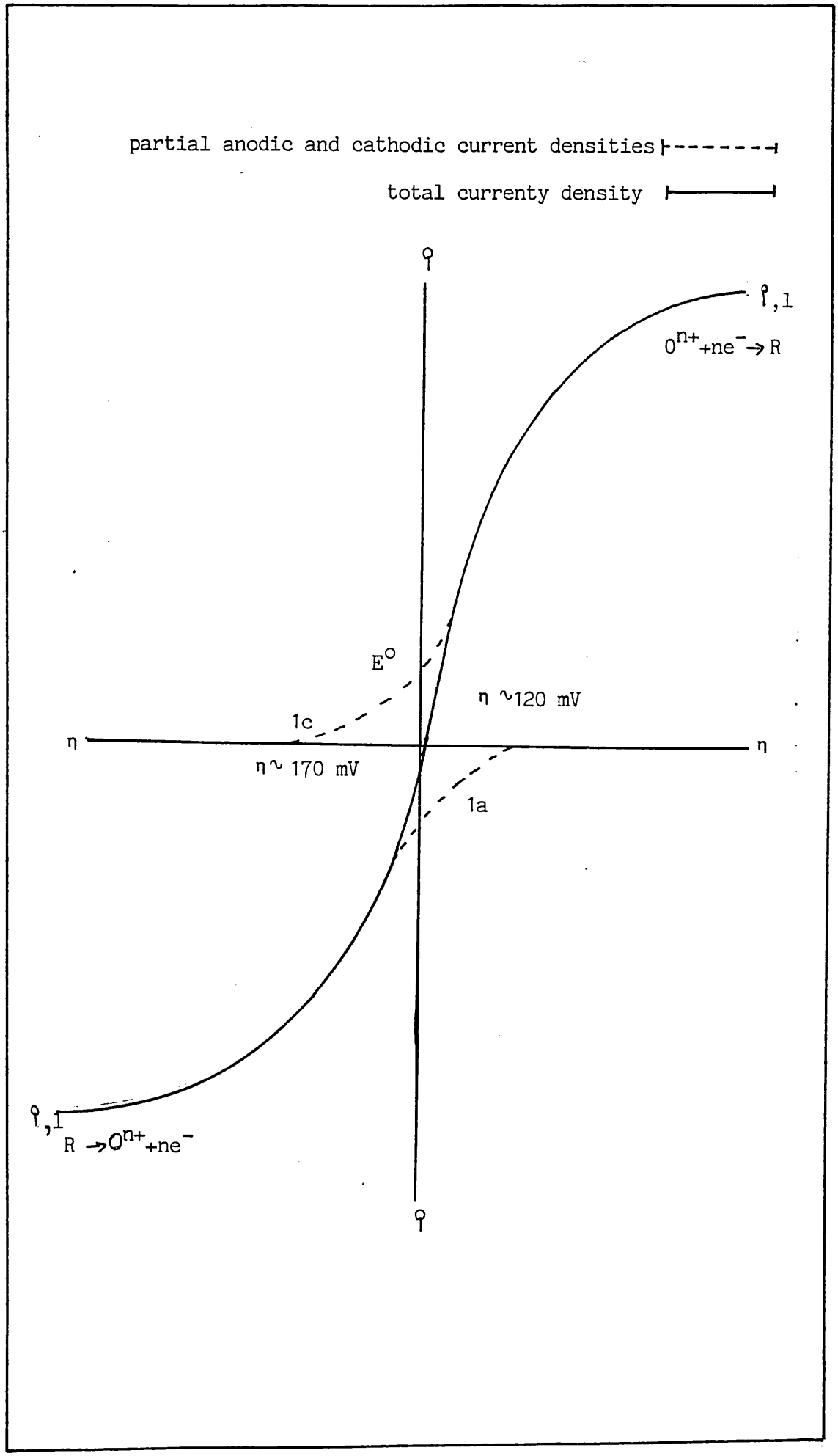


FIG A3. Current density overpotential curve for simple system, $\alpha = 0.5$, $n = 1$

A1.2.2 Electrochemical Reactions

(a) Potential

The fundamental difference between electrochemical and other reactions is that electrochemical reactions involve coupled anodic and cathodic half cell reactions.

In corrosion or leaching systems, the two half cell reactions occur at sites scattered over the surface of the mineral like tiny short circuited cells. In this project the anodic half cell reaction is the oxidation of UO_2 to oxidized products, and the cathodic half cell reaction is the reduction of peroxymonosulphuric acid or hydrogen peroxide. For theoretical purposes two general half cell reactions will be used, (A7) and (A8).

Anodic oxidation $$R \xrightarrow{k_b} O^{n+} + ne^- \qquad (A7)$$

Cathodic reaction $$O^{n+} + ne^- \xrightarrow{k_f} R \qquad (A8)$$

Figure A2 shows the current density/potential curves for two different couples (half cell reaction pairs). The first couple is slow, the rest potential is difficult to determine, and the reaction is very irreversible. The second couple is fast, the rest potential is easy to determine, and the reaction is reversible.

In this project all the half cell reactions are relatively irreversible, and resemble Figure 2(a) more than 2(b).

The rate of a single step, single electron transfer reaction is described by the Butler-Volmer equation (A9):

$$\wp = \wp_o \left[\exp \frac{-\beta n F \eta}{RT} - \exp \frac{(1-\beta) F n \eta}{RT} \right] \qquad (A9)$$

where $\wp$ = current density ($\mu A\ cm^{-2}$)

$\wp_o$ = exchange current density, i.e. the current when $E = E^0$, $\wp_{NET} = 0$, $\wp_a = \wp_c$

η = overpotential, i.e. ($E - E^0 = \eta$) (mV)

β = symmetry factor, in the simple 1 electron system $\beta = \overleftarrow{\alpha} = \vec{\alpha}$

$\vec{\alpha}$ = cathodic transfer coefficient

$\overleftarrow{\alpha}$ = anodic transfer coefficient

All other symbols have their normal meanings.

No attempt to derive the Butler-Volmer equation will be made here. Interested readers are directed to Bard and Faulkner,[64] although any standard text will probably have a derivation. The Butler-Volmer equation expresses the forward and backward reactions of every half cell reaction in the system. In the present example there are only two terms because (A7) and (A8) are complimentary reactions. The first term describes the rate of the reduction reaction (A8), the second term describes the rate of the oxidation reaction (A7). The current is proportional to the rate of reaction (A10). In this simplified Butler-Volmer equation, all reaction orders are assumed to be unity.

$$V = \frac{I}{nFA} = \frac{\varphi}{nF} \qquad (A10)$$

where I = the current (A)

V = reaction rate (mol sec^{-1} cm^{-2}) = $\frac{dn}{dt}$

In a real case where the half cell reactions are not complimentary, there would be at least two anodic terms and two cathodic terms.

Figure A3 shows the current density-overpotential curve for the system under consideration. It can be seen that when $E \sim E^0$, i.e. $\eta \sim 0$, the total current has both cathodic and anodic components. At $E = E^0$, the total current density is zero, but an equal finite current density is flowing simultaneously in both directions. The magnitude of this current density is equal to the exchange current density (φ_o).

The magnitude of the exchange current density indicates the degree of reversibility or irreversibility of the reaction, as shown in Figure A3. The exchange current density describes the kinetic properties of the cathodic and anodic reactions at $\eta = 0$, as below:

$$\varphi_o = nFk^o[O]^x [R]^y \qquad (A11)$$

where k^o = standard rate constant.

The levelling out of the anodic and cathodic current densities at the extremes of the curves is due to mass transfer limits of the system, and this current density is called the anodic or cathodic limiting current density.

It can be seen that the usefulness of the Butler-Volmer equation hinges around the magnitude and physical significance of the transfer coefficients (α) of the system. In the simple system it is taken as a measure of the symmetry of the energy barrier, and is usually assigned the value of 0.5. In more complex reactions however, the anodic ($\overleftarrow{\alpha}$) and cathodic ($\vec{\alpha}$) transfer coefficients will be shown to encompass not only the symmetry of the energy barrier, but also the number of electrons transferred in the overall and microscopic process, the number of times the rate limiting step must occur for one cycle of the overall process, and even whether a chemical or electrochemical step is rate limiting. The transfer coefficients are of paramount importance in mechanistic diagnosis, and they are normally used to test a proposed mechanism.

When ($\eta \geq 120$ mV, ($n = 1$)) the approximation that the contribution to the current of one half cell reaction is negligible when compared to the other gives rise to the Tafel equations. These are a limiting form of the Butler-Volmer equation (A9). They are normally used in their logarithmic form as a straight line plot. The cathodic Tafel Equation is reproduced below (A12).

$$\eta = \ln \varphi \frac{RT}{\vec{\alpha} nF} - \ln \varphi_o \frac{RT}{\vec{\alpha} nF} \qquad (A12)$$

There is also a low overpotential limiting form of the Butler-Volmer equation (A13). When $\eta \leq 20$ mV, the assumption that $e^x \sim 1+x$ can be employed, and equation (A9) can be rewritten:

$$\varphi = \varphi_o \left[\frac{-nF}{RT}\right] \qquad (A13)$$

In more complex systems, the Butler-Volmer equation retains its general form, but is usually quoted in terms of equation (A11).[65]

$$i = nFk_f^o[R]^x \exp \frac{\vec{\alpha} F\eta}{RT} - nFk_b^o [O^{n+}]^y \exp \frac{\overleftarrow{\alpha} F\eta}{RT} \qquad (A14)$$

cathodic reduction (A7)

anodic oxidation (A8)

where:

k_f^o and k_b^o are the heterogeneous rate constants for reduction and oxidation at E=0 on the scale of use.

x and y are the reaction orders with respect to those species.

$\overleftarrow{\alpha}$ = cathodic transfer coefficient = $[\frac{n-\phi}{\nu} - r\beta]a$

$\vec{\alpha}$ = anodic transfer coefficient = $[\frac{\phi}{\nu} + r\beta]a$

and therefore $\vec{\alpha} + \overleftarrow{\alpha} = \frac{n}{\nu}$

$\vec{\psi}$ = number of electrons transferred before the rate determining step

$\overleftarrow{\psi}$ = number of electrons transferred after the rate determining step.

ν = the stoichiometric number, i.e. the number of times the rate determining step occurs during one full cycle of the reaction.

a = the number of electrons transferred in the rate determining step

β = symmetry factor (normally taken as 0.5)

= distance across double layer to summit on the reaction co-ordinate diagram / distance across double layer

r is an arbitrary factor and depends on the nature of the rate determining step (rds)

r = 1 if rds is charge transfer

r = 0 if rds is not charge transfer

It should be noted that it is still assumed that only two complimentary half cell reactions (A7 and A8) are present. For each extra half cell reaction present, another cathodic and anodic term must be added to the Butler-Volmer equation.

Under normal leaching conditions, in this project there are at any time two (with H_2SO_5) or three (with H_2O_2) half cell reactions:

$$UO_2 \longrightarrow UO_2^{2+} + 2e^- \qquad \text{(A15)}$$

$$UO_2^{2+} \longrightarrow UO_2 \qquad \text{(A16)}$$

and

$$HSO_4 + H_2O \longrightarrow HSO_5 + 2H^+ + 2e^- \quad (A17)$$

$$HSO_5 + 2H^+ + 2e^- \longrightarrow HSO_4 + H_2O \quad (A18)$$

or

$$H_2O_2 \longrightarrow O_2 + 2H^+ + 2e^- \quad (A19)$$

$$O_2 + 2H^+ + 2e^- \longrightarrow H_2O_2 \quad (A20)$$

and

$$2H_2O \longrightarrow H_2O_2 + 2H^+ + 2e^- \quad (A21)$$

$$H_2O_2 + 2H^+ + 2e^- \longrightarrow 2H_2O \quad (A22)$$

Each of the complimentary sets of half cell reactions will have their own anodic and cathodic transfer coefficients, and their own heterogeneous rate constants. In this case, one can rule out the following reactions on thermodynamic or potential grounds: (A16), (A17), (A20) and (A21).

In a real leaching or corrosion situation, any anodic or cathodic transfer coefficients measured will be a weighted mean (according to the partial currents) of all the anodic or cathodic transfer coefficients respectively, of the system.

The major difference between the simple and the complex Butler-Volmer equation is in the transfer coefficients. The complex form of the transfer coefficients will therefore be derived. The rate of a simple one electron transfer

reaction can be expressed, under reducing Tafel conditions as:

$$i_c = Fk_c [R] \exp \frac{-\beta FE}{RT} \qquad (A23)$$

where all symbols have their normal significance. Let the total number of electrons transferred in the overall process be n. Also let the total number of electrons transferred in the rate determining step (r.d.s.) be equal to a. An arbitrary factor r will be introduced to indicate whether charge transfer is rate determining.

$$i_c = nFk_c [R] \frac{-a\beta FEr}{RT} \qquad (A23a)$$

let r = 1 when r.d.s. is charge transfer

let r = 0 when r.d.s. is not charge transfer.

In the simple 1 electron transfer reaction n = a = r = 1. Let us now set up a complex reaction scheme. The r.d.s. occurs ν times per reaction cycle.

$$A + e^- \underset{k_{-1}}{\overset{k_1}{\rightleftharpoons}} B \qquad \text{N.B. } \frac{k_1}{k_{-1}} = K_1 \qquad (A24a)$$

$$B + e^- \underset{k_{-2}}{\overset{k_2}{\rightleftharpoons}} C \qquad (A24b)$$

$$\vdots$$

$$P + e^- \rightleftharpoons R \quad \text{step } \vec{\phi} \qquad (A24c)$$

$$R + ae^- \rightarrow S \quad \text{r.d.s. } \nu \text{ times} \qquad (A24d)$$

$$S + e^- \rightleftharpoons T \quad \text{step } n\text{-}\vec{\phi} \quad -r\nu = \vec{\phi} \tag{A24e}$$

The steps which are not rate determining can be taken as a series of equilibria, therefore using the equilibrium constants and the Butler-Volmer equation, concentrations of each precourser can be expressed in terms of the concentrations of the first, or nth component, and the equilibrium constant of the corresponding step.

$$[B] = K_1 [A] \exp \frac{-FEa}{RT} \tag{A25}$$

$$[C] = K_2 [B] \exp \frac{-FEa}{RT} = K_1K_2 [A] \exp \frac{-2FEa}{RT} \tag{A26}$$

noting that the r.d.s. occurs ν times, at the end of the process:

$$[R]^\nu = (K_1K_2 \ldots k_{rds}) [A]^\nu \exp \frac{-\vec{\phi}FEa}{RT} \tag{A27}$$

If $[K_1K_2\ldots.] = \varkappa$, and by rearranging:

$$[R] = [\varkappa k_{rds}]^{1/\nu} [A] \exp \frac{-\vec{\phi}/\nu \; FEa}{RT} \tag{A28}$$

Now substitute (A28) into (A23a)

$$i_c = \eta F k_c [\varkappa k_{rds}]^{1/\nu} [A] \exp \frac{-\vec{\phi}/\nu \; FEa}{RT} \exp \frac{-a\beta FEr}{RT}$$

$$i = \eta F k_c^o [A] \ldots \exp \frac{-(\vec{\phi}/\nu + r\beta) \; aFE}{RT} \tag{A29}$$

If the analogous process for the backward reaction (A24f) is used, the anodic transfer coefficient is obtained.

$$S \longrightarrow R + se^- \qquad \text{(A24f)}$$

The cathodic transfer coefficient ($\vec{\alpha}$) is $(\vec{\psi}/\nu + r\beta)a$ (A29a)

The anodic transfer coefficient ($\overleftarrow{\alpha}$) is $(\frac{n-\vec{\psi}}{\nu} - r\beta)a$ (A29b)

hence $\overleftarrow{\alpha} + \vec{\alpha} = \frac{na}{\nu}$

Equations (A14) and (A9) differ only in the following respects:

(i) In (A14) the n values are incorporated into the transfer coefficients.

(ii) The assumption that the anodic and cathodic half cell reactions are complimentary has been dropped, hence k_o and therefore γ_o cannot be used.

(iii) The role of the transfer coefficients is revealed as controlling how the input electrical energy ($F\eta$) affects the reaction rate. Their complex dependence on energy barrier symmetry, the nature and setting of the rate determining step in the overall mechanism is incorporated into them.

To model any system fully using the Butler-Volmer equation one must have the reaction 'order' data with respect to all relevant species. As reaction order depends on mechanism, a species may have different orders in its oxidation and reduction reactions, even in the same system.

Therefore, reaction order determinations must be performed under irreversible (Tafel) conditions. In normal chemical kinetics, the concentration of one species is varied, all the others remaining constant. With electrochemical reaction orders, the additional condition that the potential drop across the mineral/solution boundary also be constant is necessary. When the potential on the mineral is caused by the presence of an oxidizing/reducing agent in situ, this condition is met. When however, the potential on the mineral is imposed externally, although the overpotential may be constant, the potential drop across the mineral/solution interface may not be. The point hinges on the fact that it is not possible to measure the potential drop across the mineral/solution interface in isolation. Hence, if the assumptions that the 'resistance' of the electrolyte and the potential drop across the double layer are approximately constant and low over all the concentration range of the order determination are tenable, then the second term in equation (96) should be negligible. If this is so, the order of reaction is obtained.

$$\left[\frac{\partial \log \rho}{\partial \log [A]}\right]_{[B][C]\ldots,\eta} = x_{(A),\text{cathodic}} + \frac{\tilde{\alpha} F}{RT}\left[\frac{\partial \Delta\phi_e}{\partial \log [A]}\right]_{[D][C]} \qquad (A30)$$

where $\Delta\phi_e$ is the potential drop across the mineral/solution interface.

Equation (A30) is simply the result of differentiating a modified Butler-Volmer equation with respect to the log concentration of [A] with constant concentrations of other components and overpotential. This whole problem will be dealt with in more detail in the practical applications section.

Finally, the whole of this discussion on the Butler-Volmer equation has tacitly assumed that the full surface of the mineral is available for reaction, and there are no adsorbed species. It is well documented[54] that sulphate specifically adsorbs onto a UO_2 surface. In electrolytic situations this is irrelevant. However, in electrochemical situations, the sulphate competes with the adsorption of electroactive agent. In most cases, because the total ionic strength $\geq$ 1.0, at these concentrations the effect can be assumed to be similar in all runs and should be absorbed in the rate constants. The other adsorption effect concerns the adsorption of reaction products, which may well be potential dependent. However, as the principle reaction products are hydrogen ion and sulphate, both of which are present in the solution, this will be ignored. Correction for surface adsorption involves the use of a surface coverage factor in the pre-experimental Butler-Volmer terms as below (A31).

$$\varphi = \varphi_o \frac{(1 - \theta)}{(1 - \theta_e)} \exp \frac{-\alpha F \eta}{RT} \qquad \text{(A31)}$$

where θ = coverage at E=E

θ_e = coverage at $E=E^0$

This equation is written assuming Tafel conditions.

(b) Temperature

So far the discussion has centred on the role of potential in determining the rate of an electrochemical reaction. Figure A4 shows the effect of potential on the activation energy. It can be seen that as the potential is altered, so too is the measured activation energy. This is because the potential is literally a measure of free energy of the electrons (A32).

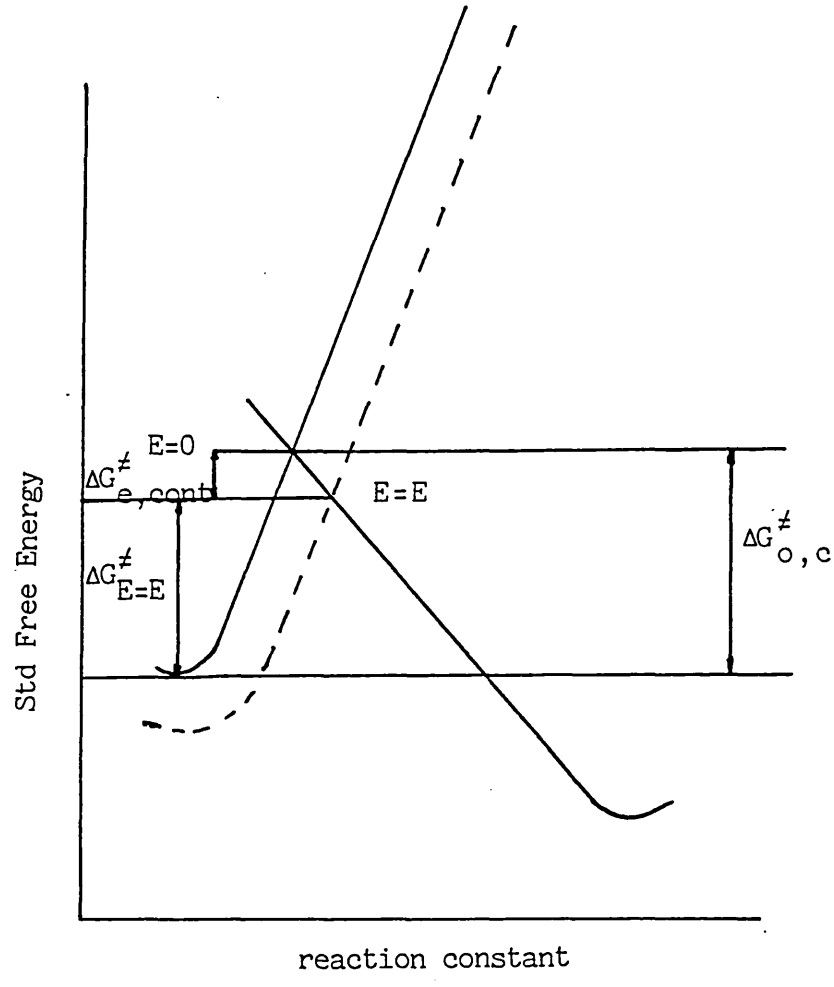
$$\Delta G^{o} = -nFE^{o} \qquad (A32)$$

However, this implies that the input electrical energy affects the rate (hence the free energy of activation) in a uniform manner. This is not so. As mentioned previously, the transfer coefficient determines how the rate of reaction is affected by potential. The contribution of potential to the activation energy is called the electrochemical contribution to the activation energy ($\Delta G^{\neq}_{e,cont}$) and is described by equation (A33).

$$\Delta G^{\neq}_{e,cont} = -\overleftarrow{\alpha} nFE \qquad (A33)$$

Algebraically, the activation energy at any potential E is:

$$\Delta G^{\neq}_{E=E} = \Delta G^{\neq}_{o,c} + \Delta G^{\neq}_{e,cont} \qquad (A34)$$



$$\Delta G^{\neq}_{E=E} = \Delta G^{\neq}_{o,c} + \Delta G^{\neq}_{e,cont}.$$

The solid lines represent the reaction path at E=0 on the scale in use.

FIG. A4: The effect of potential on the activation energy.

where $\Delta G^{\neq}_{o,c}$ is the chemical free energy of activation at E = 0 on the scale of use.

$\Delta G^{\neq}_{e,cont}$ is the potential dependent contribution to the free energy of activation.

The Arrhenius equation (A5) refers to the total free energy of activation. In a non-electrochemical reaction, this is equal to the chemical free energy of activation at E = 0 on the scale of use, ($\Delta G^{\neq}_{o,c}$). In an electrochemical system, the Arrhenius equation is modified as below (A35 and A36).

$$k_f = A \exp - \left[\frac{\Delta G^{\neq}_{o,c}}{RT} + \frac{\Delta G^{\neq}_{e,cont}}{RT}\right] \qquad (A35)$$

$$\ln k_f = \ln A - \left[\frac{\Delta G^{\neq}_{o,c}}{RT} - \frac{nFE\bar{\alpha}}{RT}\right] \qquad (A36)$$

Finally, a clarification of the different rate constants is called for. k_f and k_b are the heterogeneous rate constants at E = E of the reactions (A7 to A8). Equation (A35) can be rewritten, in potential dependent and non-dependent terms:

$$k_f = k^o_f \exp \frac{\Delta G^{\neq}_{e,cont}}{RT} \qquad (A37)$$

$$\text{where } k^o_f = A \exp - \frac{\Delta G^{\neq}_{o,c}}{RT} \qquad (A5)$$

and is called the heterogeneous rate constant at E = 0 on the scale in use.

There is of course an equivalent equation for k_b^o.

In the special case when $E = E^o$, (therefore $[O] = [R]$), then $k_f = k_b$ and in terms of equation (A37)

$$k_b^o \exp \frac{-FE\overleftarrow{\alpha}\eta}{RT} = k_f^o \exp \frac{-FE\vec{\alpha}\eta}{RT} = k^o \qquad (A38)$$

where k^o is the value of k_f and k_b at $E = E^o$ and is called standard or intrinsic rate constant.

A1.3 ELECTROLYTIC METHODS

The electrolytic experiments carried out in this project are summarised in Figure 7.

(1) Chronoamperometry

A constant potential is imposed on the system, the current versus time transient is recorded. When $t = t_o + dt$, the current is infinite. This is because the current that is passing is not faradaic (i.e. of the electrode reaction), but it is used to charge up the double layer, analogous to charging up a capacitor. Much information (including the double layer potential drop) can be obtained by using mercury wetted reed ultra fast switches and ultra fast response recorders. The timescale necessary to observe these phenomena is microseconds to milliseconds. This was not attempted in this project.

Chronoamperometry was used to determine at which point a steady state current was obtained. It was used in the electrokinetic order determinations and the steady state current-potential curves.

(2) Linear sweep voltammetry

A potential ramp is applied to the system, at a constant scan rate. The potential-current transient is recorded. Normally, the ramp is started from the pre-treatment value, so that double layer charging is less of a problem. This method can be used to actually observe individual electrode reactions occurring. As the potential is gradually increased, each of the processes in the anodic oxidation come to prominence in sequence, hence the number of intermediates in the reaction can be ascertained. Because the current is composed of faradaic and non-faradaic elements, the latter being a parabolic curve, any extra faradaic current (i.e. from the electrode reaction(s)) shows up as one or more peaks.

If a slow scan rate is used (e.g. 1 mV sec^{-1}) greater detail can be obtained, but less overall current flows, often resulting in problems with the signal to noise ratio. If a high scan rate is used (e.g. 1000 mV sec^{-1}) much less detail is obtained, but much greater current flows. The one advantage of higher scan rates is that under these conditions very fast reactions with short-lived intermediates can be differentiated.

The reason for the detail being dependent on scan rate is due to the contribution of the non-faradaic current to the overall (measured) current. When the scan rate is low, then the assumption that the potential is being scanned infinitely slowly is more nearly fulfilled. As the capacitance of the double layer changes with potential,[64] the current needed to charge it changes slowly. Therefore, the double layer (which has a time constant like any other capacitor) has more time to reach a high level of charging, i.e. get further down the φ - t curve in Figure 7(a). At high scan rates, this is not allowed to happen, therefore a much higher non-faradaic charging current flows.

In this project, 20 mV sec^{-1} was found to give good reproducible results and was chosen as the 'standard' scan rate. Where, for specific experiments, other scan rates were used, the results are suitably labelled.

(3) Cyclic voltammetry

Cyclic voltammetry is similar to linear sweep voltammetry, except that the scan is reversed at mid point. All that has been said about linear sweep voltammetry applies, with some additions.

In many cases the results of linear sweep voltammetry are disappointing because of the lack of detail. By reducing the oxidized products one can often more accurately determine the number of intermediates in the anodic reaction. By varying the anodic limit the anodic peaks can be correlated

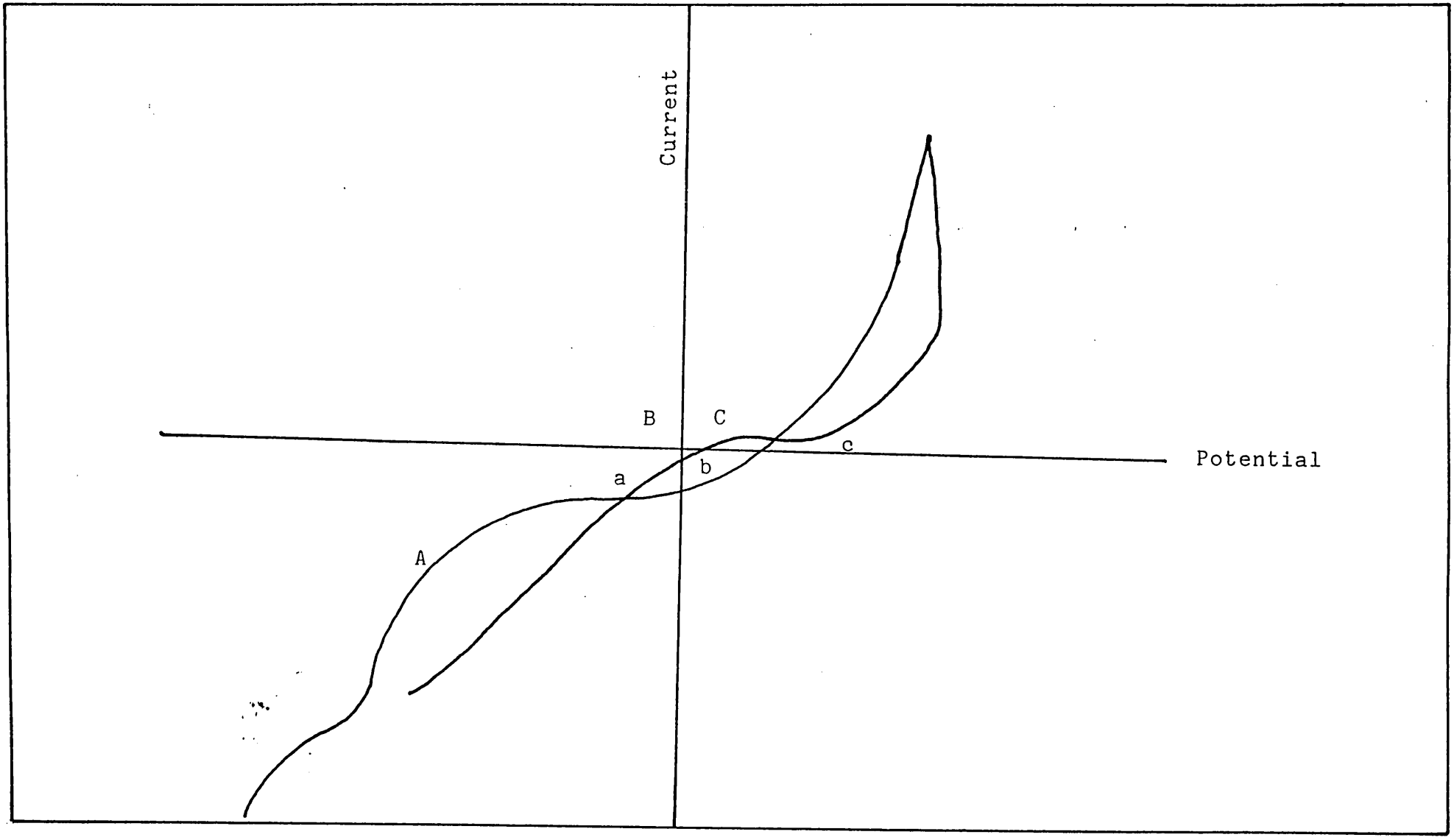


FIG. A5: A cyclic voltammogram displaying double layer polarity inversion.

with the cathodic peaks, aiding the interpretation and giving valuable information on the solubility of the products, and the reversibility of the reactions etc. By interrupting the cathodic scan at different points, for different periods of time further information on solubility of products and interproduct transformations can be gleaned.

A problem which is aggravated with cyclic voltammetry is the double layer charging problem that was discussed in the previous section. When the sweep range is wide, a situation where the polarity of the double layer may be reversed is sometimes encountered. In these cases, the apparent anodic current is more cathodic than the apparent cathodic current, as in Figure A5. In region A, an anodic reaction of some sort is proceeding (not $UO_2 \longrightarrow UO_2^{2+}$). At, or close to point a, the polarity of the double layer changes, therefore a large 'cathodic' charging current flows, reducing the anodic current. Once the double layer is charged, the anodic current increases again to anodic values (point b). Region B is the area of apparent current inversion. Area C represents the oxidation of UO_2. On the cathodic sweep the complimentary processes occur, in the same order. The point of double layer polarity inversion is not at point c. The potential range over which this occurs is explained in terms of the time the double layer takes to charge.

This problem was encountered in a few runs, but the region in which this phenomenon occurred was below that in which the cyclic voltammetry was carried out.

The effect of the double layer capacitance on the shape of the voltammograms is dealt with in the practical applications section.

(4) Cathodic stripping voltammetry

A constant (anodic) potential is imposed on the system for time = t seconds, followed by a constant rate cathodic ramp. The current-time transient is recorded for the whole experiment. The current-potential transient is recorded just prior to, and during the cathodic ramp. This method is extremely versatile and has a number of applications. The current-potential transient gives very clear cathodic stripping voltammograms analogous to the cathodic sweep in cyclic voltammetry. The reason for the improved clarity and detail is because the much greater amount of material generated in the chronoamperometric portion of this experiment increases the signal/noise ratio and also allows much greater discrimination of individual products. Cathodic stripping voltammetry is frequently used to amplify cyclic voltammograms.

The other major application of this type of experiment is a coulometric one. When the total anodic charge (passed by the system in the chronoamperometry section) and the total cathodic charge (calculated during the stripping section) are known, then film thickness and real dissolution charge can be calculated. By integration of the cathodic stripping voltammograms, film thickness can be estimated. Both the coulometric and the voltammetric experiments can be performed

simultaneously. In this project the total anodic and cathodic charge was calculated from the current versus time and cathodic stripping transients. The charges were obtained by cutting out the paper under the curves and weighing it.

There are two major sources of error in this method. The first is that when the chronoamperometric section is very short, (i.e. 0 to 20 seconds) the oxidation may continue for the first few seconds of the cathodic strip. This results in these figures being more subject to error. The second assumption is the cathodic limit on the stripping voltammograms (i.e. where the integration ceases) is an arbitrary point. However, provided the limit is the same in all cases, this should present no problems.

In this project this technique was used at five different potentials, with four to six different times at each. The times ranged from 10 to 4000 seconds, and the potentials ranged from 111 to 1011 mV (SHE). The scan (strip) rate in all cases was 20 mV sec^{-1}.

APPENDIX 2. THE COMPUTER PROGRAMS AND POTENTIAL MODELS

A2.1 The computer programs used to calculate the compositions of the kinetic runs.

A2.2 The computer programs used to process the uranium concentration data from the kinetic runs.

A2.3 The empirical equations and data bases used for the calculation of potential.

A2.1 THE COMPUTER PROGRAMS USED TO CALCULATE THE COMPOSITIONS OF THE KINETIC RUNS

In the low pH sulphate system, determinations of the concentrations of sulphate, bisulphate and hydrogen ions is made complex by the fact that the equilibrium constant (K_1) for the sulphate/bisulphate reaction (A2) are affected by ionic strength, temperature and pH. Before quantifying the way in which these variables affect the concentrations of various components, a set of equations are needed to express the concentrations of sulphate, bisulphate and hydrogen ions in terms of other variables.

$$H_2SO_4 \xrightarrow{K_{12}} HSO_4^- + H^+ \qquad (A1)$$

$$HSO_4 \xrightarrow{K_1} SO_4^{2-} + H^+ \qquad (A2)$$

All the reagents used in the kinetic runs must be included so that the derived expressions are valid over the whole range of experimental runs performed. Reagents used include:

sodium and potassium hydroxide
sodium and potassium sulphate
sodium nitrate and sodium perchlorate
sulphuric acid
peroxymonosulphuric acid
hydrogen peroxide.

The peroxymonosulphuric acid and hydrogen peroxide systems are dealt with separately, because whereas peroxymonosulphuric acid contributes to both the hydrogen ion concentration and the total ionic strength, hydrogen peroxide contributes to neither. Because it is inconvenient to design one computer program to analyse both systems correctly two variant programs were designed. One program was used to analyse the peroxymonosulphuric acid system (Nuna) and one to analyse the hydrogen peroxide system (Nina).

The Derivation of the Major Equations

The major starting equations were:

$$[TS] = [HSO_4^-] + [SO_4^=] \qquad (A3)$$

$$I_{TOT} = \tfrac{1}{2}(4[SO_4^{2-}] + [HSO_4^-] + [H^+] + [Na] + [K] + [NO_3] + [ClO_4] + [HSO_5]) \qquad (A4)$$

$$K_1 = \frac{[SO_4^{2-}][H^+]}{[HSO_4]} \qquad (A5)$$

where: I_{TOT} = total ionic strength

K_1 = the equilibrium constant for reaction (A2) (square brackets indicate concentrations)

[TS] = the concentration of total sulphate i.e. $[SO_4^{2-}] + [HSO_4^-]$

and:

[TSS]= the concentration of total sulphate not added as sulphuric acid

$[OH]_A$ = the theoretical concentration of hydroxide added assuming that none of the hydroxide has reacted with hydrogen ions.

Derivation of the equation for $[HSO_4^-]$.

$$[SO_4^=] = [TS] - [HSO_4^-] \qquad (A6)$$

Rearrangement of equation (A3) gives equation (A6). Substitution of equation (A6) into equation (A5), after rearrangement gives equation (A7).

$$[HSO_4^-] = \frac{[TS]}{(\frac{K_1}{[H^+]}) + 1} \qquad (A7)$$

A hydrogen ion balance for all the components in the system yields equation (A8), and rearrangement yields equation (A9).

$$[H^+] = 2[TS] + [HSO_5^-] - 2[TSS] - [HSO_4^-] - [OH^-]_A \qquad (A8)$$

$$[HSO_4^-] = 2[TS] + [HSO_5^-] - 2[TSS] - [H^+] - [OH^-]_A \qquad (A9)$$

Substitution by equation (A6) into equation (A4) for sulphate, and by equation (A8) into equation (A4) for hydrogen ion yields equation (A10).

$$I_{TOT} = \tfrac{1}{2}\,[4([TS] - [HSO_4^-]) + [HSO_4^-] + (2\,[TS] + [HSO_5^-] - 2\,[TSS]$$
$$\ldots\ldots\ldots - [HSO_4^-] - [OH^-]_A) \ldots\ldots\ldots$$
$$\ldots + [Na^+] + [K^+] + [NO_3^-] + [ClO_4^-] + [HSO_5^-]\,] \qquad \text{(A10)}$$

Rearrangement of equation (A10) gives equation (A11).

$$[HSO_4^-] = \frac{6[TS] + 2I_{TOT} + 2[HSO_5^-] - 2[TSS] - [OH^-]_A + [Na^+] + [K^+] + [NO_3^-]^+[ClO_4^-}{4} \qquad \text{(A11)}$$

There are now 4 independent equations for $[HSO_4^-]$, they are equations (A6), (A7), (A9), (A11).

The four equivalent equations for the hydrogen peroxide system are equations (A6), (A7), (A12), (A13).

$$[HSO_4^-] = 2\,[TS] - 2\,[TSS] - [OH^-]_A - [H^+] \qquad \text{(A12)}$$

$$[HSO_4^-] = \frac{6[TS] - 2I_{TOT} - 2[TSS] + [Na^+] - [OH^-]_A}{4} \qquad \text{(A13)}$$

None of the hydrogen peroxide runs contain potassium, nitrate or perchlorate, hence they are not included in the equations for the hydrogen peroxide system.

The program Nuna works by proposing a hydrogen ion concentration, initially, half the activity (from the pH measurements), and the assumption that $K_1^{\,o} = K_1$ is employed. $[HSO_4^-]$ and $[SO_4^=]$ are then calculated from equation (A7) at line 01160, and (A3) at line 01190.

Using these concentrations the total ionic strength is calculated by equation (A4) at line 01230. A second estimate of $[HSO_4^-]$ is then calculated by equation (A11) at line 01240, and the corresponding sulphate concentration is calculated from equation (A3) at line 01270. A third estimate of $[HSO_4^-]$ is calculated by equation (A9) at line 01280. The first and second estimates of $[HSO_4^-]$ are then compared at line 01400. If the two estimates of $[HSO_4^-]$ agree within certain limits, the second and third estimates of $[HSO_4^-]$ are also compared at line 01305. If either of these comparisons fails, the initial estimates of $[HSO_4^-]$ and $[SO_4^=]$ are replaced by the second estimates, and these data are put back into the program and used to calculate a new ionic strength at line 01230.

When both comparisons are successful, a new K_1 value is calculated in two stages using the total ionic strength and temperature data. The new K_1 value is then compared (within limits) to the old at line 01400. If the comparison is successful, all the data is printed out in various files, and the program goes to the next run. If this initial comparison fails, a second comparison is made (line 01410) with less stringent limits. If this second comparison fails, the hydrogen ion concentration is modified by adding a discrete amount to it, and the program is returned to line 01120 and the whole process is repeated, with the K_1 being replaced by K_1^o. If the second comparison is successful, the composition and ionic strength data is stored in an auxiliary file. The hydrogen

ion concentration is modified as above and the program returns to line 01120.

The potential is calculated at line 01795 using an empirical equation, the derivation of which appears later in this Appendix.

The inputted molar concentrations are corrected for temperature from lines 01020 to 01110. This is achieved by using an empirical equation derived from density data for sodium sulphate solutions, sulphuric acid solutions, and water at different temperatures.

The calculation of the K_1 value was carried out in two stages. The first was using the equation of Lindstrom and Wirth[27] for $NaHSO_4$ system. This calculates the K_1 value at T = 298K for a given ionic strength. This value was then corrected for temperature using an empirical equation which was derived from the data of Marshall and Jones.[28] It was found that the temperature variation of the data of Marshall and Jones[28] was constant to within 4% over an ionic strength range of 0.10 to 4.5.

The hydrogen peroxide version of this program (Nina) operates in an identical fashion using equations (A12) and (A13) instead of equations (A9) and (A11). Copies of both programs appear at the end of this Appendix.

A2.2 THE COMPUTER PROGRAM USED TO PROCESS THE KINETIC RATE DATA OF THE KINETIC RUNS.

The program used to analyse the raw kinetic data was called Sarah, and a copy of it appears at the end of this Appendix. The optical density measurements from the uranium analysis along with the sample time data were stored in and read from a file called Data (line 00100 and 00390). As the plot of the optical density versus uranium concentration always intercepted the origin, the slope of this graph was used to calculate the uranium concentrations directly (line 00400). The total amount of uranium leached is corrected for sample withdrawal at line 00420, after which various parameters are calculated. The results are outputted directly (line 00490) and into data files (00500).

A2.3 THE EMPIRICAL EQUATIONS AND DATA BASES USED FOR THE CALCULATION OF POTENTIAL.

For reasons discussed in Sections 2 and 3, it was not possible to measure corrosion potentials in kinetic leaching runs. It was therefore necessary to develop empirical equations (or models) to calculate the corrosion potentials under given conditions. The two variables considered relevant for the calculation of potential are temperature and the concentration of oxidising agent.

The corrosion potential of hydrogen peroxide and peroxymonosulphuric acid on UO_2 were calculated separately, but in a similar manner. The corrosion potentials of a small number of runs at different temperatures and concentrations of oxidising agent were measured. The conditions were chosen such that they encompassed the extremes of those conditions met in the main regression data base. These potentials and conditions were then used to construct an empirical model from which the potential of any run could be calculated.

For the hydrogen peroxide system, three variables were used for the empirical model. They were $\log_{10}$ concentration of hydrogen peroxide, the reciprocal of the concentration of hydrogen peroxide and temperature. The Minitab regression output from which the potential model for hydrogen peroxide was taken (MTX 2) appears at the end of this Appendix.

It can be seen from this output that 98.2% of the variance of the data is accounted for by the model. Comparisons of the measured and predicted potentials appear on the potential model output (MTX 2). A full list of the calculated potentials for all runs in the hydrogen peroxide regression analysis appears in the regression output (MTO 211) in Appendix 4.

For the peroxymonosulphuric acid system, two variables were used for the empirical model. They were $\log_{10}$concentration of peroxymonosulphuric acid, and the

temperature. The Minitab regression output from which the potential model for peroxymonosulphuric acid was taken (MTX 1) appears at the end of this Appendix.

It can be seen from this output that 99.9% of the variance of the data is accounted for by the model. Comparisons of the measured and predicted potentials appear on the potential model output (MTX 1). A full list of the calculated potentials for all runs in the peroxymonosulphuric acid regression analysis appears in the regression output (MT 113) in Appendix 4.

FIGURE A6. The computer programs used to calculate the compositions of the kinetic runs.

(a) Peroxymonosulphuric acid (NUNA)

```
00100  PROGRAM VARIOU(INPUT,OUTPUT,DATA,TAPE4=DATA,TAPE5=INPUT,
00110+ TAPE6=OUTPUT,TAPE7,TAPE8,TAPE9)
00120  DIMENSION IRUN(69),VEMP(69),VEP(69),VF(69),VG(69),VI(69),VH(69),
00130+ VM(69),VL(69),VK(69),VJ(69)
00140C FOR INFO SEE NINA          NUNA IS THE HS05 VERSION
00520C ****************INITIALIZATION SECTION*****************
00530  DO 40 J=1,69
00540  CA=0
00550  CB=0
00560  CE=0
00570  CF=0
00580  CG=0
00590  CH=0
00600  CI=0
00610  CJ=0
00620  CK=0
00630  CL=0
00640  CM=0
00650  ZA=0
00660  ZA1=0
00670  ZAL=0
00680  ZA1L=0
00690  RATI=0
00700  TOTI=0
00710  I=0
00720C I IS NO. TIMES ITERATED VIA 11 CONTINUE(998)..CONS. ITOT/COMPS
0073C  K=0
00740C K IS NO. TIMES ZA & ZA1 COMPARED(TOTAL)..FUN; NO IF STATE(999).
00750  M=0
00760C M IS THE [H] CONCENTRATION COUNTER.(997)
00761  XXX=0
00770  TEMP=0
00780  TEMPA=0
00790  TEMLA=0
00800  CEB=0
00810  CEP=0
00820  CEA=0
00830  CA1=0
00835  CA2=0
00840  CB1=0
00850  CE1=0
00860  COR1=0
00870  COR2=0
00875  ECR=0
00876  TEMP3=0
00980C ********************************************************
00910C*********************INPUT SECTION**************************************
00920  READ(4,*)IRUN(J),VEMP(J),VEP(J),VF(J),VG(J),VI(J),VH(J),VM(J),VL(J),
00930+ VK(J),VJ(J)
00950  ZA=0.01023
00955  TEMP3=VEMP(J)-30
00960  TEMPA=VEMP(J)+273.15
00970  TEMLA=ALOG10(TEMPA)
00980  CEP=-VEP(J)
00990  CE1=10**CEP
00995  CE=CE1*0.5
01000C ************************CALCULATION SECTION*********************
01010C ************TEMP. CORR. TO INITIAL CONCS**************************
01020  COR1=-1.5934+0.049152*VEMP(J)
01030  COR1=100-COR1
01040  CF=(VF(J)/100)*COR1
01050  CG=(VG(J)/100)*COR1
01060  CH=(VH(J)/100)*COR1
01070  CI=(VI(J)/100)*COR1
01080  CJ=(VJ(J)/100)*COR1
01090  CK=(VK(J)/100)*COR1
01100  CL=(VL(J)/100)*COR1
01110  CM=(VM(J)/100)*COR1
01120  40 CONTINUE
01130  M=M+1
01140  I=0
01150  RAT1=ZA/CE
01160  CA=CH/(RAT1+1)
01170  IF (CA.GT.CH) GOTO 1
01180  IF (CA.LT.0) GOTO 1
01190  CB=CH-CA
01200  10 CONTINUE
01204  IF (CA.GT.CH) GOTO 1
01206  IF (CA.LT.0) GOTO 1
01210  I=I+1
01220  IF (I.GT.50) GOTO 998
01230  TOTI=0.5*(CA+CE+CF+CI+CJ+CK+(4*CB))
01240  CA1=((6*CH)+CF+CG+CJ+(2*CI)+CK-(2*TOTI)-(2*CM)-CL)/4
01250  IF (CA1.GT.CH) GOTO 1
01260  IF (CA1.LT.0) GOTO 1


01270  CB1=CH-CA1
01280  CA2=((2*CH)-(2*CM)+CI-CL-CE)
01290  IF (ABS(CA1-CA).GT.0.001) GOTO 11
01305  IF (ABS(CA1-CA2).GT.0.01)  GOTO 11
01310  ZA=(CB1*CE)/CA1
01320  ZA1L=-1.991+(2.036*(SQRT(TOTI)))-(1.543*TOTI)+(0.8297*(TOTI**1.5))
01330  ZA1L=ZA1L-(0.1703*(TOTI*TOTI))
01340  ZA1=10**ZA1L
01350  K=K+1
01370  COR2=225.14-(6.379*VEMP(J))+(0.07335*(VEMP(J)*VEMP(J)))
01380  COR2=COR2-(0.0003169*(VEMP(J)*VEMP(J)*VEMP(J)))
01390  ZA1=(ZA1/100)*COR2
01400  IF (ABS(ZA1-ZA).LT.0.00010) GOTO 60
01410  IF (ABS(ZA1-ZA).LT.0.001) GOTO 92
01420  GOTO 1
01430  11 CONTINUE
01440  CA=CA1
01450  CB=CB1
01460  GOTO 10
01470  01 CONTINUE
01500  CE=CE+(CE1/1000)
01510  IF (M.GT.30000) GOTO 997
01520  ZA=0.01023
01530  I=0
01540  K=0
```

```
01270   CB1=CH-CA1
01280   CA2=((2*CH)-(2*CM)+CI-CL-CE)
01290   IF (ABS(CA1-CA).GT.0.001) GOTO 11
01305   IF (ABS(CA1-CA2).GT.0.01)  GOTO 11
01310   ZA=(CB1*CE)/CA1
01320   ZA1L=-1.991+(2.036*(SQRT(TOTI)))-(1.543*TOTI)+(0.8297*(TOTI**1.5))
01330   ZA1L=ZA1L-(0.1703*(TOTI*TO*I))
01340   ZA1=10**ZA1L
01350   K=K+1
01370   COR2=225.14-(6.379*VEMP(J))+(0.07335*(VEMP(J)*VEMP(J)))
01380   COR2=COR2-(0.0003169*(VEMP(J)*VEMP(J)*VEMP(J)))
01390   ZA1=(ZA1/100)*COR2
01400   IF (ABS(ZA1-ZA).LT.0.00010) GOTO 60
01410   IF (ABS(ZA1-ZA).LT.0.001) GOTO 92
01420   GOTO 1
01430   11 CONTINUE
01440   CA=CA1
01450   CB=CB1
01460   GOTO 10
01470   01 CONTINUE
01500   CE=CE+(CE/1000)
01510   IF (M.GT.50000) GOTO 997
01520   ZA=0.01028
01530   I=0
01540   K=0
01550   GOTO 50
01553   92 CONTINUE
01555   WRITE(9,103)IRUN(J),CA1,CA2,CB1,CE,TOTI,ZA1,ZA
01557   103 FORMAT(1X,I3,2X,7(F6.4,2X))
01559   GOTO 1
01680   997 CONTINUE
01690   XXX=997
01700   GOTO 30
01710   998 CONTINUE
01720   XXX=998
01730   GOTO 30
01740   999 CONTINUE
01750   XXX=999
01760   GOTO 30
01770   30 CONTINUE
01780   WRITE(8,*)IRUN(J)
01790   WRITE(8,*)'GOTO COUNTER(S) VIOLATED; DUMPED INFO'
01792   60 CONTINUE
01796   ECR=(593.330+(40.5390*(ALOG10(CI)))-(2.10586*TEMP3))
01798   WRITE(8,*)'RUN NO.    ',IRUN(J)
01800   WRITE(8,*)'THE TWO K(HA)S BEING ITERATED ARE:'
01810   WRITE(8,*)ZA,ZA1
01820   WRITE(8,*)'TRANSIENT CONCENTRATIONS OF IONS FOLLOW..'
01830   WRITE(8,*)'[HSO4]    =  ',CA1
01840   WRITE(8,*)'[SO4]     =  ',CB1
01850   WRITE(8,*)'[H] SET   =  ',CE
01855   WRITE(8,*)'[HSO4] COMP =  ',CA2
01860   WRITE(8,*)'TOTAL IONIC STRENGH =',TOTI
01870   WRITE(8,*)'[OTHER IONS] TEMP CORRECTED, FOLLOW...'
01875   WRITE(8,*)'[HSO5]     =  ',CI
01880   WRITE(8,*)'[NA]       =  ',CF
01890   WRITE(8,*)'[K]        =  ',CG
01900   WRITE(8,*)'[NO3]      =  ',CJ
01910   WRITE(8,*)'[CLO4]     =  ',CK
01920   WRITE(8,*)'[TS]       =  ',CH
01930   WRITE(8,*)'[TSS]      =  ',CM
01940   WRITE(8,*)'[OH]A      =  ',CL
01942   CEA=10**CEP
01943   CEA=CEA/CE
01945   WRITE(8,*)'PSEUDO [H] ACTIVITY COEFFICENT =',CEA
01947   WRITE(8,*)'POTENTIAL IMPOSED ON UO2 SURFACE =',ECR
01950   WRITE(8,*)'XXX  =',XXX
01960   WRITE(8,*)'M    =',M
01970   WRITE(8,*)'I    =',I
01980   WRITE(8,*)'K    =',K
02020   WRITE(7,102)IRUN(J),VEMP(J),VEP(J),CA,CB,CE,CI,CF,CG,CH,TOTI,CEA,ECR
02030   102 FORMAT(1X,I3,2X,F6.2,2X,F4.2,9(F6.4,2X),F6.2)
02035   WRITE(6,*)'RUNNING, AT RUN',IRUN(J)
02040   40 CONTINUE
02060   STOP
02070   END
```

```
UU    UU  MM    MM   CCCCCC   JJJJJJJJ   000000    333333   55555555
UU    UU  MMM  MMM  CCCCCCCC  JJJJJJJJ  00000000  33333333  55555555
UU    UU  MMMMMMMM  CC    CC      JJ    00    00        33  55
UU    UU  MM MM MM  CC            JJ    00    00        33  55
UU    UU  MM MM MM  CC            JJ    00    00      33    55
UU    UU  MM    MM  CC            JJ    00    00   3333     5555555
UU    UU  MM    MM  CC            JJ    00    00   3333      5555555
UU    UU  MM    MM  CC            JJ    00    00      33           55
UU    UU  MM    MM  CC            JJ    00    00        33         55
UU    UU  MM    MM  CC    CC      JJ    00    00        33         55
UUUUUUUU  MM    MM  CCCCCCCC  JJJJJJ    00000000  33333333  55555555
 UUUUUU   MM    MM   CCCCCC   JJJJJ      000000    333333    555555
```

FIGURE A6. The computer programs used to calculate the compositions of the kinetic runs.

(b) Hydrogen peroxide (NINA)

```
00100   PROGRAM UIHA(INPUT,OUTPUT,DATA,TAPE4=DATA,TAPE5=INPUT,
00110+  TAPE6=OUTPUT,TAPE7,TAPE8,TAPE9)
00120   DIMENSION IRUN(53),VEMP(53),VEP(53),VF(53),VI(53),VH(53),VM(53),
00130+  VL(53)
00140C  THIS PROGRAM IS DESIGNED TO CALCULATE THE ACTUAL CONCS,
00150C  OF THE VARIOUS COMPONENTS IN RUNS I AM DOING. IONS IT CAN TAKE ARE
00160C  SO4,HSO4,HSO5,NA,K,NO3,CLO4,H,([OH]A...ONLYFORCALCN.PURPOSES)
00170C  ..........THE GOAL OF THE PROGRAM IS ACHIEVED THROUGH
00180C  AN ITERATIVE PROCEEDURE AS FOLLOWS. THE ONLY IONS THAT CHANGE IN THE
00190C  RANGE BEING EXAMINED ARE SO4,HSO4,H..EMPIRICAL.EQUNS.FOR.BOTH...
00200C  TEMPERATURE AND IONIC STRENGH EFFECTS ON K(HA) ARE KNOWN.
00210C  NORMALLY.AN.ITERATIVE.LOOP.INVOLVING.BOTH.OF.THESE.EQUATIONS
00220C  WOULD.BE.USED...BUT.IN.THIS.CASE.[H] IS.UNKNOWN.........
00230C  THIS.IS.WHAT.IS.DONE.....A.SET.OF.EQUNS.TO.CALC.COMPOSITIONS..
00240C  HAVE BEEN DERIVED, THE ONLY UNKNOWN IS ITOT....WITH JUST THIS INFO
C0250C  THE COMPOSITION AT ANY ITOT CAN BE CALCULATED.....
00260C  INITIALLY KHA (THERMODYNAMIC) IS USED WITH THE PH FOR THE 'ACTIVITY'
00270C  USING THE KHA & TS RELATIONS ITOT IS CACULATED.....
00280C  THIS.... ITOT IS THEN USED TO CALCULATE COMPOSITIONS..(MY EQUNS.)..
00290C  THE COMPOSITIONS ARE NOW USED TO CALCULATE A NEW ITOT....
00300C  USING LINDSTROM'S EQUNS. A NEW KHA IS CALC. FROM ITOT...
00310C  IF NEW KHA .NE. OLD KHA COMPS. ARE CALCULATED FROM NEW ITOT...
00320C    ...ITERATION IS PERFORMED UNTIL THEY ARE EQUAL.......
00330C  NOW THESE SELF CONSISTENT VALUES OF KHA + ITOTS + COMPS ARE...
00340C  PUT INTO THE KHA EQU...IF THE KHA GIVEN BY THE COMPS IS THE ..
00350C  SAME AS THE SELF CONSISTENT KHA...WOOPEE!!!..PRINTS OUT..
00360C  IF NOT THEN KHA FORMULA & TS  ETC CALCULATES NEW COMPOSITIONS..
00370C  AND PUTS THESE BACK IN AT THE TOP.....
00380C  THIS PROGRAM IS SAME AS KAREN,LOISA, EXCEPT THAT THERE IS A SECOND
00390C  LOOP & THE NEW COMP. EQUATIONS...ALSO [I]S ARE TEMP. CORRECTED..
00400C.FOR.FURTHER.INFO.SEE.ABOVE.PROGS.....**************************
00410C     ************************************
00420C  SUBSCRIPTED VARIABLES:SAME KEY EXCEPT V NOT C PREFIX,
00430C  CA=[HSO4],CB=[SO4],CI=[H2O2],CF=[NA],CG=[K],CH=[TS],CE=[H]......
00440C  CK=[CLO4], CL=[OH] HYPOTHETICAL,  =[NO3], CM=[TSS]
00450C  TEMP=TEMPERATURE(DEG.C),TEMPA=TEMPERATURE(DEG.A),TEMLA=LOG10 TEMPA.
00460C  ZA1=TEMP. CORR.  ,ITOT,CORRECTED.K(HA),ZA=INIT. .ITERATED.K(HA),
00470C  ZA1L=LOG10 ZA1,ZA2=K(HA) IN 2ND. TEST LOOP,
00480C  ZAL=LOG10 ZA,RAT1=K(HA)/CE,CEA=A[H], TOTI=TOTAL IONIC STRENGH,
00490C  I,J,K=COUNTERS,IRUN = RUN NO,RAT2=RAT1 IN 2ND TEST LOOP,
00500C  COR1=TEMP.CORR.FOR CONCS., COR2=TEMP.CORR.FOR K(HA)
00520C  *****************INITIALIZATION SECTION******************
00530   DO 40 J=1,53
00540   CA=0
00550   CB=0
00560   CE=0
00570   CF=0
00590   CH=0
00600   CI=0
00630   CL=0
00640   CM=0
00650   ZA=0
00660   ZA1=0
00670   ZAL=0
00680   ZA1L=0
00690   RAT1=0
00700   TOTI=0
00710   I=0
00720C  I IS NO. TIMES ITEPATED VIA 11 CONTINUE(998)..CONS. ITOT/COMPS
00730   K=0
00740C  K IS NO. TIMES ZA & ZA1 COMPARED(TOTAL)..FUN; NO IF STATE(999).
00750C  M=0
00760C  M IS THE [H] CONCENTRATION COUNTER.(997)
00761   XXX=0
00770   TEMP=0
00780   TEMPA=0
00790   TEMLA=0
00800   CEB=0
00810   CEP=0
00820   CEA=0
00830   CA1=0
00835   CA2=0
00840   CB1=0
00850   CE1=0
00860   COR1=0
00870   COR2=0
00875   ECR=0
00877   TEMP3=0
00880C  ********************************************************
00910C  *********************INPUT SECTION**************************************
00920   READ(4,*)IRUN(J),VEMP(J),VEP(J),VF(J),VI(J),VH(J),VM(J),VL(J)
00950   ZA=0.01028
00955   TEMP3=VEMP(J)-30
00960   TEMPA=VEMP(J)+273.15
00970   TEMLA=ALOG10(TEMPA)


00980   CEP=-VEP(J)
00990   CE1=10**CEP
00995   CE=CE1*0.5
01000C  ************************CALCULATION SECTION**********************
01010C  ************TEMP. CORR. TO INITIAL CONCS**************************
01020   COR1=-1.5934+0.049152*VEMP(J)
01030   COR1=100-COR1
01040   CF=(VF(J)/100)*COR1
01060   CH=(VH(J)/100)*COR1
01070   CI=(VI(J)/100)*COR1
01100   CL=(VL(J)/100)*COR1
01110   CM=(VM(J)/100)*COR1
01120   50 CONTINUE
01130   M=M+1
01140   I=0
01150   RAT1=ZA/CE
01160   CA=CH/(RAT1+1)
01170   IF (CA.GT.CH) GOTO 1
01180   IF (CA.LT.0) GOTO 1
01190   CB=CH-CA
01200   10 CONTINUE
01210   I=I+1
01220   IF (I.GT.50) GOTO 999
01230   TOTI=0.5*(CA+CE+CF+(4*CB))
```

```
00920   READ(9,*)IRUN(J),TEMP(J),VEP(J),VF(J),VI(J),VH(J),VH(J),VL(J)
00950   ZA=0.01028
00955   TEMP3=VEMP(J)-30
00960   TEMPA=VEMP(J)+273.15
00970   TEMLA=ALOG10(TEMPA)


00980   CEP=-VEP(J)
00990   CE1=10**CEP
00995   CE=CE1*0.5
01000C  ************************CALCULATION SECTION**********************
01010C  ************TEMP. CORR. TO INITIAL CONCS**************************
01020   COR1=-1.5934+0.049152*VEMP(J)
01030   COR1=100-COR1
01040   CF=(VF(J)/100)*COR1
01060   CH=(VH(J)/100)*COR1
01070   CI=(VI(J)/100)*COR1
01100   CL=(VL(J)/100)*COR1
01110   CM=(VM(J)/100)*COR1
01120   50 CONTINUE
01130   M=M+1
01140   I=0
01150   RAT1=ZA/CE
01160   CA=CH/(RAT1+1)
01170   IF (CA.GT.CH) GOTO 1
01180   IF (CA.LT.0) GOTO 1
01190   CB=CH-CA
01200   10 CONTINUE
01210   I=I+1
01220   IF (I.GT.50) GOTO 999
01230   TOTI=0.5*(CA+CE+CF+(4*CB))
01240   CA1=((6*CM)+CF-(TOTI*2)-(2*CM)-CL)/4
01250   IF (CA1.GT.CH) GOTO 1
01260   IF (CA1.LT.0) GOTO 1
01270   CB1=CH-CA1
01280   CA2=((2*CM)-(2*CM)-CL-CE)
01290   IF (ABS(CA1-CA).GT.0.001) GOTO 11
01305   IF (ABS(CA1-CA2).GT.0.01)  GOTO 11
01310   ZA=(CB1*CE)/CA1
01320   ZA1L=-1.991+(2.036*(SQRT(TOTI)))-(1.543*TOTI)+(0.8297*(TOTI**1.5))
01330   ZA1L=ZA1L-(0.1703*(TOTI*TOTI))
01340   ZA1=10**ZA1L
01350   K=K+1
01370   COR2=225.14-(6.379*VEMP(J))+(0.07335*(VEMP(J)*VEMP(J)))
01380   COR2=COR2-(0.0003169*(VEMP(J)*VEMP(J)*VEMP(J)))
01390   ZA1=(ZA1/100)*COR2
01400   IF (ABS(ZA1-ZA).LT.0.00010) GOTO 60
01410   IF (ABS(ZA1-ZA).LT.0.001) GOTO 92
01420   GOTO 1
01430   11 CONTINUE
01440   CA=CA1
01450   CB=CB1
01460   GOTO 10
01470   01 CONTINUE
01500   CE=CE+(CE1/1000)
01510   IF (M.GT.100000) GOTO 997
01520   ZA=0.01028
01530   I=0
01540   K=0
01550   GOTO 50
01553   92 CONTINUE
01555   WRITE(9,103)IRUN(J),CA1,CA2,CB1,CE,TOTI,ZA1,ZA
01557   103 FORMAT(1X,I3,2X,7(F6.4,2X))
01559   GOTO 1
01680   997 CONTINUE
01690   XXX=997
01700   GOTO 30
01710   998 CONTINUE
01720   XXX=998
01730   GOTO 30
01740   999 CONTINUE
01750   XXX=999
01760   GOTO 30
01770   30 CONTINUE
01780   WRITE(8,*)IRUN(J)
01790   WRITE(8,*)'GOTO COUNTER(S) VIOLATED; DUMPED INFO'
01793   60 CONTINUE
01795   ECR=(672.14-(1.9629*TEMP3)+(46.521*(ALOG10(CI)))+(0.017532*(1/CI)))
01796   WRITE(8,*)'RUN NO.     ',IRUN(J)
01800   WRITE(8,*)'THE TWO K(HA)S BEING ITERATED ARE:'
01810   WRITE(8,*)ZA,ZA1
01820   WRITE(8,*)'TRANSIENT CONCENTRATIONS OF IONS FOLLOW..'
01830   WRITE(8,*)'[HSO4]    =  ',CA1
01840   WRITE(8,*)'[SO4]     =  ',CB1
01850   WRITE(8,*)'[H] SET   =  ',CE
01855   WRITE(8,*)'[HSO4] COMP =  ',CA2
01860   WRITE(8,*)'TOTAL IONIC STRENGH =',TOTI
01870   WRITE(8,*)'[OTHER IONS] TEMP CORRECTED, FOLLOW...'
01875   WRITE(8,*)'[H2O2]      =  ',CI
01880   WRITE(8,*)'[NA]        =  ',CF
01920   WRITE(8,*)'[IS]        =  ',CH
01930   WRITE(8,*)'[TSS]       =  ',CM


01940   WRITE(8,*)'[OHIA     =  ',CL
01942   CEA=10**CEP
01943   CEA=CEA/CE
01945   WRITE(8,*)'PSEUDO [H] ACTIVITY COEFFICENT =',CEA
01947   WRITE(8,*)'POTENTIAL IMPOSED ON UO2 SURFACE =',ECR
01950   WRITE(8,*)'XXX  =',XXX
01960   WRITE(8,*)'M    =',M
01970   WRITE(8,*)'I    =',I
01980   WRITE(8,*)'K    =',K
02020   WRITE(7,102)IRUN(J),VEMP(J),VEP(J),CA,CB,CE,CI,CF,CH,TOTI,CEA,ECR
02030   102 FORMAT(1X,I3,2X,F6.2,2X,F4.2,2X,8(F6.4,2X),F6.2)
02035   WRITE(6,*)'RUNNING AT EX  ',IRUN(J)
02040   40 CONTINUE
02060   STOP
02070   END
```

FIGURE A7. The computer program used to process the uranium concentration data from the kinetic runs (SARAH).

```
00100    PROGRAM SARAH(INPUT,OUTPUT,DATA,TAPE4=DATA,TAPE5=INPUT,
00110+ TAPE6=OUTPUT,TAPE7)
00120   DIMENSION T(15),OD(15)
00130   UTN=0
00140   UTOT=0
00150   UM=0
00160   UMM=0
00170   UIM=0
00180   UPTM=0
00190   A=0
00200   B=0
00210   C=0
00220   D=0
00230   UI=0
00240   L=0
00250   VOL=0
00260   J=0
00270   WRITE(6,*)'RUN NUMBER'
00280   READ(5,*)L
00290   WRITE(6,*)'INITIAL MASS OF URANIUM'
00300   READ(5,*)UM
00310   WRITE(6,*)'CALIBRATION CURVE'
00320   READ(5,*)C
00330   UMM=UM/270.03
00340   WRITE(6,*)'INITIAL LIQUID VOLUME'
00350   READ(5,*)VOL
00360   WRITE(6,*)'NO SPLES'
00370   READ(5,*)J
00380   DO 10 K=1,J
00390   READ(4,*)T(K),OD(K)
00400   UI=OD(K)*C
00410   UIM=UI/270.03
00420   UPTM=UIM*(VOL-(K*2-2))
00430   UTOT=UPTM+UTN
00440   UTN=UTN+(2*UIM)
00460   A=(UTOT/UMM)*0.000001
00470   B=(1-(1-A)**0.333333)
00480   D=1-(273*A)-((1-A)**0.666666)
00490   WRITE(6,103)T(K),A,B,D
00500   WRITE(7,103)T(K),A,B,D
00505   103 FORMAT(1X,F4.1,2X,3(F10.9,2X))
00510   10 CONTINUE
00520   WRITE(6,*)'T (MINS)  A  SCM   SCM+RLL '
00530   WRITE(6,*)'RUN NUMBER ',L
00540   WRITE(6,*)'PROGRAMME ENDS'
00550   STOP
00560   END
```

```
          UU    UU  MM    MM   CCCCCC   JJJJJJJJ   000000    333333   55555555
          UU    UU  MMM  MMM  CCCCCCCC  JJJJJJJJ  00000000  33333333  55555555
          UU    UU  MMMMMMMM  CC    CC      JJ    00    00        33  55
          UU    UU  MM MM MM  CC            JJ    00    00        33  55
          UU    UU  MM MM MM  CC            JJ    00    00      33    55
          UU    UU  MM    MM  CC            JJ    00    00   3333     5555555
          UU    UU  MM    MM  CC            JJ    00    00   3333          55
          UU    UU  MM    MM  CC            JJ    00    00      33         55
          UU    UU  MM    MM  CC            JJ    00    00      33         55
          UU    UU  MM    MM  CC    CC      JJ    00    00      33         55
          UUUUUUUU  MM    MM   CCCCCCCC  JJJJJJ   00000000  33333333  55555555
           UUUUUU   MM    MM    CCCCCC   JJJJJ     000000   333333    555555
```

```
13.05.33.QUEUE(SARAH=PS)
13.05.33. QUEUED PRINT FILE -SARAH
```

FIGURE A8. The Minitab regression output from which the hydrogen peroxide potential model was taken (MTX 2)

```
-- OUTPUTWIDTH 100

-- NORRIEF

-- READ'TAPE7' C1-C4
COLUMN          C1          C2          C3          C4
COUNT           11          11          11          11
ROW
  1            201.     .003087      570.100       30.
  2            202.     .000085      581.000       30.
  3            203.     .056796      612.600       30.
  4            204.     .120620      617.900       30.
  .   .   .

-- LOGT C2 C12

-- DIVI 1 C2 C6

-- NAME C1 'RUN'

-- NAME C2 'CON1'

-- NAME C12 'LCON'

-- NAME C5 'CON2'

-- NAME C6 '1/CN'

-- NAME C15 'LCN2'

-- NAME C3 'POT'

-- NAME C4 'TEMP'

-- NAME C20 'T-30'

-- SUBTR 30 C4 C20

-- MULTI C2 C2 C5

-- LOGT C5 C15

-- REGR C3 3 C12,C6,C20,C40,C41

THE REGRESSION EQUATION IS
Y =    672. +  46.5 X1 + .0175 X2
     -  1.97 X3

                                                ST. DEV.     T-RATIO =
        COLUMN      COEFFICIENT                 OF COEF.     COEF/S.D.
                        672.144                   5.358        125.44
X1      LCON             46.521                   3.686         12.62
X2      1/CN          0.017532                 0.007796          2.25
X3      T-30           -1.9692                   0.1105        -17.82

THE ST. DEV. OF Y ABOUT REGRESSION LINE IS
S =  6.232
WITH (  11- 4) =    7 DEGREES OF FREEDOM

R-SQUARED = 98.2 PERCENT
R-SQUARED = 97.5 PERCENT, ADJUSTED FOR D.F.

ANALYSIS OF VARIANCE

 DUE TO      DF            SS          MS=SS/DF
REGRESSION    3      15017.36           5005.79
RESIDUAL      7        271.83             38.83
TOTAL        10      15289.19

1
FURTHER ANALYSIS OF VARIANCE
SS EXPLAINED BY EACH VARIABLE WHEN ENTERED IN THE ORDER GIVEN

 DUE TO      DF            SS
REGRESSION    3      15017.36
LCON          1       2692.55
1/CN          1         12.59
T-30          1      12325.22

            X1           Y     PRED. Y    ST.DEV.


ROW        LCON         POT        VALUE     PRED. Y    RESIDUAL      ST.RES.
  1       -2.40      570.10       564.92        3.59        5.18         1.02
  2       -2.09      581.00       576.98        3.37        4.02         0.77
  3       -1.25      612.60       614.50        2.63       -1.90        -0.34
  4       -0.92      617.90       629.56        2.95      -11.66        -2.12R
  5       -0.22      670.60       661.90        4.68        8.70         2.11R
  6       -1.92      581.10       584.40        3.15       -3.30        -0.61
  7       -3.13      549.10       550.15        6.20       -1.05        -1.62 X
  8       -0.52      590.00       589.10        2.70        0.90         0.16
  9       -0.59      585.00       585.09        2.59       -0.89        -0.16
 10       -0.99      527.70       527.73        4.10       -0.03        -0.01
 11       -0.52      549.40       549.37        3.81        0.03         0.01

R DENOTES AN OBS. WITH A LARGE ST. RES.
X DENOTES AN OBS. WHOSE X VALUE GIVES IT LARGE INFLUENCE.

DURBIN-WATSON STATISTIC = 2.59

(X-PRIME X)INVERSE

              0           1           2           3
   0     .739399
   1     .441171     .349821
   2     .000513     .000548    -.000002
   3    -.010403    -.004852    -.000004     .000315

-- NSCORES C40,C42
```

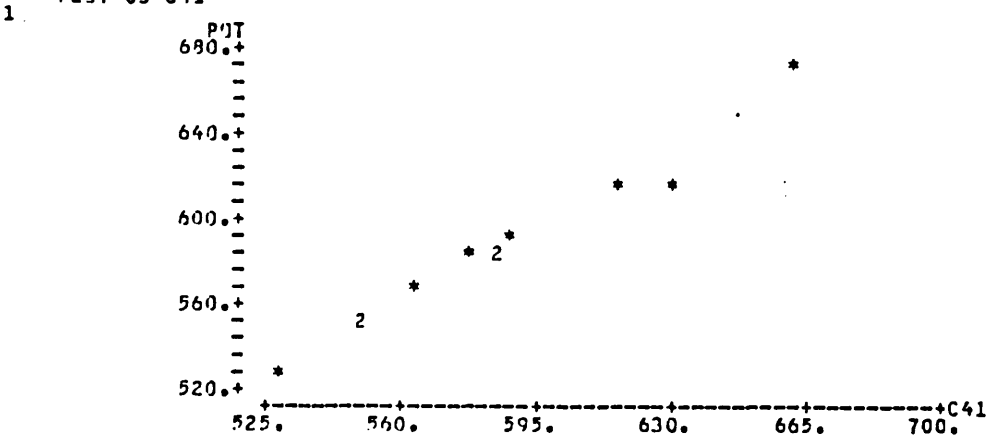
```
-- NSCORES C40,C42

-- WRITE C1,C3,C41

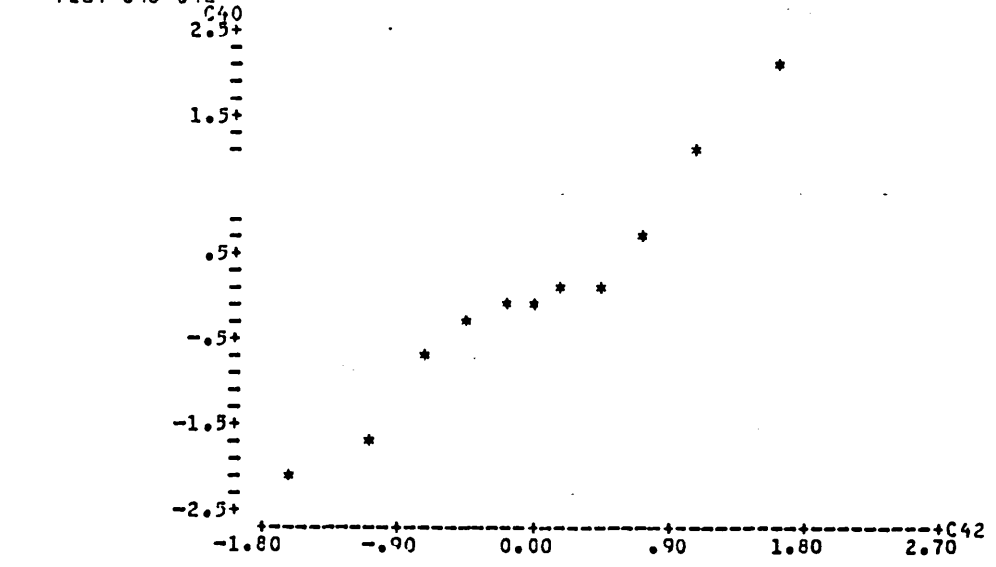
THIS FILE WAS WRITTEN USING THE FORMAT
(F5.0,F8.3,F8.3)

  201.  570.100  564.921
  202.  581.000  576.976
  203.  612.600  614.502
  204.  617.900  629.556
  205.  670.600  661.897
  206.  581.100  584.399
  200.  549.100  550.153
  300.  590.000  599.100
  301.  585.000  585.887
  302.  527.700  527.733
  303.  549.400  549.375

-- PLOT C3 C41
1
```




```
-- PLOT C40 C42
```




```
--  STOP

*** MINITAB *** STATISTICS DEPT * PENN STATE UNIV. * RELEASE 81.1 *
STORAGE AVAILABLE    5000
```

FIGURE A9. The Minitab regression output from which the peroxymonosulphuric acid potential model was taken (MTX 1).

```
-- OUTPUTWIDTH 100

-- NOBRIEF

-- READ'TAPE7' C1-C4
COLUMN          C1          C2          C3          C4
COUNT           11          11          11          11
ROW
  1            207.     .001775     484.000         30.
  2            208.     .005342     500.100         30.
  3            209.     .010523     511.700         30.
  4            210.     .052580     540.700         30.
  .   .   .

-- LOGT C2 C12

-- MULTI C2 C2 C5

-- LOGT C5 C15

-- DIVI 1 C2 C6

-- NAME C1 'RUN'

-- NAME C2 'CON1'

-- NAME C3 'POT'

-- NAME C4 'TEMP'

-- NAME C5 'CON2'

-- NAME C6 '1/CN'

-- NAME C12 'LCON'

-- NAME C20 'T-30'

-- SUBT 30 C4 C20

-- REGRESS C3 2 C12,C20,C40,C41

THE REGRESSION EQUATION IS
Y =     593. +  40.5 X1 -  2.11 X2

                                          ST. DEV.     T-RATIO =
        COLUMN      COEFFICIENT           OF COEF.     COEF/S.D.
                                            593.330        0.828        716.66
X1      LCON                               40.5390       0.4687         86.49
X2      T-30                              -2.10586      0.02101       -100.25

THE ST. DEV. OF Y ABOUT REGRESSION LINE IS
S =  1.102
WITH (  11- 3) =    8 DEGREES OF FREEDOM

R-SQUARED = 99.9 PERCENT
R-SQUARED = 99.9 PERCENT, ADJUSTED FOR D.F.

ANALYSIS OF VARIANCE

 DUE TO      DF             SS          MS=SS/DF
REGRESSION    2       14356.33           7178.17
RESIDUAL      8           9.72              1.22
TOTAL        10       14366.06

FURTHER ANALYSIS OF VARIANCE
SS EXPLAINED BY EACH VARIABLE WHEN ENTERED IN THE ORDER GIVEN

 DUE TO      DF             SS
REGRESSION    2       14356.33
LCON          1        2143.51
T-30          1       12213.83

              X1           Y        PRED. Y     ST.DEV.
ROW         LCON         POT         VALUE     PRED. Y     RESIDUAL      ST.RES.
  1        -2.75     484.000       481.816       0.729        2.184        2.64R
  2        -2.27     500.100       501.214       0.565       -1.114       -1.18
  3        -1.98     511.700       513.150       0.489       -1.450       -1.47
  4        -1.28     540.700       541.474       0.448       -0.774       -0.77
  5        -1.01     552.600       552.445       0.493        0.155        0.16


  6        -0.21     585.900       584.909       0.747        0.991        1.22
  7        -0.03     529.000       528.981       0.567        0.019        0.02
  8        -0.68     481.600       481.620       0.558       -0.020       -0.02
  9        -1.03     446.200       446.183       0.774        0.017        0.02
 10        -0.98     511.400       511.365       0.344        0.035        0.03
 11        -0.50     509.900       509.945       0.452       -0.045       -0.04

R DENOTES AN OBS. WITH A LARGE ST. RES.

DURBIN-WATSON STATISTIC = 1.44

(X-PRIME X)INVERSE

              0           1           2
  0     .563900
  1     .271500     .180753
  2    -.010295    -.004051     .000363

-- WRITE  C41,C3,C1

THIS FILE WAS WRITTEN USING THE FORMAT
(F8. 3,F8. 3,F5. 0)

401.816 484.000 207.
501.214 500.100 208.
513.150 511.700 209.
541.474 540.700 210.
```

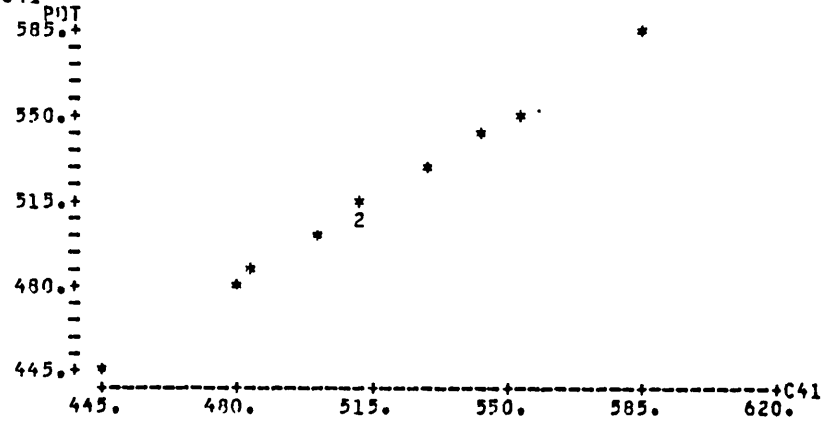
```
-- WRITE  C41,C3,C1

THIS FILE WAS WRITTEN USING THE FORMAT
(F8. 3,F8. 3,F5. 0)

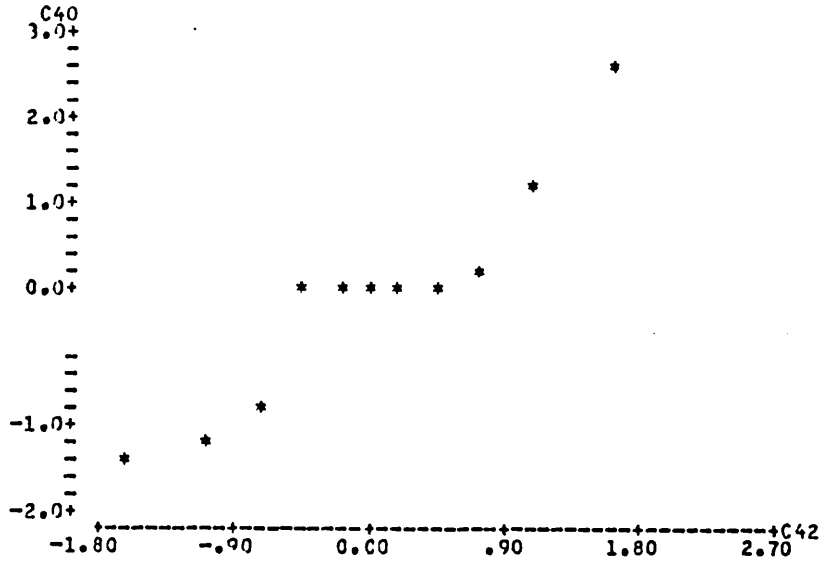
481.816 484.000 207.
501.214 500.100 208.
513.150 511.700 209.
541.474 540.700 210.
552.445 552.600 211.
584.909 585.900 212.
528.981 529.000 304.
481.620 481.600 305.
446.193 446.200 306.
511.365 511.400 307.
509.945 509.900 308.

-- NSCORES C40,G42

-- PLOT C3 C41
```




```
-- PLOT C40 C42
1
```




```
-- NOTES  ************ H2S05 ************

--  STOP

*** MINITAB *** STATISTICS DEPT * PENN STATE UNIV. * RELEASE 81.1 *
STORAGE AVAILABLE     5000
```

APPENDIX 3. THE COMPOSITION DATA AND KINETIC RESULTS

A3.1 The Peroxymonosulphuric acid system.

A3.2 The Hydrogen Peroxide System.

A3.1 THE PEROXYMONOSULPHURIC ACID SYSTEM

The kinetic data and raw composition data (uncorrected for temperature) appear in Table A1. All runs for which a unique rate line could be delineated appear in Table A1. The abbreviations used in Table A1 are defined below.

RUN	Run number
TEMP	Temperature in ^{o}C of run.
pH	pH of run
[NA]	concentration of sodium (molar)
[K]	concentration of potassium (molar)
$[HSO_5]$	concentration of peroxymonobisulphate (molar)
[TS]	total concentration of sulphate and bisulphate (molar)
[TSS]	total concentration of sulphate and bisulphate that was added in the form of a salt, as opposed to an acid (molar).
$[OH]_A$	The concentration of hydrogen ion consumed by added hydroxide (molar)
$[ClO_4]$	concentration of perchlorate (molar)
$[NO_3]$	concentration of nitrate (molar)
UO_2	The amount of uranium dioxide initially added to the reaction vessel (g).
RATE	$\frac{df(\alpha)}{dt}$ (min^{-1})
R(α)	The maximum value of α for which the plot of (α) versus time (t) is a straight line.
R(T)	The maximum value of t (mins), for which the plot of (α) versus t is a straight line.

Table A2 contains the composition data for all the peroxymonosulphuric acid runs from Table A1 which were amenable to composition analysis, and were used in the multilinear regression analysis. The abbreviations used in Table A2 are similar to those used in Table A1 with the following additions:

$[HSO_4]$ concentration of bisulphate (molar)

$[SO_4]$ concentration of sulphate (molar)

TOTI total ionic strength (molar)

$[H^+]$ hydrogen ion concentration (molar)

H The estimated activity coefficient for hydrogen ions (γ_{H^+})

$$\gamma_{H^+} = a_{H^+} / [H^+]$$

where a_{H^+} = the estimated activity of hydrogen ions (from the pH measurement)

$[H^+]$ = the estimated concentration of hydrogen ions (from composition analysis)

ECR The calculated corrosion potential (from the potential models).

All values in this Table are corrected for temperature (T=T).

TABLE A1. The kinetic and initial composition data for all peroxymonosulphuric acid runs.

RUN	TEMP	PH	[NA]	[K]	$[HSO_5]$	[TS]	[TSS]	$[OH]_A$	$[ClO_4]$	$[NO_3]$	UO_2	RATE	R(T)	R(T)
212	30.00	1.48	2.3146	0.0000	.4455	1.0785	.1008	2.1400	0.0000	0.0000	1.1547	.000073	.40	60
211	30.00	1.49	2.0542	0.0000	.0980	1.1022	.8070	.2901	0.0000	0.0000	.6753	.000011	.70	60
210	30.00	1.49	1.7898	0.0000	.0526	.9980	.8701	.0495	0.0000	0.0000	1.2256	.000004	.03	60
209	30.00	1.50	1.8506	0.0000	.0105	1.0427	.9253	0.0000	0.0000	0.0000	1.8449	.000001	.01	60
208	30.00	1.49	1.7126	0.0000	.0053	.9769	.8563	0.0000	0.0000	0.0000	3.9262	.000000	.02	60
207	30.00	1.49	1.7994	0.0000	.0018	1.0226	.8992	0.0000	0.0000	0.0000	6.6016	.000000	.00	60
160	60.00	2.49	0.0000	.8286	.5619	.1500	.0844	.0979	0.0000	0.0000	.4959	.000931	3.00	30
159	60.00	2.47	0.0000	.4821	.3404	.1000	.0512	.0393	0.0000	0.0000	.5877	.000980	4.00	45
158	61.00	1.49	0.0000	.7442	.5722	.1035	.0860	0.0000	0.0000	0.0000	.5189	.001250	6.00	45
157	60.00	1.46	0.0000	.3568	.2671	.0844	.0401	.0114	0.0000	0.0000	.5877	.000717	3.00	60
138	60.00	1.49	2.7490	0.0000	.9355	1.1252	0.0000	2.7490	0.0000	0.0000	.5024	.000951	7.50	100
137	32.00	1.49	.3871	0.0000	.1493	.1677	0.0000	.3871	0.0000	0.0000	.4679	.000085	4.00	600
136	30.00	2.50	.4350	0.0000	.1472	.1702	0.0000	.4350	0.0000	0.0000	.4499	.000155	7.50	500
135	30.00	2.52	.4669	0.0000	.1493	.1666	0.0000	.4669	0.0000	0.0000	.4767	.000188	9.00	500
134	40.00	2.49	.4437	0.0000	.1496	.1669	0.0000	.4437	0.0000	0.0000	.4492	.000244	6.00	300
133	80.00	2.50	.4393	0.0000	.1487	.1671	0.0000	.4393	0.0000	0.0000	.4524	.001510	10.00	60
132	70.00	2.50	.4437	0.0000	.1495	.1671	0.0000	.4437	0.0000	0.0000	.5394	.001100	10.00	100
131	60.00	2.48	.4437	0.0000	.1484	.1666	0.0000	.4437	0.0000	0.0000	.4918	.000587	7.00	100
130	30.00	1.50	.3902	0.0000	.1495	.1679	0.0000	.3902	0.0000	0.0000	.5130	.000048	10.00	2000
129	40.00	1.48	.3741	0.0000	.1470	.1824	0.0000	.3741	0.0000	0.0000	.4611	.000091	3.00	300
128	50.00	2.48	.4281	0.0000	.1476	.1658	0.0000	.4281	0.0000	0.0000	.5004	.000209	4.00	150
127	45.00	1.48	.3654	0.0000	.1347	.1918	0.0000	.3654	0.0000	0.0000	.5642	.000090	1.00	100
126	30.00	1.46	.3784	0.0000	.1369	.1923	0.0000	.3784	0.0000	0.0000	.5360	.000034	1.00	180
125	80.00	1.49	.3784	0.0000	.1292	.2443	0.0000	.3784	0.0000	0.0000	.4459	.000623	4.00	100
124	70.00	1.49	.3871	0.0000	.1319	.2248	0.0000	.3871	0.0000	0.0000	.4659	.000210	2.00	75
123	60.00	1.49	.3610	0.0000	.1312	.2234	0.0000	.3610	0.0000	0.0000	.4907	.000230	3.00	120
122	60.00	1.48	.3741	0.0000	.1342	.2106	0.0000	.3741	0.0000	0.0000	.4606	.000207	3.00	100
121	60.00	1.50	.3871	0.0000	.1347	.2069	0.0000	.3871	0.0000	0.0000	.5145	.000220	3.00	100
120	60.00	1.50	.4132	0.0000	.1337	.2106	0.0000	.4132	0.0000	0.0000	.4855	.000171	3.00	100
119	60.00	1.48	.3741	0.0000	.1345	.2061	0.0000	.3741	0.0000	0.0000	.5232	.000171	3.00	100
118	60.00	1.48	.4089	0.0000	.1340	.2069	0.0000	.4089	0.0000	0.0000	.6175	.000222	3.00	100
117	60.00	1.50	.8873	0.0000	.2884	.4253	0.0000	.8873	0.0000	0.0000	.4574	.000270	3.00	100
116	60.00	1.49	.7916	0.0000	.2901	.4151	0.0000	.7916	0.0000	0.0000	.4580	.000259	3.00	100
115	60.00	1.49	.8314	0.0000	.2896	.4137	0.0000	.8134	0.0000	0.0000	.4580	.000266	2.40	90
114	60.00	1.46	.8177	0.0000	.2905	.4223	0.0000	.8177	0.0000	0.0000	.4573	.000278	3.00	100
AAA														

TABLE A1. (continued)

RUN	TEMP	PH	[NA]	[K]	$[HSO_5]$	[TS]	[TSS]	[OH]A	$[CLO_4]$	$[NO_3]$	UO_2	RATE	R(α)	R(T)
112	60.00	1.54	0.0000	1.0000	.4011	.4340	0.0000	1.0000	0.0000	0.0000	.5032	.000581	4.00	100
111	60.00	1.52	0.0000	.4000	.1430	.2598	0.0000	.4000	0.0000	0.0000	.4727	.000278	3.00	100
110	60.00	1.52	0.0000	.5000	.2394	.2643	0.0000	.5000	0.0000	0.0000	.5078	.000491	5.00	100
109	60.00	1.49	0.0000	.6000	.2795	.3024	0.0000	.6000	0.0000	0.0000	.4814	.000509	5.00	100
108	60.00	1.53	0.0000	.3376	.3653	.3653	0.0000	.7500	0.0000	0.0000	.4865	.000540	5.00	100
107	60.00	1.55	1.3006	0.0000	.3113	.4909	.1079	.9208	0.0000	0.0000	.5758	.000331	3.00	100
106	60.00	1.50	1.1440	0.0000	.3257	.4728	.1129	.9228	0.0000	0.0000	.8100	.000364	3.00	100
105	60.00	1.51	1.1875	0.0000	.3431	.4903	.1189	.9723	0.0000	0.0000	.3925	.000373	3.00	100
104	60.00	1.53	1.1788	0.0000	.3337	.4955	.1157	.9571	0.0000	0.0000	.9231	.000384	3.00	100
103	60.00	1.53	1.1483	0.0000	.2990	.5387	.1036	.9752	0.0000	0.0000	.5139	.000341	3.00	100
102	60.00	1.51	1.0831	0.0000	.3727	.4040	0.0000	1.0831	0.0000	0.0000	.4776	.000370	3.00	100
101	60.00	1.55	1.1739	0.0000	.1070	.5155	0.0000	1.1739	0.0000	0.0000	.4876	.000070	.50	100
100	60.00	1.51	1.6000	0.0000	.2364	.7766	0.0000	1.6000	0.0000	0.0000	.5271	.000137	1.00	90
99	60.00	1.54	1.8500	0.0000	.5397	.6813	0.0000	1.8000	0.0000	0.0000	.5195	.000379	3.00	100
98	60.00	1.52	2.3378	0.0000	.3803	.3915	0.0000	1.0390	1.2988	0.0000	.5158	.000476	5.00	100
97	60.00	1.46	1.7663	0.0000	.3600	.3793	0.0000	.9467	.8196	0.0000	.4899	.000446	4.00	100
96	60.00	1.54	1.4121	0.0000	.3875	.4122	0.0000	.9713	.4412	0.0000	.5138	.000411	4.00	100
95	60.00	1.51	1.7312	0.0000	.4161	.4284	0.0000	.9994	0.0000	.7318	.4466	.000488	4.00	80
94	60.00	1.55	1.9574	0.0000	.3968	.4085	0.0000	1.0460	0.0000	.9114	.5341	.000494	5.00	100
93	60.00	1.52	1.2027	0.0000	.2614	.2821	0.0000	.7500	0.0000	.4527	.5332	.000425	4.00	100
92	60.00	1.51	0.0000	0.0000	2.1676	.4105	1.1774	.7548	.6588	0.0000	.4935	.000247	2.00	100
91	60.00	1.56	0.0000	2.2187	.3622	1.1953	.8154	.5879	0.0000	0.0000	.5146	.000215	2.00	100
90	60.00	1.50	0.0000	2.7066	.4171	1.5147	.9972	.7609	0.0000	0.0000	.5277	.000182	1.50	70
89	60.00	1.54	0.0000	1.0818	.3469	.5508	.1090	.8638	0.0000	0.0000	.5372	.000390	4.00	100
88	60.00	1.52	.5500	1.6010	.4620	1.5577	.8005	.5500	0.0000	0.0000	.5195	.000229	2.00	85
87	60.00	1.50	.6524	1.7685	.4132	1.6363	.8843	.6524	0.0000	0.0000	.4720	.000153	1.00	70
86	60.00	1.51	.8047	1.1228	.4055	1.2213	.5614	.8047	0.0000	0.0000	.4684	.000261	2.00	80
85	60.00	1.49	0.0000	1.6653	.4004	.7759	.1243	1.4166	0.0000	0.0000	.4566	.000331	3.00	75
84	60.00	1.55	3.2623	0.0000	.4133	2.0201	1.2730	.7163	0.0000	0.0000	.5026	.000112	1.00	100
83	60.00	1.53	2.6272	0.0000	.4349	1.5413	.8235	.9802	0.0000	0.0000	.4555	.000161	1.50	85
82	60.00	1.51	1.0003	0.0000	.1858	.4643	0.0000	1.0003	0.0000	0.0000	.4596	.000138	1.50	75
81	60.00	1.51	0.0000	.9616	.4021	.6544	0.0000	.9616	0.0000	0.0000	.4450	.000355	2.50	70
80	60.00	1.52	1.9226	0.0000	.4491	1.1524	.4112	1.1001	0.0000	0.0000	.5086	.000219	1.50	75
79	60.00	1.51	1.4919	0.0000	.4243	.8761	.1585	1.1749	0.0000	0.0000	.4907	.000218	2.00	75
78	60.00	1.55	1.2962	0.0000	.4271	.6951	0.0000	1.2962	0.0000	0.0000	.5137	.000268	2.00	75
77	30.00	2.53	1.3000	0.0000	.4819	.4683	0.0000	1.3000	0.0000	0.0000	.4549	.000121	1.30	150

TABLE A1. (continued)

RUN	TEMP	PH	[NA]	[K]	[HSO_5]	[TS]	[TSS]	[OH]A	[CLO_4]	[NO_3]	UO_2	RATE	R(α)	R(T)
76	80.00	2.45	1.5351	0.0000	.5580	.5423	0.0000	1.5351	0.0000	0.0000	.5095	.000940	3.00	30
75	70.00	2.47	1.2912	0.0000	.4765	.4743	0.0000	1.2912	0.0000	0.0000	.4473	.000722	2.50	30
74	60.00	2.45	1.4310	0.0000	.5556	.5530	0.0000	1.4310	0.0000	0.0000	.4635	.000557	3.50	75
73	50.00	2.49	1.3223	0.0000	.5193	.5169	0.0000	1.3223	0.0000	0.0000	.4474	.000363	2.20	75
72	40.60	2.51	1.5050	0.0000	.5556	.5530	0.0000	1.5050	0.0000	0.0000	.5385	.000207	1.80	100
68	80.00	.53	.6307	0.0000	.4504	.5658	0.0000	.6307	0.0000	0.0000	.5182	.000969	4.50	50
67	70.00	.55	.7090	0.0000	.4545	.5814	0.0000	.7090	0.0000	0.0000	.5239	.000420	2.50	60
66	60.00	.48	.5507	0.0000	.4306	.5508	0.0000	.5507	0.0000	0.0000	.4640	.001210	1.10	60
65	50.00	.52	.6437	0.0000	.5061	.5379	0.0000	.6437	0.0000	0.0000	.5104	.000138	.50	55
64	40.00	.52	.7071	0.0000	.5035	.5352	0.0000	.7071	0.0000	0.0000	.5360	.000052	.40	65
62	79.00	1.49	1.1788	0.0000	.4683	.4969	0.0000	1.1788	0.0000	0.0000	.5050	.000948	2.00	20
61	68.00	1.50	1.0735	0.0000	.4225	.4482	0.0000	1.0735	0.0000	0.0000	.4463	.000559	1.30	20
60	60.00	1.49	1.1420	0.0000	.4591	.4871	0.0000	1.1420	0.0000	0.0000	.4472	.000404	.70	20
59	50.00	1.51	1.2500	0.0000	.4163	.4581	0.0000	1.2500	0.0000	0.0000	.5175	.000146	.30	20
58	40.00	1.50	1.2249	0.0000	.4083	.4332	0.0000	1.2249	0.0000	0.0000	.5298	.000180	.80	15

TABLE A2. The composition data for all the peroxymonosulphuric acid runs from Table A1 used in the multilinear regression analysis.

RUN	TEMP	PH	$[HSO_4]$	$[SO_4]$	[H]	TOTI	H	ECR	$[HSO_5]$	[MA]	[K]	[TS]
211	30.00	1.49	.1632	.9403	.0788	3.0840	.4105	552.45	.0981	2.0667	0.0000	1.1035
210	30.00	1.49	.1786	.8206	.0836	2.6946	.3868	541.51	.0527	1.7919	0.0000	.9992
209	30.00	1.50	.1702	.8738	.0786	2.8036	.4023	513.11	.0105	1.8528	0.0000	1.0439
208	30.00	1.49	.1724	.8057	.0783	2.5967	.4131	501.07	.0053	1.7146	0.0000	.9781
207	30.00	1.49	.1728	.8511	.0792	2.7293	.4083	482.06	.0018	1.8005	0.0000	1.0238
138	60.00	1.49	.3366	.7733	.0981	3.5813	.3297	528.74	.9228	2.7117	0.0000	1.1099
137	32.00	1.49	.0597	.1080	.0412	.5348	.7855	555.64	.1493	.3872	0.0000	.1677
136	30.00	2.50	.0347	.1357	.0215	.5910	.1469	559.62	.1474	.4355	0.0000	.1704
135	30.00	2.52	.0115	.1553	.0062	.6275	.4847	559.75	.1485	.4675	0.0000	.1668
134	40.00	2.49	.0293	.1370	.0131	.5903	.2469	538.63	.1480	.4420	0.0000	.1663
133	80.00	2.50	.0397	.1235	.0063	.5571	.5051	454.06	.1452	.4290	0.0000	.1632
132	70.00	2.50	.0356	.1284	.0073	.5694	.4342	475.30	.1467	.4355	0.0000	.1640
131	60.00	2.48	.0323	.1320	.0084	.5764	.3929	496.33	.1464	.4377	0.0000	.1643
130	30.00	1.50	.0573	.1108	.0413	.5410	.7657	559.89	.1497	.3907	0.0000	.1681
129	40.00	1.48	.0878	.0939	.0532	.5180	.6219	538.46	.1465	.3727	0.0000	.1817
128	50.00	2.48	.0398	.1246	.0142	.5616	.2327	517.37	.1463	.4244	0.0000	.1644
127	45.00	1.48	.1010	.0896	.0545	.5054	.6079	526.34	.1339	.3631	0.0000	.1906
126	30.00	1.46	.0841	.1084	.0628	.5482	.5525	558.35	.1371	.3788	0.0000	.1925
125	80.00	1.49	.1811	.0575	.0559	.4814	.5790	451.59	.1262	.3696	0.0000	.2336
124	70.00	1.49	.1466	.0740	.0481	.5001	.6729	473.11	.1295	.3799	0.0000	.2206
123	60.00	1.48	.1504	.0700	.0670	.4914	.4943	494.15	.1294	.3561	0.0000	.2204
122	60.00	1.48	.1299	.0778	.0525	.4976	.6309	494.56	.1324	.3690	0.0000	.2077
121	60.00	1.50	.1187	.0854	.0444	.5097	.7128	494.62	.1329	.3819	0.0000	.2041
120	60.00	1.50	.1073	.1005	.0357	.5422	.8850	494.49	.1319	.4076	0.0000	.2077
119	60.00	1.48	.1244	.0789	.0494	.4955	.6702	494.60	.1327	.3690	0.0000	.2033
118	60.00	1.48	.1050	.0991	.0352	.5361	.9407	494.53	.1322	.4034	0.0000	.2041
117	60.00	1.50	.1972	.2223	.0549	1.1506	.5760	508.02	.2845	.8753	0.0000	.4195
116	60.00	1.48	.2450	.1644	.0831	1.0265	.3984	508.13	.2862	.7809	0.0000	.4095
115	60.00	1.48	.2290	.1791	.0736	1.0624	.4496	508.10	.2857	.8201	0.0000	.4031
114	60.00	1.46	.2389	.1777	.0773	1.0600	.4484	508.15	.2866	.8066	0.0000	.4166
107	60.00	1.55	.1272	.3571	.0304	1.5879	.9276	509.37	.3071	1.2830	0.0000	.4842
106	60.00	1.50	.1023	.3641	.0227	1.5156	1.3908	510.16	.3213	1.1285	0.0000	.4654
105	60.00	1.51	.0944	.3892	.0207	1.5910	1.4903	511.08	.3384	1.1714	0.0000	.4837
104	60.00	1.53	.1124	.3764	.0251	1.5675	1.1751	510.59	.3292	1.1628	0.0000	.4838
103	60.00	1.53	.1591	.3723	.0357	1.5558	.8264	508.66	.2949	1.1327	0.0000	.5314

TABLE A2. (continued)

RUN	TEMP	PH	$[HSO_4]$	$[SO_4]$	[H]	TOTI	H	ECR	$[HSO_5]$	[NA]	[K]	[TS]
102	60.00	1.51	.0806	.3180	.0189	1.4037	1.6313	512.53	.3676	1.0684	0.0000	.3985
101	60.00	1.55	.1161	.3924	.0223	1.3988	1.2616	490.56	.1055	.9844	0.0000	.5085
100	60.00	1.51	.1577	.6084	.0325	2.2176	.9497	504.52	.2332	1.5783	0.0000	.7661
99	60.00	1.54	.0838	.5883	.0199	2.4057	1.5891	519.06	.5324	1.8249	0.0000	.6721
98	60.00	1.52	.0830	.3032	.0427	2.6504	.7077	512.89	.3751	2.3061	0.0000	.3862
97	60.00	1.46	.1197	.2545	.0534	2.0485	.6494	511.93	.3551	1.7424	0.0000	.3742
96	60.00	1.54	.1729	.2337	.0677	1.6929	.4261	513.22	.3822	1.3930	0.0000	.4066
95	60.00	1.51	.1853	.2373	.0880	2.0312	.3512	514.48	.4105	1.7077	0.0000	.4226
94	60.00	1.55	.1170	.2859	.0525	2.2673	.5371	513.64	.3914	1.9309	0.0000	.4030
93	60.00	1.52	.0578	.2205	.0198	1.4252	1.5221	506.30	.2579	1.1864	0.0000	.2783
84	60.00	1.55	.9363	1.0564	.2418	4.5148	.1165	514.36	.4077	3.2181	0.0000	1.9927
83	60.00	1.53	.6914	.8290	.1900	3.6089	.1554	515.25	.4290	2.5916	0.0000	1.5204
82	60.00	1.51	.0967	.3613	.0195	1.3657	1.5848	500.28	.1833	.9867	0.0000	.4580
80	60.00	1.52	.6322	.5045	.1913	2.5906	.1579	515.82	.4430	1.8965	0.0000	1.1368
79	60.00	1.51	.5157	.3485	.1626	1.9813	.1900	514.82	.4185	1.4717	0.0000	.8642
78	60.00	1.55	.3936	.2921	.1237	1.6927	.2279	514.94	.4213	1.2786	0.0000	.6857
77	30.00	2.53	.0773	.3916	.0444	1.7360	.0664	580.50	.4825	1.3015	0.0000	.4689
76	80.00	2.45	.0952	.4344	.0135	1.9453	.2623	477.35	.5449	1.4992	0.0000	.5296
75	70.00	2.47	.1133	.3523	.0219	1.6396	.1551	495.72	.4677	1.2673	0.0000	.4655
74	60.00	2.45	.1815	.3640	.0496	1.8233	.0715	519.57	.5481	1.4116	0.0000	.5455
73	50.00	2.49	.1713	.3411	.0611	1.7113	.0529	539.52	.5148	1.3109	0.0000	.5124
72	40.60	2.51	.1114	.4394	.0481	1.9847	.0643	560.59	.5534	1.4989	0.0000	.5508
68	80.00	.53	.5119	.0407	.4203	1.0754	.7022	473.58	.4399	.6159	0.0000	.5526
67	70.00	.55	.5087	.0620	.3867	1.1427	.7289	494.88	.4461	.6959	0.0000	.5707
66	60.00	.48	.4852	.0581	.4868	1.0862	.6803	515.08	.4248	.5432	0.0000	.5433
65	50.00	.52	.4535	.0797	.4796	1.1959	.6297	539.07	.5017	.6381	0.0000	.5333
62	79.00	1.49	.2367	.2488	.0439	1.4426	.7369	476.38	.4576	1.1518	0.0000	.4855
61	68.00	1.50	.1976	.2427	.0475	1.3429	.6662	497.83	.4151	1.0547	0.0000	.4404
60	60.00	1.49	.2234	.2571	.0675	1.4493	.4796	516.21	.4529	1.1265	0.0000	.4805
59	50.00	1.51	.0654	.3887	.0195	1.6459	1.5823	535.63	.4127	1.2392	0.0000	.4541
58	40.00	1.50	.1829	.2487	.0935	1.3357	.3382	556.44	.4068	.9963	0.0000	.4316

A3.2 THE HYDROGEN PEROXIDE SYSTEM

The kinetic data and raw composition data (uncorrected for temperature) appear in Table A3. This Table is analogous to Table A1. The abbreviations used in Table A1 apply to Table A3, with the following additions:

$[H_2O_2]$ concentration of hydrogen peroxide (molar)

Table A4 is analogous to Table A2. All abbreviations retain their defined significance.

TABLE A3. The kinetic and initial composition data for all hydrogen peroxide runs.

RUN	TEMP	PH	[NA]	$[H_2O_2]$	[TS]	[TSS]	$[OH]_A$	UO_2	RATE	R(a)	R(T)
140	60.00	1.49	.1435	.1666	.1476	0.0000	.1435	.5334	.00439	10.00	20
141	60.00	1.50	.1522	.1664	.1486	0.0000	.1522	.5045	.00503	10.00	20
142	60.00	1.49	.1348	.1664	.1487	0.0000	.1348	.4744	.00470	13.00	26
143	60.00	1.50	.1566	.1666	.1475	0.0000	.1566	.4487	.00434	15.00	32
144	60.00	1.48	.1435	.1663	.1910	0.0000	.1435	.4506	.00518	12.00	22
145	30.50	1.48	.1435	.1714	.1223	0.0000	.1435	.4612	.00038	2.60	60
146	40.00	1.49	.1653	.1688	.1336	0.0000	.1653	.4479	.00069	4.00	50
147	50.00	1.49	.1479	.1685	.1376	0.0000	.1479	.4834	.00269	10.00	35
148	60.00	1.52	.1827	.1668	.1550	0.0000	.1827	.4835	.00416	7.50	18
149	70.00	1.51	.1559	.1678	.1503	0.0000	.1559	.4841	.00781	15.00	20
150	80.00	1.49	.1609	.1671	.1551	0.0000	.1609	.4355	.00619	6.00	10
151	60.00	2.51	.1920	.1742	.1041	0.0000	.1920	.5206	.00045	1.00	20
152	50.00	2.51	.1833	.1743	.1042	0.0000	.1833	.5139	.00093	1.20	16
153	40.00	2.52	.1970	.1741	.1040	0.0000	.1970	.4740	.00041	.70	16
154	30.00	2.51	.1800	.1740	.1045	0.0000	.1800	.5635	.00005	.30	50
155	69.00	2.49	.1866	.1738	.1071	0.0000	.1866	.4607	.00089	.60	7
156	80.00	2.49	.1740	.1745	.1043	0.0000	.1740	.4781	.00142	1.50	10
161	59.00	1.49	.8099	.0097	.6162	.4057	0.0000	.4622	.00018	2.00	100
162	49.00	1.48	.8314	.0099	.6017	.4157	0.0000	.6439	.00012	2.00	200
163	59.00	2.51	1.0004	.0107	.5403	.4463	.0782	.4933	.00062	5.00	80
164	50.00	2.47	1.0004	.0106	.5419	.4432	.1140	.5276	.00023	3.00	120
165	50.00	1.16	.7655	.0091	.6576	.3801	0.0000	.5020	.00007	1.00	150
166	60.00	1.59	1.1440	.1348	.7489	.5720	0.0000	.4435	.00241	2.00	10
167	60.00	1.62	.6027	.1392	.4267	.3013	0.0000	.5190	.00257	2.00	10
168	60.00	1.35	.2784	.1391	.2707	.1392	0.0000	.4918	.00339	2.00	10
169	59.00	1.55	.8403	.1359	.5883	.4202	0.0000	.4486	.00226	3.00	10
170	60.00	1.58	.5387	.2613	.3869	.2693	0.0000	.3579	.00282	3.00	10
171	30.00	.73	.2052	.1555	.3313	.1026	0.0000	1.2853	.00058	4.50	75
172	42.00	.58	0.0000	.1469	.2953	0.0000	0.0000	.6194	.00105	7.00	60
173	33.00	1.55	1.3086	.1555	.7235	.5182	.2723	.5489	.00064	4.00	60
174	70.00	1.58	1.0899	.1596	.7365	.5450	0.0000	.4425	.00454	4.00	10
176	60.00	1.92	1.8776	.2596	1.0779	.9388	0.0000	.5891	.00431	4.00	10
177	60.00	1.88	1.5015	.3045	.8787	.7508	0.0000	.4830	.00567	6.00	10
178	60.00	1.85	1.1122	.0714	.7167	.5561	0.0000	.7508	.00122	1.50	10
179	60.00	1.46	.5860	.0711	.4636	.2930	0.0000	.5005	.00180	1.50	10

TABLE A3.

RUN	TEMP	PH	[NA]	[H_2O_2]	[TS]	[TSS]	[OH]A	UO_2	RATE	R(a)	R(T)
180	60.00	.98	0.0000	.0708	.1593	0.0000	0.0000	.5099	.00233	6.00	25
181	60.00	1.12	0.0000	.0366	.1372	0.0000	0.0000	.4587	.00135	8.00	60
182	60.00	1.33	.2055	.0356	.2362	.1027	0.0000	.5107	.00095	7.00	75
183	60.00	1.70	.4918	.0355	.3791	.2459	0.0000	.5305	.00108	7.00	60
184	59.00	1.74	.6185	.0361	.4445	.3093	0.0000	.5851	.00115	7.00	60
185	60.00	1.15	0.0000	.0358	.1344	0.0000	0.0000	.4674	.00106	4.00	50
186	60.00	1.37	0.0000	.0390	.0585	0.0000	0.0000	.5550	.00152	7.00	50
187	62.00	1.53	0.0000	.0401	.0300	0.0000	0.0000	.4578	.00217	9.00	50
188	60.00	1.97	0.0000	.0402	.0121	0.0000	0.0000	.4807	.00155	4.00	20
189	60.00	1.11	0.0000	.0363	.1361	0.0000	0.0000	.5611	.00138	6.00	50
190	60.00	.87	0.0000	.0326	.2444	0.0000	0.0000	.4412	.00088	6.00	70
200	30.00	1.50	1.8305	.0007	1.0446	.9152	0.0000	1.6659	.00000	.01	50
201	30.00	1.50	1.7654	.0039	1.0039	.8730	0.0000	1.1634	.00002	.10	50
202	30.00	1.51	1.7514	.0081	.9928	.8757	0.0000	1.2909	.00002	.10	50
203	30.00	1.48	1.7804	.0568	1.0080	.8902	0.0000	1.4242	.00074	4.00	50
204	30.00	1.48	1.7003	.1206	.9678	.8501	0.0000	1.5475	.00088	6.00	60

TABLE A4. The composition data for all the hydrogen peroxide runs from Table A3 used in the multilinear regression analysis.

RUN	TEMP	PH	[HSO4]	[SO_4]	[H]	TOTI	H	ECR	[H_2O_2]	[NA]	[TS]
140	60.00	1.49	.1046	.0410	.0484	.2292	.6689	576.87	.1643	.1416	.1456
141	60.00	1.50	.1022	.0444	.0445	.2372	.7107	576.85	.1641	.1501	.1466
142	60.00	1.49	.1091	.0375	.0543	.2233	.5956	576.85	.1641	.1330	.1467
143	60.00	1.50	.0989	.0466	.0414	.2405	.7639	576.87	.1643	.1545	.1455
144	60.00	1.48	.1523	.0361	.0865	.2624	.3830	576.83	.1640	.1416	.1884
145	30.50	1.48	.0596	.0628	.0449	.2497	.7380	635.65	.1716	.1436	.1224
146	40.00	1.49	.0671	.0660	.0375	.2667	.8636	616.60	.1682	.1647	.1331
147	50.00	1.49	.0862	.0502	.0438	.2388	.7391	596.83	.1670	.1466	.1364
148	60.00	1.52	.0948	.0581	.0343	.2709	.8803	576.89	.1645	.1802	.1529
150	80.00	1.49	.1153	.0362	.0343	.2257	.9425	537.48	.1632	.1571	.1515
153	40.00	2.52	.0077	.0957	.0032	.2954	.9437	617.22	.1735	.1963	.1036
161	59.00	1.49	.3390	.2691	.0801	1.1474	.4040	523.18	.0096	.7993	.6081
162	49.00	1.48	.2892	.3076	.0830	1.2136	.3987	543.18	.0098	.8246	.5968
163	59.00	2.51	.0947	.4385	.0169	1.4265	.1831	525.01	.0106	.9873	.5332
164	50.00	2.47	.0705	.4667	.0156	1.4723	.2176	542.50	.0105	.9918	.5372
165	50.00	1.16	.4139	.2380	.1398	1.1323	.4948	539.66	.0090	.7589	.6519
166	60.00	1.59	.2941	.4446	.0583	1.6297	.4411	572.63	.1330	1.1285	.7387
167	60.00	1.62	.2053	.2156	.0455	.8539	.5277	573.26	.1373	.5945	.4209
168	60.00	1.35	.1916	.0755	.0712	.4196	.6270	573.25	.1372	.2746	.2670
169	59.00	1.55	.2761	.3045	.0597	1.1915	.4724	574.75	.1341	.8293	.5806
170	60.00	1.58	.1919	.1898	.0440	.7632	.5977	585.93	.2578	.5314	.3817
172	42.00	.58	.2602	.0337	.3304	.3613	.7961	609.86	.1462	0.0000	.2939
173	33.00	1.55	.1026	.6206	.0392	1.9663	.7194	628.76	.1555	1.3082	.7233
174	70.00	1.58	.3276	.3953	.0521	1.5153	.5051	556.29	.1567	1.0698	.7229
176	60.00	1.92	.2325	.8307	.0455	2.7266	.2643	585.80	.2561	1.8521	1.0633
177	60.00	1.88	.2155	.6513	.0405	2.1712	.3256	589.01	.3004	1.4811	.8668
178	60.00	1.85	.2679	.4391	.0522	1.5868	.2706	559.89	.0704	1.0971	.7070
179	60.00	1.46	.2714	.1859	.0682	.8307	.5081	559.80	.0701	.5781	.4573
180	60.00	.98	.1437	.0134	.1739	.1856	.6020	559.72	.0698	0.0000	.1571
181	60.00	1.12	.1226	.0127	.1510	.1608	.5024	546.63	.0361	0.0000	.1353
182	60.00	1.33	.1810	.0520	.0854	.3370	.5477	546.08	.0351	.2027	.2330
183	60.00	1.70	.2126	.1614	.0535	.6984	.3727	546.02	.0350	.4851	.3740
184	59.00	1.74	.2199	.2188	.0504	.8779	.3608	548.32	.0356	.6104	.4387
185	60.00	1.15	.1199	.0127	.1482	.1579	.4777	546.19	.0353	0.0000	.1326
186	60.00	1.37	.0500	.0077	.0671	.0739	.6353	547.90	.0385	0.0000	.0577

TABLE A4. (continued)

RUN	TEMP	PH	$[HSO_4]$	$[SO_4]$	[H]	TOTI	H	ECR	$[H_2O_2]$	[NA]	[TS]
187	62.00	1.53	.0225	.0071	.0327	.0417	.9033	544.48	.0395	0.0000	.0296
188	60.00	1.97	.0077	.0042	.0132	.0204	.8118	548.51	.0397	0.0000	.0119
189	60.00	1.11	.1215	.0127	.1500	.1597	.5175	546.47	.0358	0.0000	.1343
190	60.00	.87	.2235	.0176	.2626	.2783	.5136	544.38	.0322	0.0000	.2411
200	30.00	1.50	.1795	.8663	.0828	2.7802	.3820	550.42	.0007	1.8327	1.0458
201	30.00	1.50	.1809	.8242	.0835	2.6633	.3787	564.57	.0039	1.7675	1.0051
202	30.00	1.51	.1633	.8307	.0742	2.6569	.4165	577.01	.0081	1.7535	.9940
203	30.00	1.48	.1641	.8451	.0748	2.7009	.4425	614.53	.0569	1.7825	1.0092
204	30.00	1.48	.1650	.8039	.0745	2.5788	.4442	629.57	.1207	1.7023	.9690
205	30.00	1.47	.1588	.8840	.0731	2.8107	.4635	661.92	.6020	1.8560	1.0427
206	30.00	1.50	.1660	.8038	.0750	2.5792	.4218	594.40	.0121	1.7024	.9698

APPENDIX 4

The Minitab regression outputs for the hydrogen peroxide and peroxymonosulphuric acid systems.

FIGURE A10. The Minitab regression output for the kinetic analysis of the peroxymonosulphuric acid system.

```
-- REGPESS C34 4 C25,C3,C35,C47,C40,C41

THE REGRESSION EQUATION IS
Y =     18.6 -    .580 X1 +    .333 X2
    -11719. X3 +   8.00 X4

                                          ST. DEV.      T-RATIO =
       COLUMN      COEFFICIENT          OF COEF.      COEF/S.D.
                                          0.7651          24.25
X1     LSO4          -0.57987           0.06058          -9.57
X2     PH             0.33328           0.04375           7.62
X3     1/TK       -11718.5               429.0          -27.32
X4     E/T            7.9991            0.4061          19.70

THE ST. DEV. OF Y ABOUT REGRESSION LINE IS
S = 0.1663
WITH (  66- 5) =  61 DEGREES OF FREEDOM

R-SQUARED = 95.3 PERCENT
R-SQUARED = 94.9 PERCENT, ADJUSTED FOR D.F.

ANALYSIS OF VARIANCE

 DUE TO      DF           SS          MS=SS/DF
REGRESSION    4     33.82929           8.45732
RESIDUAL     61      1.68680           0.02765
TOTAL        65     35.51609

FURTHER ANALYSIS OF VARIANCE
SS EXPLAINED BY EACH VARIABLE WHEN ENTERED IN THE ORDER GIVEN

 DUE TO      DF           SS
REGRESSION    4     33.82929
LSO4          1      5.38059
PH            1      1.28034
1/TK          1     16.43705
E/T           1     10.73131

            X1           Y        PRED. Y      ST.DEV.
ROW       LSO4         LRTE         VALUE      PRED. Y     RESIDUAL     ST.RES.
  1      -0.03      -4.9469      -5.0113      0.0544       0.0694        0.44
  2      -0.09      -5.4202      -5.2707      0.0532      -0.1495       -0.95
  3      -0.06      -6.0969      -6.0326      0.0713      -0.0643       -0.43  X
  4      -0.09      -6.5229      -6.3331      0.0823      -0.1897       -1.31  X
  5      -0.07      -6.8980      -6.8487      0.1037       0.1497        1.15  X
  6      -0.11      -3.0218      -3.3677      0.0499       0.3459        2.18R
  7      -0.97      -4.0706      -4.2300      0.0508       0.1595        1.01
  8      -0.87      -3.8097      -4.0030      0.0610       0.1934        1.25
  9      -0.81      -3.7258      -4.0269      0.0600       0.3010        1.94
 10      -0.86      -3.6126      -3.7818      0.0509       0.1692        1.07
 11      -0.91      -2.8210      -2.9872      0.0674       0.1662        1.09  X
 12      -0.89      -2.9586      -3.1693      0.0578       0.2107        1.35
 13      -0.88      -3.2314      -3.3708      0.0499       0.1395        0.88
 14      -0.96      -4.3188      -4.2781      0.0537      -0.0407       -0.26
 15      -1.03      -4.0410      -4.0279      0.0417      -0.0131       -0.08
 16      -0.90      -3.6799      -3.5552      0.0481      -0.1247       -0.78
 17      -1.05      -4.0458      -3.9486      0.0374      -0.0971       -0.60
 18      -0.96      -4.4685      -4.3267      0.0537      -0.1418       -0.90
 19      -1.24      -3.2055      -3.1873      0.0571      -0.0182       -0.12
 20      -1.13      -3.6778      -3.4184      0.0442      -0.2594       -1.62
 21      -1.15      -3.6383      -3.5966      0.0391      -0.0417       -0.26
 22      -1.11      -3.6040      -3.6135      0.0369      -0.0706       -0.44
 23      -1.07      -3.6576      -3.6287      0.0353      -0.0289       -0.18
 24      -1.00      -3.7670      -3.6729      0.0327      -0.0941       -0.58
 25      -1.10      -3.7670      -3.6160      0.0367      -0.1510       -0.93
 26      -1.00      -3.6536      -3.6750      0.0329       0.0214        0.13
 27      -0.65      -3.5686      -3.5478      0.0225      -0.0208       -0.13
 28      -0.78      -3.5867      -3.4760      0.0234      -0.1107       -0.67
 29      -0.75      -3.5751      -3.4983      0.0229      -0.0768       -0.47
 30      -0.75      -3.5560      -3.5017      0.0232      -0.0543       -0.33

 31      -0.45      -3.4802      -3.6182      0.0264       0.1381        0.84
 32      -0.44      -3.4389      -3.6207      0.0273       0.1818        1.11
 33      -0.41      -3.4283      -3.6122      0.0284       0.1839        1.12
 34      -0.42      -3.4157      -3.6088      0.0276       0.1931        1.18
 35      -0.43      -3.4672      -3.6525      0.0270       0.1853        1.13
 36      -0.50      -3.4318      -3.5263      0.0262       0.0945        0.58
 37      -0.41      -4.1549      -4.0937      0.0335      -0.0613       -0.38
 38      -0.22      -3.8633      -3.8821      0.0361       0.0188        0.12
 39      -0.23      -3.4214      -3.5147      0.0384       0.0933        0.58
 40      -0.52      -3.3224      -3.5025      0.0257       0.1801        1.10
 41      -0.59      -3.3507      -3.5015      0.0246       0.1509        0.92
 42      -0.63      -3.3862      -3.4223      0.0238       0.0361        0.22
 43      -0.62      -3.3116      -3.4060      0.0247       0.0944        0.57
 44      -0.54      -3.3063      -3.4597      0.0251       0.1534        0.93
 45      -0.66      -3.3716      -3.5806      0.0222       0.2090        1.27
 46       0.02      -3.9508      -3.7716      0.0490      -0.1792       -1.13
 47      -0.08      -3.7932      -3.6957      0.0440      -0.0975       -0.61
 48      -0.44      -3.8601      -3.8527      0.0276      -0.0075       -0.05
 49      -0.30      -3.6596      -3.5604      0.0343      -0.0992       -0.61
 50      -0.46      -3.6615      -3.4946      0.0282      -0.1670       -1.02
 51      -0.53      -3.5719      -3.4340      0.0259      -0.1379       -0.84
 52      -0.41      -3.9172      -3.7090      0.0662      -0.2082       -1.36  X
 53      -0.36      -3.0269      -2.7932      0.0591      -0.2336       -1.50
 54      -0.45      -3.1415      -2.9577      0.0497      -0.1838       -1.16
 55      -0.44      -3.2541      -3.0782      0.0446      -0.1759       -1.10
 56      -0.47      -3.4401      -3.2571      0.0462      -0.1829       -1.15
 57      -0.36      -3.6840      -3.4636      0.0549      -0.2204       -1.40
 58      -1.39      -3.0137      -2.9222      0.0652      -0.0914       -0.60  X
 59      -1.21      -3.3768      -3.1795      0.0572      -0.1973       -1.26
 60      -1.24      -2.9172      -3.3804      0.0609       0.4632        2.99R
 61      -1.10      -3.8601      -3.5588      0.0635      -0.3013       -1.96
 62      -0.60      -3.0232      -3.0584      0.0378       0.0352        0.22
 63      -0.61      -3.2526      -3.2701      0.0287       0.0175        0.11
 64      -0.59      -3.3936      -3.3913      0.0263      -0.0024       -0.01
 65      -0.41      -3.8356      -3.7130      0.0325      -0.1226       -0.75
 66      -0.60      -3.7447      -3.8072      0.0422       0.0625        0.39

R DENOTES AN OBS. WITH A LARGE ST. RES.
X DENOTES AN OBS. WHOSE X VALUE GIVES IT LARGE INFLUENCE.
```

```
 66      -0.60      -3.7447      -3.8072      0.0422      0.0625      0.39

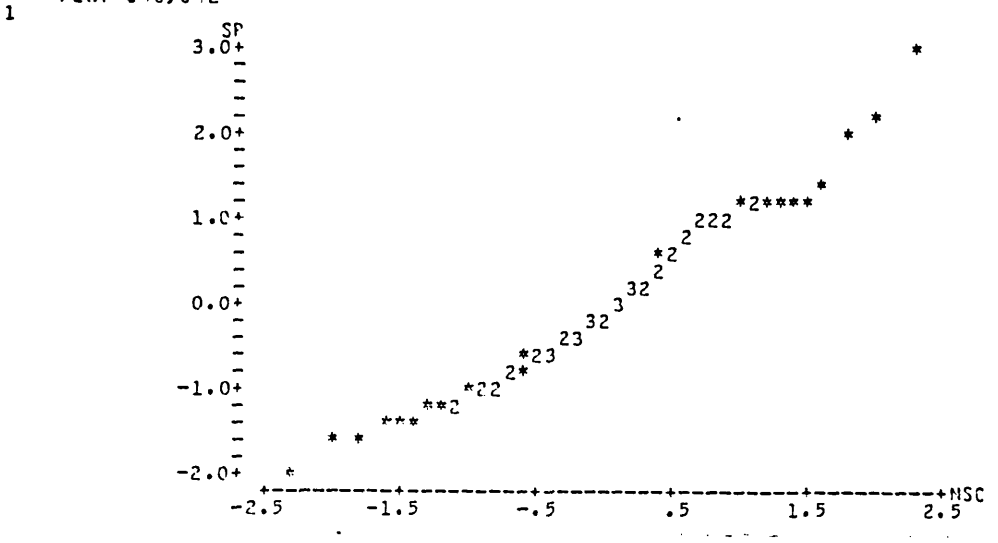
R DENOTES AN OBS. WITH A LARGE ST. RES.
X DENOTES AN OBS. WHOSE X VALUE GIVES IT LARGE INFLUENCE.

DURBIN-WATSON STATISTIC = 1.20

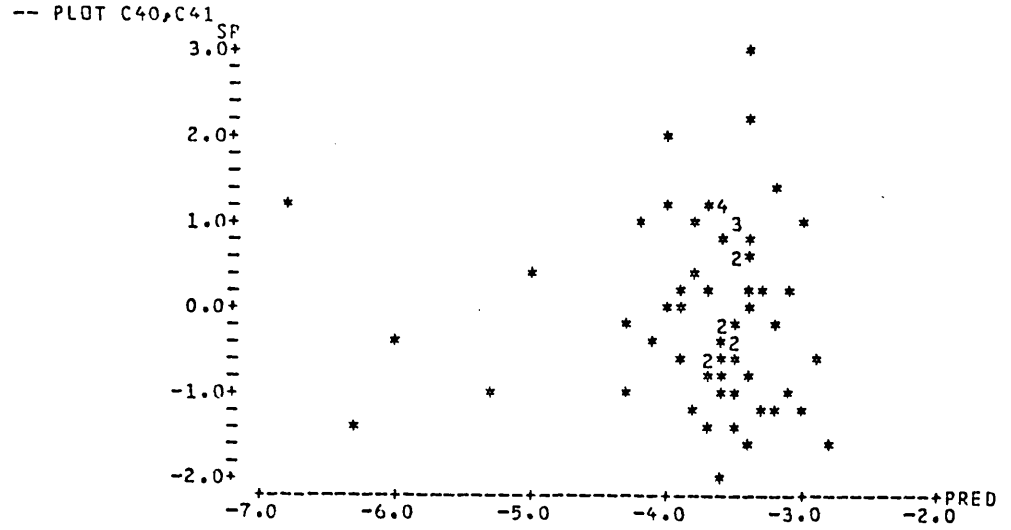
(X-PRIME X)INVERSE

                0           1           2           3           4
0             21.
1              0.          0.
2             -0.          -0.          0.
3         -11222.         -79.         30.     6655883.
4              9.          0.          -0.       -5854.          6.

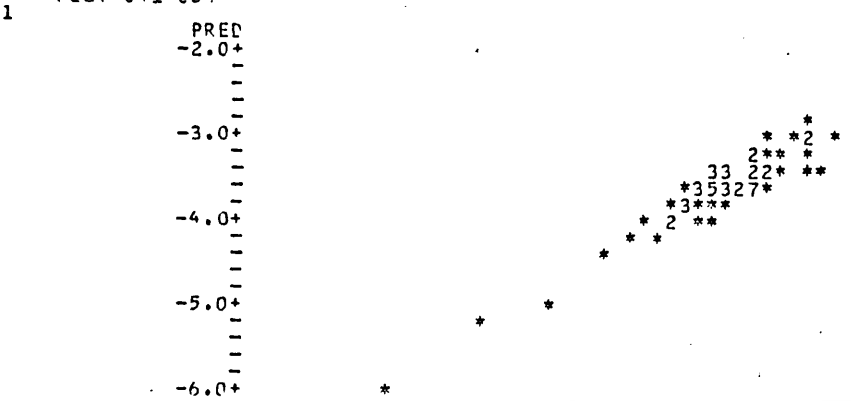
-- NSCORES C40,C42
-- PLOT C40,C42
1
```

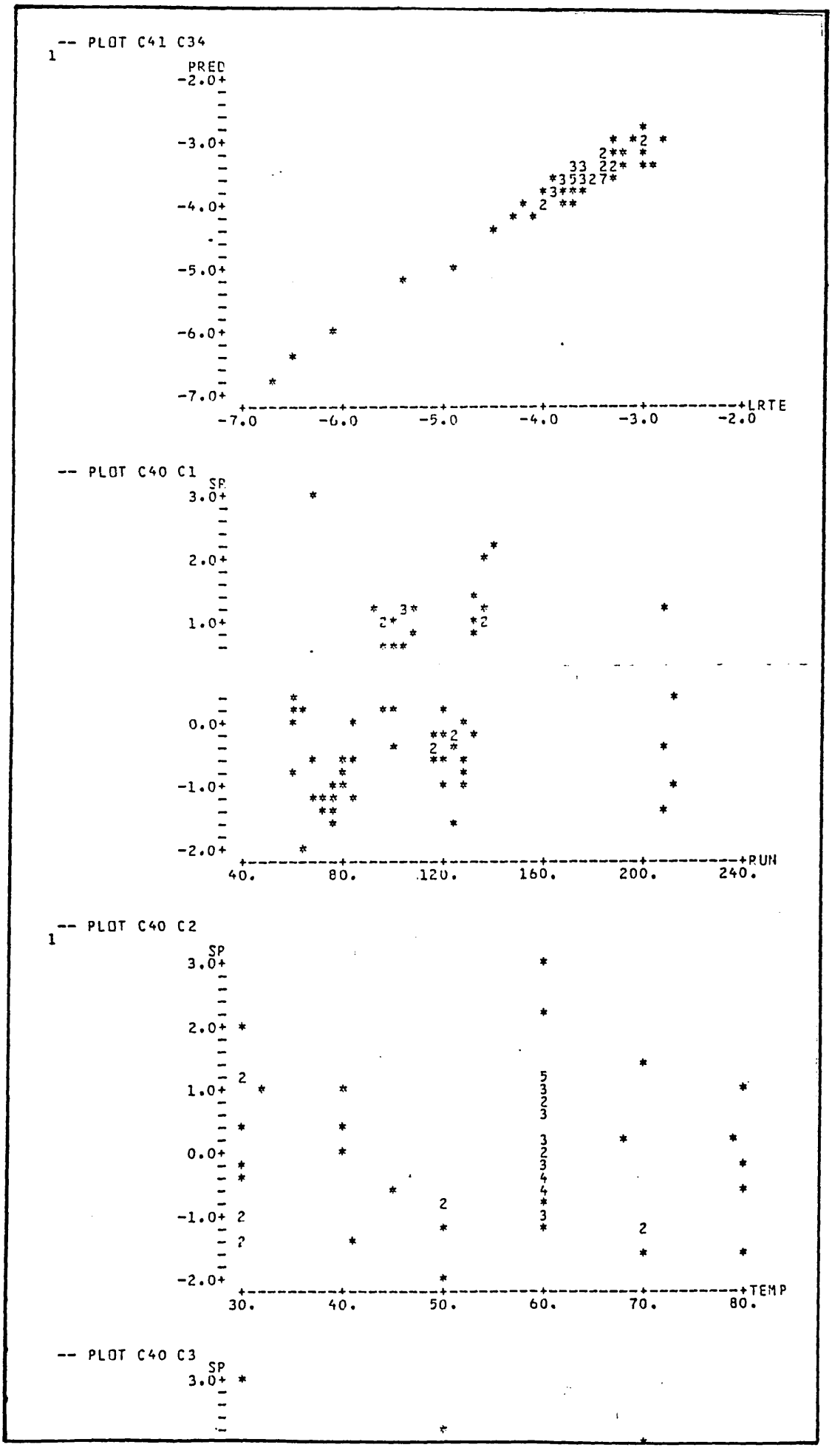



```
-- PLOT C40,C41
```

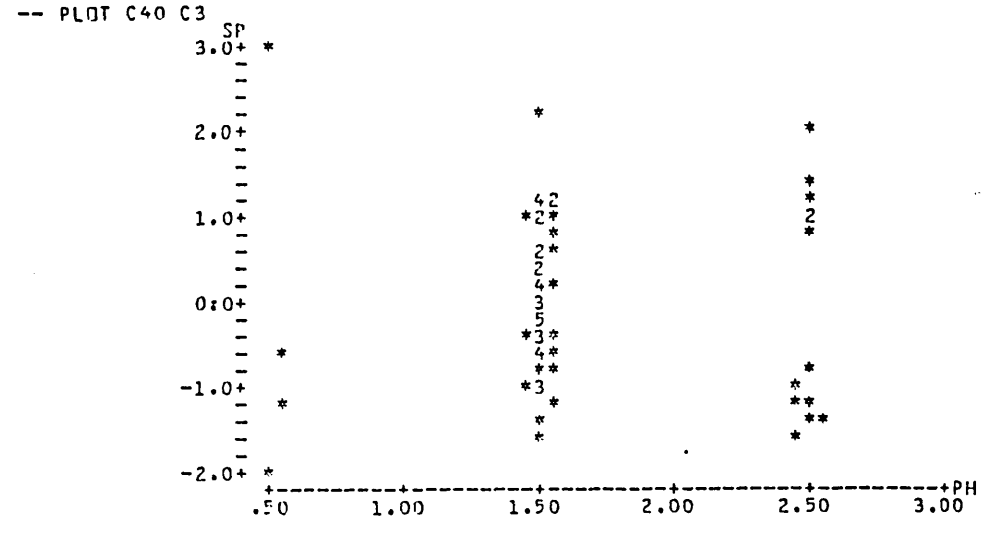



```
-- PLOT C41 C34
1
```

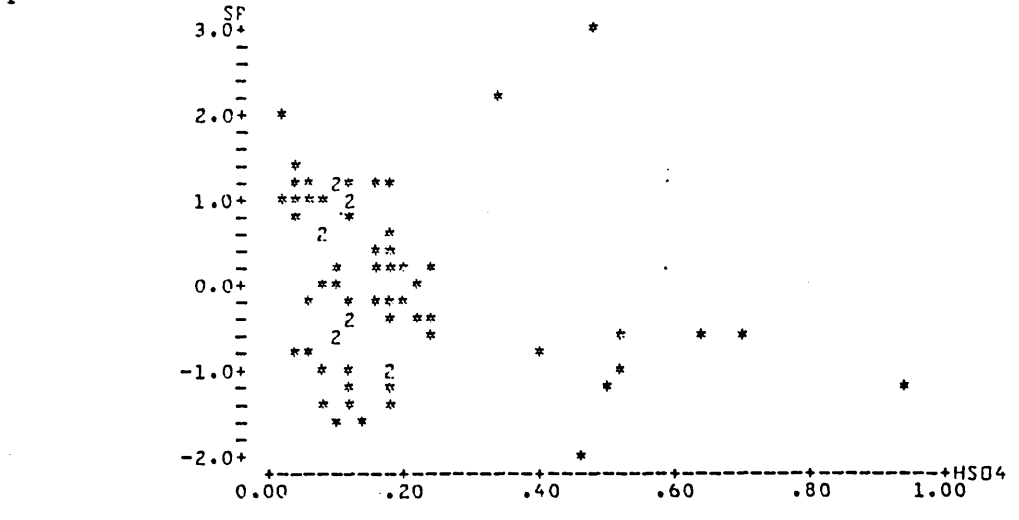



-- PLOT C41 C34
PRED
LRTE
-- PLOT C40 C1
SP
RUN
-- PLOT C40 C2
SP
TEMP
-- PLOT C40 C3
SP

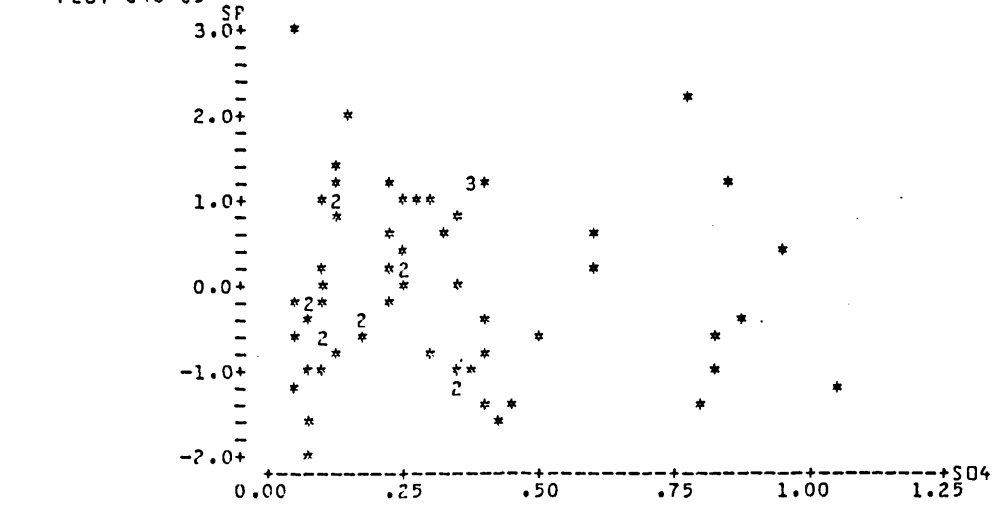
-- PLOT C40 C3



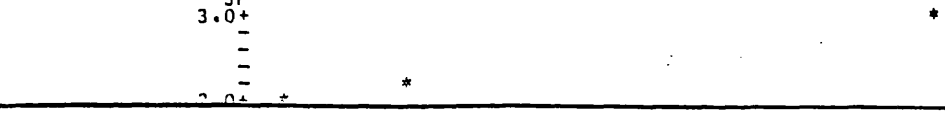
-- PLOT C40 C4



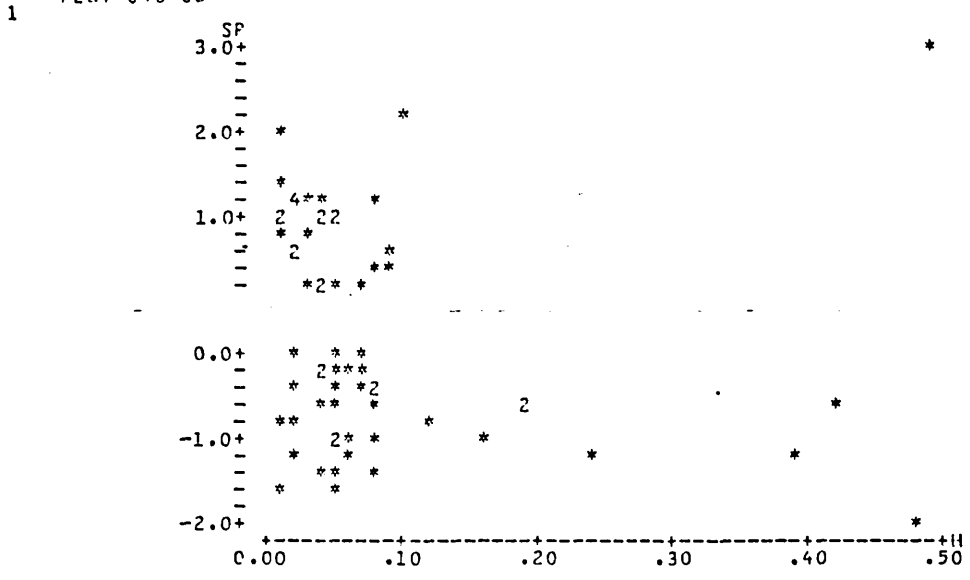
-- PLOT C40 C5



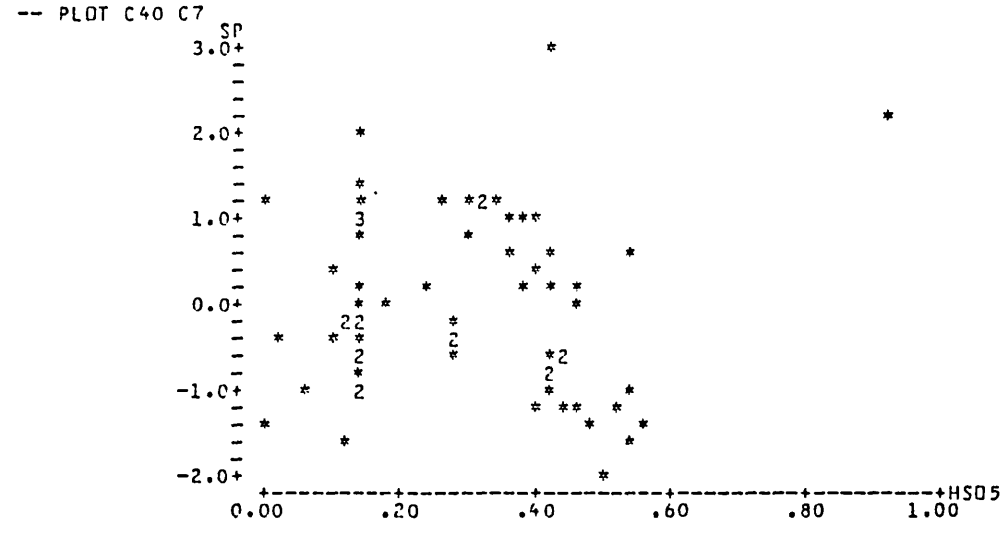
-- PLOT C40 C6



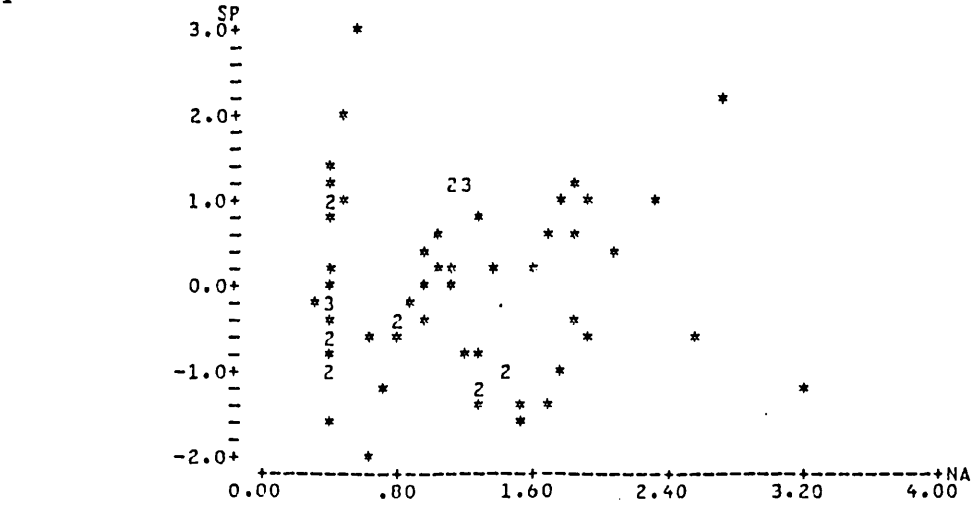
-- PLOT C40 C6



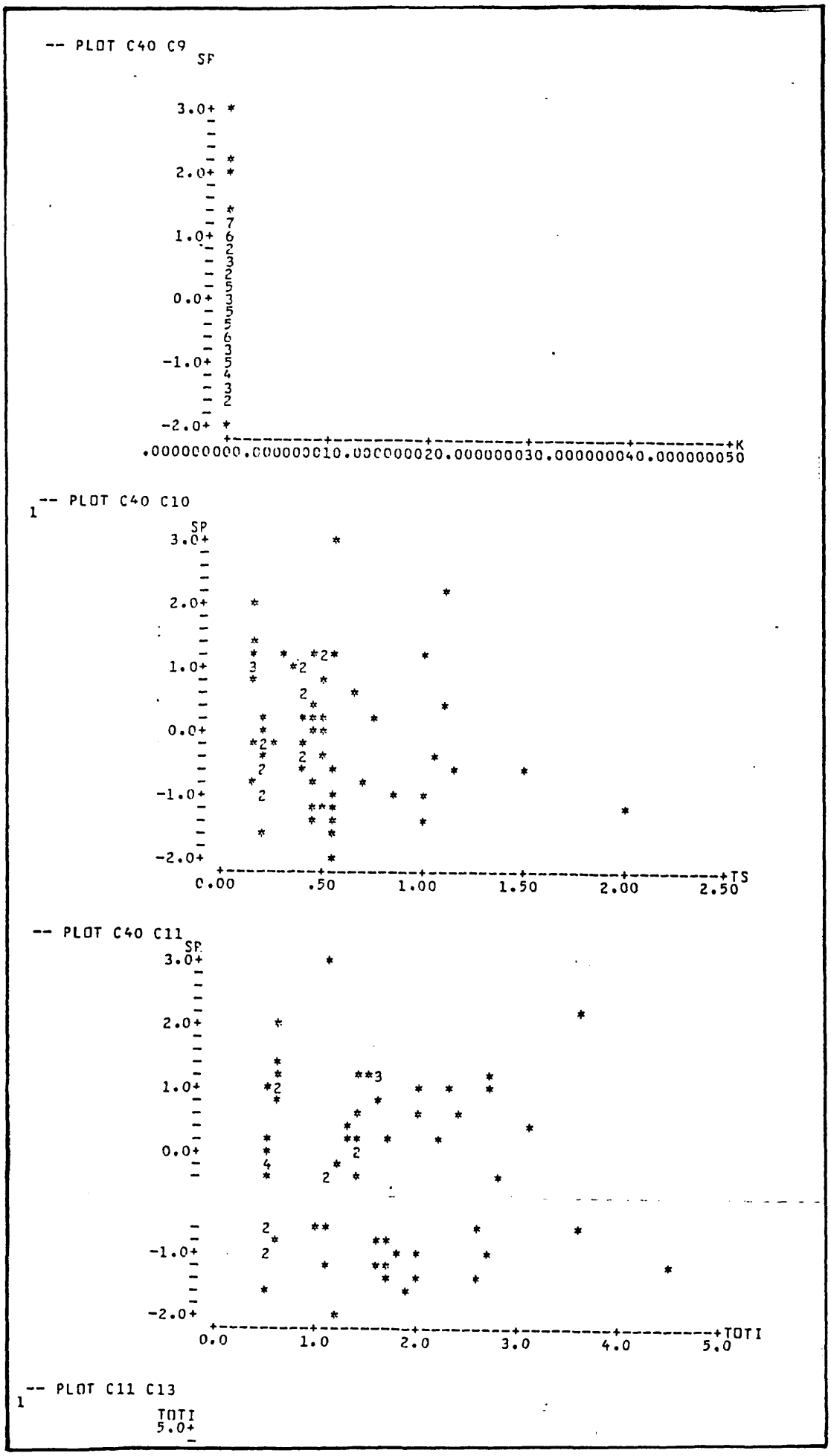
-- PLOT C40 C7



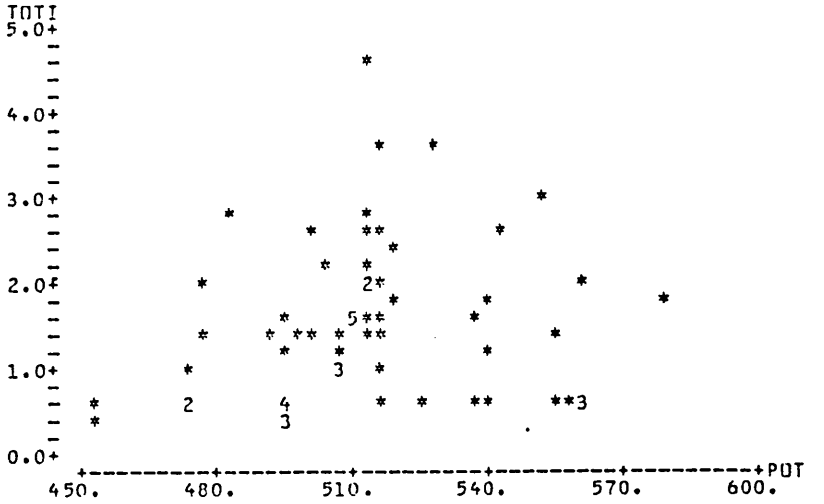
-- PLOT C40 C8



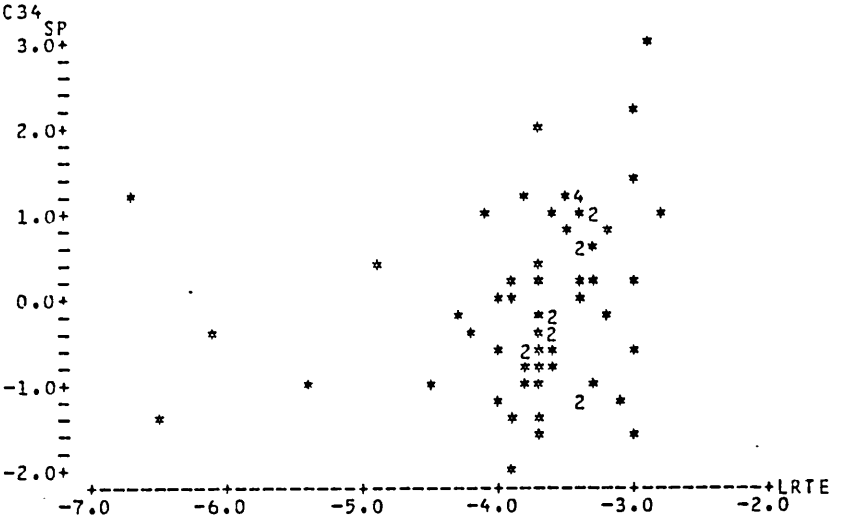
-- PLOT C40 C9


-- PLOT C40 C9
SP
3.0+
2.0+
1.0+
0.0+
-1.0+
-2.0+
.000000000.000000010.000000020.000000030.000000040.000000050
K
-- PLOT C40 C10
SP
3.0+
2.0+
1.0+
0.0+
-1.0+
-2.0+
0.00
.50
1.00
1.50
2.00
2.50
TS
-- PLOT C40 C11
SP
3.0+
2.0+
1.0+
0.0+
-1.0+
-2.0+
0.0
1.0
2.0
3.0
4.0
5.0
TOTI
-- PLOT C11 C13
TOTI
5.0+

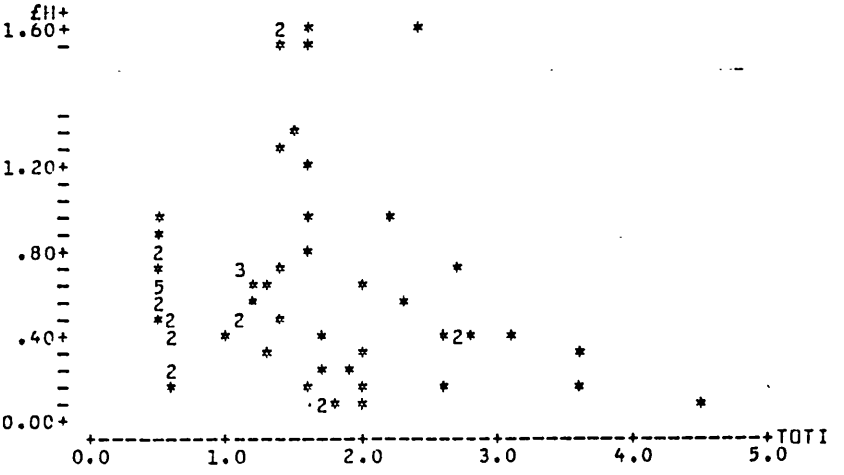
```
-- PLOT C11 C13
1
```




```
-- PLOT C40 C34
```




```
-- PLOT C12 C11
1
```




```
-- HIST C40
  SR
```

MIDDLE OF INTERVAL	NUMBER OF OBSERVATIONS	
-2.0	1	*
-1.5	6	******
-1.0	11	***********
-.5	13	*************
0.0	11	***********
.5	5	*****
1.0	13	*************

```
-- HIST C40

  SR

   MIDDLE OF    NUMBER OF
   INTERVAL     OBSERVATIONS
       -2.0           1     *
       -1.5           6     ******
       -1.0          11     ***********
        -.5          13     *************
        0.0          11     ***********
         .5           5     *****
        1.0          13     *************
        1.5           3     ***
        2.0           2     **
        2.5           0
        3.0           1     *

-- HIST C2

  TEMP

   MIDDLE OF    NUMBER OF
   INTERVAL     OBSERVATIONS
        30.          11     ***********
        35.           0
        40.           4     ****
        45.           1     *
        50.           4     ****
        55.           0
        60.          36     ************************************
        65.           0
        70.           5     *****
        75.           0
        80.           5     *****

-- HIST C3

  PH

   MIDDLE OF    NUMBER OF
   INTERVAL     OBSERVATIONS
         .4           1     *
         .6           3     ***
         .8           0
        1.0           0
        1.2           0
        1.4          21     *********************
        1.6          28     ****************************
        1.8           0
        2.0           0
        2.2           0
        2.4           7     *******
        2.6           6     ******

-- HIST C4

  HSO4


   MIDDLE OF    NUMBER OF
   INTERVAL     OBSERVATIONS
         0.0           7     *******
         .1           28     ****************************
         .2           21     *********************
         .3            1     *
         .4            1     *
         .5            5     *****
         .6            1     *
         .7            1     *
         .8            0
         .9            1     *

-- HIST C5

  SO4

   MIDDLE OF    NUMBER OF
   INTERVAL     OBSERVATIONS
         0.0           1     *
         .1           22     **********************
         .2           11     ***********
         .3            8     ********
         .4           13     *************
         .5            1     *
         .6            2     **
         .7            0
         .8            4     ****
         .9            3     ***
        1.0            0
        1.1            1     *

-- HIST C6

  H

   MIDDLE OF    NUMBER OF
   INTERVAL     OBSERVATIONS
        0.00           17     *****************
         .05           30     ******************************
         .10           11     ***********
         .15            1     *
         .20            2     **
         .25            1     *
```

```
-- HIST C6

  H

   MIDDLE OF    NUMBER OF
   INTERVAL     OBSERVATIONS
       0.00         17     *****************
        .05         30     ******************************
        .10         11     ***********
        .15          1     *
        .20          2     **
        .25          1     *
        .30          0
        .35          0
        .40          2     **
        .45          0
        .50          2     **

-- HIST C7

  HS05

   MIDDLE OF    NUMBER OF
   INTERVAL     OBSERVATIONS
        0.0          3     ***
         .1         23     ************************
         .2          2     **
         .3         10     **********
         .4         17     *****************
         .5          9     *********
         .6          1     *
         .7          0
         .8          0
         .9          1     *

1-- HIST C8

  NA

   MIDDLE OF    NUMBER OF
   INTERVAL     OBSERVATIONS
         .4         21     *********************
         .8         10     **********
        1.2         16     ****************
        1.6          9     *********
        2.0          6     ******
        2.4          2     **
        2.8          1     *
        3.2          1     *


-- HIST C9

  K
   EACH * REPRESENTS   2 OBSERVATIONS

   MIDDLE OF    NUMBER OF
   INTERVAL     OBSERVATIONS
         0.         66     *********************************

-- HIST C10

  TS

   MIDDLE OF    NUMBER OF
   INTERVAL     OBSERVATIONS
         .2         21     *********************
         .4         22     **********************
         .6         12     ************
         .8          2     **
        1.0          4     ****
        1.2          3     ***
        1.4          0
        1.6          1     *
        1.8          0
        2.0          1     *

-- HIST C12

  £H+

   MIDDLE OF    NUMBER OF
   INTERVAL     OBSERVATIONS
        0.0          4     ****
         .2         10     **********
         .4         17     *****************
         .6         14     **************
         .8          9     *********
        1.0          3     ***
        1.2          2     **
        1.4          2     **
        1.6          5     *****

-- WRITE C1,C13

THIS FILE WAS WRITTEN USING THE FORMAT
(F5. 0,F8. 3)

211. 552.453
210. 541.513
209. 513.109
208. 501.072
207. 482.059
138. 528.759
137. 555.637
```

```
        1.4
        1.6         5     *****

-- WRITE C1,C13

THIS FILE WAS WRITTEN USING THE FORMAT
(F5. 0,F8. 3)

211.  552.453
210.  541.513
209.  513.109
208.  501.072
207.  482.059
138.  528.759
137.  555.637
136.  559.622
135.  559.752
134.  538.641
133.  454.094
132.  475.328
131.  496.344
130.  559.894
129.  538.461
128.  517.385
127.  526.352
126.  558.346
125.  451.625
124.  473.132
123.  494.171
122.  494.574
121.  494.641
120.  494.508
119.  494.614
118.  494.548
117.  508.042
116.  508.147
115.  508.116
114.  508.171
107.  509.388
106.  510.183
105.  511.096


104.  510.611
103.  508.674
102.  512.554
101.  490.576
100.  504.541
 99.  519.075
 98.  512.909
 97.  511.945
 96.  513.239
 95.  514.497
 94.  513.658
 93.  506.314
 84.  514.377
 83.  515.273
 82.  500.302
 80.  515.839
 79.  514.837
 78.  514.954
 77.  580.500
 76.  477.379
 75.  495.741
 74.  519.587
 73.  539.536
 72.  560.599
 68.  473.610
 67.  494.909
 66.  515.100
 65.  539.082
 62.  476.410
 61.  497.851
 60.  516.228
 59.  535.644
 58.  556.443

--  STOP

*** MINITAB *** STATISTICS DEPT * PENN STATE UNIV. * RELEASE 81.1 *
STORAGE AVAILABLE     5000
```

FIGURE A11. The Minitab regression output for the kinetic analysis of the hydrogen peroxide system.

```
-- REGRESS C34 3 C22,C25,C48,C40,C41

THE REGRESSION EQUATION IS
Y =    18.3 -10647. X1 - .0064 X2
     +  6.42 X3

                                                ST. DEV.     T-RATIO =
        COLUMN      COEFFICIENT                 OF COEF.     COEF/S.D.
        --            18.321                     1.120         16.36
X1      1/TK        -10647.1                     530.2        -20.08
X2      LS04        -0.08642                   0.05325        -1.62
X3      E/T           6.4204                    0.4094        15.68

THE ST. DEV. OF Y ABOUT REGRESSION LINE IS
S = 0.2111
WITH (  46- 4) =  42 DEGREES OF FREEDOM

R-SQUARED = 92.4 PERCENT
R-SQUARED = 91.8 PERCENT, ADJUSTED FOR D.F.

ANALYSIS OF VARIANCE

 DUE TO      DF           SS          MS=SS/DF
REGRESSION    3      22.59170          7.53057
RESIDUAL     42       1.87091          0.04455
TOTAL        45      24.46261

1
FURTHER ANALYSIS OF VARIANCE
SS EXPLAINED BY EACH VARIABLE WHEN ENTERED IN THE ORDER GIVEN

 DUE TO      DF           SS
REGRESSION    3      22.59170
1/TK          1      11.38165
LS04          1       0.25445
E/T           1      10.95560

                X1           Y        PRED. Y     ST.DEV.
ROW          1/TK         LRTE         VALUE      PRED. Y     RESIDUAL      ST.RES.
  1       0.00300      -2.3575      -2.4047      0.0431       0.0471        0.23
  2       0.00300      -2.2984      -2.4081      0.0425       0.1097        0.53
  3       0.00300      -2.3279      -2.4018      0.0437       0.0739        0.36
  4       0.00300      -2.3625      -2.4095      0.0421       0.0470        0.23
  5       0.00300      -2.2857      -2.4006      0.0440       0.1149        0.56
  6       0.00329      -3.4202      -3.1993      0.0867      -0.2209       -1.15
  7       0.00319      -3.1612      -2.9369      0.0615      -0.2243       -1.11
  8       0.00309      -2.5702      -2.6597      0.0462       0.0894        0.43
  9       0.00300      -2.3809      -2.4173      0.0413       0.0364        0.18
 10       0.00283      -2.2083      -1.9378      0.0692      -0.2705       -1.36
 11       0.00319      -3.3872      -2.9390      0.0584      -0.4492       -2.21R
 12       0.00301      -3.7445      -3.5755      0.0650      -0.1691       -0.84
 13       0.00310      -3.9208      -3.8620      0.0565      -0.0588       -0.29
 14       0.00301      -3.2076      -3.5586      0.0688       0.3510        1.76
 15       0.00309      -3.6303      -3.8226      0.0594       0.1844        0.91
 16       0.00309      -4.1549      -3.8517      0.0570      -0.3032       -1.48
 17       0.00300      -2.6180      -2.5759      0.0570      -0.0421       -0.21
 18       0.00300      -2.5901      -2.5365      0.0465      -0.0536       -0.26
 19       0.00300      -2.4698      -2.4974      0.0391       0.0276        0.13
 20       0.00301      -2.6459      -2.5835      0.0496      -0.0624       -0.30
 21       0.00300      -2.5499      -2.2876      0.0526      -0.2622       -1.28
 22       0.00317      -2.9788      -2.9137      0.0641      -0.0651       -0.32
 23       0.00327      -3.1938      -3.2534      0.0688       0.0596        0.30

 24       0.00291      -2.3429      -2.2684      0.0734      -0.0745       -0.38
 25       0.00300      -2.3655      -2.3455      0.0741      -0.0200       -0.10
 26       0.00300      -2.2464      -2.2745      0.0718       0.0281        0.14
 27       0.00300      -2.9136      -2.8208      0.0544      -0.0928       -0.46
 28       0.00300      -2.7447      -2.7902      0.0417       0.0455        0.22
 29       0.00300      -2.6326      -2.6932      0.0538       0.0605        0.30
 30       0.00300      -2.8697      -2.9433      0.0580       0.0737        0.36
 31       0.00300      -3.0223      -3.0060      0.0414      -0.0154       -0.07
 32       0.00300      -2.9666      -3.0505      0.0437       0.0839        0.41
 33       0.00301      -2.9393      -3.0010      0.0451       0.1426        0.69
 34       0.00300      -2.9747      -2.9518      0.0582      -0.0229       -0.11
 35       0.00300      -2.8182      -2.9001      0.0664       0.0819        0.41
 36       0.00298      -2.6615      -2.8350      0.0674       0.1715        0.86
 37       0.00300      -2.8097      -2.8656      0.0780       0.0560        0.29
 38       0.00300      -2.8601      -2.9465      0.0581       0.0864        0.43
 39       0.00300      -3.0555      -2.9999      0.0539      -0.0566       -0.28
 40       0.00330      -5.6990      -5.1395      0.0999      -0.5605       -3.02RX
 41       0.00330      -4.7212      -4.8367      0.0863       0.1155        0.60
 42       0.00330      -4.6990      -4.5736      0.0765      -0.1253       -0.64
 43       0.00330      -3.1331      -3.7706      0.0668       0.6464        3.23R
 44       0.00330      -3.0580      -3.4504      0.0728       0.4014        2.03R
 45       0.00330      -2.9442      -2.7780      0.1003      -0.1663       -0.90 X
 46       0.00330      -4.2366      -4.4158      0.0718       0.1793        0.90

R DENOTES AN OBS. WITH A LARGE ST. RES.
X DENOTES AN OBS. WHOSE X VALUE GIVES IT LARGE INFLUENCE.

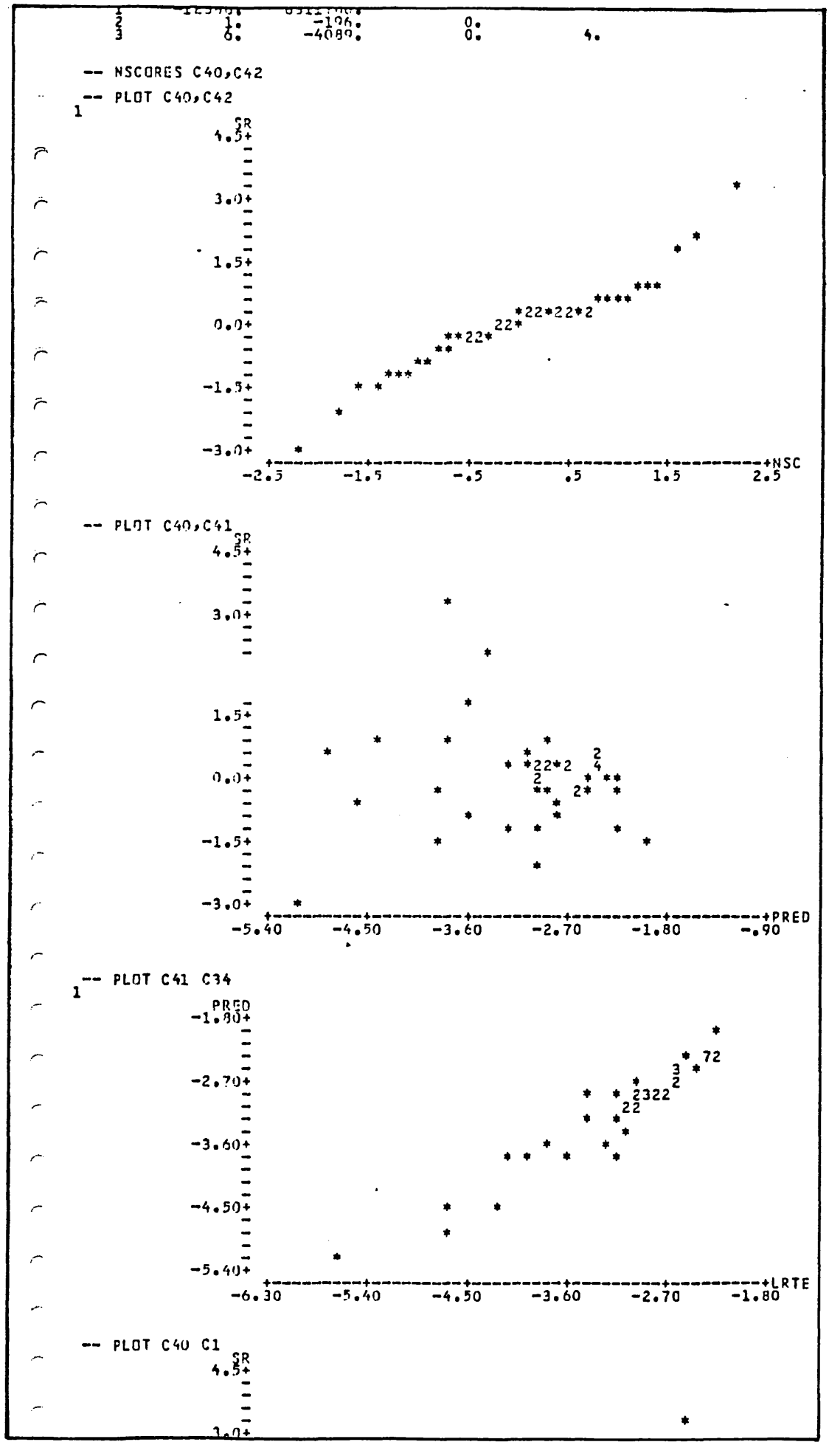
DURBIN-WATSON STATISTIC = 1.64

(X-PRIME X)INVERSE

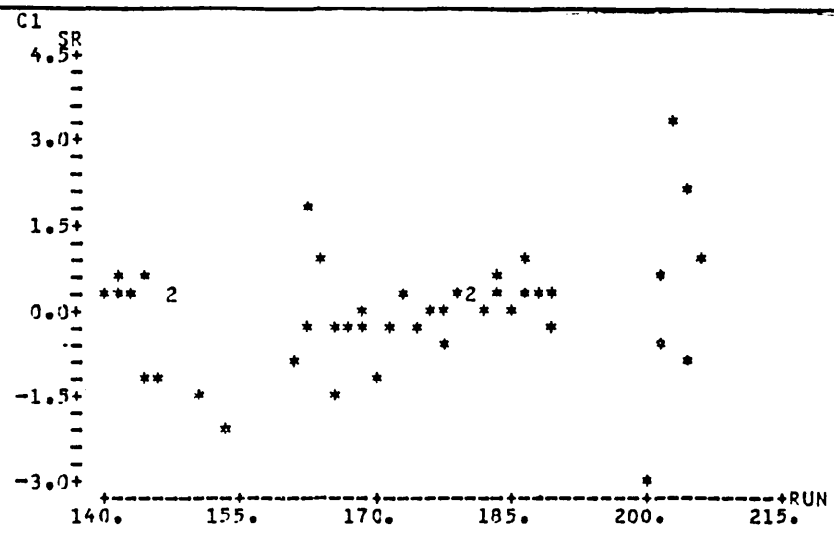
              0            1            2            3
  0         20.
  1     -12386.      6311700.
  2          1.         -196.           0.
  3          6.        -4089.           0.           4.

-- NSCORES C40,C42

-- PLOT C40,C42
1
            SR
          4.5+
             -
             -
             -
```

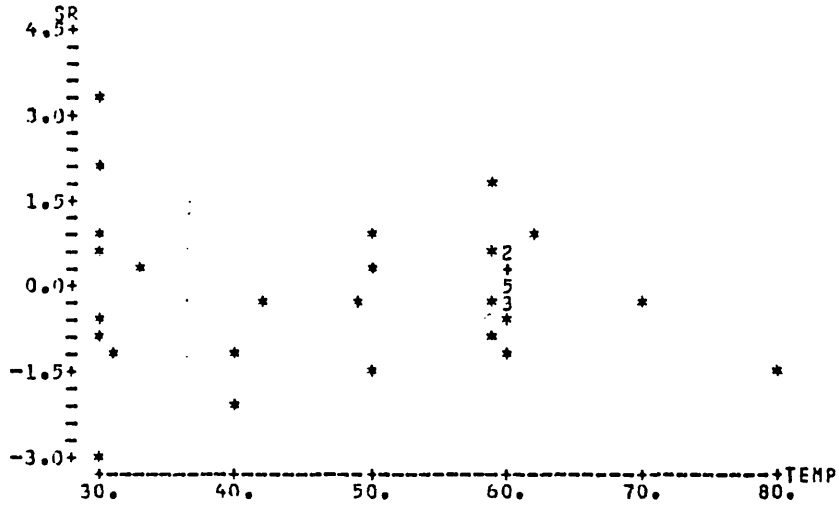

-- NSCORES C40,C42
-- PLOT C40,C42
SR
NSC
-- PLOT C40,C41
SR
PRED
-- PLOT C41 C34
PRED
LRTE
-- PLOT C40 C1
SR

-- PLOT C40 C1

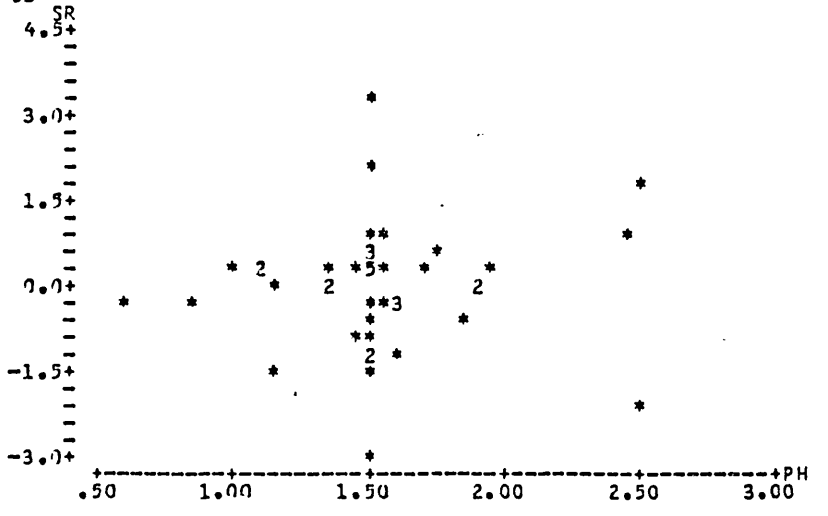


-- PLOT C40 C2

1



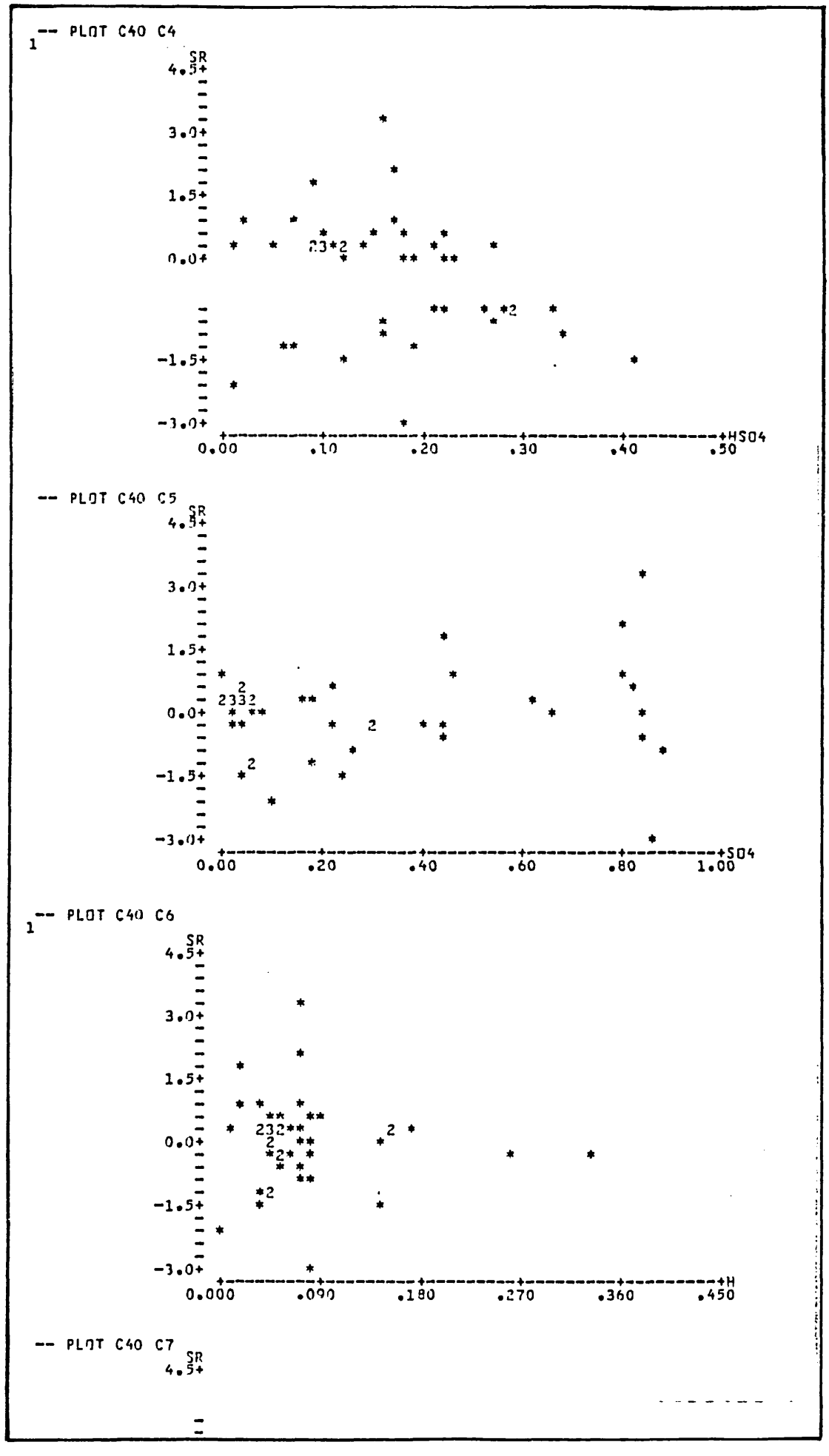
-- PLOT C40 C3

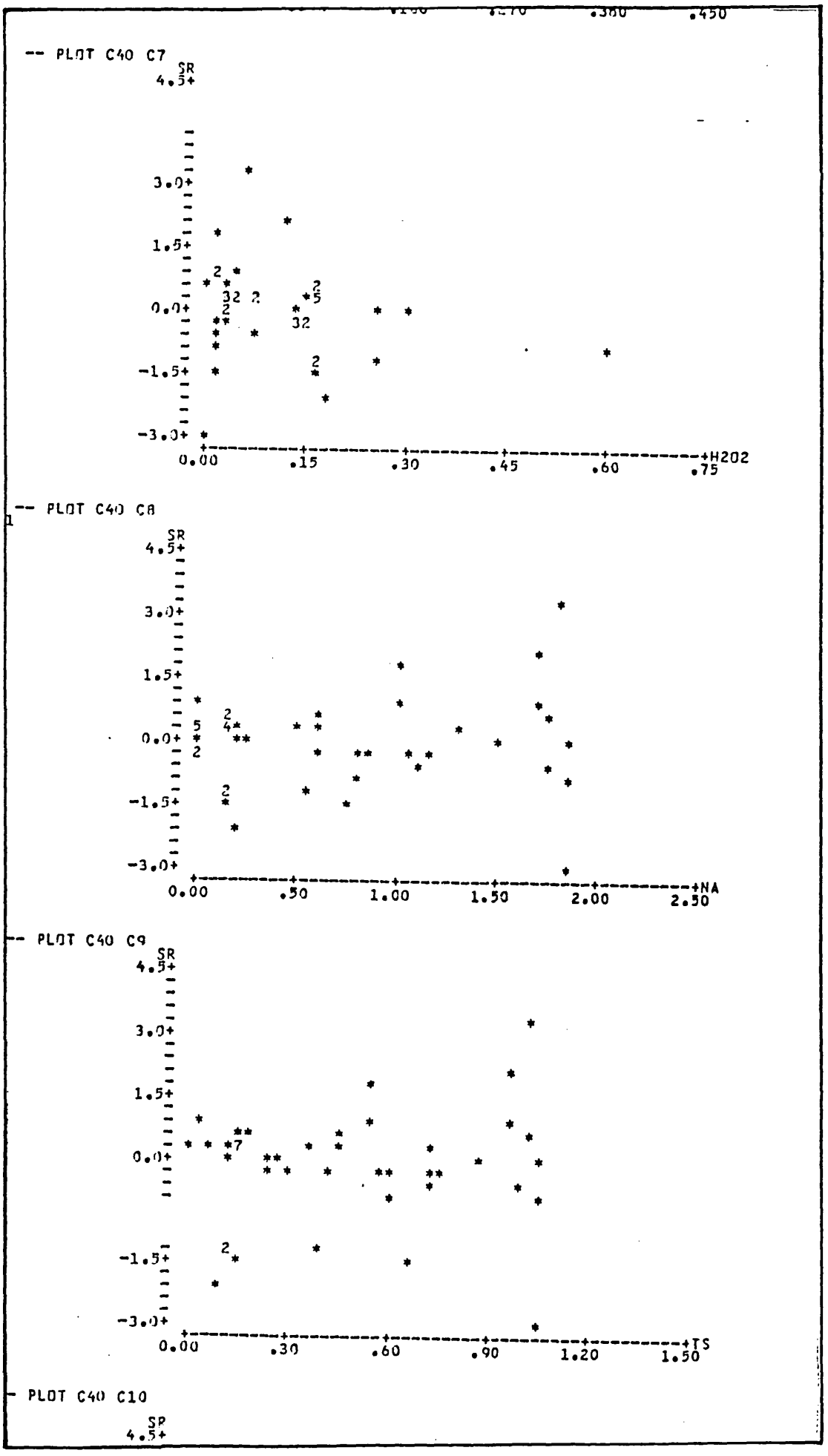


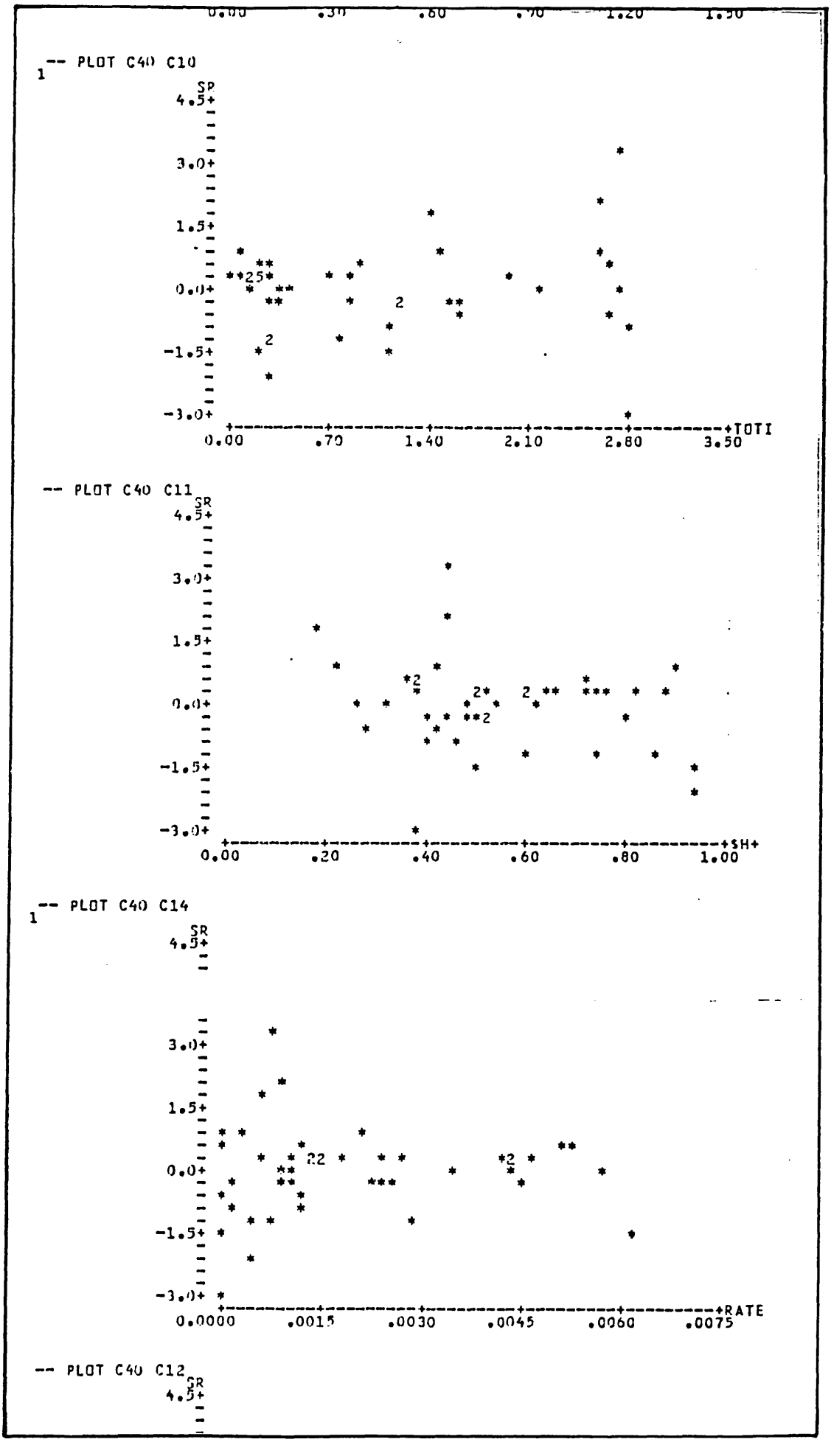
-- PLOT C40 C4

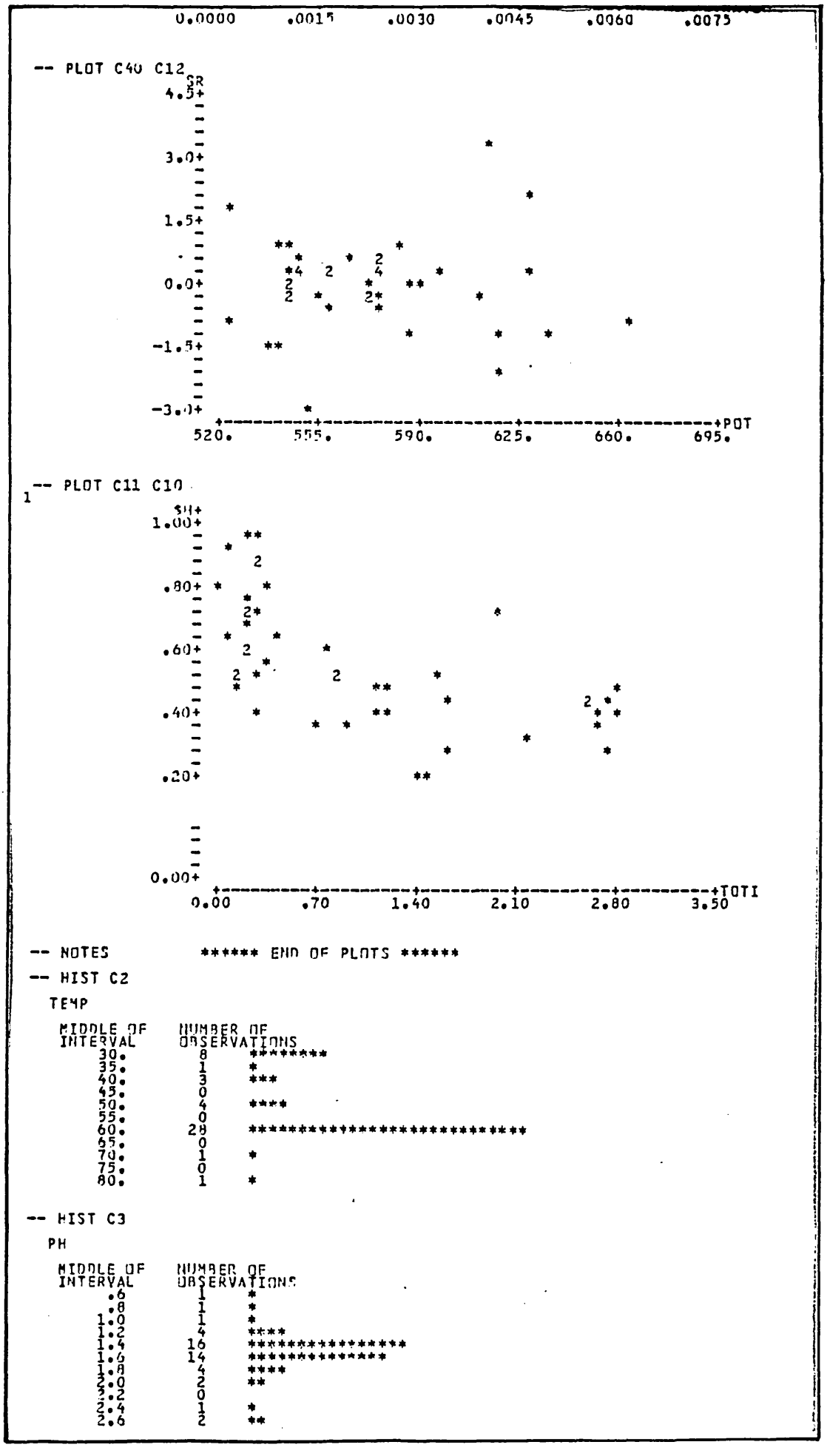
1




-- PLOT C40 C4
SR
HSO4
0.00
.10
.20
.30
.40
.50
-- PLOT C40 C5
SR
SO4
0.00
.20
.40
.60
.80
1.00
-- PLOT C40 C6
SR
H
0.000
.090
.180
.270
.360
.450
-- PLOT C40 C7
SR


.300
.360
.450
-- PLOT C40 C7
SR
4.5+
3.0+
1.5+
0.0+
-1.5+
-3.0+
0.00
.15
.30
.45
.60
.75
+H2O2
-- PLOT C40 C8
SR
4.5+
3.0+
1.5+
0.0+
-1.5+
-3.0+
0.00
.50
1.00
1.50
2.00
2.50
+NA
-- PLOT C40 C9
SR
4.5+
3.0+
1.5+
0.0+
-1.5+
-3.0+
0.00
.30
.60
.90
1.20
1.50
+TS
- PLOT C40 C10
SR
4.5+


0.00 .30 .60 .90 1.20 1.50
1 -- PLOT C40 C10
SR
4.5+
3.0+
1.5+
0.0+
-1.5+
-3.0+
0.00 .70 1.40 2.10 2.80 3.50
TOTI
-- PLOT C40 C11
SR
4.5+
3.0+
1.5+
0.0+
-1.5+
-3.0+
0.00 .20 .40 .60 .80 1.00
$H
1 -- PLOT C40 C14
SR
4.5+
3.0+
1.5+
0.0+
-1.5+
-3.0+
0.0000 .0015 .0030 .0045 .0060 .0075
RATE
-- PLOT C40 C12
SR
4.5+



-- NOTES ****** END OF PLOTS ******

-- HIST C2

TEMP

MIDDLE OF INTERVAL	NUMBER OF OBSERVATIONS	
30.	8	********
35.	1	*
40.	3	***
45.	0	
50.	4	****
55.	0	
60.	28	****************************
65.	0	
70.	1	*
75.	0	
80.	1	*

-- HIST C3

PH

MIDDLE OF INTERVAL	NUMBER OF OBSERVATIONS	
.6	1	*
.8	1	*
1.0	1	*
1.2	4	****
1.4	16	****************
1.6	14	**************
1.8	4	****
2.0	2	**
2.2	0	
2.4	1	*
2.6	2	**

```
-- HIST C4

  HSO4

   MIDDLE OF    NUMBER OF
   INTERVAL     OBSERVATIONS
       0.00          3      ***
        .05          4      ****
        .10         12      ************
        .15          7      *******
        .20         10      **********
        .25          4      ****
        .30          3      ***
        .35          2      **
        .40          1      *

-- HIST C5

  SO4

   MIDDLE OF    NUMBER OF
   INTERVAL     OBSERVATIONS
        0.0         15      ***************
         .1          7      *******
         .2          6      ******
         .3          3      ***
         .4          4      ****
         .5          1      *
         .6          1      *
         .7          1      *
         .8          6      ******
         .9          2      **


-- HIST C6

  H

   MIDDLE OF    NUMBER OF
   INTERVAL     OBSERVATIONS
       0.00          4      ****
        .05         28      ****************************
        .10          7      *******
        .15          5      *****
        .20          0
        .25          1      *
        .30          0
        .35          1      *

-- HIST C7

  H2O2

   MIDDLE OF    NUMBER OF
   INTERVAL     OBSERVATIONS
       0.00          9      *********
        .05         14      **************
        .10          1      *
        .15         18      ******************
        .20          0
        .25          2      **
        .30          1      *
        .35          0
        .40          0
        .45          0
        .50          0
        .55          0
        .60          1      *

-- HIST C8

  NA

   MIDDLE OF    NUMBER OF
   INTERVAL     OBSERVATIONS
        0.0          9      *********
         .2         13      *************
         .4          1      *
         .6          4      ****
         .8          4      ****
        1.0          4      ****
        1.2          1      *
        1.4          2      **
        1.6          0
        1.8          8      ********

-- HIST C9

  TS

   MIDDLE OF    NUMBER OF
   INTERVAL     OBSERVATIONS
        0.0          2      **
         .1         12      ************
         .2          6      ******
         .3          2      **
         .4          4      ****
         .5          3      ***
         .6          3      ***
         .7          5      *****
         .8          0
         .9          1      *
        1.0          7      *******
        1.1          1      *

-- HIST C10
```

```
  TOTI

   MIDDLE OF    NUMBER OF
   INTERVAL     OBSERVATIONS
        0.0          7      *******
         .4         15      ***************
         .8          5      *****
        1.2          4      ****


        1.6          5      *****
        2.0          2      **
        2.4          2      **
        2.8          6      ******

-- HIST C11

  $H+

   MIDDLE OF    NUMBER OF
   INTERVAL     OBSERVATIONS
         .2          2      **
         .3          3      ***
         .4         12      ************
         .5         11      ***********
         .6          5      *****
         .7          5      *****
         .8          3      ***
         .9          5      *****

-- HIST C12

  POT

   MIDDLE OF    NUMBER OF
   INTERVAL     OBSERVATIONS
       520.          2      **
       540.         14      **************
       560.          6      ******
       580.         15      ***************
       600.          2      **
       620.          5      *****
       640.          1      *
       660.          1      *

-- HIST C14

  RATE

   MIDDLE OF    NUMBER OF
   INTERVAL     OBSERVATIONS
     0.0000          8      ********
      .0005          6      ******
      .0010          9      *********
      .0015          4      ****
      .0020          2      **
      .0025          5      *****
      .0030          1      *
      .0035          1      *
      .0040          1      *
      .0045          5      *****
      .0050          2      **
      .0055          1      *
      .0060          1      *

-- HIST C40

  SR

   MIDDLE OF    NUMBER OF
   INTERVAL     OBSERVATIONS
        -3.0          1      *
        -2.5          0
        -2.0          1      *
        -1.5          3      ***
        -1.0          4      ****
         -.5          8      ********
          0.0         10      **********
           .5         13      *************
         1.0          3      ***
         1.5          0
         2.0          2      **
         2.5          0
         3.0          1      *

-- HIST C42

  NSC

   MIDDLE OF    NUMBER OF


   INTERVAL     OBSERVATIONS
        -2.0          2      **
        -1.5          3      ***
        -1.0          5      *****
         -.5          8      ********
          0.0         10      **********
           .5          8      ********
         1.0          5      *****
         1.5          3      ***
         2.0          2      **

-- WRITE C1,C12
```

```
        1.0         2     **
        1.5         3     ***
        2.0         2     **

-- WRITE C1,C12

THIS FILE WAS WRITTEN USING THE FORMAT
(F5. 0,F0. 3)

140. 576.693
141. 576.668
142. 576.568
143. 576.693
144. 576.656
145. 635.646
146. 616.540
147. 596.708
148. 576.717
150. 537.182
153. 617.164
161. 523.012
162. 543.080
163. 524.842
164. 542.305
165. 539.549
166. 572.448
167. 573.087
168. 573.072
169. 574.583
170. 585.754
172. 609.786
173. 628.744
174. 556.053
176. 585.621
177. 589.834
178. 559.715
179. 559.630
180. 559.544
181. 546.460
182. 545.906
183. 545.850
184. 548.154
185. 546.018
186. 547.730
187. 544.298
188. 548.336
189. 546.295
190. 544.209
200. 550.419
201. 564.579
202. 577.013
203. 614.537
204. 629.566
205. 661.910
206. 584.406

--  STOP

*** MINITAB *** STATISTICS DEPT * PENN STATE UNIV. * RELEASE 81.1 *
STORAGE AVAILABLE     5000
```

ACKNOWLEDGEMENTS

I wish to take this opportunity to thank Dr. John Monhemius, who, as my supervisor has been a constant source of encouragement and guidance.

I would like to extend my thanks to Professor Burkin and Dr. G.H. Kelsall for many stimulating conversations and discussions.

I wish to thank the members of the Hydrometallurgy Group, past and present, for their friendship and support, especially Salvador Aguayo Salinas, Ray Cooke, and Simon Curling.

I wish to thank John Burgess for his superb technical assistance, and friendship. Thanks are also due to Mike Haddon and Dan Waters for their assistance at various times.

I would like to acknowledge the gift of uranium dioxide spheres and plates from UKAEA (Harwell).

The funding for this project comes from an SERC CASE award in conjunction with Interox Chemicals Ltd., whom I wish to thank for making this work possible. My special thanks go to the Hydrometallurgy Group at Widnes, including David Mobbs, Colin Fowler and Diana Anderson.

For her patience and magnificent typing, I wish to thank Sylvia Greenwood. For her massive personal support and sacrifice, I wish to thank Marion, my wife.

Finally, I must also thank Pat, Ken and family for their encouragement, and also the gentle acceptance of the chaos we have caused them.

There are many who deserve a place on this page; the friends from Woodberry, Bradford, Upminster and beyond. Let it be understood that you have my sincere gratitude and thanks. Thank you.

S.F. Watts
Royal School of Mines,
London.
1st September 1985

REFERENCES

1. HALPERN, J. 'Some aspects of the Physical Chemistry of Hydrometallurgy', J. Metals 9 (1957) p.280.
2. SOHN, H.Y. 'Fundamentals of the Kinetics of Heterogeneous Reaction Systems in Extractive Metallurgy' in Rate Processes of Extractive Metallurgy. Editors Sohn, H.Y. and Wadsworth, M.E. Plenum, New York, (1979).
3. LEVICH, V.G. Physiochemical Hydrodynamics. Prentice Hall (1962).
4. HARRIOT, P. 'Mass Transfer to Particles: Part 1 Suspended in Agitated Tanks', AIChE 8 (1962) p.93.
5. PEARSON, R. & WADSWORTH, M.E. 'A Kinetic Study of the Dissolution of UO_2 in Carbonate Solutions' Trans. Metall. Soc. AIME (1958), p.294.
6. LAXEN, P.A. 'The Dissolution of Uranium Dioxide as an Electron Transfer Reaction'. Symposium, Sao Paulo 1970. Proceedings published 1970. The Recovery of Uranium from its Ores, p.321.
7. KATZ, J.J. & RABINOVITCH, E. The Chemistry of Uranium the Element, its Binary and Related Compounds (USAEC). Dover Publications Inc., New York, (1951).
8. ZACHARIASEN, W.H. Report N-1973, April 24th 1945 (Chicago Project). *Reference 7

9. RUNDLE, R.E., BAENZIGER, N.L., WILSON, A.S. & McDONALD, R.A. 'The Structures of Carbines, Nitrides and Oxides of Uranium'. J. Am. Chem. Soc. 70 (1948), pp.99-105.

10. SCHEOP, A. & BILLIET, V. *Reference 7
Bull. Soc. Geol. Belg. 58 (1935), p.198.

11. VON ARKEL, A. *Reference 7
Physica 4 (1924) p.286.

12. GOLDSCHMIDT, THOMASSEN. *Reference 7
Videnskapsselskapets Skrifter 1 (2) p.8.

13. FRIED, DAVIDSON, Reports CN 2689, CN 3053, March-June 1945 (Chicago Project) *Reference 7

14. JOLIBOIS, P. *Reference 7
Compt. Rend. 224 (1947) p.1393.

15. GRONVOLD, F. & HARALDSEN, H. Nature 162 (1948) p.69.

16. BILTZ, H., MULLER, H. 'Uranoxyde'. Z. Anorg. Allgem. Chem. 163 (1927) p.161.

17. MARLOW, P.G., RUSSELL, J.P. & HARDY, J.R. 'Raman Scattering in UO_2'. J. Phys. Chem. 70 (1966) p.409.

18. DARMAYON, P.H. 'The Economics of Uranium Supply and Demand'. IAEA Bull. 23 (1981) (2) p.3.

19. SWANSON, FUYAT, ASTM. 32-1404. NBS Circular 539 (1953) (2) p.33.

20. HOKESTRA, H.R., SIEGEL, S., GALLAGHER, H.
J. Inorg. Nucl-Chem. 32 (1970) p.3237.

21. KOZHINA, I., SOLNTSEV, From A.S.T.M. Index Card number 32-1404.

22. NAITO, ISHIII, HAMAGUCHI, OSHIMA, Solid State Comm. 5 (1967) p.349.

23. WEISSBART, J. From A.S.T.M. Index Card number 9-206.

24. PAQUETTE, J., LEMISE, R.J. 'A Description of the Chemistry of Aqueous Solutions of Uranium and Plutonium to 200°C using Potential-pH Diagrams.' Nucl. Sci. and Eng. 79 (1981) p.26.

25. DIAS, M.J.P. 'A Statistical Approach to the Precipitation of Iron as Jarosite' PhD Thesis (1979). Department of Metallurgy, Imperial College, University of London.

26. BAES, C.F. 'Estimation of HSO_4^- Dissociation in $H_2SO_4/NaHSO_4$ Solutions'. J. Amer. Chem. Soc. 79 (1957), p.5611.

27. LINDSTROM, R.E., WIRTH, H.E. 'Estimation of the Bisulphate Ion Dissociation in Solutions of Sulfuric Acid and Sodium Bisulphate'. J. Phys. Chem. 73 (1969) (1) p.218.

28. MARSHALL, W.L., JONES, E.V. 'The Second Dissociation Constant of H_2SO_4 in the Temperature range 25°-350° from $CaSO_4$ Solubility Measurements'. J. Phys. Chem. 70 (1966) (12) p.4028.

29. YOUNG, SMITH. 'Thermodynamic Properties of Mixtures of Electrolytes in Aqueous Solutions'. J. Phys. Chem. 50 (1954) p.716.

30. MAJIMA, H., AWAKURA, Y. 'Ion Activities of H_2SO_4, Sulphate and Water in Concentrated Sulphuric Acid Solution'. Ryuson to Kogyo 37 (1984) (1) p.1.

31. SCHORTMANN, W.E., DESESA, M.A. 'Kinetics of the Dissolution of UO_2 in CO_3/HCO_3 solutions'. 2nd U.N. International Conference for the Peaceful Uses of Atomic Energy. Geneva, June 1958. Proceedings published, P/505.

32. IVEZ, D.J.G., JANZ, G.S. Reference Electrodes: Theory and Practice. Academic Press (1961), New York.

33. BURKIN, A.R., MONHEMIUS, A.J. 'Acid Leaching of Uranium Ores Using Hydrogen Peroxide and Caro's Acid'. Joint 8th Hydrometallurgical Meeting, Montreal, 28th August 1978.

34. BURKIN, A.R., MANNING, G.D., MONHEMIUS, A.J. 'Applications of Hydrogen Peroxide and Peroxysulphuric Acids in Hydrometallurgy'. Hydrometall. '81. Proc. Soc. Ind. Symp. 1981. B5/1-B5/13.

35. HABASHI, F., THURSTON, G.A. 'Kinetics and Mechanism of the Dissolution of Uranium Dioxide'. Energia Nucleare 14 (1967) (4) p.238.

36. HABASHI, F. 'Kinetics of Corrosion of Metals'. J. Chem. Educ. 42 (1965) p.318.

37. SIPOS, L., LEFTIC, L.J., BRONICA, M., GALUS, Z. 'Electrochemical Redox Mechanism of Uranium in Acidic Perchlorate Solutions'. J. Electroanal. Chem. 32 (1971) p.35.

38. NICOL, M.J., NEEDES, C.R.S. 'The Mechanism of the Anodic Dissolution of Uranium Dioxide'. N.I.M. Report PIN 171 September 25th 1973 (N.I.M. number 7079).

39. NICOL, M.J., NEEDES, C.R.S., FINKELSTEIN, N.P. 'Electrochemical Model for the Leaching of Uranium Dioxide: 1-Acid Media', in Leaching and Reduction in Hydrometallurgy, Ed. Burkin,A.R. IMM, (1975).

40. NICOL, M.J., FINKELSTEIN, N.P. 'Electrochemical Model for the Leaching of Uranium Dioxide: 2-Alkaline Carbonate Media' in Leaching and Reduction in Hydrometallurgy Ed. Burkin, A.R. IMM, (1975).

41. NICOL, M.J., NEEDES, C.R.S. 'The Anodic Dissolution of UO_2-I in Perchlorate Solutions' Electrochim. Acta. 20 (1975) p.585.

42. NICOL, M.J., NEEDES, C.R.S. 'The Anodic Dissolution of UO_2-II in Carbonate Solutions'. Electrochim. Acta. 22 (1977) p.1381.

43. NEEDES, C.R.S., NICOL, M.J. 'A Study of some Redox Reactions at a UO_2 Surface' N.I.M. Report PIN 165 September 15th 1973 (N.I.M. number 7073).

44. JOHNSON, L.H., SHOESMITH, D.W., LUNANSKY, G.E., BAILEY, M.G., TREMAINE, P.R. 'Mechanisms of Leaching and Dissolution of UO_2 Fuel' Nucl. Tech. 56 (1982) p.238.

45. SUNDER, S., SHOESMITH, D.W., BAILEY, M.G. STANCHELL, F.W., McINTYRE, N.S. 'Anodic Oxidation of UO_2. Part I. Electrochemical and X-Ray Photoelectron Spectroscopic Studies in Neutral Solutions'. J. Electroanal. Chem. 130 (1981) p.163.

46. KELSALL, G.H. Private Communication.

47. SUNDER, S., SHOESMITH, D.W., BAILEY, M.G., WALLACE, G.J. 'Anodic Oxidation of UO_2. Part II. Electrochemical and X-Ray Photoelectron Spectroscopic Studies in Alkaline Solutions'. Received from Dr. S. Sunder, to be published in J. Electroanal. Chem.

48. PAQUETTE, J., LEMIRE, R.J. 'A Description of the Chemistry of Aqueous Solutions of Uranium and Plutonium to 200°C using potential-pH Diagrams'. Nucl. Sci. and Eng. 79 (1981) p.26.

49. SUNDER, S., SHOESMITH, D.W., BAILEY, M.G., WALLACE, G.J. 'Mechanism of Oxidative Dissolution of UO_2 Under Waste Disposal Vault Conditions'. Canadian Nuclear Society Conference, Winnipeg, September 1982.

50. GRANDSTAFF, D.E. 'A Kinetic Study of the Dissolution of Uraninite' Econ. Geol. 71 (1976) p.1493.

51. HISKEY, J.B. 'Hydrogen Peroxide Leaching of Uranium in Carbonate Solutions'. Inst. Min. Metall. Trans. (1979) C145.

52. HISKEY, J.B. 'Kinetics of UO_2 Dissolution in Ammonium Carbonate' Trans. Inst. Min. Metall. (Section C: Extraction Metallurgy) 88 (1979).

53. HAQUE, K.E., RITCEY, G.M. 'Comparison of Oxidants for the Leaching of Uranium Ores in Sulphuric Acid'. C.I.M. Bull. 75 (1982) (841) p.127.

54. CELEDA, J., GOMEZ LARA, J. 'The Kinetics and Mechanism of the Dissolution of Uranous-Uranic Oxide in H_2SO_4 in the presence of Fe^{2+}, J. Inorg. Chem. 27 (1965) p.2561.

55. PETERS, E., HALPERN, J. 'Kinetics and Dissolution of Pitchblende' C.I.M.M. Bull. 56 (1953) p.380.

56. MACKAY, T.L., WADSWORTH, M.E. 'A Kinetic Study of the Dissolution of UO_2 in Sulphuric Acid'. Trans. A.I.M.E. (Metall. Soc.) 212 (1958) p.597.

57. ELIGWE, C.A., TARMA, A.E., DEVRIES, F.W. 'Extraction of Uranium from Low Grade Ore with H_2SO_4/H_2O_2 Agitated Reactor at 1600 rpm'. 4th Annual Uranium Seminar, Corpus Christi, Texas, September 14th-17th 1980 South Texas Mining Section of A.I.M.E.

58. ELIGWE, C.A., TARMA, A.E., DEVRIES, F.W. 'Kinetics of Uranium Extraction from a New Mexico Ore by H_2SO_4-H_2O_2'. Metall. 2 (36/1/82) Seite 135.

59. ELIGWE, C.A., TARMA, A.E., DEVRIES, F.W. 'Extraction of Uranium from Ores by the HSS Process'. To be published in Hydrometallurgy.

60. LAXEN, P.A. 'A Kinetic Study of the Dissolution of Uraninites in Sulphuric Acid' in Research in Chemical and Extractive Metallurgy; Australas. Inst. Min. and Metall. Melbourne, (1967).

61. SOBKOWSKI, J., STUGLIK, Z., MINC, S. 'Kinetics of the Reaction Between U_3O_8 and Fe III ions in Sulphuric Acid'. Nukleonika 11 (1966) p.799.

62. SKLIBOVA-KLABULORA, J., NEUMANN, L. 'Mechanism and Kinetics of the Dissolution of Uranium IV Oxide in Sulphuric Acid with Iron III ions' Colln. Czech. Chem. Commun. (English Edition) 33 (1968) p.1678.

63. EARY, L.E., CATHLESS, L.M. 'A Kinetic Model of UO_2 Dissolution in Acid H_2O_2 Solutions that includes Uranium Peroxide Hydrate Precipitation' Met. Trans. B. 14B (1983) p.325.

64. BARD, A.J., FAULKNER, L.R. Electrochemical Methods-Fundamentals and Applications. John Wiley and Sons (1980), New York.

65. BOCKRIS, J.O.M., REDDY, A.K.N. Modern Electrochemistry (Volume 2) Macdonald and Co. (Publishers) Ltd. (1970). London. Then by Plenum, New York.

66. BOX, G.E.P., HUNTER, G.H., HUNTER, S.H. Statistics for Experimenters. John Wiley and Sons (1978). New York.

67. MANNING, G.D. Leaching of Synthetic Uranium Dioxide with Hydrogen Peroxide, Caro's Acid and Ferric Iron Solutions. Received from Dr. A.J. Monhemius Royal School of Mines, London.

68. THOMPSON, M., WALSH, J.N. A Handbook of Inductively Coupled Plasma Spectrometry. Blackie & Son Ltd. (1983), London.

69. AMELL, A.R., LANGMUIR, D. 'Factors Influencing the solution rates of UO_2 under conditions applicable to in situ leaching'. U.S. Department of the Interior: Bureau of Mines, Contract HO272019, Nov. 20th 1978.

70. GERLACH, J., KUZECI, E. 'Application of Carbon Paste electrodes to elucidate Hydrometallurgical Dissolution Processes with Special Regard to Chalcocite and Covellite'. Hydrometallurgy 11 (1983) p.345.

71. BARIKOV, V.G., ROZHDESTVENSKAYA, Z.B., SONGINA,O.A. 'Voltammetry with a Mineral-Carbon-Paste Electrode' Ind. Lab. 1960, p.928.

74. VARIOUS AUTHORS, 'Caro's Acid Laboratory Procedure for Hydrometallurgy' Document A.O.5.2. Interox Chemicals Ltd.

75. FLANAGAN, J. 'Peroxymonosulphate, Peroxymonobarates and Peroxocarbonates' Research Report No.1 (January 1983), School of Chemistry, Imperial College, London.

76. BERTHOLOT, M. Compt. Rend. 86 (1878) p.20.

77. CARO, H. Z. Ang. Ch. (1878) 58 (1898) p.845.

78. FRIEDERICH, W. Z. Anerg. Ch. 73 (1912) p.325.

79. KIRKY, J. Ann. Univ. Turku. Ser. Al. 61 (1963).

80. SPIRO, M. Electrochim. Acta 24 (1979) p.213.

81. STEELE, W.V., APPELMAN, E.H. 'The Standard Enthalpy of Formation of Peroxymonosulphate (HSO_5) and the Standard Electrode Potential of the Peroxymonosulphate-Bisulphate Couple' J. Chem. Thermodynamics 14 (1982) p.337.

82. BALL, D.L., EDWARDS, J. J. Am. Chem. Soc. 78 (1956) p.1125.

83. GOODMAN, J.F., ROBSON, P. J. Chem. Soc. (1963) p.2871.

84. JOHNSON, D.A., FLORENCE, T.M. 'Spectrophotometric Determination of Uranium VI with 2-(5-bromo-2-pyridylazo)-5-diethylaminophenol' Anal. Chim. Acta. 53 (1971) p.73.

85. JOHNSON, D.A., FLORENCE, T.M. 'A Study of some Pyridylazo Dye Stuffs as Chromogenic Reagents and the Elucidation of the Nature of their Metal Complex Spectra'. Talanta 22 (1975) p.253.

86. SAJIK, W.M. 'Synthesis and Acid Leaching of Brannerite (UTi_2O_6)' PhD Thesis (1981). Dept. of Metallurgy, Imperial College, University of London.

87. UNKNOWN. Perkin-Elmer Model 2380 Atomic Absorption Spectrophotometer, Perkin Elmer (1978).

88. UNKNOWN. Analytical Methods for Atomic Absorption Spectroscopy Perkin Elmer (1978).

89. VOGEL, A.I. A Textbook of Quantitative Inorganic Analysis. 3rd Edition, Longman (1961).

90. UNKNOWN. Manual of Analytical Practice and Procedure Standard issue in all Quality Control Laboratories of the Rhone-Poulenc Group of Companies.

91. JONES, D.W. Undergraduate Inorganic Chemistry Lectures (Symmetry) University of Bradford.

92. MAJIMA, H., AWAKA, Y. 'Measurement of the Activity of Electrolytes and the Application of Activity to Hydrometallurgical Studies'. Metall. Trans.B. 128 (1981) p.141.

93. ROFFIA, S., LAVACCHIELLI, M. 'Potential Sweep Voltammetry with Uncompensated Ohmic Potential Drop. Irreversible Charge Transfer'. J. Electroanal. Chem. 22 (1969) p.117.

94. IMBEAUX, J.C., SAVEANT, J.M. 'Linear Sweep Voltammetry. Effect of Uncompensated Cell Resistance and Double Layer Charging on Polarisation Curves'. J. Electroanal. Chem. 28 (1970) p.325.